HISTORICAL WATER-QUALITY DATA, PUERCO RIVER BASIN, ARIZONA AND NEW MEXICO

By Laurie Wirt, Peter C. Van Metre, and Barbara Favor

U.S. GEOLOGICAL SURVEY
Open-File Report 91—196

Prepared in cooperation with
OFFICE OF NAVAJO AND HOPI INDIAN RELOCATION,
U.S. BUREAU OF INDIAN AFFAIRS,
THE NAVAJO NATION,
ARIZONA DEPARTMENT OF WATER RESOURCES,
ARIZONA DEPARTMENT OF ENVIRONMENTAL QUALITY, and
NEW MEXICO ENVIRONMENTAL IMPROVEMENT DIVISION

Tucson, Arizona
June 1991

U.S. DEPARTMENT OF THE INTERIOR

MANUEL LUJAN, JR., *Secretary*

U.S. GEOLOGICAL SURVEY

Dallas L. Peck, *Director*

For additional information
write to:

District Chief
U.S. Geological Survey
375 South Euclid Avenue
Tucson, Arizona 85719

Copies of this report can be
purchased from:

U.S. Geological Survey
Books and Open-File Reports Section
Federal Center, Box 25425
Denver, Colorado 80225

Table 7.--Monthly average, minimum, and maximum values for treated mine discharge, Kerr-McGee Church Rock I Mine, 1980-84

[Values are in the following units: °F, degrees Fahrenheit; MGD, million gallons per day; mg/L, milligrams per liter; µg/L, micrograms per liter; pCi/L, picocuries per liter; dashes indicate no data]

Month		Temperature (°F)	Discharge (MGD)	pH (Standard units)	Total suspended sediment, (mg/L)	Molybdenum, total (µg/L as Mo)	Selenium, total (µg/L as Se)	Uranium, total (µg/L as U)	Vanadium, total (µg/L as V)	Radium-226, dissolved (pCi/L as Ra-226)
					1980					
January	Average	------	-----	-----	-----	-----	----	-----	---	-----
	Minimum	------	-----	-----	-----	-----	----	-----	---	-----
	Maximum	------	-----	-----	-----	-----	----	-----	---	-----
February	Average	------	-----	-----	-----	-----	----	-----	---	-----
	Minimum	------	-----	-----	-----	-----	----	-----	---	-----
	Maximum	------	-----	-----	-----	-----	----	-----	---	-----
March	Average	------	-----	-----	-----	-----	----	-----	---	-----
	Minimum	------	-----	-----	-----	-----	----	-----	---	-----
	Maximum	------	-----	-----	-----	-----	----	-----	---	-----
April	Average	------	-----	-----	-----	-----	----	-----	---	-----
	Minimum	------	-----	-----	-----	-----	----	-----	---	-----
	Maximum	------	-----	-----	-----	-----	----	-----	---	-----
May	Average	------	5.5	-----	<2	-----	----	-----	---	-----
	Minimum	------	-----	8.5	-----	-----	----	-----	---	-----
	Maximum	------	5.5	8.8	<2	-----	----	1,400	---	1.5
June	Average	------	5.5	-----	<2	-----	----	-----	---	-----
	Minimum	------	-----	8.7	-----	-----	----	-----	---	-----
	Maximum	------	5.5	8.8	<2	-----	----	1,300	---	1.2
July	Average	------	5.5	-----	<2	-----	----	-----	---	-----
	Minimum	------	-----	8.6	-----	-----	----	-----	---	-----
	Maximum	------	5.5	9.0	<2	460	38	1,300	12	2.4
August	Average	------	5.5	-----	<2	-----	----	-----	---	-----
	Minimum	------	-----	8.5	-----	-----	----	-----	---	-----
	Maximum	------	5.5	8.7	<2	420	38	1,200	17	1.4
September	Average	------	5.5	-----	<2	-----	----	-----	---	-----
	Minimum	------	-----	8.5	-----	-----	----	-----	---	-----
	Maximum	------	5.5	8.7	<2	450	25	1,200	13	1.8
October	Average	------	5.5	-----	<2	-----	----	-----	---	-----
	Minimum	------	-----	8.6	-----	-----	----	-----	---	-----
	Maximum	------	5.5	8.8	<2	440	25	1,000	20	1.7
November	Average	60	5.5	-----	<2	-----	----	-----	---	-----
	Minimum	------	-----	8.6	-----	-----	----	-----	---	-----
	Maximum	62	5.5	8.7	<2	430	35	1,600	31	1.6
December	Average	58.9	5.5	-----	<2	-----	----	-----	---	-----
	Minimum	------	-----	8.6	-----	-----	----	-----	---	-----
	Maximum	61	5.5	8.7	<2	440	34	1,100	28	1.3
Standard deviation (σ)	Average	.778	0	-----	0	-----	----	-----	---	-----
	Minimum	------	-----	.071	-----	-----	----	-----	---	-----
	Maximum	.707	0	.104	0	14	6	185	8	.376
Mean	Average	59.5	5.5	-----	<2	-----	----	-----	---	-----
	Minimum	------	-----	8.58	-----	-----	----	-----	---	-----
	Maximum	61.5	5.5	8.78	<2	440	33	1,260	20	1.61

Table 7.--Monthly average, minimum, and maximum values for treated mine discharge, Kerr-McGee Church Rock I Mine, 1980-84--Continued

Month		Temperature (°F)	Discharge (MGD)	pH (Standard units)	Total suspended sediment, (mg/L)	Molybdenum, total (µg/L as Mo)	Selenium, total (µg/L as Se)	Uranium, total (µg/L as U)	Vanadium, total (µg/L as V)	Radium-226, dissolved (pCi/L as Ra-226)
					1981					
January	Average	36.0	5.5	-----	<2.0	-----	----	-----	---	-----
	Minimum	------	-----	8.5	-----	-----	----	-----	---	-----
	Maximum	59.0	5.5	8.7	<2.0	450	38	1,300	26	0.94
February	Average	56.0	5.5	-----	<2.0	-----	----	-----	---	-----
	Minimum	------	-----	8.6	-----	-----	----	-----	---	-----
	Maximum	60.0	5.5	8.8	<2.0	460	56	1,350	16	3.2
March	Average	57.6	5.5	-----	<2.0	-----	----	-----	---	-----
	Minimum	------	-----	8.6	-----	-----	----	-----	---	-----
	Maximum	60.0	5.5	8.8	<2.0	440	33	1,600	9	.6
April	Average	61.0	3.5	-----	<2.0	-----	----	-----	---	-----
	Minimum	------	-----	8.5	-----	-----	----	-----	---	-----
	Maximum	68.0	3.5	8.8	<2.0	480	49	1,400	6	1.0
May	Average	63.25	3.5	-----	<2.0	-----	----	-----	---	-----
	Minimum	------	-----	8.6	-----	-----	----	-----	---	-----
	Maximum	66.0	3.5	8.9	3.1	490	61	1,400	12	2.85
June	Average	61.25	3.4	-----	<2.0	-----	----	-----	---	-----
	Minimum	------	-----	8.5	-----	-----	----	-----	---	-----
	Maximum	68.0	3.4	8.9	3.1	490	61	1,300	9	.93
July	Average	74.0	3.72	-----	<2.0	450	40	-----	8	-----
	Minimum	------	-----	8.7	-----	-----	----	-----	---	-----
	Maximum	78.0	3.95	8.8	<2.0	470	48	1,400	9	1.48
August	Average	72.0	3.78	-----	<2.0	560	47	-----	9	.44
	Minimum	------	-----	8.4	-----	-----	----	-----	---	-----
	Maximum	75.0	4.54	8.8	<2.0	850	54	1,400	19	.86
September	Average	69.0	3.67	-----	<2.0	910	25	-----	16	-----
	Minimum	------	-----	8.7	-----	-----	----	-----	---	-----
	Maximum	72.0	4.42	8.9	<2.0	1,000	28	1,200	20	.51
October	Average	63.0	3.20	-----	<2.0	480	68	1,180	50	1.04
	Minimum	58.0	-----	8.25	-----	-----	----	-----	---	-----
	Maximum	67.0	3.56	8.82	<2.0	480	91	1,300	55	2.2
November	Average	57.9	3.48	-----	2.2	480	52	1,100	15	.42
	Minimum	52.0	-----	8.7	-----	-----	----	-----	---	-----
	Maximum	62.0	3.77	8.8	3.0	490	91	1,300	50	.51
December	Average	54.0	3.38	-----	<2.0	450	48	1,100	6	.62
	Minimum	49.0	-----	8.6	-----	-----	----	-----	---	-----
	Maximum	59.0	3.90	8.8	<2.0	480	59	1,300	12	1.08
Standard deviation (σ)	Average	------	0.911	-----	0.058	179	14	46	16	0.288
	Minimum	------	-----	0.134	-----	-----	----	-----	---	-----
	Maximum	------	.829	.052	0.410	180	20	99	16	.913
Mean	Average	------	4.01	-----	2.02	560	47	1,130	17	.63
	Minimum	------	-----	8.55	-----	-----	----	-----	---	-----
	Maximum	------	4.25	8.81	2.18	550	56	1,350	20	1.35

Table 7.--Monthly average, minimum, and maximum values for treated mine discharge, Kerr-McGee Church Rock 1 Mine, 1980-84--Continued

Month		Temperature (°F)	Discharge (MGD)	pH (Standard units)	Total suspended sediment, (mg/L)	Molybdenum, total (µg/L as Mo)	Selenium, total (µg/L as Se)	Uranium, total (µg/L as U)	Vanadium, total (µg/L as V)	Radium-226, dissolved (pCi/L as Ra-226)
					1982					
January	Average	50.9	3.46	-----	<2.0	460	45	1,500	17	0.39
	Minimum	46.0	-----	8.3	-----	-----	----	-----	---	-----
	Maximum	54.0	3.81	8.6	<2.0	480	51	1,700	41	.64
February	Average	54.8	3.56	-----	<2.0	470	46	1,400	12	.24
	Minimum	50.0	-----	8.6	-----	-----	----	-----	---	-----
	Maximum	60.0	3.85	8.8	<2.0	480	53	1,600	23	.35
March	Average	56.1	3.59	-----	<2.0	460	42	1,400	14	.29
	Minimum	51.0	-----	8.6	-----	-----	----	-----	---	-----
	Maximum	62.0	3.86	8.9	<2.0	480	51	1,500	46	.32
April	Average	59.3	3.71	-----	<2.0	440	29	1,400	30	.30
	Minimum	54.0	-----	8.8	-----	-----	----	-----	---	-----
	Maximum	66.0	4.06	9.03	<2.0	450	39	1,500	33	.51
May	Average	63.8	3.71	-----	<2.0	470	61	1,400	48	.52
	Minimum	59.0	-----	8.7	-----	-----	----	-----	---	-----
	Maximum	68.0	3.96	8.9	<2.0	470	65	1,500	94	.77
June	Average	67.8	3.59	-----	<2.0	450	37	1,500	27	2.25
	Minimum	64.0	-----	8.7	-----	-----	----	-----	---	-----
	Maximum	72.0	3.82	8.9	<2.0	460	38	2,000	28	8.0
July	Average	72.3	3.45	-----	<2.0	500	40	2,000	30	.69
	Minimum	67.0	-----	8.5	-----	-----	----	-----	---	-----
	Maximum	75.0	3.69	8.9	<2.0	510	48	2,700	80	.90
August	Average	74.0	3.43	-----	<2.0	440	30	1,750	20	1.23
	Minimum	72.0	-----	8.3	-----	-----	----	-----	---	-----
	Maximum	76.0	3.80	8.8	<2.0	500	37	2,100	45	1.89
September	Average	68.0	3.46	-----	<2.0	400	26	1,980	9	.46
	Minimum	61.0	-----	8.1	-----	-----	----	-----	---	-----
	Maximum	73.0	3.72	8.9	<2.0	560	33	2,100	17	.57
October	Average	62.0	3.36	-----	<2.0	-----	----	-----	---	.00
	Minimum	59.0	-----	8.2	-----	-----	----	-----	---	-----
	Maximum	64.0	3.80	8.9	<2.0	600	42	2,600	29	.45
November	Average	58.0	3.42	-----	<2.0	-----	----	-----	---	.00
	Minimum	55.0	-----	8.5	-----	-----	----	-----	---	-----
	Maximum	59.0	3.79	8.8	<2.0	470	68	2,100	17	.59
December	Average	57.0	3.27	-----	<2.0	490	----	-----	---	.00
	Minimum	50.0	-----	8.6	-----	-----	----	-----	---	-----
	Maximum	59.0	3.50	9.0	<2.0	510	70	1,500	29	.40
Standard deviation (σ)	Average	7.27	0.134	-----	0	28	11	250	12	.66
	Minimum	7.77	-----	0.219	-----	-----	----	-----	---	-----
	Maximum	17.37	0.138	.111	0	44	18	430	24	2.16
Mean	Average	62.0	3.50	-----	<2.0	460	40	1,590	23	.70
	Minimum	57.3	-----	8.5	-----	-----	----	-----	---	-----
	Maximum	61.67	3.81	8.9	<2.0	500	46	1,910	40	1.28

Table 7.--Monthly average, minimum, and maximum values for treated mine discharge, Kerr-McGee Church Rock I Mine, 1980-84--Continued

Month		Temperature (°F)	Discharge (MGD)	pH (Standard units)	Total suspended sediment, (mg/L)	Molybdenum, total (µg/L as Mo)	Selenium, total (µg/L as Se)	Uranium, total (µg/L as U)	Vanadium, total (µg/L as V)	Radium-226, dissolved (pCi/L as Ra-226)
					1983					
January	Average	58.0	3.33	-----	<2.0	-----	----	-----	---	-----
	Minimum	55.0	-----	8.5	-----	-----	----	-----	---	-----
	Maximum	60.0	3.69	8.9	<2.0	510	82	1,600	<4	.05
February	Average	59.0	3.45	-----	<1.0	-----	----	-----	---	-----
	Minimum	57.0	-----	8.5	-----	-----	----	-----	---	-----
	Maximum	63.0	3.70	8.9	<1.0	510	27	1,300	14	.00
March	Average	60.0	3.40	-----	<1.0	-----	----	-----	---	-----
	Minimum	56.0	-----	8.6	-----	-----	----	-----	---	-----
	Maximum	64.0	3.60	8.8	<1.0	480	29	1,100	14	.03
April	Average	61.0	3.42	-----	<2.0	-----	----	-----	---	-----
	Minimum	55.0	-----	8.7	-----	-----	----	-----	---	-----
	Maximum	66.0	4.97	8.8	<2.0	460	28	1,000	<40	.08
May	Average	66.0	3.34	-----	<2.0	-----	----	-----	---	-----
	Minimum	60.0	-----	8.7	-----	-----	----	-----	---	-----
	Maximum	72.0	3.52	8.8	<2.0	550	32	1,200	<40	.06
June	Average	71.0	3.23	-----	<2.0	-----	----	-----	---	-----
	Minimum	66.0	-----	8.6	-----	-----	----	-----	---	-----
	Maximum	74.0	3.45	8.8	<2.0	560	43	1,500	<40	.22
July	Average	76.0	3.35	-----	<2.0	-----	----	-----	---	-----
	Minimum	75.0	-----	8.5	-----	-----	----	-----	---	-----
	Maximum	77.0	3.80	8.8	<2.0	650	97	1,200	40	.35
August	Average	77.0	3.44	-----	<2.0	-----	----	-----	---	-----
	Minimum	75.0	-----	8.5	-----	-----	----	-----	---	-----
	Maximum	78.0	3.67	8.8	<2.0	560	12	1,300	22	.80
September	Average	73.0	3.80	-----	<2.0	-----	----	-----	---	-----
	Minimum	65.0	-----	8.3	-----	-----	----	-----	---	-----
	Maximum	76.0	4.00	8.7	<2.0	510	10	1,400	5	.53
October	Average	67.0	3.51	-----	<2.0	-----	----	-----	---	-----
	Minimum	66.0	-----	8.4	-----	-----	----	-----	---	-----
	Maximum	70.0	3.74	8.8	<2.0	540	75	1,500	8	.035
November	Average	61.0	3.52	-----	<2.0	-----	----	1,450	---	.132
	Minimum	52.0	-----	8.4	-----	-----	----	-----	---	-----
	Maximum	68.0	3.88	8.7	<2.0	580	63	1,600	30	.27
December	Average	57.0	3.46	-----	<2.0	-----	----	1,670	---	.08
	Minimum	52.0	-----	8.4	-----	-----	----	-----	---	-----
	Maximum	60.0	3.62	8.7	<2.0	600	76	1,820	36	.11
Standard deviation (σ)	Average	7.217	0.141	-----	-----	-----	----	156	---	0.037
	Minimum	8.167	-----	0.124	-----	-----	----	-----	---	-----
	Maximum	6.481	0.397	0.067	-----	55	32	237	15	.410
Mean	Average	65.5	3.44	-----	<2.0	-----	----	1,560	---	0.106
	Minimum	61.2	-----	8.5	-----	-----	----	-----	---	-----
	Maximum	69.0	3.80	8.8	<2.0	540	64	1,380	24	.295

Table 7.--Monthly average, minimum, and maximum values for treated mine discharge, Kerr-McGee Church Rock I Mine, 1980-84--Continued

Month		Temperature (°F)	Discharge (MGD)	pH (Standard units)	Total suspended sediment, (mg/L)	Molybdenum, total (µg/L as Mo)	Selenium, total (µg/L as Se)	Uranium, total (µg/L as U)	Vanadium, total (µg/L as V)	Radium-226, dissolved (pCi/L as Ra-226)
					1984					
January	Average	59.0	3.44	-----	-----	-----	----	1,030	---	0.12
	Minimum	56.0	-----	8.4	-----	-----	----	-----	---	-----
	Maximum	62.0	3.73	8.6	-----	570	73	1,320	320	.14
February	Average	60.0	3.34	-----	-----	-----	----	1,690	---	.13
	Minimum	56.0	-----	8.4	-----	-----	----	-----	---	-----
	Maximum	63.0	3.67	8.7	-----	480	74	1,940	410	.18
March	Average	62.0	3.49	-----	-----	-----	----	1,770	---	.17
	Minimum	59.0	-----	8.3	-----	-----	----	-----	---	-----
	Maximum	64.0	3.91	8.6	-----	<587	<101	1,930	<27	.28
April	Average	------	-----	-----	-----	-----	----	-----	---	-----
	Minimum	------	-----	-----	-----	-----	----	-----	---	-----
	Maximum	------	-----	-----	-----	-----	----	-----	---	-----
May	Average	------	-----	-----	-----	-----	----	-----	---	-----
	Minimum	------	-----	-----	-----	-----	----	-----	---	-----
	Maximum	------	-----	-----	-----	-----	----	-----	---	-----
June	Average	------	-----	-----	-----	-----	----	-----	---	-----
	Minimum	------	-----	-----	-----	-----	----	-----	---	-----
	Maximum	------	-----	-----	-----	-----	----	-----	---	-----
July	Average	------	-----	-----	-----	-----	----	-----	---	-----
	Minimum	------	-----	-----	-----	-----	----	-----	---	-----
	Maximum	------	-----	-----	-----	-----	----	-----	---	-----
August	Average	------	-----	-----	-----	-----	----	-----	---	-----
	Minimum	------	-----	-----	-----	-----	----	-----	---	-----
	Maximum	------	-----	-----	-----	-----	----	-----	---	-----
September	Average	------	-----	-----	-----	-----	----	-----	---	-----
	Minimum	------	-----	-----	-----	-----	----	-----	---	-----
	Maximum	------	-----	-----	-----	-----	----	-----	---	-----
October	Average	------	-----	-----	-----	-----	----	-----	---	-----
	Minimum	------	-----	-----	-----	-----	----	-----	---	-----
	Maximum	------	-----	-----	-----	-----	----	-----	---	-----
November	Average	------	-----	-----	-----	-----	----	-----	---	-----
	Minimum	------	-----	-----	-----	-----	----	-----	---	-----
	Maximum	------	-----	-----	-----	-----	----	-----	---	-----
December	Average	------	-----	-----	-----	-----	----	-----	---	-----
	Minimum	------	-----	-----	-----	-----	----	-----	---	-----
	Maximum	------	-----	-----	-----	-----	----	-----	---	-----
Standard deviation (σ)	Average	1.528	0.076	-----	-----	-----	----	406	---	0.026
	Minimum	1.732	-----	.058	-----	-----	----	-----	---	-----
	Maximum	1.000	.125	.058	-----	58	16	355	200	.072
Mean	Average	60.0	3.42	-----	-----	-----	----	1,500	---	.14
	Minimum	57.0	-----	8.4	-----	-----	----	-----	---	-----
	Maximum	63.0	3.77	8.6	-----	550	83	1,730	252	.20

Table 8.--Water-quality data for mine discharges, United Nuclear Corporation Old Church Rock Mine, 1980-82

[Values are in the following units: μS/cm, microsiemens per centimeter at 25° Celsius; mg/L, milligrams per liter; μg/L, micrograms per liter; pCi/L, picocuries per liter; dashes indicate no data]

Date	pH (Standard units)	Molybdenum, total (μg/L as Mo)	Selenium, total (μg/L as Se)	Uranium, total (μg/L as U)	Vanadium, total (μg/L as V)
Untreated water					
11-17-80[1]	----	---	--	-----	--
11-02-82[1]	----	---	--	-----	--
Treated water					
11-17-80[1]	----	---	--	-----	--
07-20, 21-82[2] [3]	9.03	110	15	1,160	28
11-02-82[1]	----	---	--	-----	--

Date	Zinc, total (μg/L as Zn)	Gross beta, total (pCi/L)	Radium-226, dissolved (pCi/L as Ra-226)	Radium-226, total (pCi/L as Ra-226)	Total suspended sediment (mg/L)
Untreated water					
11-17-80	---	4,008±879	--------	--------	---
11-02-82	---	530±100	--------	--------	---
Treated water					
11-17-80	---	646±64	--------	--------	---
07-20, 21-82[2]	<50	------	5.37±.12	5.49±.11	4.8
11-02-82	---	322±30	--------	--------	---

[1]Data from United Nuclear Corporation

[2]24-hour composite sample.

[3]Data from U.S. Environmental Protection Agency.

Table 9.--Water-quality data for mine discharges, United Nuclear Corporation Northeast Church Rock Mine, 1975-82

[Values are in the following units: µS/cm, microsiemens per centimeter at 25° Celsius; mg/L, milligrams per liter; µg/L, micrograms per liter; pCi/L, picocuries per liter; dashes indicate no data]

Date	Specific conductance (µS/cm)	pH (Standard units)	Calcium, total (mg/L as Ca)	Sodium, total (mg/L as Na)	Potassium, total (mg/L as K)	Sulfate, total (mg/L as SO_4)	Chloride, total (mg/L as Cl)	Bicarbonate, (mg/L as HCO_3)	Total solids dissolved (mg/L)
Untreated water									
11-13-80	---	----	----	-----	-----	-----	-----	-----	---
11-17-80[1]	---	----	----	-----	-----	-----	-----	-----	---
10-06-81[2]	---	----	----	-----	-----	-----	-----	-----	---
11-02-82[1]	---	----	----	-----	-----	-----	-----	-----	---
Treated water									
03-04-75[1 3]	---	----	----	-----	-----	-----	-----	-----	---
03-05-75[1 3]	---	----	----	-----	-----	-----	-----	-----	---
03-06-75[1 3]	---	----	----	-----	-----	-----	-----	-----	---
10-24-77[4]	681	8.82	----	144.9	-----	67.2	24.2	-----	383
11-13-78[4]	623	----	8.0	149.5	1.56	107.6	25.4	229.6	419
08-29-79[1]	---	----	----	-----	-----	-----	-----	-----	---
11-01-79[4]	923	7.66	27.6	144.9	1.56	361.5	20.4	32.6	587
03-05-80[4]	725	----	13.4	147.2	1.56	126.1	26.2	256	453
11-17-80[1]	---	----	----	-----	-----	-----	-----	-----	---
10-06-81[3]	---	----	----	-----	-----	-----	-----	-----	---
11-02-82[1]	---	----	----	-----	-----	-----	-----	-----	---
07-20,21-82[3 5]	---	8.16	----	-----	-----	-----	-----	-----	---

Date	Nitrate+nitrite, total (mg/L as NO_2+NO_3)	Ammonia, total (mg/L as NH_3)	Aluminum, total (µg/L as AL)	Antimony, total (µg/L as Sb)	Arsenic, total (µg/L as As)	Barium, total (µg/L as Ba)	Beryllium, total (µg/L as Be)	Cadmium, total (µg/L as Cd)	Chromium, total (µg/L as Cr)	Copper, total (µ/L as Cu)
Untreated water										
11-13-80	----	-----	----	---	---	-----	---	---	---	---
11-17-80	----	-----	----	---	---	-----	---	---	---	---
10-06-81	----	-----	----	---	---	-----	---	---	---	---
11-02-82	----	-----	----	---	---	-----	---	---	---	---
Treated water										
03-04-75[3]	----	-----	----	---	---	-----	---	---	---	---
03-05-75[3]	----	-----	----	---	---	-----	---	---	---	---
03-06-75[3]	----	-----	----	---	---	-----	---	---	---	---
10-24-77	----	0.036	----	---	<5	880	---	---	---	---
11-13-78	0.46	.19	----	---	<5	381	---	<1	---	---
08-29-79	----	-----	----	<20	<20	-----	<20	<20	<20	<20
11-01-79	0.34	1.25	<250	---	<5	707	---	<1	---	---
03-05-80	----	-----	----	---	<5	311	---	<1	---	---
11-17-80	----	-----	----	---	---	-----	---	---	---	---
10-06-81	----	-----	----	---	---	-----	---	---	---	---
11-02-82	----	-----	----	---	---	-----	---	---	---	---
07-20,21-82[3]	----	-----	----	---	---	-----	---	---	---	---

See footnotes at end of table.

Table 9.--Water-quality data for mine discharges, United Nuclear Corporation Northeast Church Rock Mine, 1975-82--Continued

Date	Lead, total (µg/L as Pb)	Mercury, total (µg/L as Hg)	Molybdenum, total (µg/L as Mo)	Nickel, total (µg/L as Ni)	Selenium, total (µg/L as Se)	Silver, total (µg/L as Ag)	Uranium, total (µg/L as U)	Vanadium, total (µg/L as V)	Zinc, total (µg/L as Zn)
Untreated water									
11-13-80	---	-----	----	----	--	-----	-----	-----	-----
11-17-80	---	-----	----	----	--	-----	-----	-----	-----
10-06-81	---	-----	----	----	--	-----	-----	-----	-----
11-02-82	---	-----	----	----	--	-----	-----	-----	-----
Treated water									
03-04-75[3]	---	-----	200	----	60	-----	7,600	500	-----
03-05-75[3]	---	-----	200	----	60	-----	6,500	400	-----
03-06-75[3]	---	-----	100	----	10	-----	7,600	400	-----
10-24-77	---	-----	<10	----	94	-----	1,200	-----	-----
11-13-78	<5	-----	65	----	74	-----	1,320	30	<1
08-29-79	<20	<0.20	<20	<20	22	<20	-----	50	<20
11-01-79	<5	-----	<10	----	53	-----	1,260	<10	<250
03-05-80	<5	-----	10	----	82	-----	516	24	<250
11-17-80	---	-----	----	----	--	-----	-----	-----	-----
10-06-81	---	-----	----	----	--	-----	-----	-----	-----
11-02-82	---	-----	----	----	--	-----	-----	-----	-----
07-20,21-82[3]	---	-----	14	----	43	-----	870	10	<50

Date	Gross alpha, total (pCi/L)	Gross beta, total (pCi/L)	Lead-210, total (pCi/L as Pb-210)	Polonium-210, total (pCi/L as Po-210)	Radium-226, dissolved (pCi/L as Ra-226)	Radium-226, total (pCi/L as Ra-226)
Untreated water						
11-13-80	---------	----------	---------	---------	---------	24.1±0.8
11-17-80	---------	6,442±551	---------	---------	---------	---------
10-06-81	3,100±100	----------	1,200±100	900±200	---------	550±170
11-02-82	---------	876±150	---------	---------	---------	---------
Treated water						
03-04-75[3]	---------	----------	---------	---------	19.8	---------
03-05-75[3]	---------	----------	---------	---------	22.9	---------
03-06-75[3]	---------	----------	---------	---------	27.3	---------
10-24-77	---------	----------	---------	9.7±5.6	---------	1.9±.8
11-13-78	900±60	----------	---------	---------	---------	2.0±.1
08-29-79	---------	----------	---------	---------	---------	---------
11-01-79	650±80	----------	---------	---------	---------	.81±.24
03-05-80	282±18	----------	---------	---------	---------	3.89±.15
11-17-80	---------	326±32	---------	---------	---------	---------
10-06-81	280±30	----------	10±2	10±1	---------	2.5±.8
11-02-82	---------	342±32	---------	---------	---------	---------
07-20,21-82[3]	---------	----------	---------	---------	1.35±.07	1.14±.10

See footnotes at end of table.

Table 9.--Water-quality data for mine discharges, United Nuclear Corporation Northeast Church Rock Mine, 1975-82--Continued

Date	Radium-228, total (pCi/L as Ra-228)	Thorium-228, total (pCi/L as Th-228)	Thorium-230, total (pCi/L as Th-230)	Thorium-232, total (pCi/L as Th-232)	Total suspended sediment, (mg/L)
Untreated water					
11-13-80	---	-------	-------	-------	----
11-17-80	---	-------	-------	-------	----
10-06-81	---	0.0±.1	210±10	0.1±0.1	----
11-02-82	---	-------	-------	-------	----
Treated water					
03-04-75[3]	---	-------	-------	-------	33
03-05-75[3]	---	-------	-------	-------	47
03-06-75[3]	---	-------	-------	-------	71
10-24-77	---	-------	-------	-------	----
11-13-78	0±2	-------	-------	-------	4.2
08-29-79	---	-------	-------	-------	----
11-01-79	---	-------	-------	-------	0
03-05-80	---	-------	-------	-------	4.5
11-17-80	---	-------	-------	-------	----
10-06-81	---	-0.2±.2	0.1±.1	0.0±.1	----
11-02-82	---	-------	-------	-------	----
07-20,21-82[3]	---	-------	-------	-------	2.6

[1]Data from United Nuclear Corporation

[2]Data from Bruce Gallaher (New Mexico Health and Engineering Department, written commun., 1982).

[3]24-hour composite sample.

[4]Data from New Mexico Health and Engineering Department, Environmental Improvement Division, Water Pollution Control Board.

[5]Data from U.S. Environmental Protection Agency.

Table 10.--Water-quality data for tailings-pond solution, 1979-80

[Values are in the following units: µS/cm, microsiemens per centimeter at 25° Celsius; mg/L, milligrams per liter; µg/L, micrograms per liter; pCi/L, picocuries per liter; dashes indicate no data]

Date	Specific conductance (µS/cm)	pH (Standard units)	Calcium, total (mg/L as Ca)	Magnesium, total (mg/L as Mg)	Sodium, total (mg/L as Na)	Potassium, total (mg/L as K)	Sulfate, total (mg/L as SO_4)	Chloride, total (mg/L as Cl)	Fluoride, total (mg/L as F)
02-05-79[1] [2]	-----	1.92	----	50.8	519	----	4,802	50.0	2.47
11-01-79[1] [2]	1,589	8.66	20.0	4.5	315.1	1.95	434.7	19.4	----
03-05-80[3] [4]	702	----	10.0	----	-----	1.56	108.6	12.2	----

Date	Bicarbonate, (mg/L as HCO_3)	Total solids dissolved (mg/L)	Nitrate+nitrite, total (mg/L as NO_2+NO_3)	Ammonia, total (mg/L as NH_3)	Aluminum, total (µg/L as AL)	Arsenic, total (µg/L as As)	Barium, total (µg/L as Ba)	Cadmium, total (µg/L as Cd)	Chromium, total (µg/L as Cr)
02-05-79[1]	-----	---	----	----	-----	70	<100	--	150
11-01-79[1]	372.1	899	0.02	0.07	5,170	<5	940	<1	---
03-05-80[3]	258.2	441	----	----	-----	<5	201	<1	---

Date	Cobalt, total (µg/L as Co)	Iron, total (µg/L as Fe)	Lead, total (µg/L as Pb)	Manganese, total (µg/L as Mn)	Molybdenum, total (µg/L as Mo)	Selenium, total (µg/L as Se)	Uranium, total (µg/L as U)	Vanadium, total (µg/L as V)	Zinc, total (µg/L as Zn)
02-05-79[1]	950	157,500	200	14,000	40	--	4,090	---	----
11-01-79[1]	----	-------	<5	------	<10	29	1,140	95	<250
03-05-80[3]	----	-------	<5	------	9	82	3,260	<10	<250

Date	Gross alpha, total (pCi/L)	Radium-226, total (pCi/L as Ra-226)	Thorium-230, total (pCi/L as Th-230)	Total suspended sediment, (mg/L)
02-05-79[1]	---------	209.5	10,225	-----
11-01-79[1]	5,300±300	4.2±1.3	------	175
03-05-80[3]	1,890±100	38.9±1.3	------	11.1

[1]Sample from United Nuclear Corporation Old Church Rock, last settling pond.

[2]Data from United Nuclear Corporation

[3]Sample from United Nuclear Corporation, Northeast Church Rock.

[4]Data from New Mexico Health and Engineering Department, Environmental Improvement Division, Water Pollution Control Board.

This document provides the United Nuclear Corporation (UNC) response to the U.S. Nuclear Regulatory Commission's (NRC's) June 4, 2013, Request for Additional Information (RAI) on the Report Entitled "Technical Analysis Report in Support of License Amendment Request for Revised Groundwater Protection Standards Based on Updated Background Concentrations, Source Materials License SUA-1475, Groundwater Corrective Action Program, United Nuclear Corporation Church Rock Mill and Tailings Site, New Mexico April 2012". NRC comments are shown in blue text and UNC responses are shown in black text.

1) Comment: In Section 2, Identification of Samples Representative of Background Water Quality, Page 2; the establishment of monitoring wells having samples representative of background water quality in the 2008 N.A. Water Systems report [Agencywide Document Access and Management System (ADAMs) Accession Number ML083530220] was not formally reviewed or approved by the U.S. Nuclear Regulatory Commission (NRC). The NRC staff believes that this section, as drafted, incorrectly implies that the 2008 N.A. Water Systems report was submitted and approved by the NRC staff.

Technical Basis: The current amendment request has chosen to utilize the same monitoring well network in the Southwest Alluvium and Zone 1 that was previously assessed during NRC review of Amendment No. 37 for the Technical Analysis Report revised in 2006 [ML006073004]. However, a key difference in the current submittal is that the time interval from the background wells includes two additional years of data than that was not previously assessed and includes data from Zone 3 background wells. Therefore, the monitoring wells associated with the current licensing request were reevaluated to determine if they are representative of background conditions for the newly proposed time interval.

Path Forward: United Nuclear Corporation (UNC) should revise this section to clearly state that the 2008 N.A. Water Systems report was reviewed and approved only by the U.S. Environmental Protection Agency (EPA). The NRC will be reviewing the selected background wells to ensure they are representative of background water quality.

UNC RESPONSE

UNC will make the requested modification to the text.

2) Comment: The Technical Analysis Report – April 2012 does not discuss the algorithmic method (if only dependent on higher order statistics and the value of k samples) used or the mathematical method used to determine the Upper Predictable Limit (UPL) 95 for the nonparametric background statistic.

Technical Basis: The report is deficient in documenting how the ProUCL software calculates the nonparametric UPL 95.

Path Forward: Provide a detailed explanation of how the nonparametric UPL 95 is determined.

UNC RESPONSE

Summary

Potential background threshold values (BTVs) were calculated for the License Amendment Request using the EPA's software package ProUCL (Singh et al., 2010). The statistic selected to estimate BTVs is the upper prediction limit at 95 percent confidence (UPL95) of an anticipated number of future samples. Most background constituent of concern (COC) sample sets are left-censored (i.e., contain non-detected results in the lower part of the analytical range) and do not follow frequency distributions (e.g., normal or log-normal) for which parametric estimation methods are applicable. Because it is difficult to reliably perform goodness-of-fit tests for data distributions on left-censored sample sets, the ProUCL software technical guidance (Singh et al., 2010) emphasizes the use of distribution-free non-parametric methods including the Kaplan-Meier Method (KM), and others, for the estimation of UPL95 statistics. Specification of the future number of samples is required for the calculation of UPL95 statistics. The appropriate number of future samples was based on the anticipated number of sampling locations in each hydrostratigraphic unit and anticipated future sampling frequencies and durations.

The Kaplan-Meier method is a non-parametric statistical method used to estimate the mean and standard deviation of populations with censored data; these estimates are then used by ProUCL in a parametric UPL95 calculation. The number of future samples (k) is used to adjust the exceedance probability (based upon the Bonferroni inequality) to select the appropriate critical value (i.e., t-statistic or z-statistic) for the UPL95 calculation. Detailed calculation methods and reference citations are provided in the following discussion.

Discussion

Kaplan-Meier Method

The Kaplan-Meier estimation method, also known as the product limit estimate (PLE), is a recommended statistical method to analyze environmental data containing non-detected values (Singh, 2011). According to EPA statistical guidance (Unified Guidance, EPA, 2009), the Kaplan-Meier estimator was originally devised to estimate survival probabilities for right-censored samples (Kaplan and Meier, 1958), such as in medical studies of cancer treatments. Because it is non-parametric, there is no requirement that the underlying population be normal or transformable to normality. EPA also incorporates the Kaplan-Meier procedure to calculate a UPL for left-censored data without a discernible distribution within its ProUCL software (Singh et al., 2010).

The Kaplan-Meier method is applied by ordering and assigning ranks to each of the detected values and accounting for non-detected values to create a cumulative distribution function (CDF). Starting at the largest detected value, the proportion of concentrations below each detected value (the estimator) is calculated. The estimator for left-censored data thus depends on a series of conditional probabilities, where the frequency of lower concentrations depends on how many larger concentrations have already been observed (EPA, 2009).

The equations used to calculate the Kaplan-Meier estimator in the EPA Unified Guidance (EPA, 2009) are excerpted below. Equations are also presented in Singh et al. (2010; see Section 4.6) and Singh (2011), using a slightly different notation.

In mathematical notation, suppose there are m distinct values in the sample (out of a total of n measurements), including distinct reporting limits. Order these values from least to greatest and denote them as $x_{(1)}$, $x_{(2)}$, ..., $x_{(m)}$. Let n_i for i = 1 to m denote the 'risk set' associated with value $x_{(i)}$. The risk set represents the total number of measurements — both detects and non-detects — no greater than $x_{(i)}$. Since a non-detect with a RL larger than $x_{(i)}$ is potentially (but not necessarily) larger than $x_{(i)}$, nondetects with RL > $x_{(i)}$ are not included in n_i. A further term di identifies the number of detected measurements exactly equal to $x_{(i)}$.

With these definitions in place and letting X denote a random variable concentration from the true underlying distribution, the Kaplan-Meier estimator is constructed from the pair of probabilities:

$$\Pr\left(X \le x_{(m)}\right) = 1 \qquad [15.1]$$

$$\Pr\left(X \le x_{(i)} \middle| X \le x_{(i+1)}\right) = 1 - \frac{d_{i+1}}{n_{i+1}} \quad \text{for } i = 1 \text{ to } m \qquad [15.2]$$

where $x_{(m+1)} = +\infty$, $d_{m+1} = 0$, and $n_{m+1} = n$ all by definition. Equation [15.2] represents the conditional probability that the concentration does not exceed $x_{(i)}$ given that it does not exceed $x_{(i+1)}$. The final Kaplan-Meier CDF estimate (F_{KM}) for each i = 1 to m–1 (each distinct detected value) is given by a product of these conditional probabilities and can be expressed as:

$$F_{KM}\left(x_{(i)}\right) = \Pr\left(X \le x_{(i)}\right) = \left(1 - \frac{d_{i+1}}{n_{i+1}}\right) \times \left(1 - \frac{d_{i+2}}{n_{i+2}}\right) \times \ldots \times \left(1 - \frac{d_m}{n_m}\right) = \prod_{k=i}^{m-1}\left(1 - \frac{d_{k+1}}{n_{k+1}}\right) \qquad [15.3]$$

The mean and standard deviation estimates are calculated using the following equations excerpted from the Unified Guidance (EPA, 2009).

$$\hat{\mu}_{KM} = \sum_{i=1}^{m} x_{(i)} \cdot \left[F_{KM}\left(x_{(i)}\right) - F_{KM}\left(x_{(i-1)}\right)\right] \quad [15.4]$$

$$\hat{\sigma}_{KM} = \sqrt{\sum_{i=1}^{m} \left(x_{(i)} - \hat{\mu}_{KM}\right)^2 \cdot \left[F_{KM}\left(x_{(i)}\right) - F_{KM}\left(x_{(i-1)}\right)\right]} \quad [15.5]$$

where $x_{(0)} = 0$, and $F_{KM}(x_{(0)}) = F_{KM}(0) = 0$ by definition.

Example spreadsheet calculations for the Kaplan-Meier CDF, mean, and standard deviation using the Church Rock Site Zone 3 background arsenic data are provided in Table 1. The resulting mean and standard deviation estimates are then used as the sample mean and standard deviation in parametric equations for the UPL, as demonstrated in the following section.

UPL95 and UPL$_k$95

UPLs are often used as background threshold values (BTVs) for point-by-point individual site observation comparisons. A UPL95 calculated for a background data population represents an upper limit for which a single independently obtained observation from that population will be below, or equal to, with a confidence level 95%. Accordingly, there is a 5% probability that a single sample drawn from the population would be above the UPL95.

ProUCL contains parametric and non-parametric methods to calculate UPLs and other BTVs. A parametric UPL that can be used to compare a single future sample comparison based on the Kaplan-Meier estimates of mean and population standard deviation can be calculated using following equation (excerpted from Singh, 2011):

> **Upper Prediction Limit (UPL):** For small samples (e.g., fewer than 30 samples), UPL can be computed using the critical value from the Student's t-distribution; and for large datasets, UPL can be computed using the critical values from normal distribution.
>
> $$UPL = \hat{\mu}_{KM} + t_{((1-\alpha),(n-1))} * \hat{\sigma}_{KM}\sqrt{1+\frac{1}{n}}$$
>
> $$UPL = \hat{\mu}_{KM} + z_{\alpha} * \hat{\sigma}_{KM}\sqrt{1+\frac{1}{n}}$$
>
> $\hat{\mu}_{KM}$ = Kaplan Meier estimate of mean based upon data x_i, $i = 1, 2, \ldots, n$;
>
> $\hat{\sigma}_{KM}$ = Kaplan Meier estimate of population standard deviation;
>
> $t_{((1-\alpha),(n-1))} = (1-\alpha)^{th}$ critical value from t-distribution with degrees of freedom of $(n-1)$;
>
> $z_{\alpha} = \alpha^{th}$ critical value from standard normal distribution

However, should k future observations be compared against a UPL designed for one future comparison, the overall probability of exceeding the UPL (i.e., the false positive rate) increases in accordance with the following equation (Singh, 2011):

$$\alpha_{actual} = 1-(1-\alpha)^k$$

Singh (2011) summarizes an adjustment that can be made to a UPL95 equation (based upon the Bonferroni inequality) to account for one or more future observations and uses the notation UPL_k95 to represent a 95% UPL for k (>=1) future observations. In the adjusted equation, the exceedance probability α is divided by the number of k future samples and used to generate the appropriate critical value (i.e., t-statistic or z-statistic) for the UPL95 calculation:

$$UPL_k95 = \left(\bar{x} + t_{((1-0.05/k),n-1)} s \sqrt{1+\frac{1}{n}} \right)$$

The preceding equation shows a normal-distribution based UPL95 calculation with the population mean and standard deviation, rather than Kaplan-Meier estimates of the population mean and standard deviation. The use of the analogous equation for the UPL_k95 based on the Kaplan-Meier estimates of the population mean and standard deviation is not explicitly described in the ProUCL technical guidance manual, but referred to in Section 5.4.1.1 (Singh et al., 2010). The calculation is made in ProUCL when performing non-parametric background statistics for censored datasets (i.e., with NDs) and more than one "different or future k values" has been entered as an option. The results of this analysis are identified in the ProUCL output (for a selected 95% confidence level) as the "95% KM UPL for Next k Observations".

It should also be noted that ProUCL does not appear to provide an option to use the z-statistic from the standard normal distribution (i.e., rather than the t-statistic from Student's t-test) to calculate the Kaplan-Meier UPL95 for multiple future k values from a large background dataset (i.e., greater than 30 samples). However, the use of the t-statistic is considered acceptable because the t-statistic approaches the z-statistic as the number of samples (i.e., degrees of freedom in the Student's t-test) increase, and the Church Rock site background datasets for the three hydrostratigraphic units are relatively large (i.e., a minimum of 185 to a maximum of 429 samples).

Example spreadsheet calculations for the Church Rock Zone 3 arsenic UPL95 for 216 future samples are provided in Table 2. The resulting UPL95 estimate (0.757 mg/l) is identical to that provided in Table 6 and Appendix C in the License Amendment request.

3) Comment: Remedial action of Zone 3 is reported in numerous documents to have begun in 1983 at the Northeast Pump-Back wells. However, a December 7, 1981, quarterly report [ADAMs No. ML101050277] from UNC to the New Mexico Natural Resources Department indicates that ten 400 series seepage extraction pumps in Section 36 and three 300 Series pumps around the tailings area were being utilized prior to 1981. While the document does not identify each of the 13 wells, early cross-sections and monitoring well maps indicate that many of the 400 and 300 series wells were screened within Zone 3.

Technical Basis: Information on seepage extraction prior to commencement of remedial action activities would provide accurate information necessary for the NRC staff to determine those influences that may have affected the transport of seepage from the tailings cells and burrow pits.

Path Forward: Provide further detailed information about the wells used for seepage extraction prior to commencement of remedial actions for each of the hydrostratigraphic units.

UNC RESPONSE

Summary

The referenced text from the December 7, 1981, quarterly report (UNC, 1981c) reads as follows:

> *The ten 400-Series seepage extraction pumps on Section 36 were turned off on September 14, 1981, and so were the three 300-Series pumps around the tailings area on November 30, 1981. Therefore, no seepage extraction water is being returned to the borrow pits now.*

The United States Nuclear Regulatory Commission (NRC) has suggested that the use of the terminology "seepage extraction pumps" in the referenced quarterly report implies that these wells were pumping what was previously determined to be seepage-impacted water from Zone 3. During the July 11, 2013, teleconference, NRC indicated the following additional concerns related to historical pumping of the 300- and 400-series wells: (1) due to the downgradient position of the 400-series wells, this pumping may have temporarily expanded the seepage-impacted area into background (i.e., non-impacted) areas; and (2) subsequent to the cessation of 400-series well pumping, background groundwater may have become re-established in the temporarily impacted areas, such that the evidence of impact was lessened and previously impacted monitoring wells might be included improperly in the statistical evaluations of background concentrations.

Our review of the available historical information indicates that three 300-series wells screened in multiple hydrostratigraphic units were pumped for approximately 11 months. Based on their proximity to the Central Tailings Cell, these wells likely extracted seepage-impacted water. The ten 400-series wells were pumped for approximately five months prior to September 1981 and it is unlikely that the 400-series wells were pumping seepage-impacted water during this period. Historical investigations were not able to clearly distinguish between seepage impacted and background waters in Zone 3; therefore, historical seepage-impact delineations are not as reliable as comparisons made via our current capabilities, which use the evolution of bicarbonate concentrations as the best geochemical indicator of differentiating seepage-impacted from other water types. Additionally, variations in

monitoring well construction may have affected the historical interpretations of seepage impact. We will address each of these topics below in support of a conclusion that the 1981 pumping of the 300- and 400-series wells was inconsequential with respect to the extent of seepage impacts.

Discussion

UNC has reviewed available historical documents related to pumping of the 300-series and 400-series wells conducted prior to the initiation of Zone 3 remedial action in 1983. A March 6, 1981, UNC letter report (UNC, 1981a) indicates that UNC operated the Central Cell seepage interception system, comprising four 300-series wells (340, 304, 323A, and 335) in early 1981 (see Figures 1 and 2). Three of these wells (340, 304, and 323A) appear to be the 300-series wells referenced in the December 1981 quarterly report (UNC, 1981c). The March 1981 letter report (UNC, 1981a) contains daily pumping records for these wells for February 1 through March 6, 1981, and indicates that 1,075,000 gallons were pumped during February 1981. The March 1981 letter report (UNC, 1981a) also provides pH and conductivity measurements collected from January 5 to March 6, 1981. These data suggest that well 340 replaced well 335 as a pumping well because pH and conductivity measurements ceased for well 335 in mid-January and are subsequently initiated for well 340.

Based on this information it appears that the three 300-series wells operated for approximately 11 months until they were shut down in November 1981. However, the location and construction of these wells indicate that the pumping would not have significantly affected the Zone 3 seepage-impact area. The well locations near the Central Cell (see Figures 1 and 2) are too distant from the Zone 3 downgradient background areas and well construction records indicate that these wells are open to multiple hydrostratigraphic units. The screened interval for each of the wells extends from the lower part of Zone 3, through Zones 2 and Zone 1 and into the top of Mancos Shale; the sandpack for each well extends from the bottom of the well to (or near) the ground surface.

It appears that the 400-series wells described in the December 1981 quarterly report (UNC, 1981c) were pumped for a period of approximately five to seven months, prior to being turned off in September 1981. According to the UNC database and master wells table, the 400-series wells were installed between February 1981 and April 1981. The March 1981 letter report (UNC, 1981a), which summarizes plans to install the 400-series wells between wells TWQ-115D and TWQ-148, further constrains the 400-series wells operating period. The report indicates that only three of the wells (401, 402, and 403, see Figures 1 and 3) had been installed at the time of the report and that pumping had been initiated at one well (402), at a rate of approximately 8 gpm, on February 27, 1981. Wells 401 and 403 were not being pumped because they were being redeveloped and redrilled, respectively.

UNC files contain a partial copy of a report related to the 400-series well installation and pumping (UNC, 1981b; titled Report 2, Northern Collection System; dated May 20, 1981; no author listed) which indicates that pumps were installed in ten 400-series wells (401, 402, 403A, 422, 424, 433, 435, 438, 444, and 446) in early 1981. This report summarizes the results of pumping tests conducted at wells 402 and 438 at rates of approximately 5 gpm prior to the initiation of "extractive pumpage" on April 29, 1981, from all extraction wells. Therefore, the combined pumping of the ten 400-series wells was limited to approximately five months ending September 14, 1981. The aggregate pumping rate for the ten well system is not documented.

There is additional information indicating that the ten 400-series wells were pumped together for only five months. Billings & Associates (1982) references a five-month operation period for the 400-series wells in a report providing recommendations for the future Zone 3 seepage control system. Water level hydrographs for wells 411 and 420 prepared by Billings & Associates (1984, attached) show a response to pumping corresponding to that described Northern Collection System report. The hydrographs also show that the wells recovered fully and that the Zone 3 water level continued to rise in response to the continuing mine dewatering discharge (i.e., background water). Billings & Associates (1984) also indicates that neither of these wells appeared to be contaminated when they were last sampled.

It is unlikely that the 400-series wells were pumping seepage-impacted water during this period. Billings & Associates (1982) notes that several feet of drawdown were documented in the Well 126/127 area (south of the 400-series wells) after five months of pumping and that water quality "worsened" in the eastern half of the 400 Series wells during the pumping, but there is no evidence presented that the 400-series wells were pumping seepage-impacted water. As was typical in the early part of the site investigation, Billings & Associates (1982) was not able to clearly distinguish geochemical differences between seepage-impacted and background waters and stated that "Without clear and undebatable background water quality data existing at the UNC site, the determination of the degree of contamination is based on professional judgment and opinion". Billings & Associates (1982) indicated that the general shape of the seepage-impacted water could be discerned using total dissolved solids (TDS) and sulfate concentrations, and suggested a TDS concentration of 4,000 mg/l as a general criterion for seepage impacts. These historical determinations were likely limited by inconsistent well construction. For example, the March 6, 1981, letter report (UNC, 1981a) provides well chemistry data for wells 402 and 401, which have quite different construction. Well 402 is screened across Zone 3 and the top of Zone 2 (although the sandpack extends into the Dilco Coal Member), while well 401 is screened across multiple hydrostratigraphic zones (i.e., Dilco, Zone 3, Zone 2, Zone 1, and the Mancos Shale). The May 20, 1981, Northern Collection System report (UNC, 1981b) suggests that wells completed in the Dilco or at the Dilco/Zone 3 interface have inferior water quality to those completed only in Zone 3 or Zone 1 of the Upper Gallup sandstone. It is further suggested that elevated concentrations of TDS, sulfate, manganese, molybdenum, and uranium may be correlatable to localized carbonaceous deposits in the Dilco shale and sandy shale.

The 400-series well area was not seepage-impacted in the mid- to late 1980s. Canonie (1987) used pH as the primary indicator of seepage impact and stated that all other indicators, such as TDS, thorium-230, heavy metals, and ammonia follow the trend set by pH. This seepage impact delineation shows that the 400-series well area was not seepage-impacted as of May 1986. EPA subsequently utilized TDS as the primary indicator in the Remedial Investigation (EPA, 1988), which also showed that the 400-series well area was not seepage-impacted.

The current seepage-impact delineation methodology has been used to track the seepage-impact progression for approximately ten years and is more reliable than previous single parameter delineations because the current method more fully considers the geochemical response to the acid seepage front by considering the following (N.A. Water Systems, 2008a):

- The key indicators of seepage impact are pH and bicarbonate; the analysis considers empirically derived concentration ranges and time-series of these two indicator parameters.
- Time trends in the concentration of major ions; in particular, decreasing ratios of Ca:Mg are associated with degrading groundwater quality.
- Time trends in the concentrations of many metals and radionuclides will usually increase as the buffering capacity degrades in Zone 3.

UNC considers the five-month pumping of the 400-series wells to be volumetrically minor in comparison to the combination of the remediation pumping initiated at the northeast corner of the impoundment in October 1983 and the subsequent Zone 3 pumping, initiated in 1989 and 2005. Assuming a pumping rate of 5 gpm per well (i.e., equal to pumping rates used for pumping tests of wells 402 and 438) during the five month period, the 400-series would have pumped approximately 11,000,000 gallons. In comparison, Earth Tech (2002) shows that the total volume pumped from the Zone 3 wells from 1989 to 2000 was approximately 160,000,000 gallons. Additionally, approximately 14,100,000 gallons were extracted from the current Zone 3 pumping system pumping from January 2005 to June 2012 (Chester Engineers, 2013). Any slight, short-term shifts in the distribution of background and seepage-impacted waters that might have occurred due to the 400-series pumping in 1981 would likely have been substantially reversed due to the continued mine dewatering discharge and recharge into Zone 3 over the several intervening years. UNC concludes that the small proportion of water removed in the early 1980s was volumetrically insignificant and of too short duration to adversely influence the current methodology used to discriminate between background and seepage-impacted groundwater. Finally, we should point out that the underlying premise of this comment as expressed during the July 11, 2013, teleconference is perhaps misplaced. The procedure to discriminate background from seepage-impacted is via a statistical analysis of chemical attributes and is not influenced or confounded by pumping history which only influences the location and timing of seepage-impacts. UNC has in fact solved the background determination problem that was previously inhibitive – rather than using a well's location or sampling time to establish background, the water chemistry is the only variable that should be considered.

4) Comment: Molybdenum concentrations have been observed in far downgradient Zone 3 wells at concentrations greater than expected for being impacted by mining alone. The origin of the high molybdenum concentrations is unclear due to the lack of groundwater data available prior to 1989.

Technical Basis: It would be unlikely that the concentrations were a result of mining effluents discharged to the Southwest Alluvium or seepage from the drying pads at the Quivira facilities which contained a minimum amount of water. The Upper Gallup Sandstone is known to be fractured in the vicinity of the site. The NRC staff is concerned that fracture controlled flow could account for the unusually high concentrations observed at distant downgradient wells including the tendency of the plume to migrate toward the north-northeast instead of in the down dip direction to the northwest. Molybdenum concentrations obtained from a limited number of sampling events for the North Pond and Burrow Pits 1 and 2 ranged from 0.001 mg/l to 18.7 mg/l.

Path Forward: Provide further explanation of the high concentrations of molybdenum found downgradient in Zone 3 and historic sampling results from the tailings ponds and burrow pits during operations.

UNC RESPONSE

Summary

Elevated molybdenum concentrations observed in samples from Zone 3 wells outside the tailings seepage plume have historically been considered to be representative of background conditions. The United States Nuclear Regulatory Commission (NRC) comment contemplates instead that molybdenum is an indicator of seepage impacts and could be preferentially transported from the tailings ponds via fracture-controlled flow pathways to locations beyond the geochemically-established extent of seepage impacts. This alternative interpretation of the historical data is considered to be implausible for the following reasons:

1. The geochemical interaction of tailings seepage with aquifer materials is well known and the distribution of tailings seepage-impacted waters is reliably indicated by key parameters pH and bicarbonate (HCO_3^-). Elevated molybdenum concentrations were present at background locations in the absence of known indicators of tailings seepage.

2. It is highly implausible that molybdenum would migrate completely independently of all other well-known seepage-impact parameters. Even if there were fracture zones with enhanced permeability extending from the tailings cells to the northern part of Section 36 and molybdenum was more highly concentrated in seepage-impacted water, then the comment purports that the fractures transmit molybdenum preferentially more than any other dissolved constituent. We can identify no possible physical or chemical mechanism that would bring this about.

3. The observed distribution of molybdenum concentrations in the three site hydrostratigraphic units demonstrates that molybdenum is not a suitable indicator of tailings seepage at the Church Rock site. Molybdenum has a high natural variance in both seepage-impacted and

background water in Zone 3, and as a consequence the water types are not amenable to differentiation on the basis of molybdenum data.

More plausible explanations for the observed site molybdenum concentration distributions are related to its complex environmental geochemistry and the presence of potential natural geologic sources of molybdenum such as coal beds and carbonaceous shales in the Zone 3 and Zone 2 bedrock and the overlying Dilco Member of the Crevasse Canyon Formation. Molybdenum concentrations in water are also complicated by inconsistent well construction in Zone 3; certain wells have screened or sandpacked intervals that coincide with, or adjoin, the Zone 2 coal, while other wells have screened or sandpacked intervals that extend from the Dilco or Zone 3 to the Mancos Shale underlying Zone 1. Additional details regarding these issues are provided in the following section.

Discussion

Historical molybdenum concentrations detected in samples from several Zone 3 wells near the northern Section 36 boundary (e.g., wells EPA-1, EPA-11, and 0504 B) frequently exceeded 5 mg/l and have a maximum of 75 mg/l. Many of these detected concentrations are among the highest measured at any location on the site (including samples collected directly from the tailings ponds and borrow pits) and, in previous analyses, have been considered representative of background conditions prior to impact by tailings seepage.

A portion of the dewatering fluids discharged from the Northeast Church Rock (NECR) Mine and Kerr-McGee Church Rock I Mine into Pipeline Arroyo infiltrated the previously unsaturated alluvium and bedrock to form the current background groundwater at the Church Rock Mill Site. This mine dewatering discharge was a source of some molybdenum to the Zone 3 background groundwater; however, historical discharge monitoring data indicate that molybdenum concentrations in these mine-related waters were typically lower than those reported in Zone 3 background groundwater. NPDES monitoring data show that the treated NECR Mine discharge had molybdenum concentrations were in the range of <0.010 to 0.2 mg/l (1975-1982) and the Kerr-McGee Church Rock I Mine discharge (1980-1984) had a mean concentration of approximately 0.5 mg/l (Wirt et al., 1991). Blickwedel (2006) shows that a NECR mine vent shaft sample and several Pipeline Arroyo surface water samples had molybdenum concentrations similar to the NECR mine discharge results. These analyses do not encompass the entire operating period of the mines and therefore may not account for all of the variability in concentrations discharged to the Arroyo.

Zone 3 is fractured sandstone in which groundwater flows both through the pores in the rock (i.e., primary porosity) and through a network of interconnected fractures (i.e., secondary porosity). The geochemical interaction of acidic tailings seepage with aquifer materials is well known and the distribution of tailings seepage-impacted waters is reliably indicated by the key parameters pH and bicarbonate (HCO_3^-). The aquifer materials neutralize the acidic seepage, causing a relatively gradual increase of the bicarbonate concentration indicative of carbonate mineral dissolution, followed by a rapid decrease in bicarbonate and pH as the buffering capacity of the formation is exhausted (BBL, 2006). Historical Zone 3 groundwater quality data (see Chester Engineers, 2013, Appendix B) from fully seepage-impacted wells indicate that it takes from one to three years, from the onset of geochemical changes associated with the arrival of seepage-impacted groundwater, for full seepage impact to

develop (unless the constituent transport is affected by pumping). Once the buffering capacity of the formation is exhausted, acidic conditions will remain indefinitely. The use of pH and bicarbonate as plume indicators, and to distinguish background from seepage-impacted water quality, is well documented (N. A. Water Systems, 2008a and 2008b) and has been accepted for various uses (including an NRC License Amendment, the site Human Health Risk Assessment, and the site Five Year Review) by NRC, the United States Environmental Protection Agency (EPA), and New Mexico Environment Department (NMED).

NRC has expressed concern that the source of elevated molybdenum concentrations observed in the northern Zone 3 wells is tailings seepage that migrated through hypothetical fracture zones (i.e., enhanced permeability zones or conduits) from the tailings disposal cells to the well locations. Similarly EPA, in the Remedial Investigation Report (1988), speculates (without supporting evidence) that higher downgradient molybdenum concentrations could result from a single discrete introduction of contamination into the groundwater system. However, historical data show that elevated molybdenum concentrations were present at background locations in the absence of other known indicators of tailings seepage. It is implausible that the chemical signature of acidic seepage-impacted water traveling in an enhanced fracture system would be limited to elevated molybdenum concentrations, independent of the other more typical seepage indicator parameters (i.e., low pH and bicarbonate concentrations). There are no identified physical or geochemical mechanisms under which these conditions would occur and no means for elevated concentrations to be sustained over time such as in samples from well EPA-1 or exhibit variability over time such as in samples from well 0504B.

UNC also considers this potential migration pathway to be unlikely based on the distribution of molybdenum concentrations in the three site hydrostratigraphic units, which demonstrates that the molybdenum is not a suitable indicator of tailings seepage at the Church Rock site. Although there are a few historical examples of significantly elevated molybdenum concentrations in the North Pond and Borrow Pit 2, these are likely to be related to very low pH conditions (i.e., pH <2.0) which do not persist for substantial distances in the areas outside the tailings ponds.

The following tables summarize the results of the molybdenum analyses from the background and exposure point concentration (EPC) statistical evaluations (N.A. Water Systems, 2008a and 2008b) for each of the three hydrostratigraphic units.

Summary Statistics for Molybdenum (mg/L) in Background Water (N.A. Water Systems, 2008a)

Zone	Total Data	Percent Nondetect	Minimum Detected	Maximum Detected	Mean of Detected	Median of Detected	UCL95 of Mean
Z3	184	14.13%	0.02	.75	11.88	3.76	17.43
Z1	234	97.9%	0.03	0.27	0.12	0.13	0.132
SWA	391	99.5%	0.03	0.03	N/A	N/A	N/A

Summary Statistics for Molybdenum (mg/L) in Impacted Groundwater (N.A. Water Systems, 2008b)

Zone	Total Data	Percent Nondetect	Minimum Detected	Maximum Detected	Mean of Detected	Median of Detected	UCL95 of Mean
Z3	70	54.3%	0.1	5	1.084	0.3	0.739
Z1	16	100.0%	N/A	N/A	N/A	N/A	N/A
SWA	96	100.0%	N/A	N/A	N/A	N/A	N/A

Two observations regarding these summary data demonstrate that molybdenum should not be considered a viable indicator of tailings seepage impacts. First, there is a wide, overlapping range of molybdenum concentrations observed in the Zone 3 background and impacted wells; however, significantly higher concentrations and greater variance are found in background data. Molybdenum was detected in approximately 86% of the background samples and in only approximately 46% of the impacted samples. During the two-year EPC statistical evaluation period (July 2006 through April 2008 inclusive), only two of the 10 seepage-impacted wells (0504 B and NBL-01) had molybdenum concentrations exceeding 0.4 mg/l, including the maximum detected concentration at NBL-01 (5 mg/L). Both of these wells also had elevated molybdenum concentrations prior to observing other geochemical evidence of seepage impact (i.e., changes in pH and bicarbonate). These data show that molybdenum is a poor indicator to distinguish background from seepage-impacted water. Second, molybdenum was not detected in any sample of seepage-impacted water from Zone 1 and the Southwest Alluvium (SWA) during the two-year EPC evaluation period and was detected only infrequently at low concentration in the background water sample data. If molybdenum were a significant component of the tailings seepage and that seepage was the source of highly elevated downgradient molybdenum concentrations in Zone 3, it should also be detected in impacted water in the other hydrostratigraphic units as well. These conclusions are supported by a review of the annual report data (Chester Engineers, 2013).

More plausible explanations for the observed site molybdenum concentration distributions are related to its complex environmental geochemistry and the potential presence of natural geologic sources of molybdenum. Hem (1985) indicates that the dominant molybdenum species change at pH values of 2 and 5 and that above pH 5 the molybdate ion (MoO_4^{-2}) is dominant. Hem (1985) further indicates that many of the metallic elements have molybdates of low solubility and that ferrous molybdate specifically limits solubility in relatively iron-rich waters below pH 5. This suggests a sensitivity to pH and effects related to the availability of other dissolved metals that would favor higher molybdenum solubility at higher pH (i.e., under background conditions existing after the influx of mine discharge water) than at lower pH (i.e., impacted conditions).

Hem (1985) notes that molybdenum is also present in fossil fuels and it is well known that molybdenum is often present in coal combustion products (i.e., fly ash). This is of interest because coal beds and carbonaceous shales are locally present in the Dilco Coal Member of the Crevasse Canyon Formation (which overlies Zone 3), the lower part of Zone 3, and Zone 2 (which underlies Zone 3 and is considered a shale and coal unit). These coals and carbonaceous shales may be a significant source background molybdenum concentrations and many plausible geochemical reactions related to the other metals present. Well construction, particularly the position of screened and/or sandpacked intervals with respect to these coal beds and carbonaceous shales, varies among the Zone 3 wells. For example, a review of construction information for four northern Section 36 wells indicates that they either penetrated Zone 2 or were completed near the base of Zone 3:

- EPA-1 – Total drilled depth 250 ft bgs, screened from 215 to 240 ft bgs, with a sandpack from 210 to 251 ft bgs. The Zone 2 contact is indicated to be within the sandpack at 244 ft bgs. Therefore the well sandpack is approximately 6 to 7 feet into Zone 2.
- EPA-10 – Total drilled depth 206 ft bgs, screened from 155 to 195 ft bgs, with a sandpack from 151 to 205 ft bgs. The Zone 2 contact is indicated to be within the screened interval at 194 ft bgs and the entire thickness of Zone 2 (10 ft) is within the drilled depth of the well.
- EPA-11 – Total drilled depth 180 ft bgs, screened from 136 to 171 ft bgs, with a sandpack from 133 to 180 ft bgs. The Zone 2 contact is indicated to be within the sandpack at 175 ft bgs. Therefore the well is approximately 5 feet into Zone 2.
- 0504 B – Total drilled depth 172 ft bgs, screened from 120 to 170 ft bgs, with a sandpack from 120 to 170 ft bgs. The bottom of Zone 3 is indicated to be just below the sandpack at 172 ft bgs.

Regarding the Dilco coal, UNC files contain a partial copy of a report related to the 400-series well installation and pumping in Section 36 (UNC, 1981b; titled Report 2, Northern Collection System; dated May 20, 1981; no author listed), which suggests that wells completed in the Dilco or at the Dilco/Zone 3 interface have inferior water quality to those completed only in Zone 3 or Zone 1 of the Upper Gallup sandstone. It is further suggested that elevated concentrations of TDS, sulfate, manganese, molybdenum, and uranium may be correlatable to localized carbonaceous deposits in the Dilco shale and sandy shale.

The Mancos Shale, which underlies Zone 1, is another possible source of molybdenum at certain well locations. Canonie (1987) considered the Mancos Shale to be the likely source of anomalously high TDS,

elevated magnesium, and acidic pH found in several alluvium wells. Bush and Morrison (2012) have also determined that the Mancos Shale can be the source of elevated background concentrations of certain parameters (e.g., uranium, nitrate, selenium, sulfate). Certain wells constructed in the early 1980s (e.g., wells 147 and 401) have screened intervals and/or sandpacked intervals that extend from Zone 3 through Zone 2 and Zone 1 into the Mancos Shale.

In conclusion, there are no identified physical or chemical mechanisms that could result in the transport of molybdenum from the tailings ponds in the absence of other geochemical evidence of seepage impacts. More plausible explanations for the observed site molybdenum concentration distributions are related to its complex environmental geochemistry and the presence of potential natural geologic sources of molybdenum such as coal beds and carbonaceous shales in the Dilco Coal, Zone 3, and Zone 2, as well as the Mancos Shale.

REFERENCES FOR ENCLOSURE 1

BBL, 2006, UNC Church Rock Site In-Situ Alkalinity Stabilization Pilot Study, United Nuclear Corporation, Gallup, New Mexico. June.

Billings & Associates, Inc., 1982, Design of a Seepage Control System for Zone 3 (Upper Gallup) Northeast of the North Pond. December.

Billings & Associates, Inc., 1984, Well Construction and Well Hydrograph Data. November 11, 1984.

Blickwedel, Roy S., 1986, Regulatory Significance of the Occurrence and Distribution of Dissolved Uranium in Groundwaters of the Southwest Alluvium, Church Rock Site, New Mexico. March.

Bush, Richard P. and Stan J. Morrison, 2012, Evaluation of Background Concentrations of Contaminants in an Unusual Desert Arroyo Near a Uranium Mill Tailings Disposal Cell – 12260, Paper presented at the WM2012 Conference, Phoenix, Arizona, February 26 – March 1, 2012.

Canonie Environmental Services Corp., 1987, Reclamation Engineering Services, Geohydrologic Report, Church Rock Site, Gallup, NM. May.

Chester Engineers, 2013, Annual Review Report – 2012 – Groundwater Corrective Action, Church Rock Site, Church Rock, New Mexico. January.

Earth Tech, 2002, Annual Review Report – 2002 – Groundwater Corrective Action, Church Rock Site, Gallup, New Mexico. December.

Hem, John D., 1985, Study and Interpretation of the Chemical Characteristics of Natural Water. USGS Water-Supply Paper 2254, US Government Printing Office, Alexandria VA, 1985.

Kaplan, E.L. and O. Meier, 1958, Nonparametric Estimation from Incomplete Observations. Journal of the American Statistical Association, Vol. 53. 457-481. June.

N.A. Water Systems, 2008a, Revised Submittal – Calculation of Background Statistics with Comparison Values, UNC Church Rock Mill & Tailings Site, Church Rock, New Mexico. October 17, 2008.

N.A. Water Systems, 2008b, Revised Submittal – Estimated UCL95 Statistics and EPCs in Impacted Groundwater, UNC Church Rock Mill & Tailings Site, Church Rock, New Mexico. December 5, 2008.

Singh A., N. Armbya, and A. K. Singh, 2010, ProUCL Version 4.1.00 Technical Guide (Draft) Statistical Software for Environmental Applications for Data Sets with and without Nondetect Observations. EPA/600/R-07/041). May.

Singh A., 2011, Statistical Methods Used to Establish Background Datasets Using Sampled Data Collected From DTLS and Surface and Subsurface Soils of Three RBRAs of the Two Formations and Compute Estimates of Background Threshold Values Based Upon Established Background Datasets (With and Without Nondetect Observations for the Santa Susana Field Laboratory Investigation (Appendix B of the October 2011 Final Radiological Background Study Report) Santa Susana Field Laboratory, Ventura County, California), EPA Contract No.: EP-S3-07-05,

Work Assignment Number: 021TATA09QL, Prepared for: U.S. Environmental Protection Agency Region 9, 75 Hawthorne Street, San Francisco, California 94105. October.

United Nuclear Corporation (UNC), 1981a, Letter from T.F. Bailey (UNC) to T. Baca (New Mexico Environmental Improvement Division (NMEID). March 6, 1981.

United Nuclear Corporation (UNC), 1981b, File Information: Report 2, Northern Collection System; No author listed. May 20, 1981.

United Nuclear Corporation (UNC), 1981c, Quarterly Report – UNC Mining and Milling, Northeast Church Rock Tailings Facility, File No. 3346. Letter from S. D. Misra (UNC) to S. E. Reynolds (State Engineer, New Mexico Natural Resources Department). December 7, 1981.

U.S. Environmental Protection Agency (EPA), 2009, Statistical Analysis of Groundwater Monitoring Data at RCRA Facilities – Unified Guidance. EPA 530-R-09-007. March.

U.S. Environmental Protection Agency (EPA), 1988, Draft Final Remedial Investigation, United Nuclear Corporation, Churchrock Site. U.S. Environmental Protection Agency. August.

Wirt, Laurie, Peter C. Van Metre, and Barbara Favor, 1991, Historical Water-Quality Data, Puerco River Basin Arizona and New Mexico. USGS Open-File Report 91-196, United States Geological Survey, Tucson Arizona. June.

TABLES

11	0.011	2	91	0.489247312	0.00011828	6.4673E-05
12	0.012	2	93	0.5	0.000129032	6.30159E-05
13	0.013	3	96	0.516129032	0.000209677	9.20705E-05
14	0.014	3	99	0.532258065	0.000225806	8.96494E-05
15	0.015	1	100	0.537634409	8.06452E-05	2.90869E-05
16	0.016	2	102	0.548387097	0.000172043	5.66027E-05
17	0.017	4	106	0.569892473	0.000365591	0.000110106
18	0.018	3	109	0.586021505	0.000290323	8.02876E-05
19	0.019	2	111	0.596774194	0.000204301	5.20186E-05
20	0.02	1	112	0.602150538	0.000107527	2.52668E-05
21	0.021	1	113	0.607526882	0.000112903	2.4535E-05
22	0.022	4	117	0.629032258	0.000473118	9.5256E-05
23	0.023	1	118	0.634408602	0.000123656	2.31037E-05
24	0.024	1	119	0.639784946	0.000129032	2.24042E-05
25	0.025	1	120	0.64516129	0.000134409	2.17155E-05
26	0.026	1	121	0.650537634	0.000139785	2.10375E-05
27	0.029	2	123	0.661290323	0.000311828	3.8136E-05
28	0.031	1	124	0.666666667	0.000166667	1.78088E-05
29	0.035	2	126	0.677419355	0.000376344	3.08388E-05
30	0.036	2	128	0.688172043	0.000387097	2.96978E-05
31	0.037	1	129	0.693548387	0.000198925	1.42892E-05
32	0.043	1	130	0.698924731	0.000231183	1.11567E-05
33	0.044	1	131	0.704301075	0.000236559	1.06722E-05
34	0.047	1	132	0.709677419	0.000252688	9.28342E-06
35	0.05	2	134	0.720430108	0.000537634	1.59827E-05
36	0.054	3	137	0.73655914	0.000870968	1.92575E-05
37	0.055	2	139	0.747311828	0.000591398	1.2106E-05
38	0.059	1	140	0.752688172	0.000317204	4.69583E-06
39	0.06	1	141	0.758064516	0.000322581	4.38343E-06
40	0.062	1	142	0.76344086	0.000333333	3.79087E-06
41	0.066	1	143	0.768817204	0.000354839	2.7348E-06
42	0.069	1	144	0.774193548	0.000370968	2.05564E-06
43	0.071	1	145	0.779569892	0.00038172	1.65664E-06
44	0.084	1	146	0.784946237	0.000451613	1.11488E-07
45	0.087	1	147	0.790322581	0.000467742	1.29795E-08
46	0.088	1	148	0.795698925	0.000473118	1.64868E-09
47	0.095	1	149	0.801075269	0.000510753	2.23408E-07
48	0.107	1	150	0.806451613	0.000575269	1.82937E-06
49	0.113	1	151	0.811827957	0.000607527	3.213E-06
50	0.133	1	152	0.817204301	0.000715054	1.06208E-05
51	0.137	1	153	0.822580645	0.000736559	1.26185E-05
52	0.14	1	154	0.827956989	0.000752688	1.42297E-05
53	0.142	1	155	0.833333333	0.000763441	1.53575E-05
54	0.149	1	156	0.838709677	0.000801075	1.96438E-05
55	0.156	1	157	0.844086022	0.00083871	2.4457E-05
56	0.175	1	158	0.849462366	0.00094086	4.01772E-05
57	0.176	1	159	0.85483871	0.000946237	4.11121E-05
58	0.181	1	160	0.860215054	0.000973118	4.59479E-05
59	0.183	1	161	0.865591398	0.000983871	4.79575E-05
60	0.19	1	162	0.870967742	0.001021505	5.53298E-05
61	0.193	1	163	0.876344086	0.001037634	5.86506E-05
62	0.195	1	164	0.88172043	0.001048387	6.09183E-05
63	0.21	1	165	0.887096774	0.001129032	7.92967E-05
64	0.224	1	166	0.892473118	0.001204301	9.86327E-05
65	0.242	1	167	0.897849462	0.001301075	0.00012659
66	0.253	1	168	0.903225806	0.001360215	0.00014539
67	0.303	1	169	0.908602151	0.001629032	0.000247243
68	0.318	1	170	0.913978495	0.001709677	0.000283041
69	0.34	1	171	0.919354839	0.001827957	0.00033992
70	0.357	1	172	0.924731183	0.001919355	0.000387438
71	0.481	1	173	0.930107527	0.002586022	0.000828033
72	0.523	1	174	0.935483871	0.002811828	0.00101475
73	0.538	1	175	0.940860215	0.002892473	0.001086032
74	0.57	1	176	0.946236559	0.003064516	0.001246185
75	0.573	1	177	0.951612903	0.003080645	0.001261764
76	0.604	1	178	0.956989247	0.003247312	0.001428413
77	0.613	1	179	0.962365591	0.003295699	0.00147873
78	0.688	1	180	0.967741935	0.003698925	0.001931913
79	0.714	1	181	0.97311828	0.00383871	0.002103134
80	0.728	1	182	0.978494624	0.003913978	0.002198341
81	0.768	1	183	0.983870968	0.004129032	0.002481974
82	0.776	1	184	0.989247312	0.004172043	0.002540765
83	0.955	1	185	0.994623656	0.005134409	0.004036178
84	1.01	1	186	1	0.005430108	0.004564856
					0.088553763	**0.187067608**

Cumulative Probability Distribution Function

$$F_{KM}(x_{(i)}) = \Pr(X \le x_{(i)}) = \left(1-\frac{d_{i+1}}{n_{i+1}}\right)\times\left(1-\frac{d_{i+2}}{n_{i+2}}\right)\times\ldots\times\left(1-\frac{d_m}{n_m}\right) = \prod_{k=i}^{m-1}\left(1-\frac{d_{k+1}}{n_{k+1}}\right)$$

TABLE 2
UPLk95 Calculations Showing Difference Between Use of Z-Statistic and T-Statistic
UNC Church Rock Site, Church Rock, New Mexico

COPC	n	k	KM Mean	KM SD	α	Probability α/k	1-α/k	Critical Value Normal Dist. (z)	Calculated UPL Using z-statistic	t-statistic	Calculated UPL Using t-statistic	ProUCL UPL
As	186	1	0.0886	0.187	0.05	0.050000	0.950000	1.645	0.397	1.653	0.399	0.399
As	186	4	0.0886	0.187	0.05	0.012500	0.987500	2.241	0.509	2.260	0.512	0.512
As	186	16	0.0886	0.187	0.05	0.003125	0.996875	2.734	0.601	2.766	0.607	0.607
As	186	40	0.0886	0.187	0.05	0.001250	0.998750	3.023	0.656	3.065	0.6635	0.6635
As	186	136	0.0886	0.187	0.05	0.000368	0.999632	3.376	0.722	3.433	0.733	0.733
As	186	216	0.0886	0.187	0.05	0.000231	0.999769	3.501	0.745	3.565	0.757	0.757
As	186	544	0.0886	0.187	0.05	0.000092	0.999908	3.740	0.790	3.817	0.805	0.805

Note: the actual k value for Zone 3 = 216

Equation for t-statistic based calculation

$$UPL_k 95 = \left(\bar{x} + t_{((1-0.05/k),n-1)} s \sqrt{1 + \frac{1}{n}} \right)$$

Note: The Kaplan-Meier estimates of the population mean and standard deviation are substituted into the preceding equation to make the UPL calculation (Singh, 2011).

FIGURES

FIGURE 1
Composite (Multiple Formation) Wells in the 300-400 Series
United Nuclear Corporation Church Rock Site,
Church Rock, New Mexico

CHESTER ENGINEERS

FIGURE 2
Zone 1 Wells in the 300-400 Series
United Nuclear Corporation Church Rock Site,
Church Rock, New Mexico

CHESTER ENGINEERS

FIGURE 3
Zone 3 Wells in the 300-400 Series
United Nuclear Corporation Church Rock Site,
Church Rock, New Mexico

CHESTER ENGINEERS

Attachments

Well Hydrographs

BILLINGS & ASSOCIATES, INC.
Rt. 3, Box 739
Kimberling City, MO 65686
(417) 739-4492

DATABASE MANAGEMENT INTERPRETIVE COMMENTS

WELL: 411

Well 411 is a Zone 3 well north of the 400 Series at the same location as the KMEID well. The water level shows good response to the pumping of the 400 Series and is an excellent long distance observation well for analysis. The well does not appear to be contaminated.

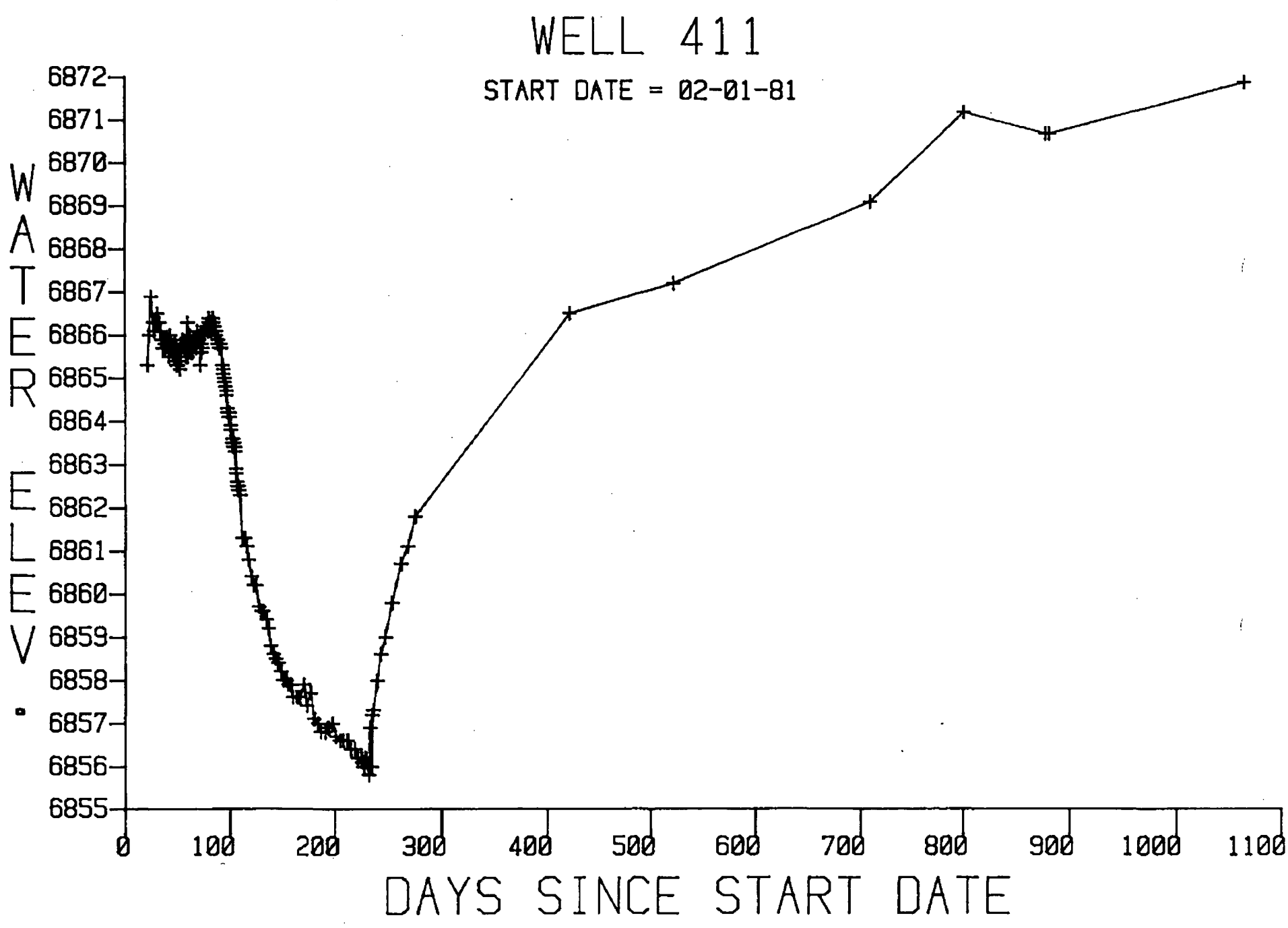
WELL 411
START DATE = 02-01-81
WATER ELEV.
6872
6871
6870
6869
6868
6867
6866
6865
6864
6863
6862
6861
6860
6859
6858
6857
6856
6855
0
100
200
300
400
500
600
700
800
900
1000
1100
DAYS SINCE START DATE

BILLINGS & ASSOCIATES, INC.
Rt. 3, Box 739
Kimberling City, MO 65686
(417) 739-4492

WELL: 420

DATE: 11-11-84

SUBJECT: Interpretive Comments

Well 420 is a Zone 3 observation well in the 400 Series pumping system. The well was probably not contaminated at the last sampling (1982). The well demonstrates response to pumping and the later, general rise in Zone 3 water level.

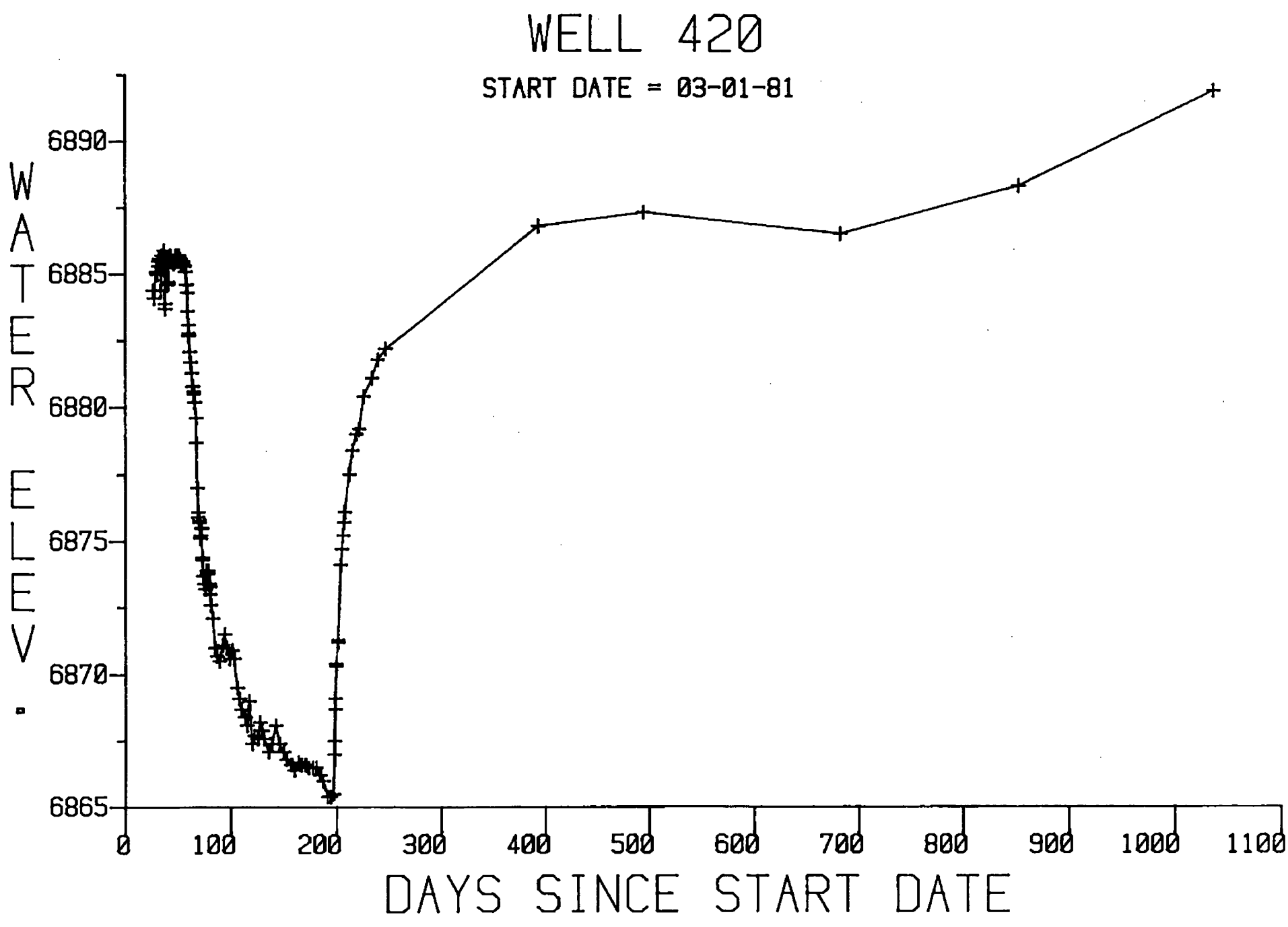
WELL 420
START DATE = 03-01-81
WATER ELEV.
6890
6885
6880
6875
6870
6865
0
100
200
300
400
500
600
700
800
900
1000
1100
DAYS SINCE START DATE

GEOCHEMISTRY OF GROUND WATER IN THE GALLUP, DAKOTA, AND MORRISON AQUIFERS, SAN JUAN BASIN, NEW MEXICO

By William L. Dam

U.S. GEOLOGICAL SURVEY
Water-Resources Investigations Report 94-4253

A Contribution of the Regional Aquifer-System Analysis Program

Albuquerque, New Mexico
1995

U.S. DEPARTMENT OF THE INTERIOR

BRUCE BABBITT, *Secretary*

U.S. GEOLOGICAL SURVEY

Gordon P. Eaton, *Director*

For additional information write to:

District Chief
U.S. Geological Survey
Water Resources Division
4501 Indian School Road NE, Suite 200
Albuquerque, New Mexico 87110

Copies of this report can be purchased from:

U.S. Geological Survey
Earth Science Information Center
Open-File Reports Section
Box 25286, Mail Stop 517
Denver Federal Center
Denver, Colorado 80225

CONTENTS

	Page
Abstract	1
Introduction	2
Purpose and scope	2
Previous studies	2
Acknowledgments	4
Geology and hydrology	5
Gallup aquifer	9
Dakota aquifer	9
Morrison aquifer	10
Geochemistry of Gallup, Dakota, and Morrison aquifers	16
Methods	16
Major constituents and pH	23
Minor and trace constituents	37
Dissolved gases	45
Stable isotopes	45
Radioactive isotopes	51
Physical and geochemical processes	57
Summary and conclusions	70
References cited	72

ILLUSTRATIONS

Figure 1.	Map showing location of the San Juan structural basin, Colorado Plateau, and study area	3
2.	Map showing structural elements of the San Juan structural basin and adjacent areas and generalized pattern of ground-water flow in rocks of Jurassic and Cretaceous age	6
3.	Diagram showing time- and rock-stratigraphic framework and nomenclature	7
4.	Diagrammatic hydrogeologic section of the San Juan Basin	8
5.	Map showing hydraulic heads in the Dakota aquifer and Entrada Sandstone relative to the Morrison aquifer, 1985-86	13
6.	Water-level hydrographs for three wells completed in the Morrison aquifer, 1957-87	14
7.	Map showing potentiometric surface of the Morrison aquifer, 1985-86	15
8.	Map showing location of sampled water wells completed in the Gallup aquifer	17
9.	Map showing location of sampled water wells completed in the Dakota aquifer	18
10.	Map showing locations of sampled water wells completed in the Morrison aquifer and of geohydrologic sections	19
11.	Geohydrologic sections showing well completion in the Morrison aquifer	22

ILLUSTRATIONS--Concluded

Page

Figures 12-14. Maps showing values of pH for water from water wells completed in the:
- 12. Gallup aquifer 28
- 13. Dakota aquifer 29
- 14. Morrison aquifer 30

15-17. Maps showing chemical-constituent diagrams of water from water wells completed in the:
- 15. Gallup aquifer 31
- 16. Dakota aquifer 32
- 17. Morrison aquifer 33

18-20. Trilinear diagrams of major ion chemistry from water wells completed in the:
- 18. Gallup aquifer 34
- 19. Dakota aquifer 35
- 20. Morrison aquifer 36

21-23. Maps showing concentration of chloride in water from water wells completed in the:
- 21. Gallup aquifer 38
- 22. Dakota aquifer 39
- 23. Morrison aquifer 40

24. Graph showing oxygen and deuterium isotopic ratios in water from water wells completed in the Gallup, Dakota, and Morrison aquifers 49

25. Map showing deuterium isotopic ratio in water from water wells completed in the Morrison aquifer 50

26. Map showing carbon-13 isotopic ratio in water from water wells completed in the Gallup aquifer 52

27. Map showing carbon-13 isotopic ratio in water from water wells completed in the Morrison aquifer 53

28. Map showing ratio of chlorine-36 to stable chlorine isotopes in water from water wells completed in the Morrison aquifer 56

29. Graph showing ratio of bromide/chloride versus chloride concentrations for water samples from the Gallup, Dakota, and Morrison aquifers 59

30. Map showing location, well number, and group for water wells completed in the Morrison aquifer used in analysis of chlorine-36 data shown in figures 31-33 60

31. Graph showing chlorine-36/chlorine versus chlorine-36 for water from the Morrison aquifer 61

32. Graph showing chlorine-36/chlorine versus inverse of chloride concentration for water from the Morrison aquifer 63

33. Graph showing chlorine-36/chlorine versus inverse of chloride concentration for water from the Morrison aquifer--expanded scale 64

34. Plot showing concentration of dissolved silica versus field pH and temperature of water samples from the Morrison aquifer 68

TABLES

Page

Table 1. Data for wells sampled from 1986 to 1989 21

2-4. Selected properties of and constituents in water from the:

2. Gallup aquifer 24
3. Dakota aquifer 25
4. Morrison aquifer 26

5. Concentrations of dissolved nutrients and dissolved organic carbon in water from the Gallup, Dakota, and Morrison aquifers 42

6. Concentration of dissolved trace constituents in water from the Gallup, Dakota, and Morrison aquifers 43

7. Concentrations of dissolved gases in water from the Morrison aquifer 45

8. Isotopic ratios of stable isotopes in water from the Gallup, Dakota, and Morrison aquifers 47

9. Activities of tritium, carbon-14, and chlorine-36 isotopes in water from the Gallup, Dakota, and Morrison aquifers 54

10. Two chemical analyses of water from the Entrada Sandstone. 65

CONVERSION FACTORS, VERTICAL DATUM, AND ABBREVIATED WATER-QUALITY TERMS

Multiply	By	To obtain
foot (ft)	0.3048	meter (m)
mile (mi)	1.609	kilometer (km)
square mile (mi^2)	2.590	square kilometer (km^2)
gallon (gal)	3.785	liter (L)
gallon per minute (gal/min)	0.06309	liter per second (L/s)

Temperature in degrees Celsius (°C) can be converted to temperature in degrees Fahrenheit (°F) by using the equation:

$$°F = 1.8 \times °C + 32$$

Sea level: In this report, sea level refers to the National Geodetic Vertical Datum of 1929--a geodetic datum derived from a general adjustment of the first-order level nets of the United States and Canada, formerly called Sea Level Datum of 1929.

Al	Aluminum, in micrograms per liter
Ag	Silver, in micrograms per liter
Ar	Argon, in milligrams per liter
As	Arsenic, in micrograms per liter
B	Boron, in micrograms per liter
Ba	Barium, in micrograms per liter
Be	Beryllium, in micrograms per liter
Br^-	Bromide, in milligrams per liter
$\delta^{13}C$	Carbon-13/carbon-12 ratio, in per mil PDB (Peedee belemnite, Cretaceous Peedee Formation of South Carolina)
^{14}C	Carbon-14, in uncorrected percent modern carbon
$CaCO_3$	Calcium carbonate, in milligrams per liter
Ca^{2+}	Calcium, in milligrams per liter
Cd	Cadmium, in micrograms per liter
Cl^-	Chloride, in milligrams per liter
$^{36}Cl/10^{15}Cl$	Atomic ratio of ^{36}Cl atoms to 10^{15} atoms of Cl^{35} and Cl^{37}
Co	Cobalt, in micrograms per liter
CO_2	Carbon dioxide, in milligrams per liter
CO_3^{2-}	Carbonate, in milligrams per liter
Cr	Chromium, in micrograms per liter
Cu	Copper, in micrograms per liter
D	Deuterium
DO	Dissolved oxygen, in milligrams per liter
F^-	Fluoride, in milligrams per liter
Fe	Iron, in micrograms per liter
g	Gram
δD	Deuterium/hydrogen ratio, in per mil V-SMOW (Vienna-Standard Mean Ocean Water)
^3H	Tritium, in tritium units
HCO_3^-	Bicarbonate, in milligrams per liter
Hg	Mercury, in micrograms per liter
T	
HS^-	Bisulfide
I^-	Iodide, in milligrams per liter
K^+	Potassium, in milligrams per liter
Li	Lithium, in micrograms per liter
Mg^{2+}	Magnesium, in milligrams per liter
meq/L	Milliequivalents per liter
mg/L	Milligrams per liter
mmol/L	Millimoles per liter
Mn	Manganese, in micrograms per liter
Mo	Molybdenum, in micrograms per liter
N	Nitrogen, in milligrams per liter

Na^+	Sodium, in milligrams per liter
Ni	Nickel, in micrograms per liter
NO_3^-	Nitrate, in milligrams per liter
NO_2^-	Nitrite, in milligrams per liter
$\delta^{18}O$	Oxygen-18/oxygen-16 ratio, in per mil V-SMOW (Vienna-Standard Mean Ocean Water)
P	Phosphorus, in milligrams per liter
Pb	Lead, in micrograms per liter
pCi/L	Picocuries per liter
pCO_2	Partial pressure of carbon dioxide
pH	Negative log activity of hydrogen ion
PO_4	Phosphorous, in milligrams per liter
$\delta^{34}S$	Sulfur-34/sulfur-32 ratio, in per mil Canyon Diablo meteorite standard
SiO_2^0	Silica, in milligrams per liter
SO_4^{2-}	Sulfate, in milligrams per liter
Se	Selenium, in micrograms per liter
Sr^{2+}	Strontium, in micrograms per liter
µg/L	Micrograms per liter
µm	Micron
V	Vanadium, in micrograms per liter
Zn	Zinc, in micrograms per liter

BLANK

GEOCHEMISTRY OF GROUND WATER IN THE GALLUP, DAKOTA, AND MORRISON AQUIFERS, SAN JUAN BASIN, NEW MEXICO

By William L. Dam

ABSTRACT

Ground water was sampled from wells completed in the Gallup, Dakota, and Morrison aquifers in the San Juan Basin, New Mexico, to examine controls on solute concentrations. Samples were collected from 38 wells primarily from the Morrison aquifer (25 wells) in the northwestern part of the basin. A series of samples was collected along ground-water flow paths; dissolved constituents varied horizontally and vertically.

The understanding of the flow system changed as a result of the geochemical analyses. The conceptual model of the flow system in the Morrison aquifer prior to the study reported here assumed the Westwater Canyon Member of the Morrison aquifer as the only significant regional aquifer; flow was assumed to be two dimensional; and vertical leakage was assumed to be negligible. The geochemical results indicate that the Westwater Canyon Member is not the only major water-yielding zone and that the flow system is three dimensional. The data presented in this report suggest an upward component of flow into the Morrison aquifer. The entire section above and below the Morrison aquifer appears to be controlled by a three-dimensional flow regime where saline brine leaks near the San Juan River discharge area.

Predominant ions in the Gallup aquifer were calcium bicarbonate in recharge areas and sodium sulfate in discharge areas. In the Dakota aquifer, predominant ions were sodium bicarbonate and sodium sulfate. Water in the Morrison aquifer was predominantly sodium bicarbonate in the recharge area, changing to sodium sulfate downgradient.

Chemical and radioisotopic data indicate that water from overlying and underlying units mixes with recharge water in the Morrison aquifer. Recharge water contained a large ratio of chlorine-36 to chlorine and a small ratio of bromide to chloride. Approximately 10 miles downgradient, samples from four wells completed in the Morrison aquifer were considerably different in composition compared to recharge samples. Oxygen stable isotopes decreased by 2.8 per mil and deuterium decreased 26 per mil, relative to recharge. Carbon-14 radioisotope activities were not detectable. Chloride-36 radioisotope ratios were small and bromide to chloride concentration ratios were large. These results suggest two potentially viable processes: ion filtration or trapping of ancient dilute water recharged under a humid climate. For water samples near the San Juan River, pH decreased to about 8.0, chloride concentrations increased to more than 100 milligrams per liter, and ratios of chlorine-36 to chlorine and bromide to chloride were small. Leakage of deep basin brine into the fresher water of the Morrison aquifer appears to control ion concentrations.

INTRODUCTION

In October 1984, the U.S. Geological Survey (USGS) began a regional assessment of the San Juan structural basin aquifer systems in New Mexico, Colorado, Arizona, and Utah as part of its national Regional Aquifer-System Analysis (RASA) program (Bennett, 1979).

The San Juan Basin is located in New Mexico, Colorado, Arizona, and Utah, covering an area of approximately 21,600 mi^2 (fig. 1). The basin, a structural depression in the eastern part of the Colorado Plateau, is approximately 140 mi wide by 200 mi long, and land-surface altitudes range from about 4,500 ft in the northwest to about 11,000 ft in the southeast.

The San Juan Basin is an arid region where development of energy and water resources is essential to the economy. Surface-water resources are fully allocated, so ground-water resources are vital to industries, municipalities, and ranchers.

Purpose and Scope

This report presents geochemical and isotopic data used in examining sources of solutes and hydrologic and chemical controls that affect the concentration and distribution of solutes in aquifers in the San Juan Basin. The Gallup, Dakota, and Morrison aquifers were chosen for detailed geochemical analysis because of available water wells having known completion data, ground-water modeling results, and mineralogical analyses. These aquifers are equivalent stratigraphically to the Gallup Sandstone, Dakota Sandstone, and Morrison Formation. These aquifers are used extensively as water supplies for industry, communities, and livestock.

The report examines in detail the geochemistry of the three aquifers. The scope is constrained primarily to the northwestern part of the basin due to limited areal distribution of wells completed in a single aquifer and disturbances to the natural ground-water system by mining and petroleum industries in other parts of the basin. The main focus of this report is on the Morrison aquifer from the communities of Sanostee to Shiprock. Data for the Gallup and Dakota aquifers are provided for purposes of comparison and examination of vertical changes in flow and water quality. Hydrologic and water-quality data for the underlying Entrada Sandstone also are evaluated for the effects that water from this unit may have had on the Morrison aquifer.

Previous Studies

The hydrogeology of the San Juan Basin was described comprehensively by Stone and others (1983). USGS Hydrologic Investigations Atlases (HA 720-A through 720-J) have been published for 10 major aquifers in the basin (Craigg and others, 1989, 1990; Kernodle and others, 1989, 1990; Dam and others, 1990a, b; Levings and others, 1990a, b; and Thorn and others, 1990a, b). Data are presented on maps and in tables to describe the geology, hydrology, and water quality for each aquifer.

The only previous study that examined the regional San Juan Basin ground-water geochemistry of Jurassic and Cretaceous aquifers was performed by Berry (1959). He collected physical and chemical data from water wells, producing oil or gas wells, and drill-stem tests.

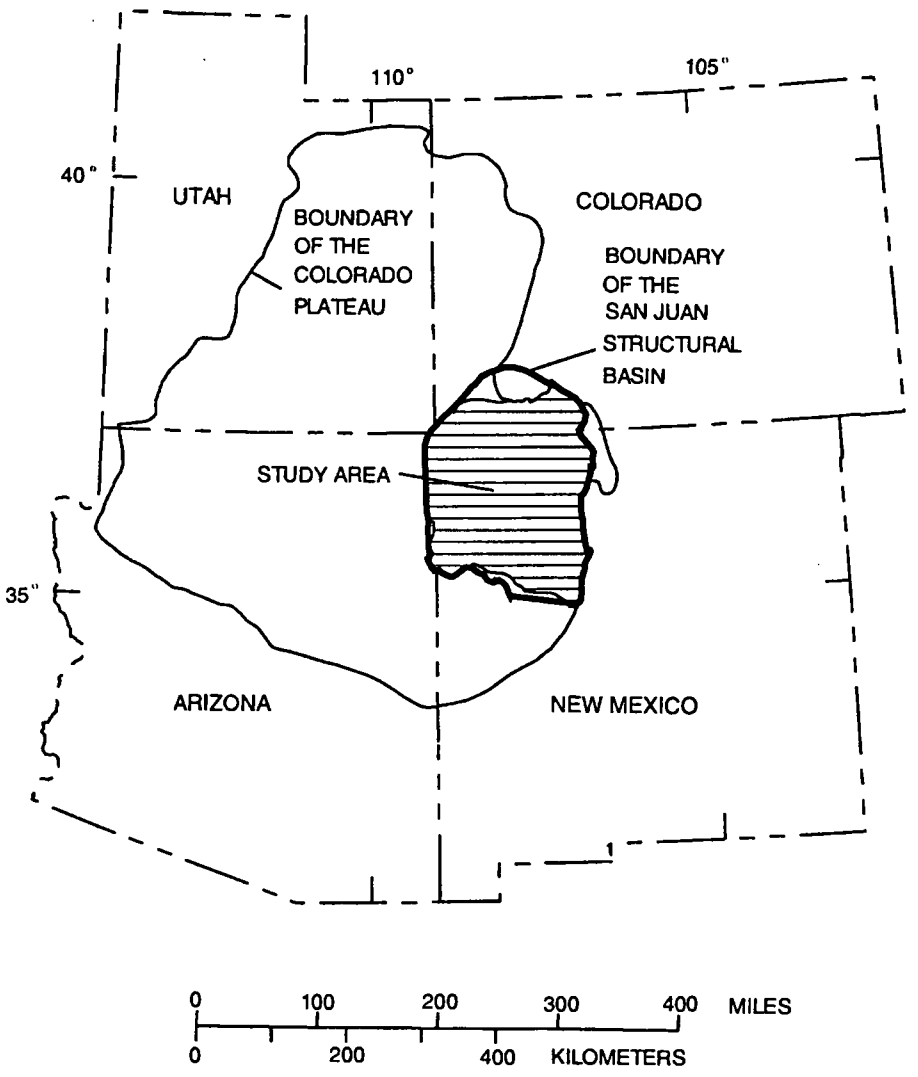

Figure 1.--Location of the San Juan structural basin, Colorado Plateau, and study area.

The direction of ground-water flow in Jurassic and Cretaceous aquifers, according to Berry (1959), was predominantly toward the lowest outcrop in the northwestern part of the basin. Normal hydrodynamic conditions existed along the flanks of the San Juan Basin. Conversely, in the central San Juan Basin, referred to by Berry as the "Inner Basin," hydraulic-pressure sinks and increased salinities were observed in all Cretaceous aquifers. Berry hypothesized that saline water containing dissolved-solids concentrations ranging from 30,000 to 270,000 parts per million entered the Entrada Sandstone from dissolved evaporite minerals such as halite contained in the overlying Todilto Limestone Member of the Wanakah Formation. The saline water in the Entrada Sandstone moved to the west and was trapped on the western side of the central basin due to the synclinal structures of the basin. Saline water in the Entrada Sandstone and freshwater in the Dakota aquifer were separated by the Brushy Basin Member of the Morrison Formation; this shale, acting as a semipermeable membrane, created an osmotic pressure system. Osmotic pressure, Berry proposed, caused the relatively dilute water from the Dakota aquifer to pass through the Brushy Basin Member. This caused a decrease in hydraulic pressure and left behind solutes that increased the salinity in the Dakota. The dilute water flowed into sandstones of the Morrison aquifer and Entrada Sandstone, increasing the hydraulic pressure and decreasing the dissolved-solids concentration. Similar osmotic-pressure phenomena for all Cretaceous sequences of sandstones and shales in this basin were observed (Berry, 1959).

Phillips and others (1986b) evaluated stable and radioactive isotopic data obtained from the Ojo Alamo and Nacimiento aquifers (in rocks of Paleocene age) in the central San Juan Basin. They found that waters collected from the two aquifers were of Pleistocene age and contained lighter oxygen and deuterium isotopes than modern precipitation and ground water. They proposed trends of decreased mean annual temperature and increased winter precipitation as factors affecting the stable-isotope contents.

Acknowledgments

The author acknowledges the people of the Navajo Nation who allowed and assisted in collection of water samples from their wells. Officials with ARCO Oil and Gas Company and El Paso Natural Gas Company also permitted access to wells, and Exxon Company, USA supplied well information. The Bureau of Land Management and the National Park Service provided access and information on selected wells. Information on oil and gas injection wells was obtained from the New Mexico Oil Conservation Division. Dr. Fred Phillips and Geoff Jones provided chlorine-36 results through a cooperative agreement with the New Mexico Institute of Mining and Technology. Several professors at the University of New Mexico provided assistance and technical advice in data collection and interpretation, including Drs. Laura Crossey, Douglas Brookins, and Crayton Yapp.

GEOLOGY AND HYDROLOGY

The San Juan Basin is a northwest-trending, asymmetric structural depression formed during the Laramide orogeny (Late Cretaceous-early Tertiary age) at the eastern edge of the Colorado Plateau (fig. 1). In many places, structural boundaries of the basin are well defined, whereas in other places, the basin merges gradually into adjacent depressions or uplifts (Kelley, 1951, p. 124-127). The structural boundaries consist principally of large, elongate, domal uplifts; low, marginal platforms; and abrupt monoclines as shown in figure 2. Faulting is common especially in the southeastern part of the basin. Maximum structural relief in the basin is about 10,000 ft. The Hogback Monocline, Nacimento Uplift, and Chaco Slope bound the central San Juan Basin.

The San Juan Basin contains a thick sequence of nearly horizontal beds of sedimentary rocks, ranging in age from Cambrian through Tertiary, but principally from Pennsylvanian through Tertiary (fig. 3). The maximum thickness of this sequence of rocks is about 14,000 ft at the trough-like structural center of the basin (Fassett and Hinds, 1971, p. 4). The sedimentary rocks, primarily sandstone and shale, dip from the basin margins toward the center of the basin. Volcanic rocks of Tertiary age and various deposits of Quaternary age also are present in the basin.

Ground-water flow directions for Jurassic and Cretaceous aquifers are shown in a generalized areal form in figure 2. Recharge occurs along outcrops in mountainous regions along the basin boundaries; ground water circulates toward major discharge areas in the northwestern, southwestern, and southeastern parts of the basin (Frenzel and Lyford, 1982, p. 7).

A diagrammatic hydrogeologic section showing major aquifers, confining layers, and direction of ground-water flow is shown in figure 4. Major aquifers include the rocks of Tertiary age, undivided; Kirtland Shale and Fruitland Formation; Pictured Cliffs Sandstone; Mesaverde Group, undivided; Gallup Sandstone; Dakota Sandstone; Morrison Formation; Entrada Sandstone; and San Andres Limestone and Glorieta Sandstone. Thick shale beds act as confining layers between the sandstone aquifers. Ground water generally flows from the recharge areas at the outcrops downdip through permeable zones. Vertical leakage between aquifers is known to occur; however, the magnitude is not known and leakage rates through intervening shale beds probably are small in most areas (Stone and others, 1983, p. 23). Large upward vertical leakage rates are thought to occur along the Hogback Monocline in the northwestern part of the basin and in the Puerco Fault Zone in the southeastern part of the basin (fig. 2) (Stone and others, 1983, p. 23).

The geology and hydrology of the Gallup, Dakota, and Morrison aquifers are described briefly, including the structure, stratigraphy, depositional environment, petrology, mineralogy, ground-water flow patterns, water levels, and hydraulic characteristics. Additional information can be found in Stone and others (1983); Craigg and others (1989); Kernodle and others (1989); and Dam and others (1990a).

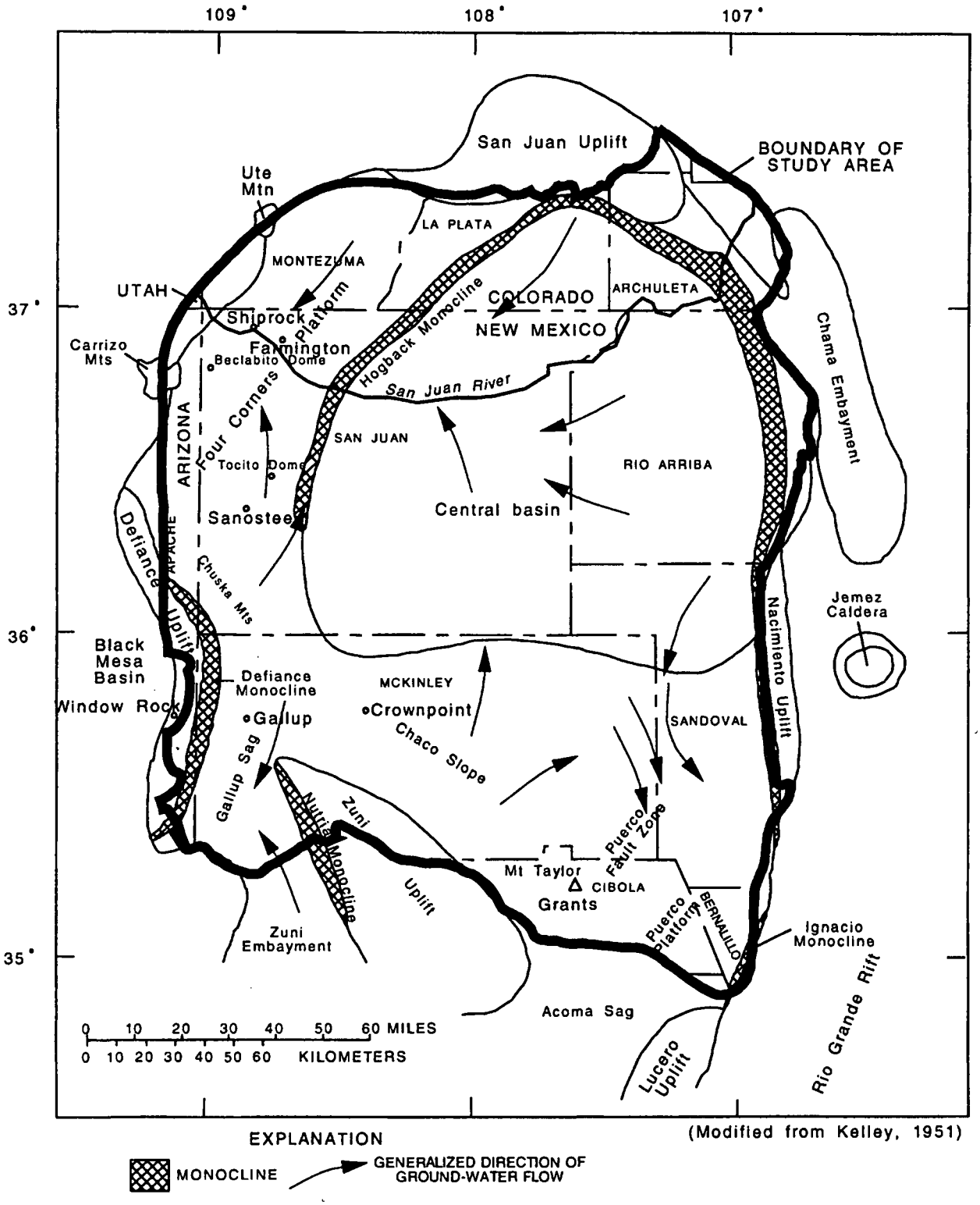

Figure 2.--Structural elements of the San Juan structural basin and adjacent areas and generalized pattern of ground-water flow in rocks of Jurassic and Cretaceous age.

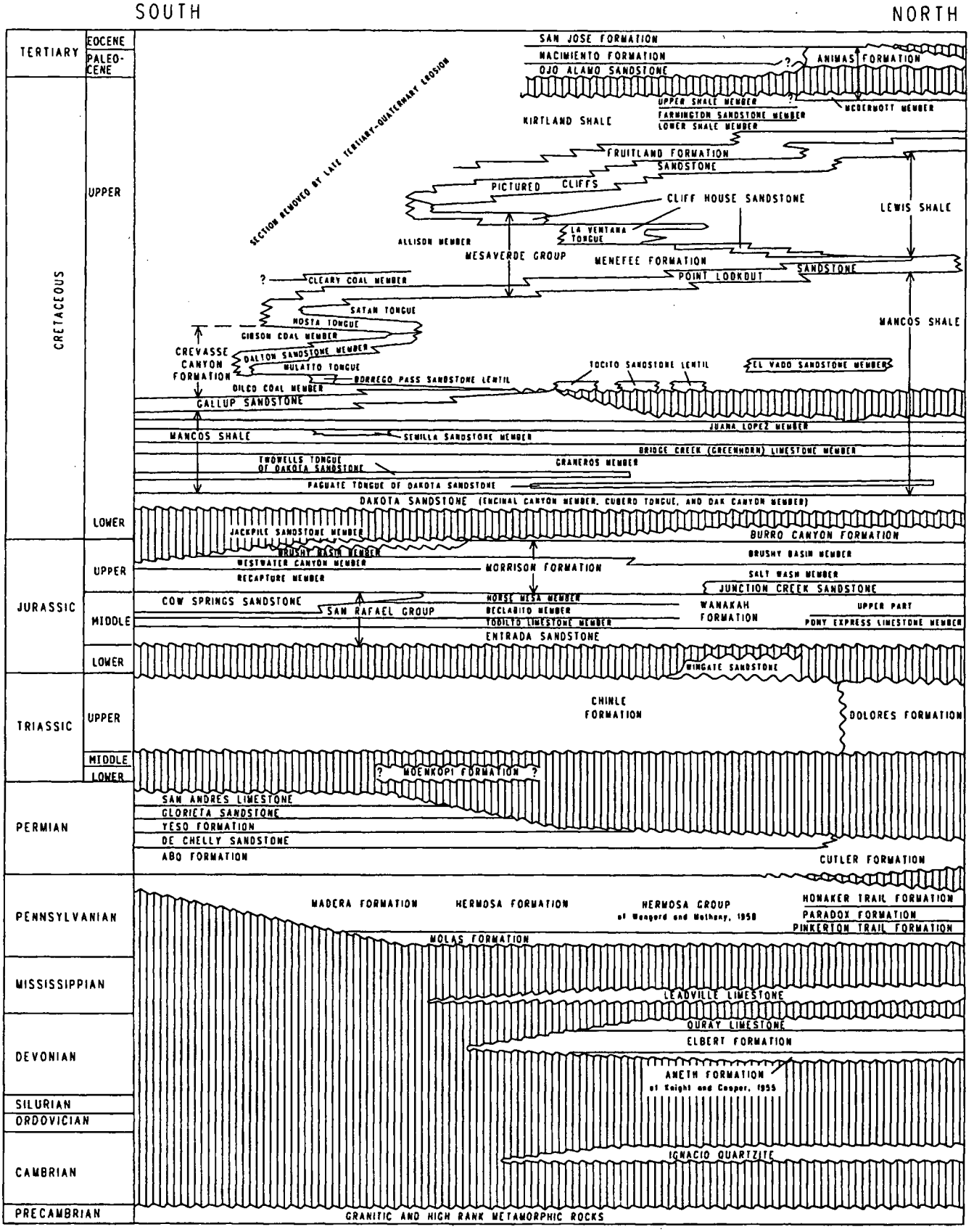

(Modified from Molenaar, 1977a,b, and 1989)

Figure 3.--Time- and rock-stratigraphic framework and nomenclature. Ruled lines indicate a hiatus in the sequence of beds.

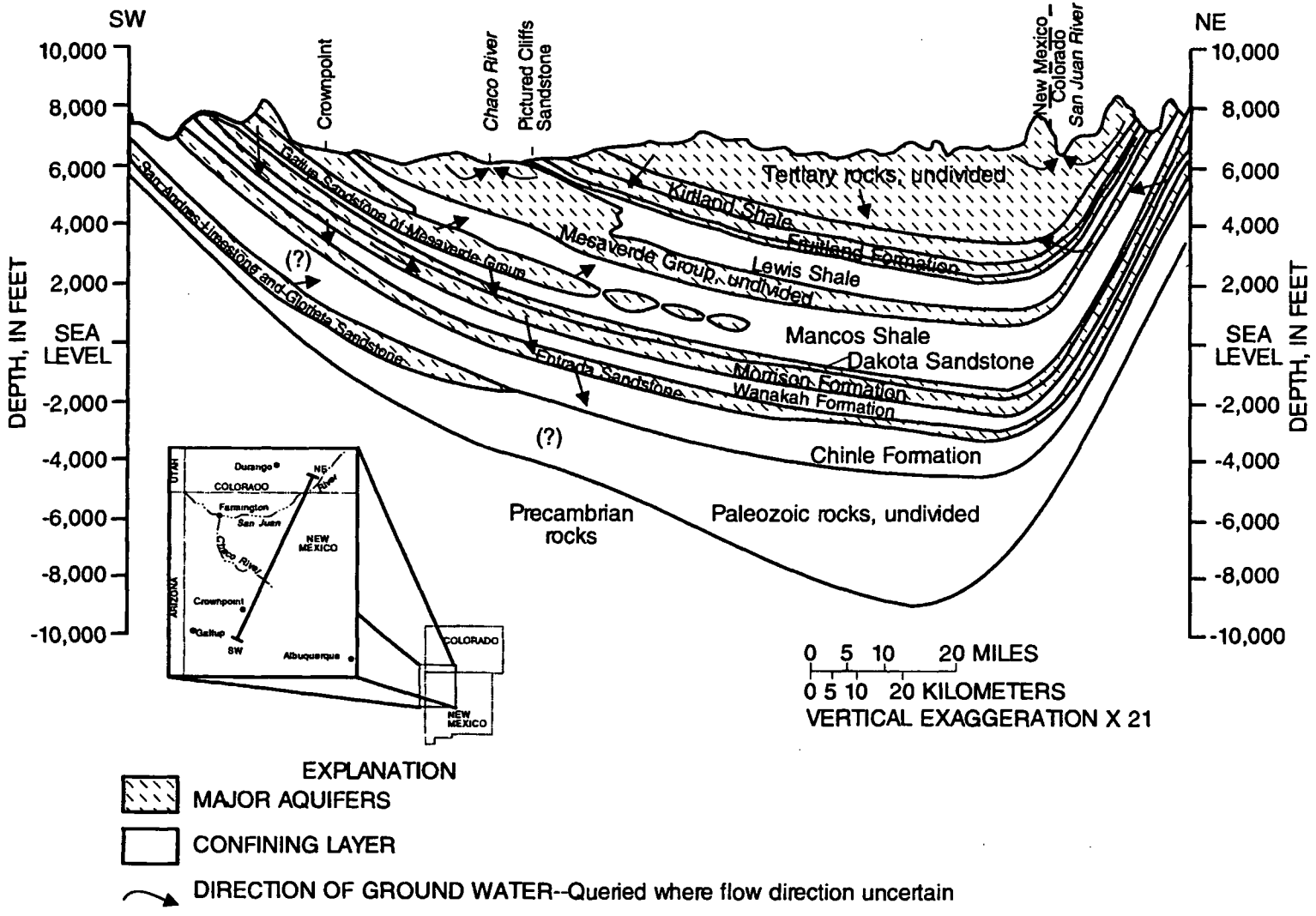

Figure 4.--Diagrammatic hydrogeologic section of the San Juan Basin (modified from Stone and others, 1983).

Gallup Aquifer

The Gallup aquifer is a hydrogeologic unit corresponding to the Gallup Sandstone. The Gallup Sandstone is of Late Cretaceous age (Molenaar, 1973, 1974). The unit has a smaller areal extent than the other major Upper Cretaceous sandstones in the San Juan structural basin and occurs only in New Mexico and a small part of Arizona. The Gallup crops out in an arcuate pattern around the western and southern margin of the basin where it typically forms erosion-resistant cliffs and dip slopes. Thickness of the Gallup decreases from about 600 ft near the outcrops along the margin of the basin to zero along the northwest-trending pre-Niobrara erosion limit. Depth to the top of the Gallup Sandstone ranges from zero in areas of outcrop to about 4,500 ft in an area about 20 mi south of the town of Farmington (Kernodle and others, 1989). The altitude of the top of the Gallup decreases from a maximum of about 7,500 ft northeast of Window Rock, Arizona, to about 1,500 ft above sea level southwest of Farmington. The Gallup represents the first major regression of the Upper Cretaceous sea in the San Juan structural basin and also represents deposition in marine and nonmarine environments. As originally defined by Sears (1925) and discussed in detail by Dane and others (1957), the Gallup consists of various rocks including sandstone (the predominant rock type), conglomerate, shale, carbonaceous shale, and coal. Minerals found in the Gallup include quartz (70-90 percent), feldspar (5-25 percent), glauconite, chlorite, sericite, chert, zircon, tourmaline, hematite, limonite, magnetite, ilmenite, dolomite, and ankerite (Kaharoeddin, 1971).

The Gallup aquifer is a source of water for domestic, livestock, municipal, and industrial uses. Recharge to the aquifer is from infiltration of precipitation and streamflow on outcrops and from vertical leakage of water through confining beds. Areas of recharge are in the southwestern and northeastern parts of the basin. Ground-water flow from these areas moves generally toward the central part of the basin and to the west, northwest, and southeast parts (fig. 2). However, the remaining body of the Gallup aquifer is cut off in a northwest-southeast pattern such that flow of water is not continuous throughout the entire basin (fig. 3). The Gallup aquifer occurs under both water-table and artesian conditions. Water wells generally are near the western and southern margins of the basin and primarily in McKinley County; flowing wells are mostly in the northern part of the county. The reported or measured discharge from 32 water wells completed in the Gallup aquifer ranges from 1 to 645 gal/min and the median is 30 gal/min (Kernodle and others, 1989). Water levels significantly below land surface were found in the Grants mineral belt near Crownpoint and near Gallup, New Mexico, and Window Rock, Arizona.

Dakota Aquifer

The Dakota aquifer is a hydrogeologic unit corresponding to the Dakota Sandstone. The Dakota Sandstone generally is thought to be of earliest Late Cretaceous age, although the lowermost part may be of latest Early Cretaceous age (Fassett, 1977, p. 225). The Dakota crops out around the basin margins where it typically caps mesas and forms erosion-resistant dip slopes and hogbacks. The Dakota Sandstone unconformably overlies the Morrison Formation (Late Jurassic age) throughout much of the basin; however, it unconformably overlies the Burro Canyon Formation (Early Cretaceous age) in the northern part of the basin (fig. 3). The upper contact of the Dakota is conformable with the Mancos Shale, and intertonguing of these two units is common near the contact. Stratigraphy of the Dakota is complex. The unit consists of a main sandstone body in the north, which branches into various members and tongues depending on location in the San Juan Basin. Thickness of the Dakota generally ranges from a few tens of feet to about 500 ft; Stone and others (1983, p. 37) reported that a range of 200 to 300 ft probably is

common. Data reported by Molenaar (1977b, p. 160-161) and Stone and others (1983, fig. 66) and data obtained from Petroleum Information Corporation, Denver, Colorado, indicate that the thickness of the Dakota generally increases from the western, northwestern, and northern margins of the basin toward the eastern, southeastern, and southern margins. Depth to the Dakota ranges from zero in areas of outcrop to about 8,500 ft in the northeastern part of the basin. The top of the Dakota decreases from a maximum altitude of about 9,500 ft along the northern basin margin to about 1,500 ft below sea level in the northeastern part of the study area (Craigg and others, 1989).

The Dakota was deposited on an erosional surface in this region; the strata represent a transition from nonmarine alluvial-plain deposition in the lower part of the aquifer to marine shorezone deposition in the upper part. Marine and nonmarine depositional environments were interpreted by Walters and others (1987); the primary depositional area for nonmarine rocks was along the west side of the present basin. The Dakota contains three principal lithologies in different parts of the basin. It typically consists of a sequence of buff to brown, crossbedded, poorly sorted, coarse-grained conglomeratic sandstone and moderately sorted, medium-grained sandstone in the lower part; dark-gray carbonaceous shale with brown siltstone and lenticular sandstone beds in the middle part; and yellowish-tan, fine-grained sandstone interbedded with gray shale in the upper part (Owen, 1973, p. 39-48; Merrick, 1980, p. 45-47). Mineralogy, in mean percentage, as determined by Walters and others (1987, p. 269), for the marine (first number) and nonmarine (second number) deposits consists of the following: quartz (28 percent, 26 percent), illite (22 percent, 32 percent), kaolinite (16 percent, 22 percent), calcite (8.3 percent, 0.87 percent), dolomite (7.3 percent, 0.42 percent), mixed clay (5.7 percent, 9.8 percent), smectite (4.4 percent, 2.9 percent), potassium feldspar (4.2 percent, 4.7 percent), chlorite (2.7 percent, 0.29 percent), and plagioclase (2.4 percent, 1.3 percent).

The Dakota aquifer is a source of water for domestic, livestock, and industrial uses, and water wells generally are near the margins of the basin. Water in the Dakota aquifer occurs under both water-table and artesian conditions. Recharge to the aquifer is from infiltration of precipitation and streamflow on outcrops and from vertical leakage of water through confining beds. Within the basin, areas of stress from ground-water development in the Dakota aquifer are localized. These areas may represent oil or gas production, injection for disposal of brine, secondary recovery or repressurization of producing zones, or uranium-mine dewatering of the underlying Morrison aquifer that induces downward flow in the Dakota. The reported or measured discharge from 29 water wells completed in the Dakota aquifer ranged from 1 to 200 gal/min and the median is 13 gal/min (Craigg and others, 1989). Water levels in numerous wells were several hundred feet below land surface. Only one well, in the northwestern part of the basin, was flowing.

Morrison Aquifer

The Morrison aquifer is a hydrogeologic unit corresponding to the Morrison Formation. The Morrison Formation is of Late Jurassic age (Cadigan, 1967, p. 6) and crops out around the basin margins. Major sandstones in the Morrison typically form erosion-resistant cliffs and dip slopes, whereas shale units form topographic saddles. The Morrison is present throughout the San Juan Basin (Green and Pierson, 1977, p. 151) and conformably overlies the Wanakah Formation or Cow Springs Sandstone of Late Jurassic age (Condon and Peterson, 1986, p. 24) throughout most of the basin. In the northern part of the basin, the Morrison conformably overlies and probably intertongues with the Junction Creek Sandstone of Late Jurassic age (fig. 3). In the San Juan Basin, the Morrison Formation consists of five members (Gregory, 1938; Craig and others, 1955; Cadigan, 1967; Green and Pierson, 1977; Owen, 1984). These members, in ascending

order, are: the Salt Wash Member, Recapture Member, Westwater Canyon Member, Brushy Basin Member, and Jackpile Sandstone Member. The thickness of the Morrison ranges from about 200 ft near Grants to about 1,100 ft in the northwestern part of the basin (Dam and others, 1990a). Depth to the top of the Morrison ranges from zero in areas of outcrop to about 8,500 ft in the northeastern part of the basin (Dam and others, 1990a). The top of the Morrison decreases from a maximum altitude of about 10,000 ft along the northern basin margin to about 1,500 ft below sea level in the northeastern part of the basin. Morrison Formation strata were deposited in various continental environments including eolian, stream channels, flood plains, and lakes (Green and Pierson, 1977, p. 151; Turner-Peterson and others, 1986). A semiarid to arid climate existed during deposition of the Morrison (Turner-Peterson and Fishman, 1989).

The Morrison Formation generally consists of yellowish-tan to pink, fine- to coarse-grained, locally conglomeratic sandstones, which are interbedded with sandy siltstones and green to reddish-brown shales and claystones; minor limestone beds also are in the aquifer (Woodward and Schumacher, 1973, p. 3-5; Green and Pierson, 1977, p. 151; Stone and others, 1983, p. 38). The Salt Wash Member was deposited by meandering and braided streams and consists of very fine to medium-grained sandstone interbedded with mudstone (Hansley, 1990, p. H4). The Recapture Member was deposited in fluvial, lacustrine, and eolian environments; lithology consists of very fine to fine-grained sandstones interbedded with mudstones and claystones. The Westwater Canyon Member was deposited by braided streams draining source areas in the western and southwestern parts of the basin. Sandstones are fine to medium grained and locally conglomeratic; interbedded mudstones and claystones are bentonitic (Hansley, 1990). The Brushy Basin Member consists of thick bentonitic to zeolitic mudstones interbedded with thin fluvial sandstones that were deposited in a saline, alkaline lake. The Jackpile Sandstone Member was deposited in the southeastern part of the basin by braided streams; sandstones are fine to medium grained and locally conglomeratic.

Hansley (1986 and 1990) described in detail the mineralogy and diagenesis of members of the Morrison Formation. Minerals from core samples in the southern part of the basin and from outcrop samples along the rim of the basin include amorphous silica, potassium feldspar, albite, calcite, anhydrite, barite, hematite, pyrite, garnet, staurolite, and zeolite. Whitney and Northrop (1987, p. 357) examined clay mineralogy and found smectite, interstratified illite/smectite, chlorite, and kaolinite. Crossey (1989) recognized two groups of clay minerals on the basis of grain size in the Westwater Canyon Member: (1) coarse-grained lithologies contain a mixed-layer illite/smectite that is highly expandable, kaolinite, and chlorite; and (2) fine-grained lithologies contain a more illitic mixed-layer illite/smectite with traces of chlorite.

The initial interpretation of the ground-water flow system in the Morrison aquifer is based on work by Kelly (1977), Frenzel and Lyford (1982), Stone and others (1983), and data from the files of the U.S. Geological Survey, Albuquerque, New Mexico. The conceptual model of the flow system in the Morrison aquifer assumed the Westwater Canyon Member to be the only significant regional aquifer (Kelly, 1977); the other members were considered important only as local aquifers. The Brushy Basin and Recapture Members were thought to serve as semiconfining layers above and below the Westwater Canyon throughout the basin except in the southwestern part where the Brushy Basin is absent.

Flow in the Morrison aquifer previously was assumed to be two dimensional. Vertical leakage into the Morrison from above or below was unknown and assumed to be negligible (Stone and others, 1983, p. 23). Minimal hydraulic-head data not representing a single time period were available for units overlying and underlying the Morrison to determine vertical flow

components. Data for the Dakota and Morrison aquifers were for 1985-86 and data for the Entrada Sandstone were pre-1959. Figure 5 shows a comparison of hydraulic heads for the Dakota aquifer and the Entrada relative to the Morrison aquifer. Hydraulic heads for the Dakota aquifer and Entrada were measured in the well, whereas hydraulic heads for the Morrison aquifer were interpolated from the Morrison potentiometric-surface map for that well site. The heads for wells in the Dakota (for 1985-86) generally are lower than those interpolated from the Morrison potentiometric surface.

Underlying the Morrison aquifer is the Wanakah Formation; however, no hydraulic-head data were available for this formation. The Entrada Sandstone underlies the Wanakah Formation. The only head data available for the Entrada were obtained from a dissertation by Berry (1959), which contains a potentiometric-surface map of the Entrada with five data points. The dates of measurement for these wells are unknown, but they were made prior to 1959. The head values for the Entrada indicate a northerly flow direction similar to the Morrison aquifer. Figure 5 shows the estimated hydraulic-head differences between the Entrada Sandstone and the Morrison aquifer at the locations of five wells. Comparison of heads in the Entrada (pre-1959) with those in the Morrison (1985-86) (fig. 5) shows that the Entrada heads in four wells were from 13 to 110 higher than in the Morrison. Because hydraulic-head values in the Morrison had declined, pre-1985 water levels in the Morrison were sought for comparison with pre-1959 water levels. Hydrographs for three wells completed in the Morrison aquifer that span the period 1957-90 were used to determine water-level trends in the Morrison during this time. These hydrographs, shown in figure 6, indicate a decline in hydraulic head in the Morrison during this period. The declines range from approximately 4 feet to more than 70 feet. Although the declines in the Morrison are shown for almost a 30-year period, the declines are believed to have occurred after the mid- to late 1970's when uranium test drilling was conducted and many of the test holes were completed as wells in the Morrison aquifer and allowed to flow continuously. On the basis of these tentative comparisons, even with the declines in the Morrison of as much as 70 feet, the head in the Entrada would still be several tens of feet higher than the head in the Morrison. Therefore, an upward component of flow into the Morrison aquifer is assumed.

The potentiometric contours shown in figure 7 indicate that recharge to the Morrison aquifer north of the Chuska Mountains along the New Mexico-Arizona State line has a significant component that is north, parallel to the north-trending outcrop. Along the north flanks of the Chuska Mountains, the Morrison dips primarily to the east, but northward the easterly dip flattens and a northerly dip develops toward the Four Corners Platform (fig. 2). This change in dip accounts for the much larger outcrop area, and recharge in this area moves north parallel to the outcrop to the discharge area near Four Corners.

The discharge areas for the Morrison are considered to be in the northwestern part of the area near Four Corners where the San Juan River has breached the Morrison aquifer, the southwestern part of the area southwest of Gallup, and the southeastern part of the area northeast of Grants (see fig. 2 for general areas of discharge as indicated by converging arrows). In the northwestern part of the basin north of the Chuska Mountains, the general gradient is to the north (fig. 7); in the area northeast of the city of Gallup, areas of localized dewatering for uranium mining have resulted in substantial head declines.

The reported or measured discharge from 53 water wells completed in the Morrison aquifer ranges from 1 to 401 gal/min; the median discharge is 32 gal/min (Dam and others, 1990a). Heads of wells completed in the Morrison Formation are typically above land surface in San Juan County and below land surface in McKinley and Cibola Counties.

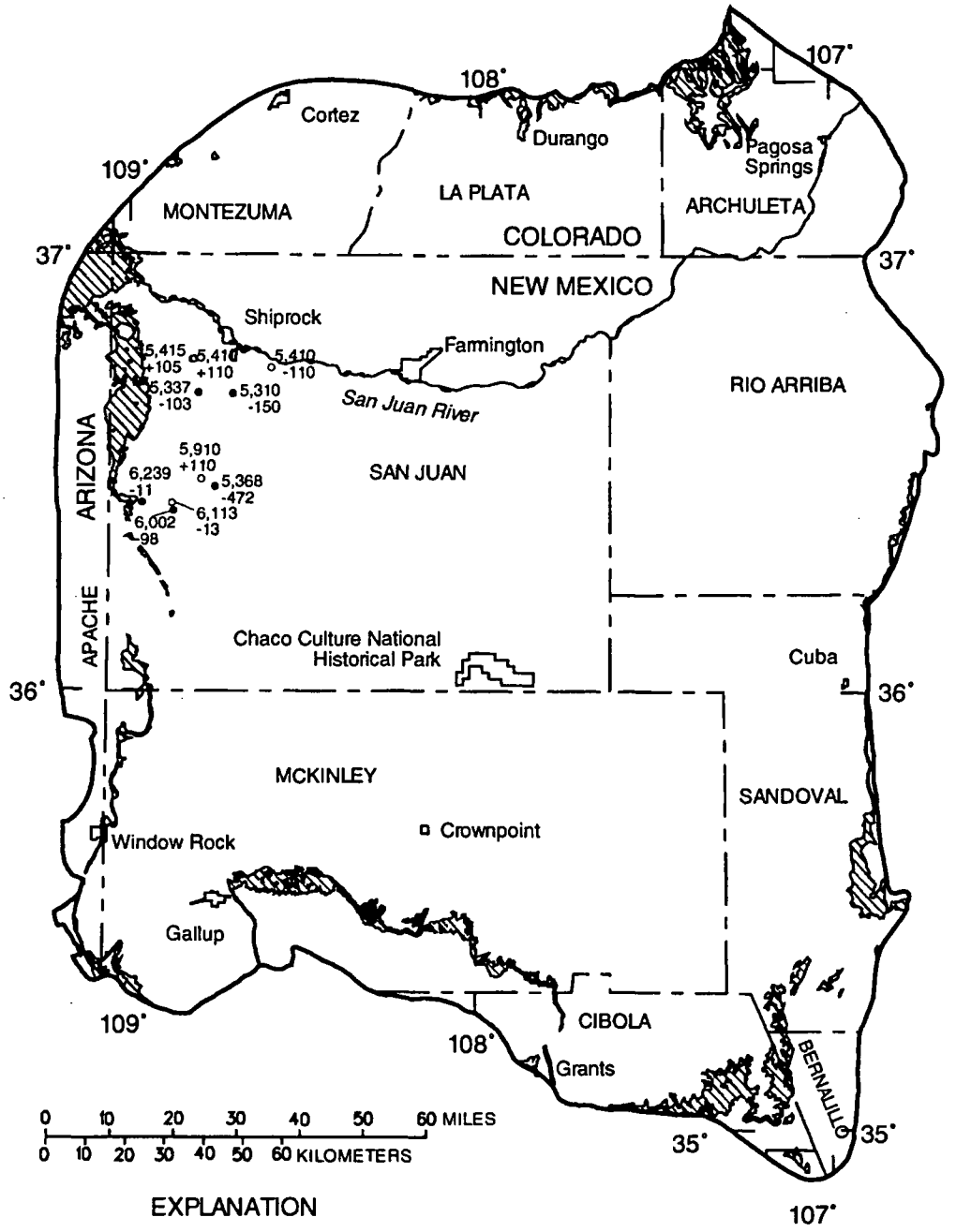

Figure 5.--Hydraulic heads in the Dakota aquifer and Entrada Sandstone relative to the Morrison aquifer, 1985-86.

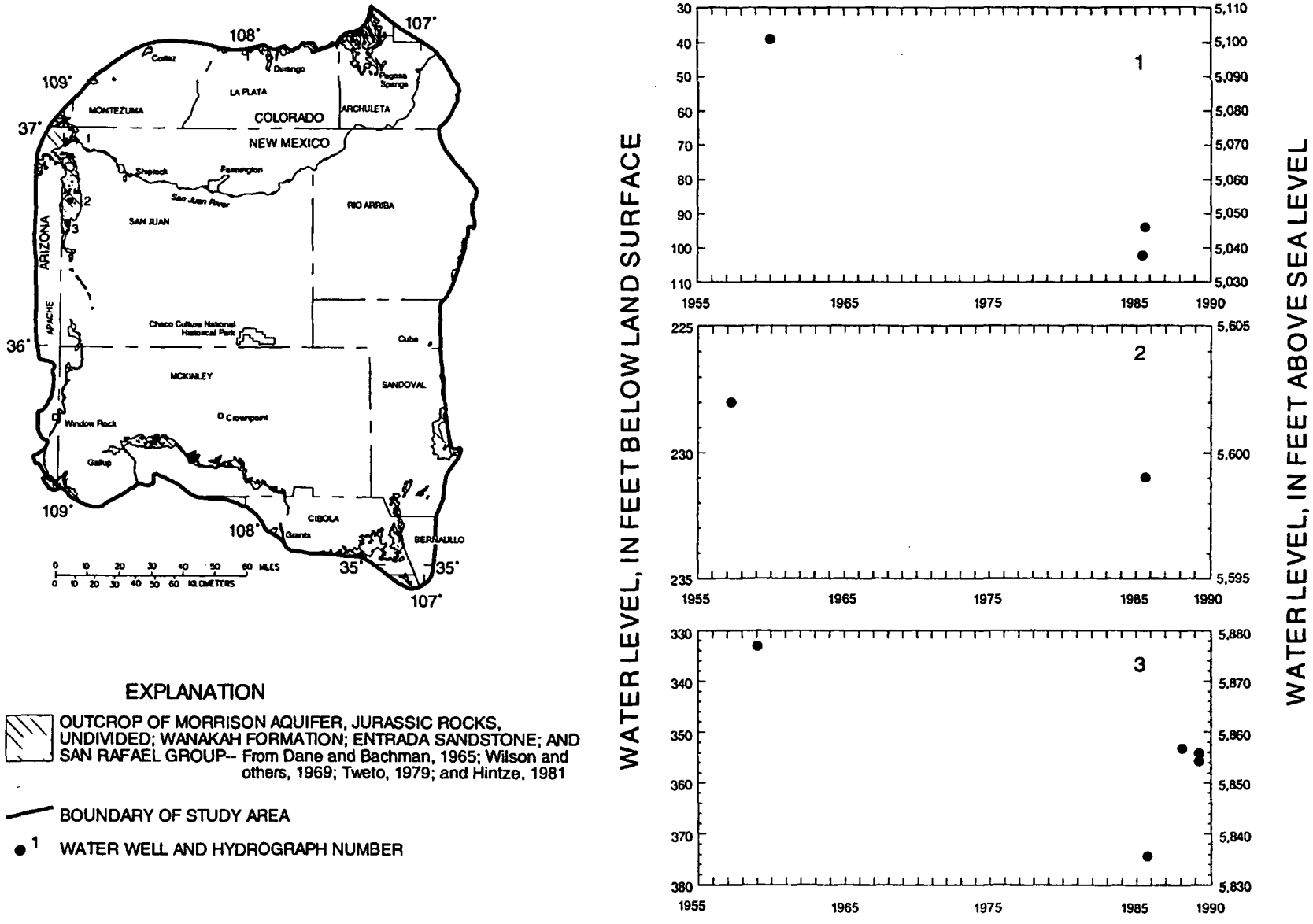

Figure 6.--Water-level hydrographs for three wells completed in the Morrison aquifer, 1957-87.

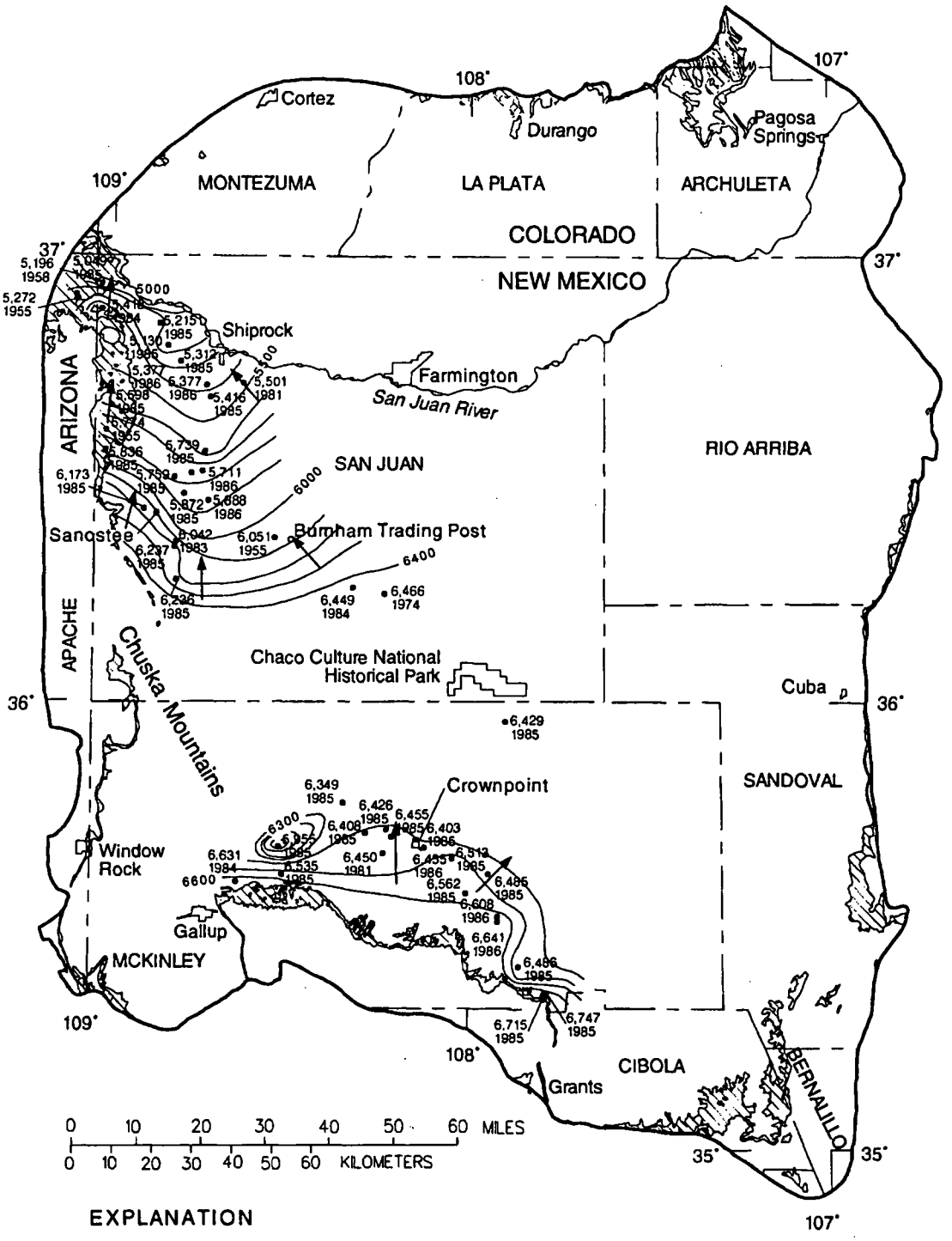

Figure 7.--Potentiometric surface of the Morrison aquifer, 1985-86.

GEOCHEMISTRY OF GALLUP, DAKOTA, AND MORRISON AQUIFERS

This section describes the methods used to collect the data including essential water well information. Geochemical data are discussed by type of constituent including major, minor, and trace elements; gases; and isotopes. Physical and geochemical processes controlling solute concentrations then are evaluated.

Methods

The field sampling methods used to collect the geochemical data are detailed in Dam (1988) and follow standard USGS procedures (Claassen, 1982; Knapton, 1985). Nonflowing wells were pumped for a sufficient duration to remove at least three borehole volumes of water. Field techniques were used to measure specific conductance, pH, temperature, DO, alkalinity, and sulfide. Alkalinity was used to calculate HCO_3^- and CO_3. Samples were collected and preserved for analysis of major, minor, and trace elements; stable and radioactive isotopes; and dissolved-organic carbon. Dissolved gases were collected in the field using double-chamber glass tubes under a vacuum. Carbon-14 samples were collected onsite by precipitation of strontium carbonate in a stainless-steel tank as described in Dam (1988). Chloride-36 samples were treated with nitric acid and silver nitrate to precipitate silver chloride and stored in light-proof brown bottles. An anion-exchange resin was used to concentrate chloride when chloride concentration was less than 10 mg/L. Preparation of the ^{36}Cl samples for analysis (primarily to remove interfering sulfur-36) is described in Jones and Phillips (1990).

All samples collected for laboratory analysis of major, minor, and trace elements were analyzed at the USGS National Water Quality Laboratory (NWQL) in Denver, Colorado. Gas samples were kept on ice and sent to the USGS laboratory in Reston, Virginia, for analysis. These samples were analyzed for N, oxygen, Ar, CO_2, methane, and ethane. Rapid analysis was necessary to ensure that loss of vacuum did not result in sample contamination from the air. Stable isotopes of oxygen and hydrogen and the radioisotope ^3H were analyzed at the USGS laboratory in Reston, Virginia. Carbon-13/carbon-12 and sulfur-34/sulfur-32 stable isotopes were analyzed by Global Geochemistry, and ^{14}C isotopes were analyzed by Kruger, Inc. These laboratories are under contract to the NWQL. The University of Rochester, in Rochester, New York, analyzed ^{36}Cl isotopes using a tandem accelerator mass spectrometer.

Geochemical data for analysis and interpretation were obtained by sampling 38 wells and using analyses from the USGS NWIS (National Water Information System) data base for 21 wells (figs. 8-10). Locations of water wells sampled for geochemical data are shown in figure 8 for the Gallup aquifer (wells 1-10), in figure 9 for the Dakota aquifer (wells 11-13), and in figure 10 for the Morrison aquifer (wells 14-38). The abundance of wells completed in the Morrison aquifer is a result of uranium exploration (without development or mining) in the early 1980's. Additional chemical analyses obtained from the NWIS data base augmented the geochemical data for the Gallup (15 wells) and Dakota (6 wells) aquifers.

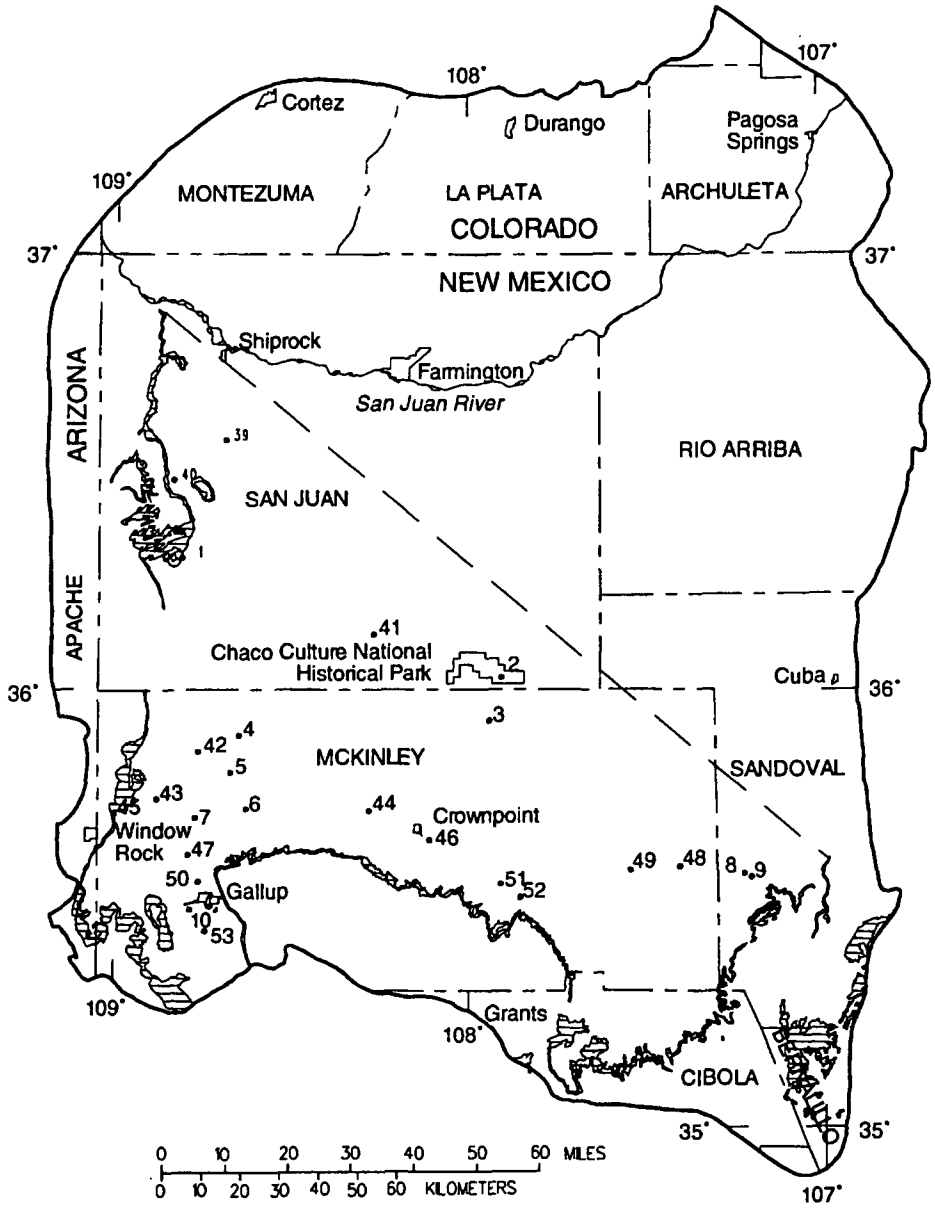

EXPLANATION

OUTCROP OF GALLUP AQUIFER--In Arizona includes Pescado Tongue of Mancos Shale. In southeastern part of the study area mapped as part of the Mesaverde Group, undivided. From Dane and Bachman, 1965, and Hackman and Olson, 1977

APPROXIMATE SUBSURFACE EXTENT OF GALLUP AQUIFER--From Molenaar, 1973

BOUNDARY OF STUDY AREA

• 1 WATER WELL--Wells 1-10 were sampled from 1986 to 1989; wells 39-53 were sampled prior to 1986 and the analyses are from the National Water Information System data base

Figure 8.--Location of sampled water wells completed in the Gallup aquifer.

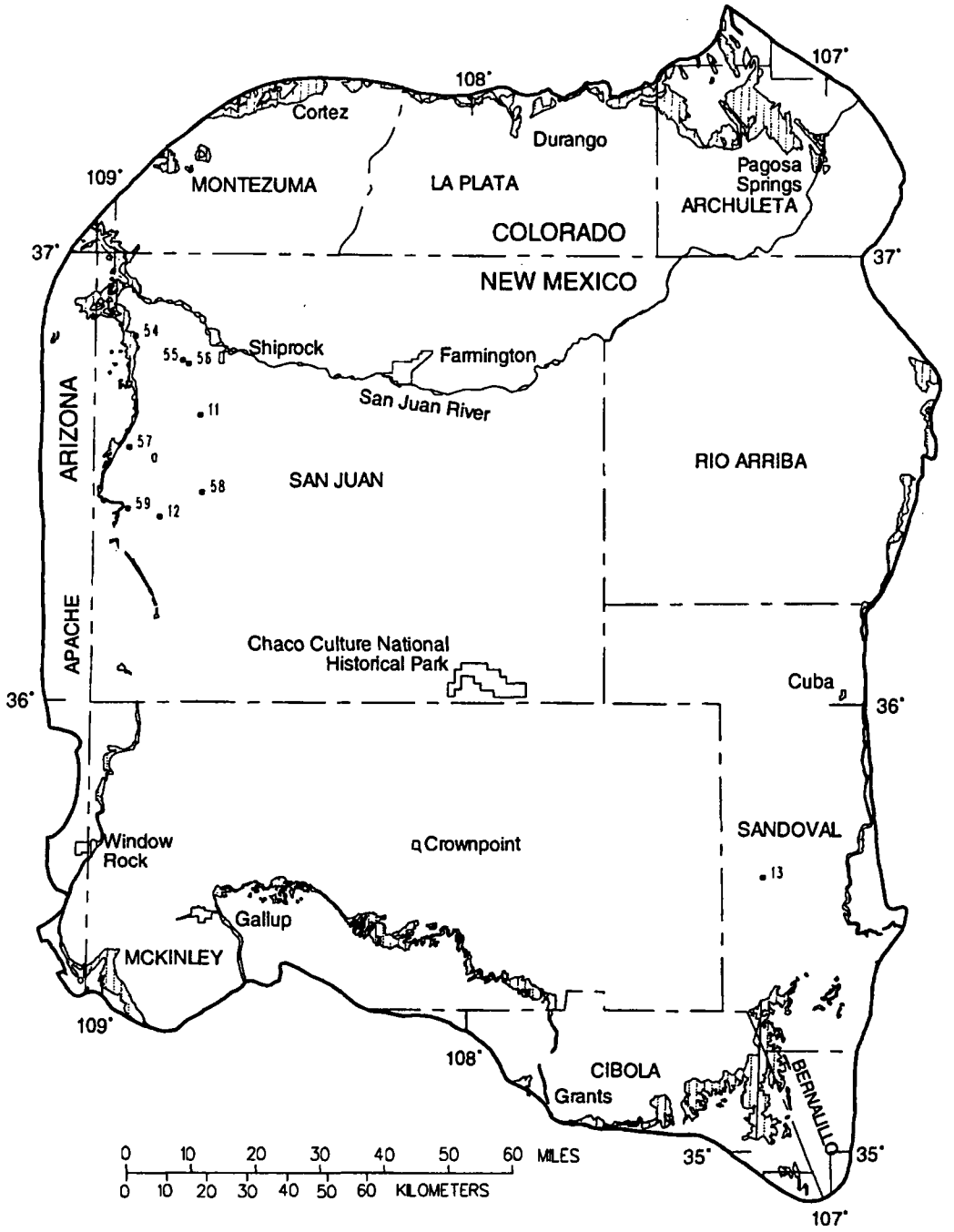

EXPLANATION

OUTCROP OF DAKOTA AQUIFER, MANCOS SHALE, AND BURRO CANYON FORMATION--From Dane and Bachman, 1965; Wilson and others, 1969; and Tweto, 1979

BOUNDARY OF STUDY AREA

•11 WATER WELL--Wells 11-13 were sampled from 1986 to 1989; wells 54-59 were sampled prior to 1986 and the analyses are from the National Water Information System data base

Figure 9.--Location of sampled water wells completed in the Dakota aquifer.

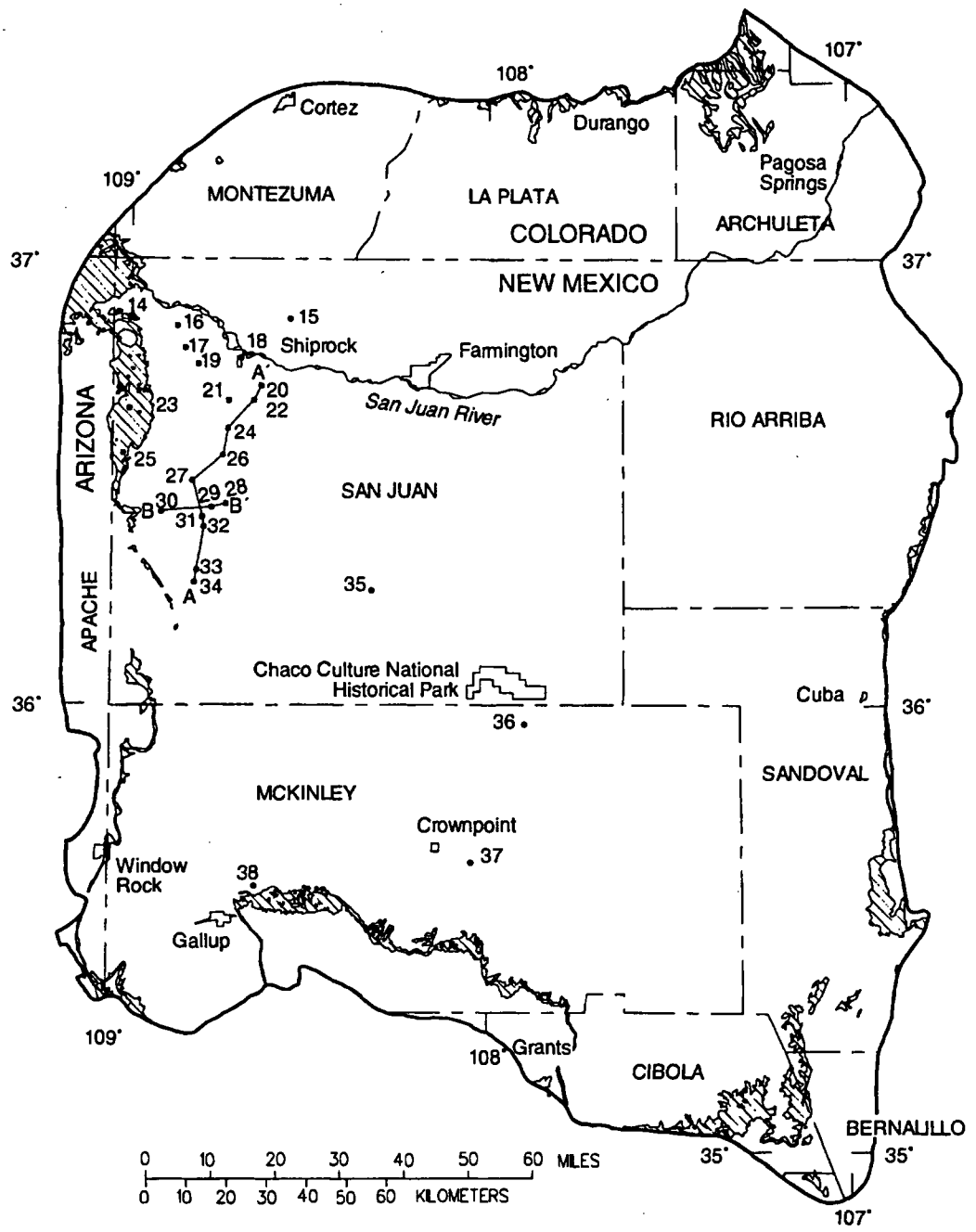

EXPLANATION

OUTCROP OF MORRISON AQUIFER, JURASSIC ROCKS, UNDIVIDED; WANAKAH FORMATION; ENTRADA SANDSTONE; AND SAN RAFAEL GROUP--From Dane and Bachman, 1965; Wilson and others, 1969; Tweto, 1979; and Hintze, 1981

BOUNDARY OF STUDY AREA

A —— A' LINE OF GEOHYDROLOGIC SECTION--See figure 11

• 14 WATER WELL--Wells 14-38 were sampled from 1986 to 1989

Figure 10.--Locations of sampled water wells completed in the Morrison aquifer and of geohydrologic sections.

Table 1 provides data pertaining to the 38 wells sampled from 1986 to 1989. Well depths range from 150 to 5,250 ft. The part of the Gallup, Dakota, or Morrison aquifer that was sampled, as shown in table 1, is the thickness of the interval open to the aquifer; the interval thickness ranges from 31 to 876 ft. Most wells sampled were completed as open holes, so water was obtained from the entire open interval as opposed to one or more perforated intervals in the casing. Eight wells were completed with multiple perforated intervals so the well was open to selected zones; the perforated intervals were summed to determine the total thickness of the interval open to the aquifer that was sampled (table 1). Two geohydrologic sections for 12 wells completed in the Morrison aquifer are shown in figure 11. Section A-A' depicts nine wells in a north-trending line. Well 32 is the only well open solely to the Westwater Canyon Member; the other wells are open to varying combinations of the Westwater Canyon, Recapture, or Salt Wash Members of the Morrison Formation. Several wells are completed below the Morrison aquifer and open to the Wanakah Formation. Section B-B' depicts three wells in an east-trending line. Wells 29 and 30 are completed solely in the Morrison aquifer, whereas well 28 extends 155 feet into the Wanakah Formation. Flowing, artesian conditions occurred at most wells, facilitating sample collection. Most of these wells (22 of 29) (table 1) had the capacity to be shut in for a head measurement and therefore could be turned off after sampling was completed. However, seven wells (7, 11, 18, 20, 21, 32, and 33) could not be shut in for a head measurement or turned off to prevent continuous discharge. Six wells were equipped with windmills with positive-displacement piston pumps and three wells were equipped with submersible pumps. These data are listed in table 1.

Table 1.--Data for wells sampled from 1986 to 1989

[See figures 8-10 for location of wells. Type of lift: F, natural flow; P, piston; S, submersible. --, not reported]

Well number	Aquifer	Altitude of land surface (feet above sea level)	Depth of well (feet below land surface)	Thickness of interval open to aquifer (feet)	Type of lift	Shut-in capacity for flowing wells
1	Gallup	5,890	150	--	F	Yes
2	Gallup	6,195	3,090	60	F	Yes
3	Gallup	6,401	--	--	F	Yes
4	Gallup	5,990	1,239	80	F	Yes
5	Gallup	6,048	1,743	160	F	Yes
6	Gallup	6,379	1,082	502	P	--
7	Gallup	6,365	1,850	225	F	No
8	Gallup	6,430	969	64	F	Yes
9	Gallup	6,165	602	120	F	Yes
10	Gallup	6,515	667	64	S	--
11	Dakota	5,342	1,464	555	F	No
12	Dakota	6,035	521	147	P	--
13	Dakota	6,130	1,840	55	F	Yes
14	Morrison	5,545	604	342	P	--
15	Morrison	5,440	2,736	430	S	--
16	Morrison	5,120	2,000	782	F	Yes
17	Morrison	5,100	2,035	691	F	Yes
18	Morrison	4,941	1,777	295	F	No
19	Morrison	5,270	2,013	280	F	Yes
20	Morrison	5,060	2,300	788	F	No
21	Morrison	5,290	2,597	770	F	No
22	Morrison	5,139	2,520	747	F	Yes
23	Morrison	5,831	555	60	P	--
24	Morrison	5,270	2,682	876	F	Yes
25	Morrison	6,206	702	149	P	--
26	Morrison	5,522	1,992	247	F	Yes
27	Morrison	5,735	1,912	526	F	Yes
28	Morrison	5,595	2,034	834	F	Yes
29	Morrison	5,670	1,912	505	F	Yes
30	Morrison	6,090	1,751	275	F	Yes
31	Morrison	5,840	2,125	613	F	Yes
32	Morrison	5,830	1,691	410	F	No
33	Morrison	5,905	2,349	858	F	No
34	Morrison	6,010	2,518	768	F	Yes
35	Morrison	5,750	5,250	250	F	Yes
36	Morrison	6,330	3,988	31	F	Yes
37	Morrison	6,795	2,605	400	S	--
38	Morrison	6,825	410	110	P	--

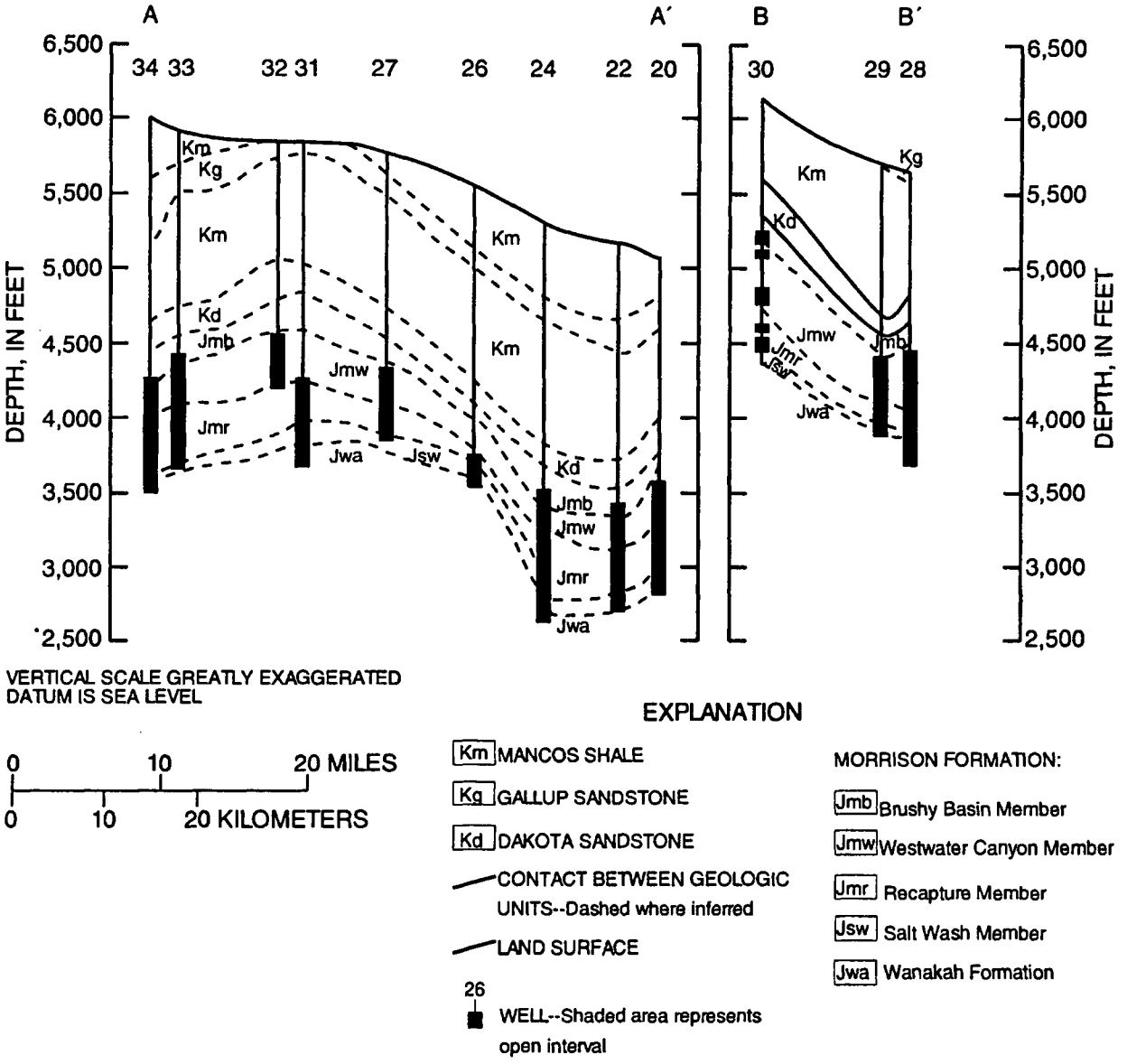

Figure 11.--Geohydrologic sections showing well completion in the Morrison aquifer. Lines of section are shown in figure 10 (modified from Dam, 1988).

Major Constituents and pH

Chemical analyses are shown for 61 water samples collected during 1986 through 1989 from 38 wells completed in the Gallup (table 2), Dakota (table 3), and Morrison aquifers (table 4). In addition, data from NWIS are presented for the Gallup aquifer (15 wells) and the Dakota aquifer (6 wells). Several wells, particularly wells completed in the Morrison aquifer, were sampled more than once during 1986 through 1989 to supplement the initial suite of constituents collected and to identify a possible change of constituent concentrations with time.

Concentrations of major ions (Ca^{2+}, Mg^{2+}, Na^{+}, K^{+}, HCO_3^{-}, CO_3^{2-}, SO_4^{2-}, and Cl^{-}) generally were found to be reproducible in samples collected from the Gallup and Dakota aquifers. Concentrations of major ions were found to change over time for samples collected from several wells completed in the Morrison aquifer.

Three of 10 wells in the Gallup aquifer were sampled twice between 1986 and 1987. Major ion concentrations differed by less than 10 percent for Na^{+}, alkalinity, and SiO_2^{0} (table 2). Only one of three wells completed in the Dakota aquifer that were sampled during the investigation was sampled twice (table 3). Differences greater than 10 percent were detected between Ca^{2+}, Mg^{2+}, Na^{+}, and K^{+} concentrations from two analyses for well 13. However, SO_4^{2-}, Cl^{-}, and several other properties and constituents differed by less than 10 percent between the two analyses. Three of six chemical analyses obtained from the NWIS data base for the Dakota aquifer indicated that major ion concentrations were within 10 percent (table 3).

Fifteen of 25 wells completed in the Morrison aquifer were sampled more than once between 1986 and 1989 (table 4). Concentrations of major ions in water samples collected from 9 of the 15 wells were reproducible within 10 percent. Thus, concentrations of several major ions in samples collected from 6 of 15 wells differed by more than 10 percent. Concentrations of Ca^{2+}, HCO_3^{-}, and Cl^{-} varied between sampling periods for wells 18, 20, 22, 25, 28, and 33, and Mg^{2+}, Na^{+}, and SO_4^{2-} concentrations varied by more than 10 percent in samples from wells 20 and 28. Because major ion concentrations in water from well 30 were nearly identical except for Cl^{-}, which changed from 4.7 to 2.7 mg/L, and for K^{+}, which changed from 2.3 to 1.9 (table 4), well 30 was not included with the six wells.

Several factors may contribute to the non-reproducibility of the samples with time. These include discharge of large volumes of water between sampling periods, a large open interval, and pump type–such as piston, which can introduce oxygen into the water resulting in chemical reactions. The range in discharge at wells 18, 20, 22, and 33 was 16 to 65 gal/min. At a discharge rate of only 20 gal/min over the minimum duration of 354 days between the 1986 and 1987 sampling dates, more than 10 million gal of water would have been discharged at each of these four wells. However, well 32 flowed continuously for the 3 years of sample collection, 1986-88, yet analytical results were reproducible within 10 percent. A smaller open interval for well 32 (410 ft) compared with well 33 (858 ft) may account for the difference in analytical results. Well 28 was constructed with a large open interval (834 ft) (table 1). Well 25 was constructed with a relatively small open interval (149 ft) (table 1); however, a windmill piston pump was used to obtain the water sample.

Table 2.–Selected properties of and constituents in water from the Gallup aquifer

[See figure 8 for location of wells; pH, standard units; °C, degrees Celsius; concentrations in milligrams per liter; <, less than; –, not reported]

Well number	Date of sample	Field pH	Temperature (°C)	Dissolved oxygen	Sulfide (H_2S+HS^-)	Calcium (Ca^{2+})	Magnesium (Mg^{2+})	Sodium (Na^+)	Sodium plus potassium (Na^++K^+)	Potassium (K^+)	Bicarbonate (HCO_3^-)	Carbonate (CO_3^{2-})	Alkalinity (as $CaCO_3$)	Sulfate (SO_4^{2-})	Chloride (Cl^-)	Fluoride (F^-)	Bromide (Br^-)	Iodide (I^-)	Silica (SiO_2^0)	Dissolved solids
1	07-01-88	7.90	16.7	1.2	<0.05	42	17	96	--	6.4	310	0	254	120	7.8	0.30	0.074	0.006	14	455
2	04-22-86	8.20	32.8	--	--	10	2.1	630	--	3.3	380	0	307	910	46	1.6	.18	.004	17	1,799
	10-21-87	8.33	32.9	--	.14	7.4	2.4	670	--	3.2	334	10	290	1,100	49	1.6	.066	.005	16	2,000
3	04-21-86	8.60	32.7	--	--	7.0	1.2	669	--	2.3	240	10	213	1,000	81	.70	.16	.004	17	1,900
4	07-15-88	8.57	24.4	--	.15	1.2	.28	220	--	1.1	451	14	394	84	4.1	1.2	.034	.005	12	559
5	06-30-87	8.81	26.0	--	--	3.8	.18	400	--	1.0	295	22	277	530	44	1.2	.15	.006	12	1,200
	06-28-88	8.81	25.0	--	.14	3.6	.15	400	--	.90	288	17	264	550	45	1.1	--	--	12	--
6	06-30-88	8.99	19.9	--	--	1.7	.62	230	--	.70	336	22	311	180	5.0	.70	.054	.005	11	639
7	06-28-88	9.00	20.7	--	.11	2.3	.29	140	--	.70	222	14	206	84	9.5	.30	.056	.005	13	374
8	12-03-87	8.73	18.4	--	.05	5.2	2.0	630	--	2.4	252	10	224	1,200	23	.60	.11	.004	12	2,000
9	04-29-86	9.10	18.0	--	--	1.4	.03	129	--	.80	259	20	244	31	4.3	.50	.044	.008	12	330
	08-11-87	8.83	18.0	--	.12	1.3	.31	130	--	.70	293	26	244	35	3.3	.70	--	--	13	330
10	06-30-88	9.20	16.9	--	--	.28	.06	170	--	.70	290	17	266	85	20	.80	.068	.005	9.9	444
39	05-26-64	7.8	18.5	--	--	33	6.7	--	1,000	--	410	0	336	1,700	180	3.5	--	--	12	3,200
40	07-03-74	8.0	--	--	--	400	120	150	--	2.0	170	13	161	1,500	20	.4	--	--	--	2,700
41	10-29-74	8.5	--	--	--	4.2	.7	580	--	3.6	520	19	457	480	240	3.0	--	--	16	1,600
42	10-14-64	7.8	--	--	--	37	11	--	25	--	200	0	167	19	2.8	.4	--	--	14	210
43	09-08-69	8.2	--	--	--	74	15	37	--	2.0	240	7	209	95	9.9	.3	--	--	--	390
44	01-28-72	8.2	--	--	--	12	4.8	120	--	2.0	190	0	156	140	4.6	.6	--	--	--	430
45	01-20-71	8.0	--	--	--	92	17	36	--	2.0	260	0	213	140	7.1	.5	--	--	--	450
46	03-10-70	7.8	--	--	--	80	26	87	--	5.0	270	0	221	260	8.9	.4	--	--	--	650
47	07-31-70	8.4	32.0	--	--	11	3.0	270	--	2.7	280	6	243	310	50	.8	--	--	16	810
48	09-19-62	8.2	24.5	--	--	9.5	2.1	720	--	3.0	310	0	254	1,200	42	.8	--	--	13	2,190
49	10-02-62	7.9	24.0	--	--	9.4	5.0	360	--	3.0	280	0	230	560	12	.8	--	--	14	1,100
50	10-14-64	8.5	--	--	--	12	3.6	--	220	--	250	7	205	270	21	.5	--	--	16	680
51	07-18-73	8.1	--	--	--	100	36	180	--	3.1	210	10	189	580	7.1	.7	--	--	--	1,100
52	09-18-62	8.8	20.0	--	--	3.1	.9	400	--	1.8	350	18	315	440	73	1.2	--	--	15	1,100
53	08-30-57	8.4	15.5	--	--	11	3.3	--	440	--	610	8	500	200	180	4.4	--	--	10	1,200

Table 3.--Selected properties of and constituents in water from the Dakota aquifer

[See figure 9 for location of wells; pH, standard units; °C, degrees Celsius; concentrations in milligrams per liter; --, not reported; >, greater than]

Well number	Date of sample	Field pH	Temperature (°C)	Sulfide (H_2S+HS^-)	Calcium (Ca^{2+})	Magnesium (Mg^{2+})	Sodium (Na^+)	Sodium plus potassium (Na^++K^+)	Potassium (K^+)	Bicarbonate (HCO_3^-)	Carbonate (CO_3^{2-})	Alkalinity (as $CaCO_3$)	Sulfate (SO_4^{2-})	Chloride (Cl^-)	Fluoride (F^-)	Bromide (Br^-)	Iodide (I^-)	Silica (SiO_2^0)	Dissolved solids
11	07-23-87	8.47	18.1	0.05	21	11	390	--	3.8	277	10	241	640	57	0.90	0.16	0.006	8.6	1,300
12	06-29-88	8.78	18.1	--	2.0	.16	100	--	1.1	215	10	192	25	2.6	.30	.038	.005	12	262
13	04-29-86	8.90	19.5	--	2.3	1.1	700	--	1.7	390	30	376	910	85	1.5	.24	.005	10	1,900
	12-03-87	8.91	19.5	>1.5	170	95	270	--	2.2	--	--	--	980	78	1.6	--	--	11	--
54	04-27-60	7.6	15.5	--	24	.5	780	--	3	280	0	230	1,100	260	2.2	--	--	8.5	2,320
55	09-21-66	8.0	--	--	53	10	1,300	--	11	360	12	315	1,600	720	8.2	--	--	--	3,780
56	06-27-52	--	--	--	19	3.1	--	690	--	170	6	149	980	280	1.3	--	--	13	2,080
	09-21-66	8.4	--	--	19	2.4	690	--	9	140	12	135	1,000	290	2.0	--	--	--	2,060
57	07-22-70	8.6	--	--	7.0	--	320	--	--	260	12	233	480	15	.3	--	--	--	961
	09-24-74	8.6	--	--	6.0	1.2	360		2	250	23	243	470	18	.4	--	--	8.7	1,040
58	06-08-67	9.4	--	--	2.0	1.2	120		--	160	26	175	70	15	.3	--	--	--	302
	01-08-70	9.4	--	--	1.0	--	130		2	180	34	204	68	12	.3	--	--	--	310
59	07-03-74	8.2	--	--	54	7.3	120		2	300	13	268	130	11	.2	--	--	9.8	512

Table 4.–Selected properties of and constituents in water from the Morrison aquifer

[See figure 10 for location of wells; pH, standard units; °C, degrees Celsius; concentrations in milligrams per liter; --, not reported; <, less than detection limit]

Well number	Date of sample	Field pH	Temperature (°C)	Dissolved oxygen	Sulfide (H_2S + HS^-)	Calcium (Ca^{2+})	Magnesium (Mg^{2+})	Sodium (Na^+)	Potassium (K^+)	Bicarbonate (HCO_3^-)	Carbonate (CO_3^{2-})	Alkalinity (as $CaCO_3$)	Sulfate (SO_4^{2-})	Chloride (Cl^-)	Fluoride (F^-)	Bromide (Br^-)	Iodide (I^-)	Silica (SiO_2^0)	Dissolved solids
14	06-10-88	7.56	17.0	--	--		13	42	1.3	286	0	234	79	11	0.60	0.135	0.008	28	361
15	07-21-87	7.52	39.9	--	35	50	28	1,700	18	305	0	250	3,800	210	1.6	.38	.033	33	6,000
16	06-24-86	9.20	19.9	--	--	1.1	.08	130	1.0	244	29	247	33	10	2.0	.050	.006	17	350
	06-08-88	9.37	20.1	--	.07	1.2	.06	140	.90	273	14	248	33	11	2.8	--	--	17	350
17	07-02-86	8.50	23.0	--	--	40	3.4	810	3.6	124	4	110	1,700	61	1.6	.13	.015	13	2,700
18	06-16-86	8.00	31.0	--	--	58	14	800	7.7	58	0	49	1,600	110	2.0	.13	.015	14	2,600
	06-09-87	8.03	31.1	--	<.05	110	14	810	7.2	71	0	60	2,100	57	1.9	--	--	14	3,200
19	07-14-87	7.74	29.1	--	.24	33	12	1,300	9.0	383	0	310	1,500	750	8.0	.05	.073	18	3,800
20	06-19-86	7.60	33.0	--	--	78	31	1,400	19	158	0	130	3,200	190	2.1	.20	.035	16	5,000
	06-10-87	7.80	31.0	--	.18	160	15	890	10	81	0	68	2,500	120	2.1	--	--	14	3,800
21	06-18-86	8.30	--	--	--	39	3	770	4.6	128	0	105	1,600	67	1.1	.15	.021	14	2,600
22	06-19-86	8.00	28.8	--	--	98	25	740	8.2	51	0	48	1,900	60	1.9	.12	.016	16	2,900
	06-10-87	8.03	30.5	--	.07	160	23	690	8.2	57	0	45	2,000	83	2.0	--	--	16	3,000
23	06-10-88	9.65	17.1	--	--	1.3	.06	120	.70	176	26	188	37	23	.80	.235	.018	11	308
24	07-01-86	8.10	18.0	--	--	14	8.1	290	2.7	327	0	265	390	38	1.3	.12	.005	12	920
25	06-09-88	8.87	16.9	5.0	--	14	5.9	54	2.1	156	7	140	21	10	.50	.074	.004	16	213
	04-25-89	9.12	16.0	--	--	5.0	1.6	60	1.0	117	10	112	23	8.3	.40	--	--	10	167
26	06-17-86	9.30	27.2	--	--	1.0	.04	110	.40	143	30	166	52	4.2	.40	.019	.002	19	300
	07-22-87	9.39	27.6	--	.16	2.6	.16	110	.60	176	34	200	35	4.1	.40	--	--	18	290
	07-01-88	9.33	27.1	--	.19	.98	.09	120	.40	159	43	202	48	3.9	.30	--	--	18	310
27	06-18-86	9.40	23.9	--	--	.80	.04	81	.30	156	34	182	9.8	1.1	.30	.014	.002	17	220
	06-11-88	9.65	23.9	--	--	.90	<.01	88	.30	166	29	184	10	.80	.30	--	--	18	230
28	06-30-86	9.33	22.0	--	--	1.8	.20	130	.90	170	36	199	71	28	.40	.032	.006	19	370
	07-17-87	9.45	21.3	--	<.05	3.1	.46	190	1.2	164	38	197	170	64	.90	--	--	17	570
	07-01-88	9.26	21.3	--	--	2.1	.37	160	.90	171	34	196	90	37	.60	--	--	18	430
29	06-29-88	9.51	23.3	--	--	.73	.03	110	.40	200	36	224	24	2.5	.80	.030	.003	16	290
	11-22-88	9.41	20.9	--	--	.86	<.01	120	.50	193	38	222	22	3.0	.70	--	--	17	297
30	07-23-87	8.37	24.0	1.0	<.05	11	.89	68	2.3	200	0	163	13	4.7	2.0	.010	<.001	18	220
	01-05-89	8.58	16.1	--	--	11	.89	70	1.9	200	0	164	13	2.7	.80	--	--	18	216
31	01-05-89	9.06	22.0	--	--	1.3	.06	66	.70	134	22	146	3.0	1.6	.20	--	--	16	174
32	06-24-86	9.05	21.9	--	--	1.0	.07	71	.60	151	14	147	5.6	1.6	.20	.018	.001	19	190
	07-15-87	9.31	22.4	<1.0	.10	.93	.05	72	.60	144	19	148	4.8	1.5	.30	--	--	19	190
	06-11-88	9.42	23.6	--	--	.95	.06	71	.50	149	19	154	5.2	1.1	.30	--	--	18	190
33	07-15-87	9.52	26.6	<	--	.85	.04	120	.50	168	34	194	38	12	.60	--	--	18	290
	06-29-88	9.53	--	--	--	.66	.01	110	.60	164	34	190	36	8.4	.50	--	--	19	290
	11-23-88	9.25	21.3	--															
34	07-16-87	8.96	25.5	<1.0	.71	1.8	.17	190	1.2	301	17	270	130	7.1	1.7	--	--	15	509
	11-22-88	8.88	23.9	--	--	1.9	.19	190	1.0	295	19	274	130	7.8	1.9	.062	.005	14	510
35	06-11-87	7.88	51.8	--	<.05	27	.42	240	2.3	173	0	142	430	19	1.2	.10	.009	35	840
36	04-24-86	8.20	42.2	--	--	12	.09	359	2.1	190	6	165	560	14	1.5	.16	.009	25	1,099
	10-22-87	8.31	37.4	--	.12	13	.15	340	2.0	188	5	162	580	17	1.6	.081	.012	25	1,100
37	10-02-87	9.05	30.5	--	.07	1.4	.32	200	.90	308	22	288	150	6.5	.40	.035	.006	14	550
38	07-01-87	7.64	15.0	4.3-5.0	--	49	17	180	2.6	344	0	282	290	7.9	.30	.10	.006	--	720
	07-14-88	7.64	15.4	--	--	51	17	180	2.4	344	0	282	310	7.2	.20	--	--	17	750

Values of pH were reproducible at most wells, and all samples were alkaline (above 7.0). Values of pH in water samples from the Gallup and Dakota aquifers were typically below 9.0 (figs. 12 and 13). Values of pH in water samples from the Morrison aquifer ranged from 7.52 to 9.65; water from 10 wells exceeded a pH of 9.0, indicating highly alkaline conditions. The areal distribution of pH in water from the Morrison aquifer indicates that highly alkaline water in the northwestern part of the basin generally is neutralized as it moves in a northerly direction (fig. 14). The pH in water along Morrison outcrop areas was typically below 9.0 except for one sample that had the highest pH value measured at 9.65. The pH of samples from wells located near Shiprock was typically below 8.0.

The distribution of major cations and anions found in water from the three aquifers is shown in figures 15 through 20. Two types of diagrams were used to depict ion concentrations: (1) chemical-constituent diagrams modified from Stiff (1951) to indicate spatial variations in ion concentrations, and (2) trilinear diagrams developed by Piper (1944) to relate variations in the relative percentage of ion concentrations.

Predominant ions in water from the three aquifers generally were Ca^{2+}, Na^{+}, HCO_3^{-}, and SO_4^{2-}, as shown in figures 15-17. Bicarbonate represents part of the alkalinity value in these figures. Major ions in water from the Gallup aquifer were predominantly Ca^{2+}-HCO_3^{-} in the southwestern outcrop area and Na^{+}-HCO_3^{-} in the northwestern outcrop area. The majority of samples were predominantly Na^{+}-HCO_3^{-} in the southwestern area of the basin and Na^{+}-SO_4^{2-} in the southeastern and central parts of the basin (fig. 15).

Predominant ions in water in the Dakota aquifer were Na^{+}-HCO_3^{-} for three samples located farthest south in the northwestern part of the basin. Predominant ions were Na^{+}-SO_4^{2-}, with minor HCO_3^{-}, for samples to the north and one sample in the southeastern part of the basin (fig. 16).

Distinct chemical groups of major ion distribution were observed in samples from wells completed in the Morrison aquifer (fig. 17). Chemical changes were observed in well samples from south to north in the general direction of flow. For one sample near the outcrop located near Gallup, New Mexico, Na^{+}-HCO_3^{-}-SO_4^{2-} were predominant ions. Predominant ions near Crownpoint consisted of Na^{+}-HCO_3^{-} and predominant ions south and northwest of Chaco Culture National Historical Park consisted of Na^{+}-SO_4^{2-}. In the northwestern part of the basin, the predominant ions in 10 samples from the southern and outcrop areas were Na^{+}-HCO_3^{-} and in 8 samples from the northern area were Na^{+}-SO_4^{2-}. Predominant ions in two samples near Four Corners consisted of Ca^{2+}-HCO_3^{-} and Na^{+}-HCO_3^{-}. In the western part of the basin, water is dilute and ion concentrations progressively increased northward toward Shiprock.

Points in figures 18-20 represent the percentage of a cation, in meq/L, relative to the total sum of cations and the percentage of an anion, in meq/L, relative to the total sum of anions. The intersection of the two percentages is depicted in the quadrangular portion of the trilinear diagram. Calcium concentrations constitute approximately 0 to 35 percent of the total cations in the Gallup, Dakota, and Morrison aquifers (figs. 18-20).

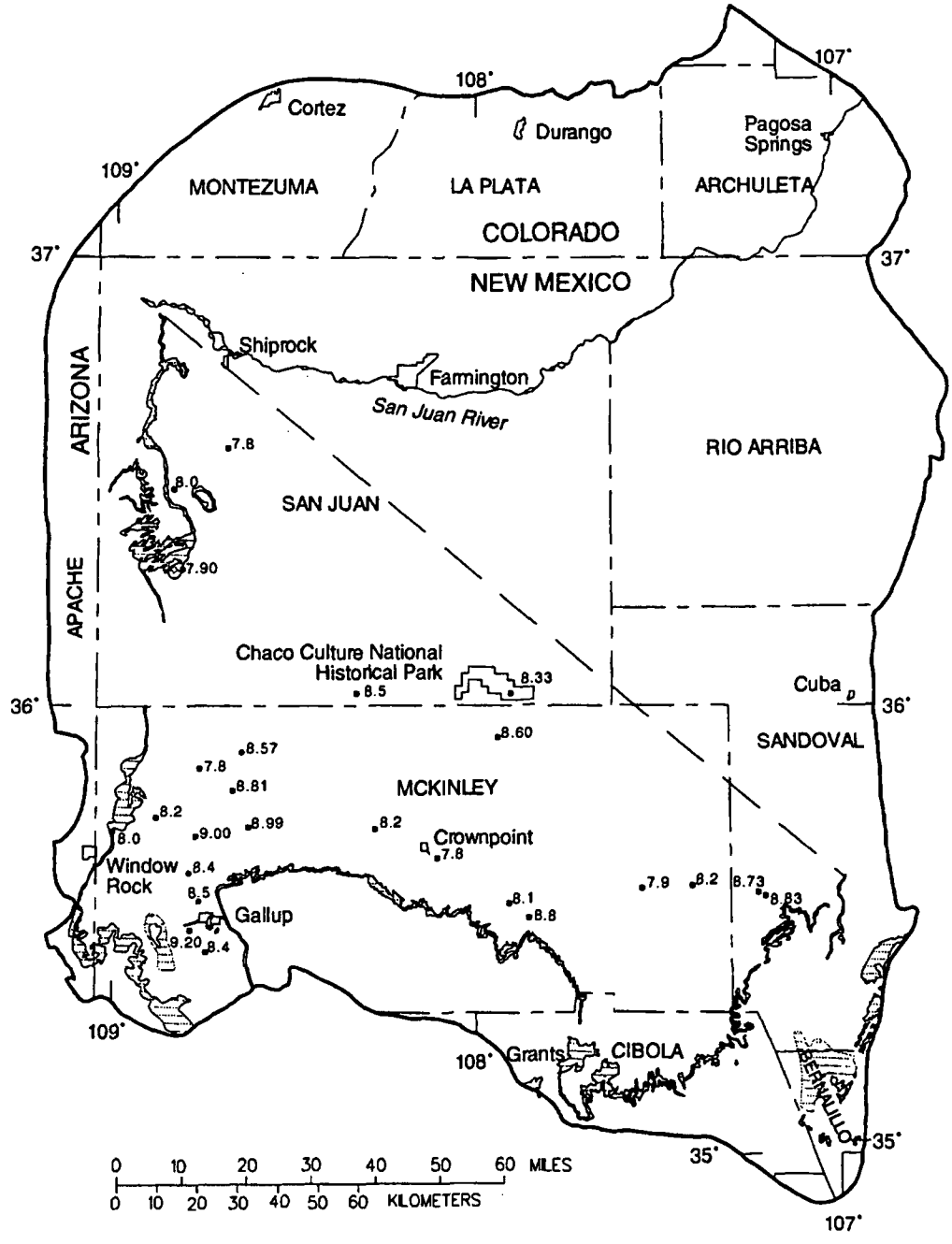

EXPLANATION

OUTCROP OF GALLUP AQUIFER--In Arizona includes Pescado Tongue of Mancos Shale. In the southeastern part of the study area mapped as part of the Mesaverde Group, undivided. From Dane and Bachman, 1965; and Hackman and Olson, 1977

APPROXIMATE SUBSURFACE EXTENT OF GALLUP AQUIFER--From Molenaar, 1973

BOUNDARY OF STUDY AREA

•7.8 WATER WELL--Number is pH, in standard units

Figure 12.--Values of pH for water from water wells completed in the Gallup aquifer.

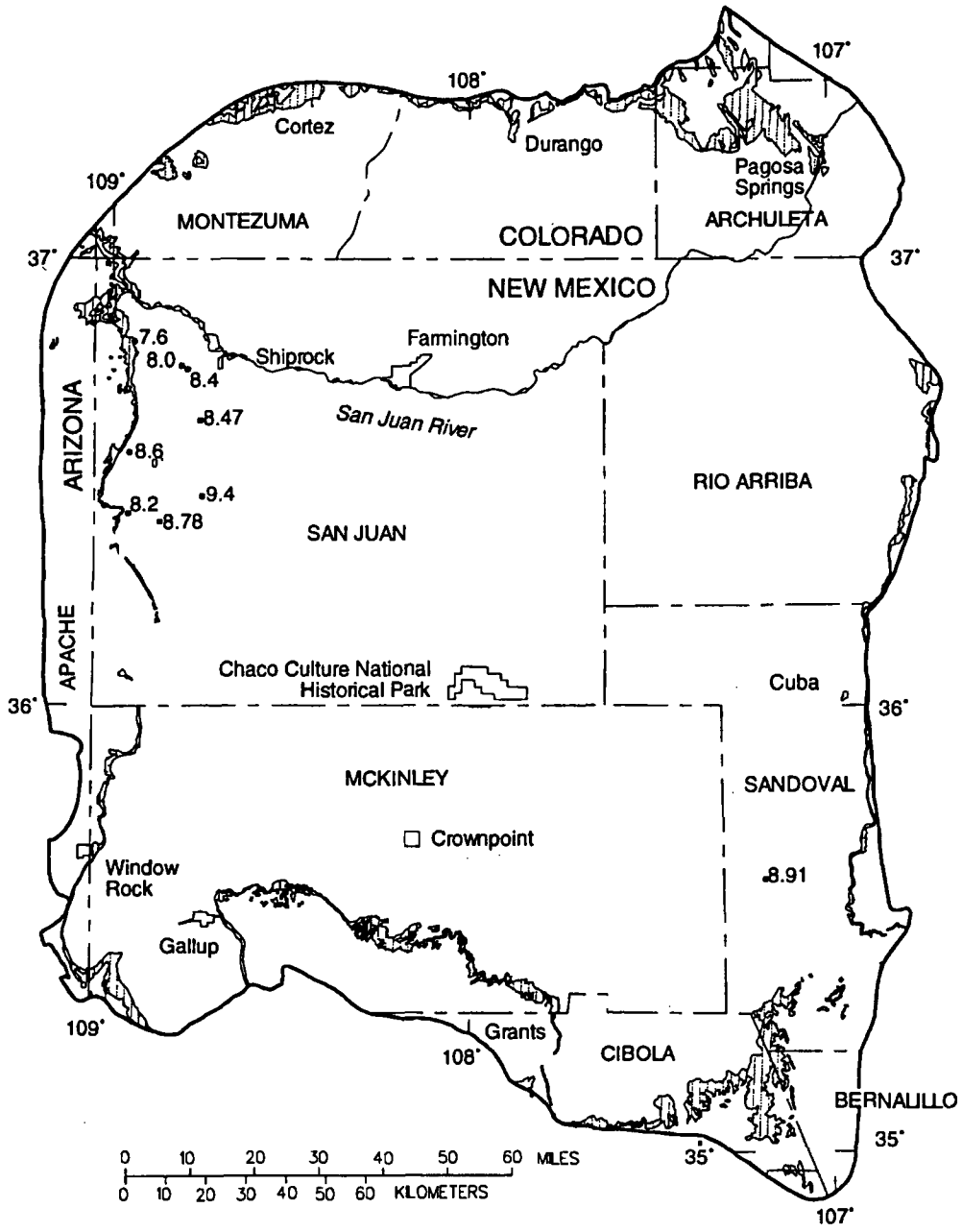

EXPLANATION

OUTCROP OF DAKOTA AQUIFER, MANCOS SHALE, AND BURRO CANYON FORMATION:-- From Dane and Bachman, 1965; Wilson and others, 1969; and Tweto, 1979

BOUNDARY OF STUDY AREA

• 9.4 WATER WELL--Number is pH, in standard units

Figure 13.--Values of pH for water from water wells completed in the Dakota aquifer.

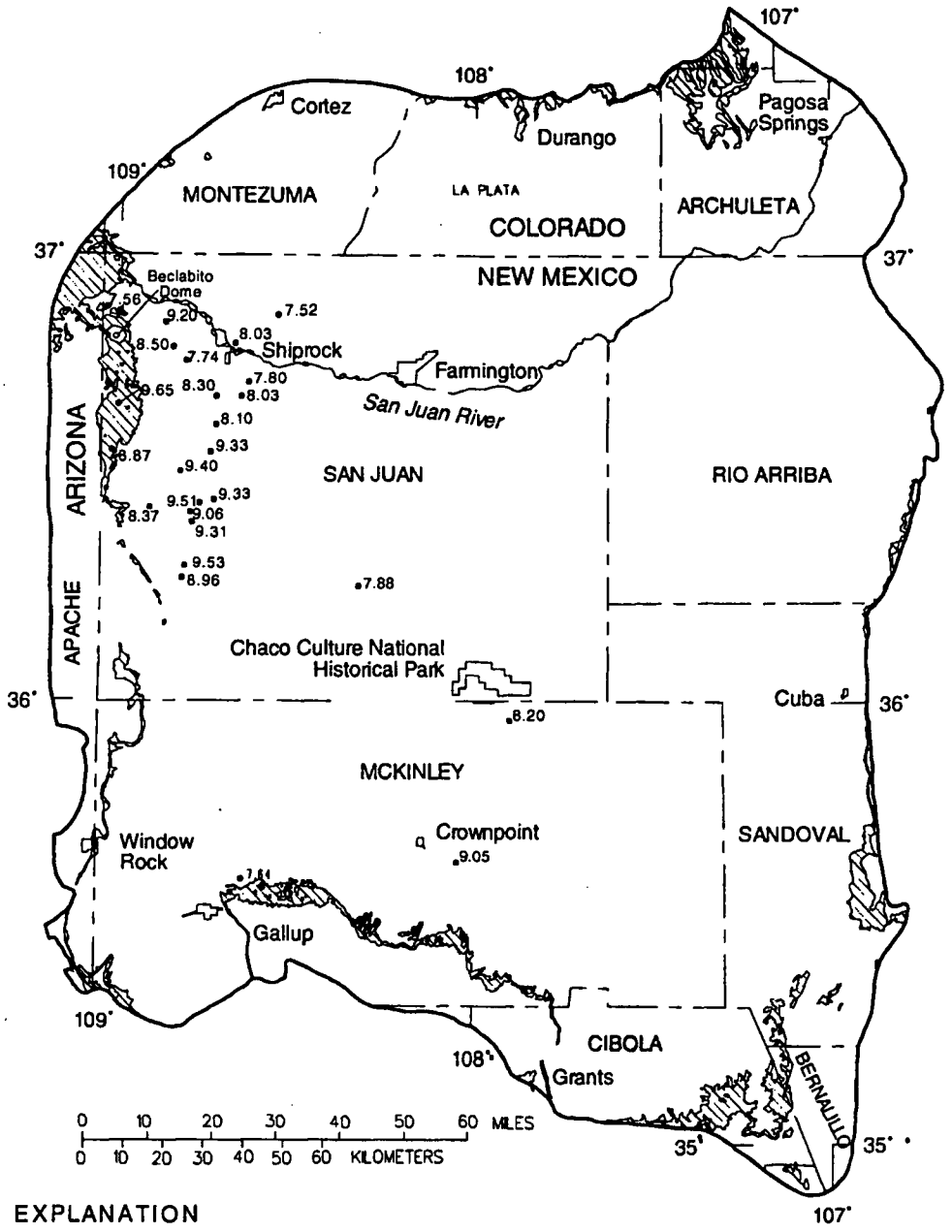

Figure 14.--Values of pH for water from water wells completed in the Morrison aquifer.

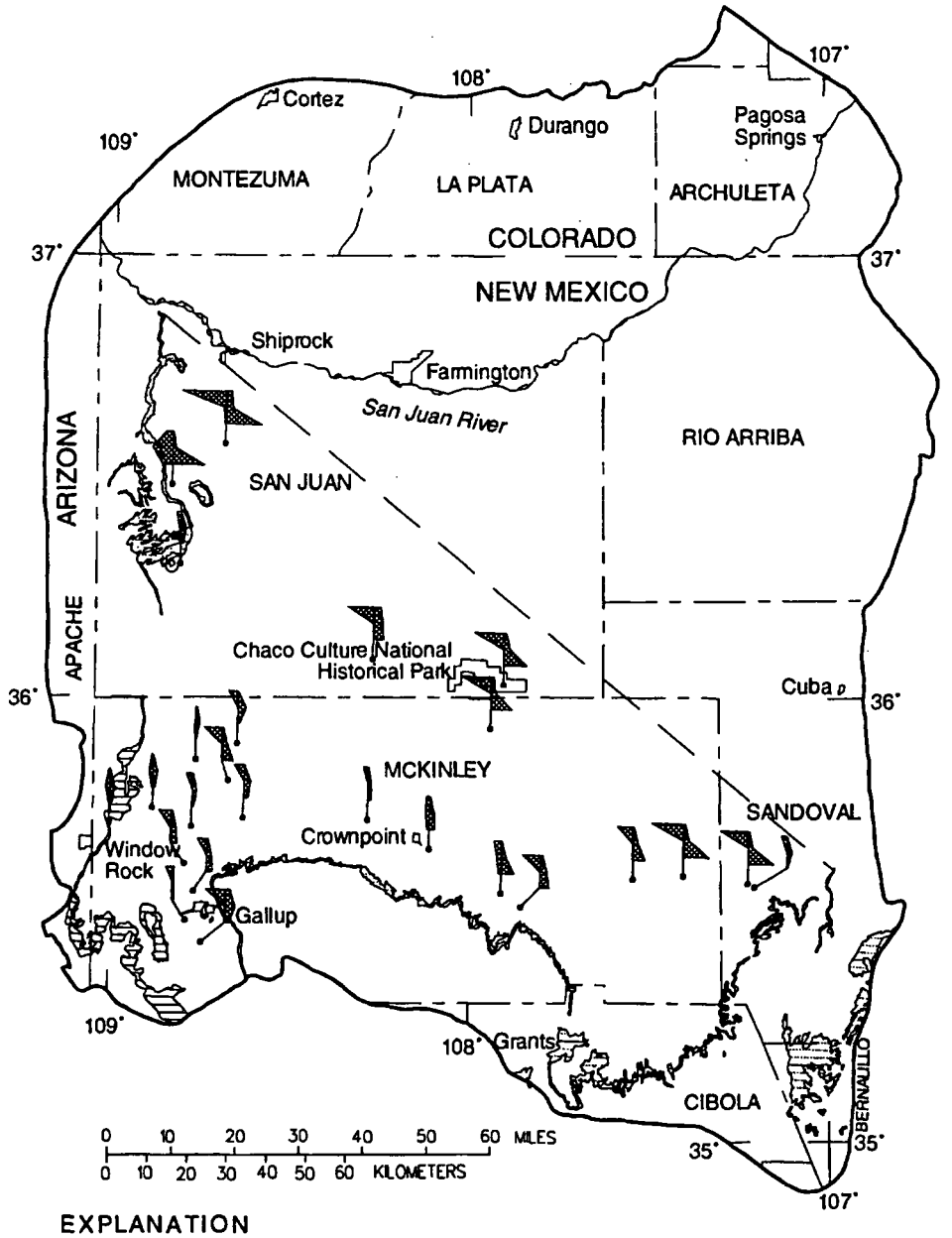

EXPLANATION

OUTCROP OF GALLUP AQUIFER--In Arizona includes Pescado Tongue of Mancos Shale. In the southeastern part of the study area mapped as part of the Mesaverde Group, undivided. From Dane and Bachman, 1965; and Hackman and Olson, 1977

APPROXIMATE SUBSURFACE EXTENT OF GALLUP AQUIFER--From Molenaar, 1973

BOUNDARY OF STUDY AREA

WATER WELL

CHEMICAL-CONSTITUENT DIAGRAM (modified from Stiff, 1951)

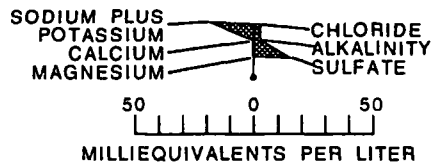

Figure 15.--Chemical-constituent diagrams of water from water wells completed in the Gallup aquifer.

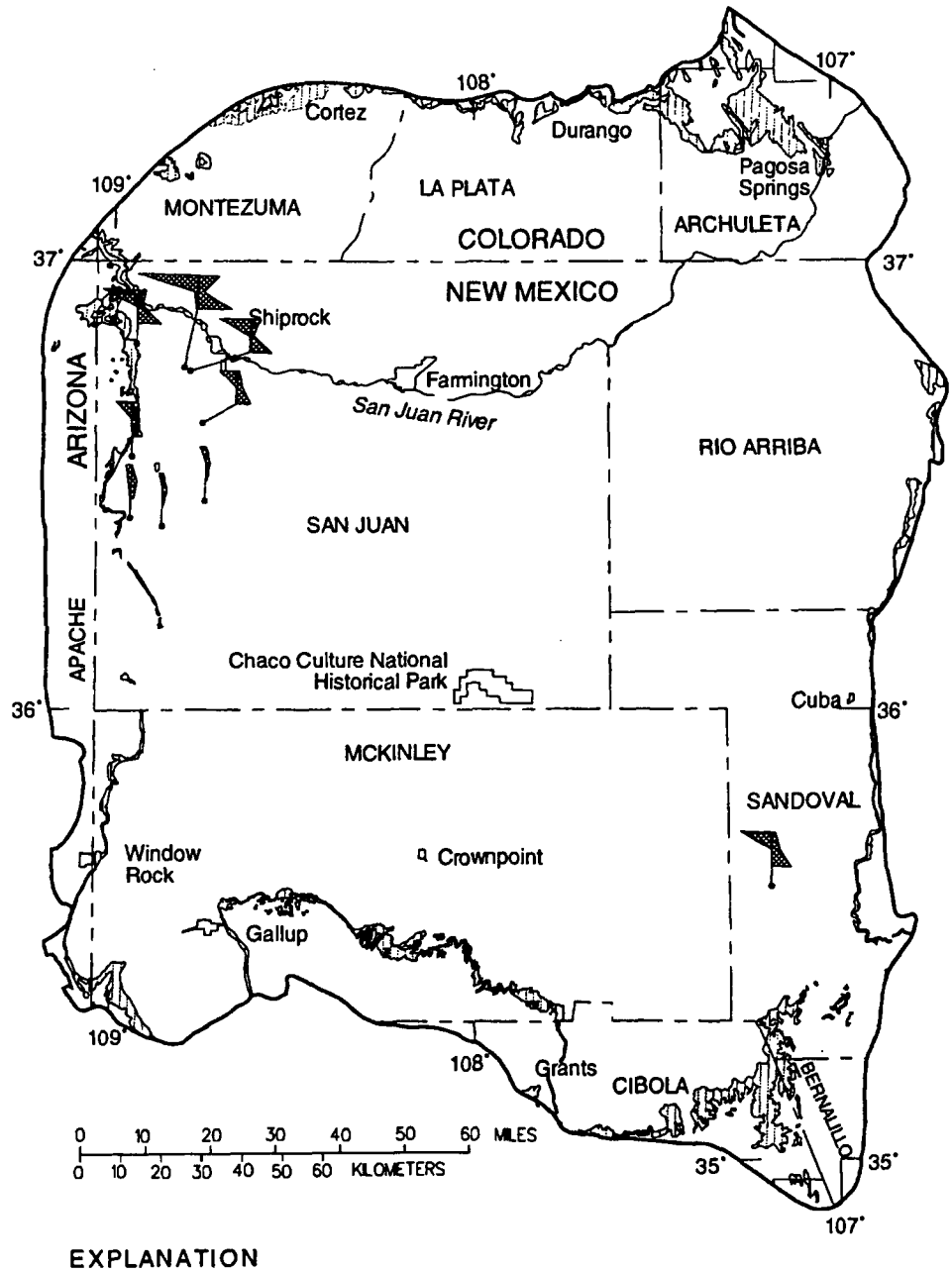

EXPLANATION

OUTCROP OF DAKOTA AQUIFER, MANCOS SHALE, AND BURRO CANYON FORMATION--From Dane and Bachman, 1965; Wilson and others, 1969; and Tweto, 1979

BOUNDARY OF STUDY AREA

WATER WELL

CHEMICAL-CONSTITUENT DIAGRAM (modified from Stiff, 1951)

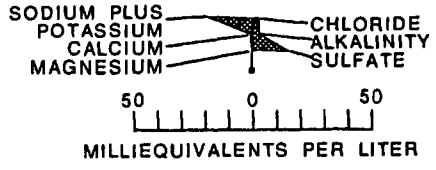

Figure 16.--Chemical-constituent diagrams of water from water wells completed in the Dakota aquifer.

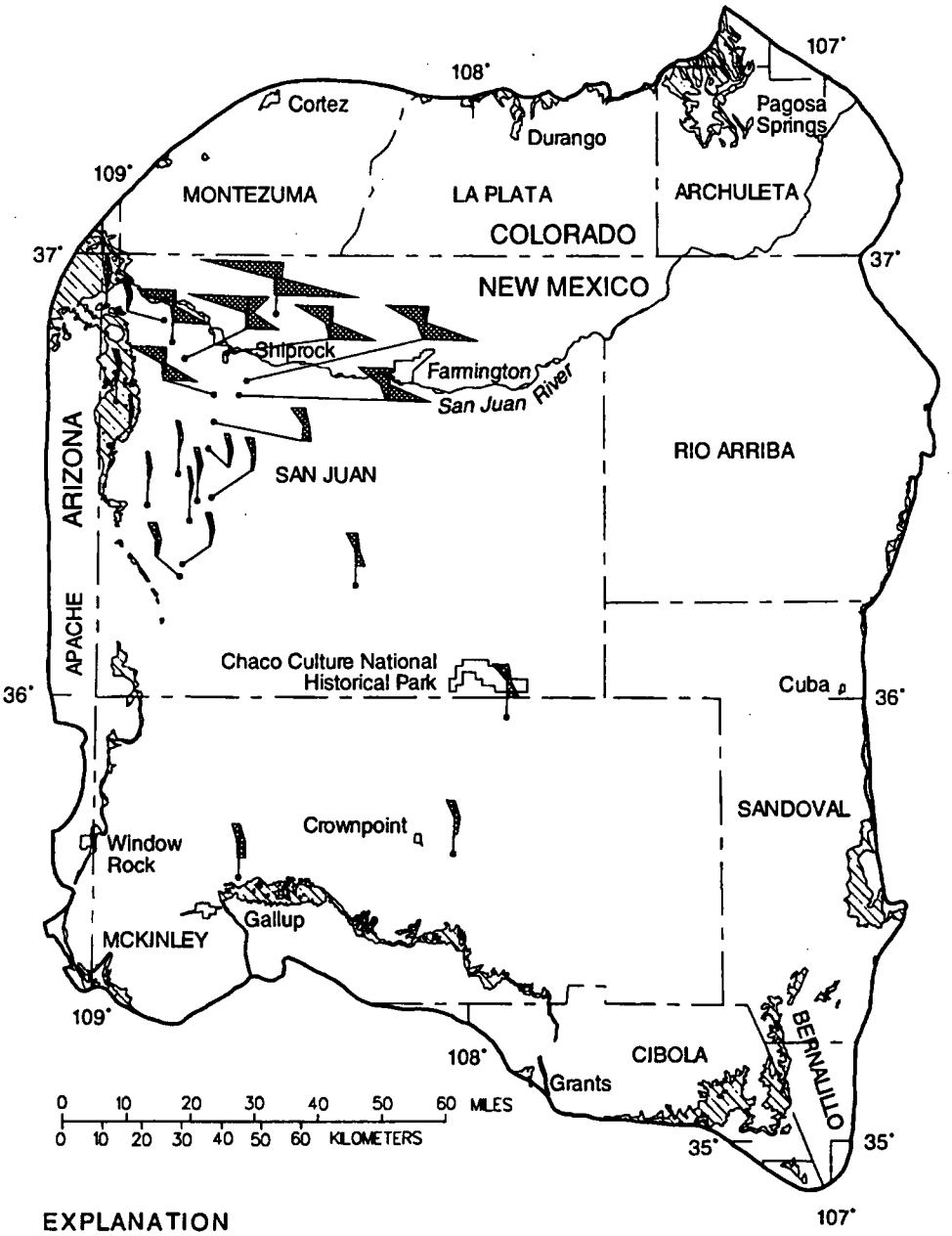

EXPLANATION

OUTCROP OF MORRISON AQUIFER, JURASSIC ROCKS, UNDIVIDED; WANAKAH FORMATION; ENTRADA SANDSTONE; AND SAN RAFAEL GROUP--From Dane and Bachman, 1965; Wilson and others, 1969; Tweto, 1979; and Hintze, 1981

BOUNDARY OF STUDY AREA

WATER WELL

CHEMICAL-CONSTITUENT DIAGRAM (modified from Stiff, 1951)

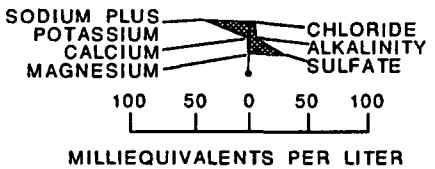

Figure 17.--Chemical-constituent diagrams of water from water wells completed in the Morrison aquifer.

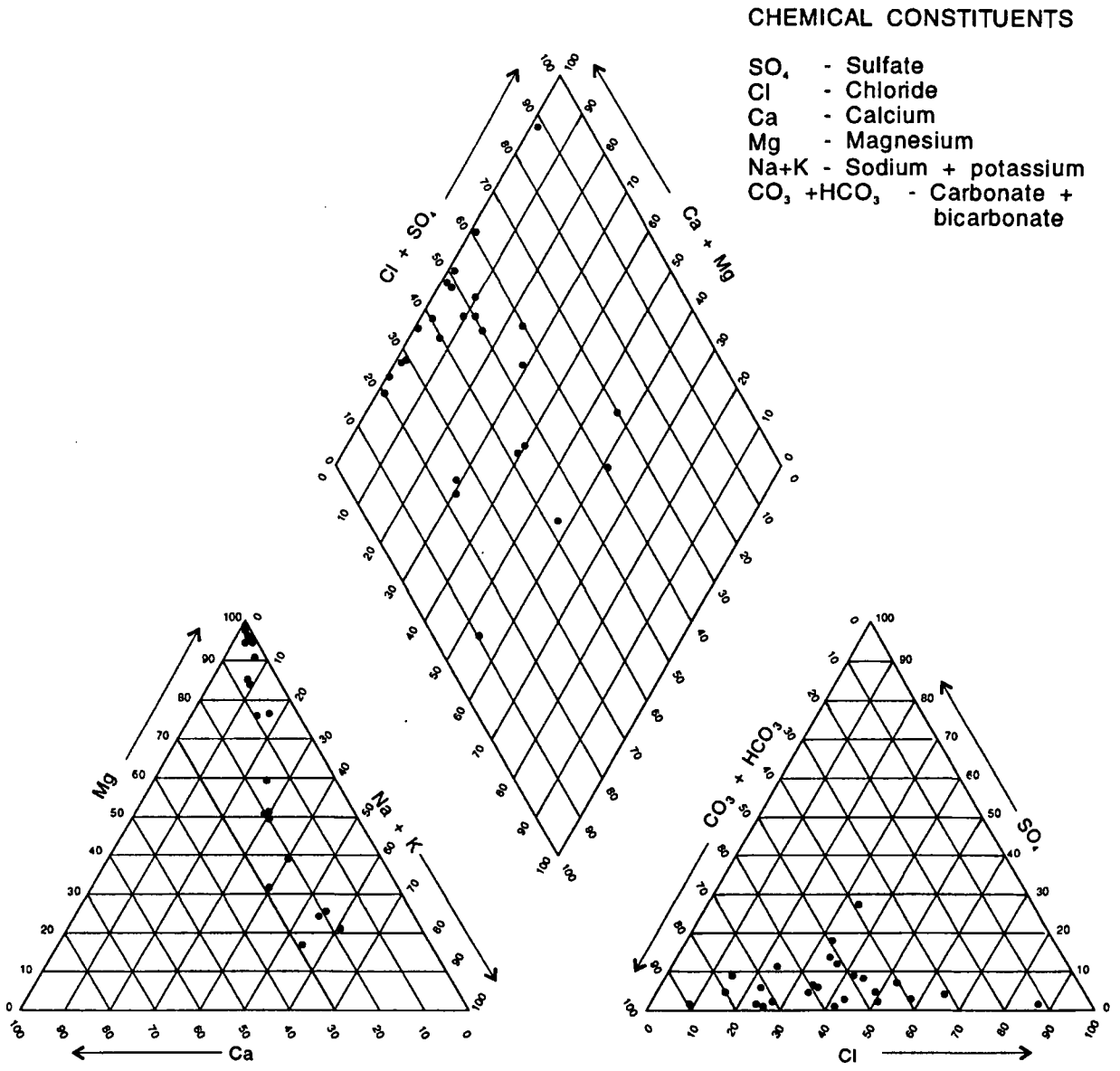

Figure 18.--Trilinear diagram of major ion chemistry from water wells completed in the Gallup aquifer.

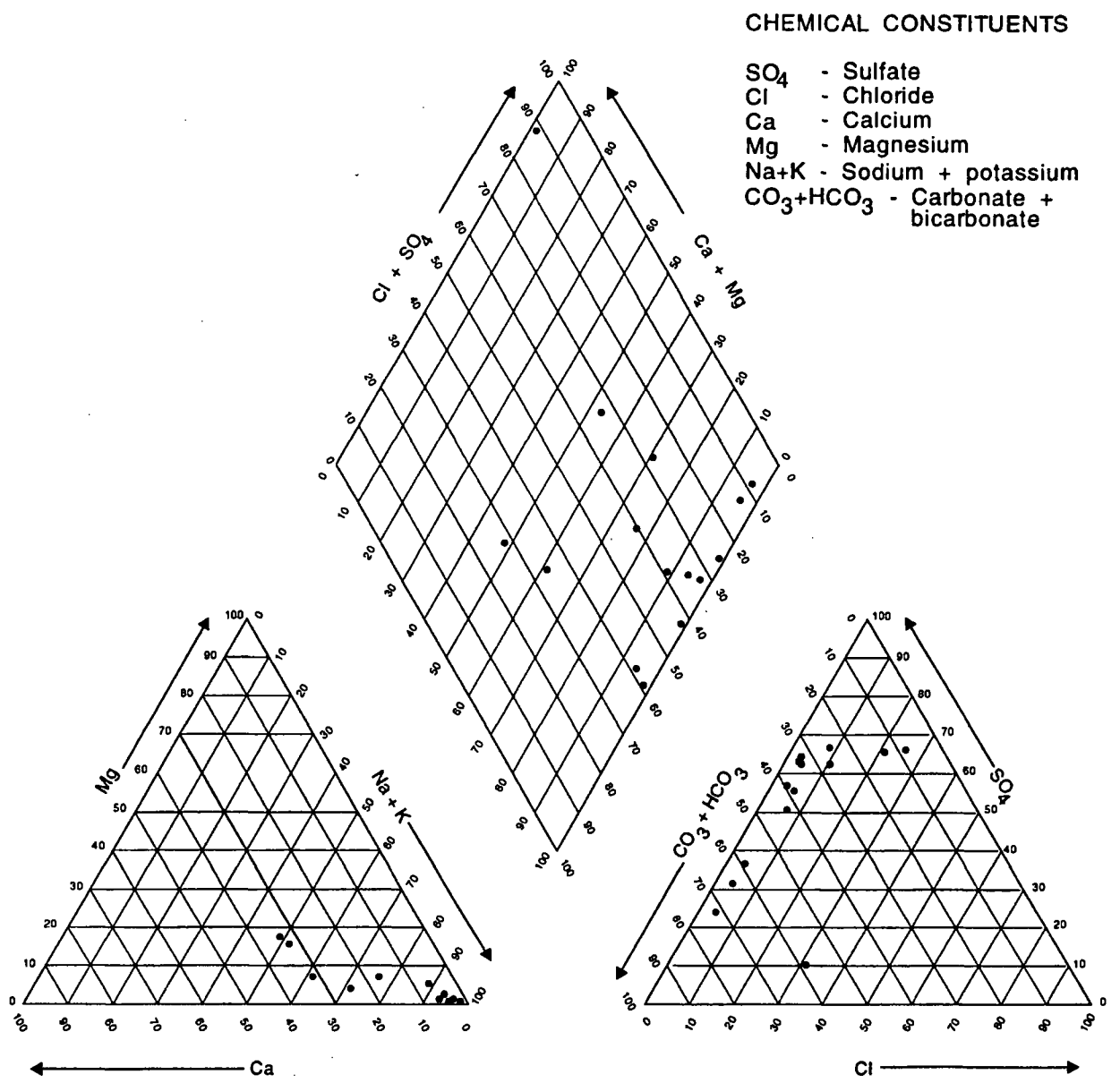

Figure 19.--Trilinear diagram of major ion chemistry from water wells completed in the Dakota aquifer.

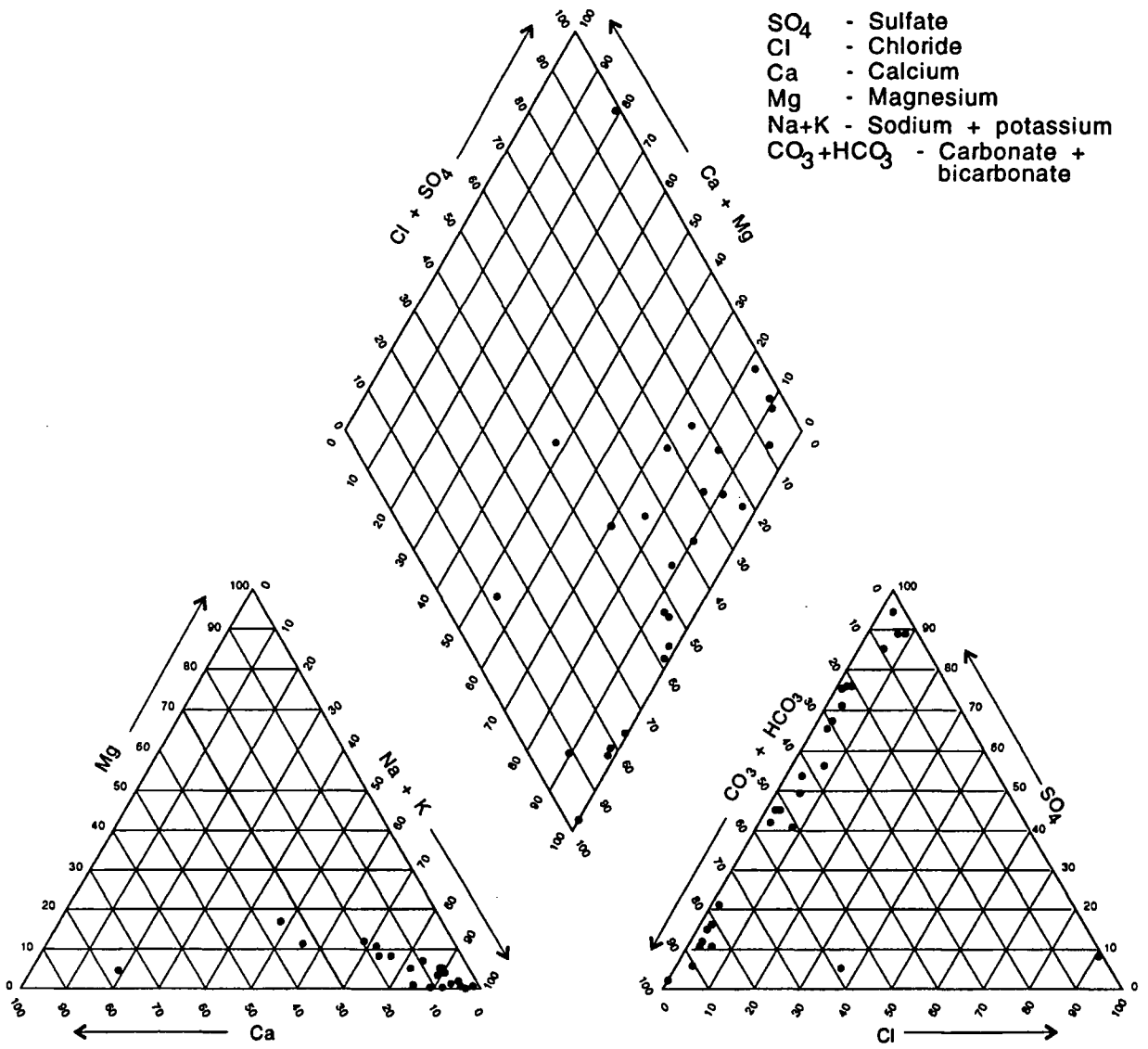

Figure 20.--Trilinear diagram of major ion chemistry from water wells completed in the Morrison aquifer.

Chloride concentrations were small (less than 25 mg/L) in samples on or near recharge areas for the three aquifers (figs. 21-23). Downgradient, chloride concentrations generally increased by one to two orders of magnitude. Two samples from wells completed in the outcrop area of the Gallup aquifer contained less than 8 mg/L of Cl^- (fig. 21). Chloride concentrations ranged from 2.8 to 180 mg/L in samples downgradient from the western outcrop areas. For three water samples from the Gallup aquifer in the northwestern area, chloride concentrations ranged from 7.8 to 180 mg/L, increasing to the north in the general direction of ground-water flow (fig. 21). Similar trends were observed for the Dakota aquifer (fig. 22). Chloride concentrations were less than 20 mg/L for four samples and increased to the north toward Shiprock to a maximum of 720 mg/L. In outcrop areas of the Morrison aquifer, small chloride concentrations (less than 25 mg/L) as well as large increases (750 mg/L) toward Shiprock were observed (fig. 23). However, six samples at and downgradient from Sanostee contained extremely low chloride values ranging from 0.80 to 3.9 mg/L.

Minor and Trace Constituents

Concentrations of selected minor and trace constituents are shown for the Gallup, Dakota, and Morrison aquifers (tables 2-4, respectively). Dissolved oxygen and sulfide data were used to establish the redox (oxidation-reduction) potential of the water samples. The occurrence of DO in water along outcrop areas generally is anticipated although difficult to measure precisely. Wells sampled on or near outcrops were equipped with piston pumps that can transfer oxygen from the air to the water. For example, at well 38 the DO concentration in water ranged from 4.3 to 5.0 mg/L (table 4), increasing as the rate of pumping decreased. Therefore, values of DO shown in tables 2 and 4 are very approximate. Sulfide was detected in water from several wells downgradient from the outcrop area; this indicates reducing conditions. However, sulfide did not consistently increase to the north toward Shiprock, suggesting that localized conditions, such as the presence of organic matter or availability of reactive iron, may have affected sulfate reduction reactions. Sulfide consists largely of hydrogen sulfide gas (H_2S) and the bisulfide (HS^-) ion. Above a pH of 7.0, sulfide will occur predominantly as HS^- (Stumm and Morgan, 1981, p. 443). Therefore, the alkaline water found in the three aquifers indicates that HS^- was the predominant sulfide species.

Fluoride concentrations generally are small in water samples from the three aquifers (tables 2-4); however, a larger percentage of F^- concentrations were greater than 2 mg/L in samples from wells completed in the Dakota aquifer. The F^- concentration exceeded 2 mg/L for samples from 3 of 25 wells completed in the Gallup aquifer, 2 of 9 wells completed in the Dakota aquifer, and 3 of 25 wells completed in the Morrison aquifer. The 2-mg/L value is the recommended maximum contaminant level set by the U.S. Environmental Protection Agency (1986). The Dakota aquifer commonly contains elevated concentrations of F^- in the San Juan Basin (Craigg and others, 1989) and in other parts of the Western United States (Lawton and others, 1984, p. 227).

To further define geochemical and hydrologic processes within the aquifers, samples were analyzed for Br^- and I^- concentrations (tables 2-4). Bromide solid phases are highly soluble, and concentrations of bromide in most natural water are not affected by redox reactions, sorption, or precipitation reactions (Whittemore, 1988). Bromide concentrations ranged from 0.010 mg/L in water from well 30 to 0.38 mg/L in water from well 15. Both wells were completed in the Morrison aquifer, and bromide concentrations for the Gallup and Dakota aquifers were within this range (tables 2-4). For water from downgradient wells northeast of well 30 where chloride decreased in concentration, Br^- concentrations increased only slightly (as much as three times higher) relative to the Br^- concentration at well 30.

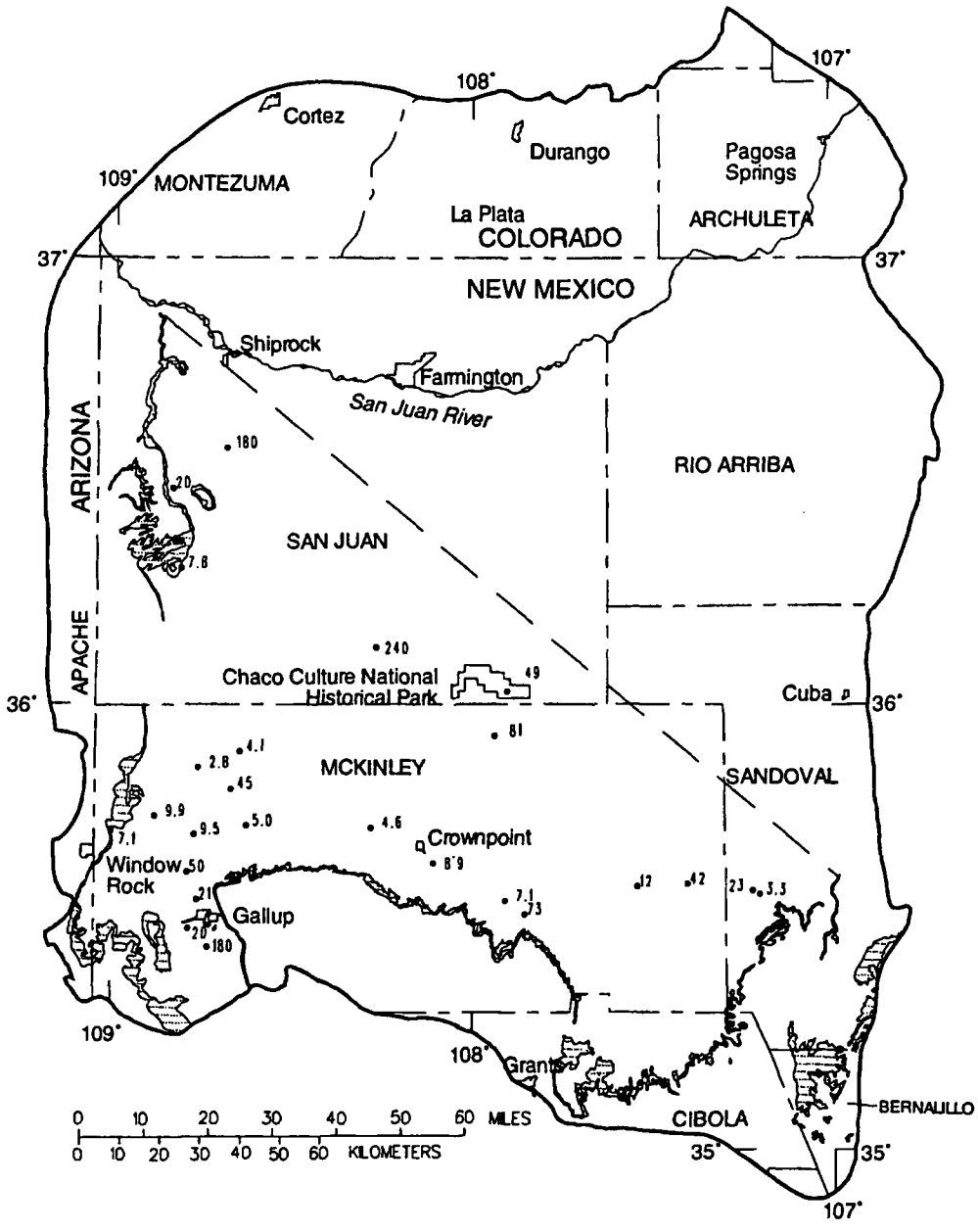

EXPLANATION

OUTCROP OF GALLUP AQUIFER--In Arizona includes Pescado Tongue of Mancos Shale. In the southeastern part of the study area mapped as part of the Mesaverde Group, undivided. From Dane and Bachman, 1965; and Hackman and Olson, 1977

APPROXIMATE SUBSURFACE EXTENT OF GALLUP AQUIFER--From Molenaar, 1973

BOUNDARY OF STUDY AREA

• 81 WATER WELL--Number is concentration of chloride, in milligrams per liter

Figure 21.--Concentration of chloride in water from water wells completed in the Gallup aquifer.

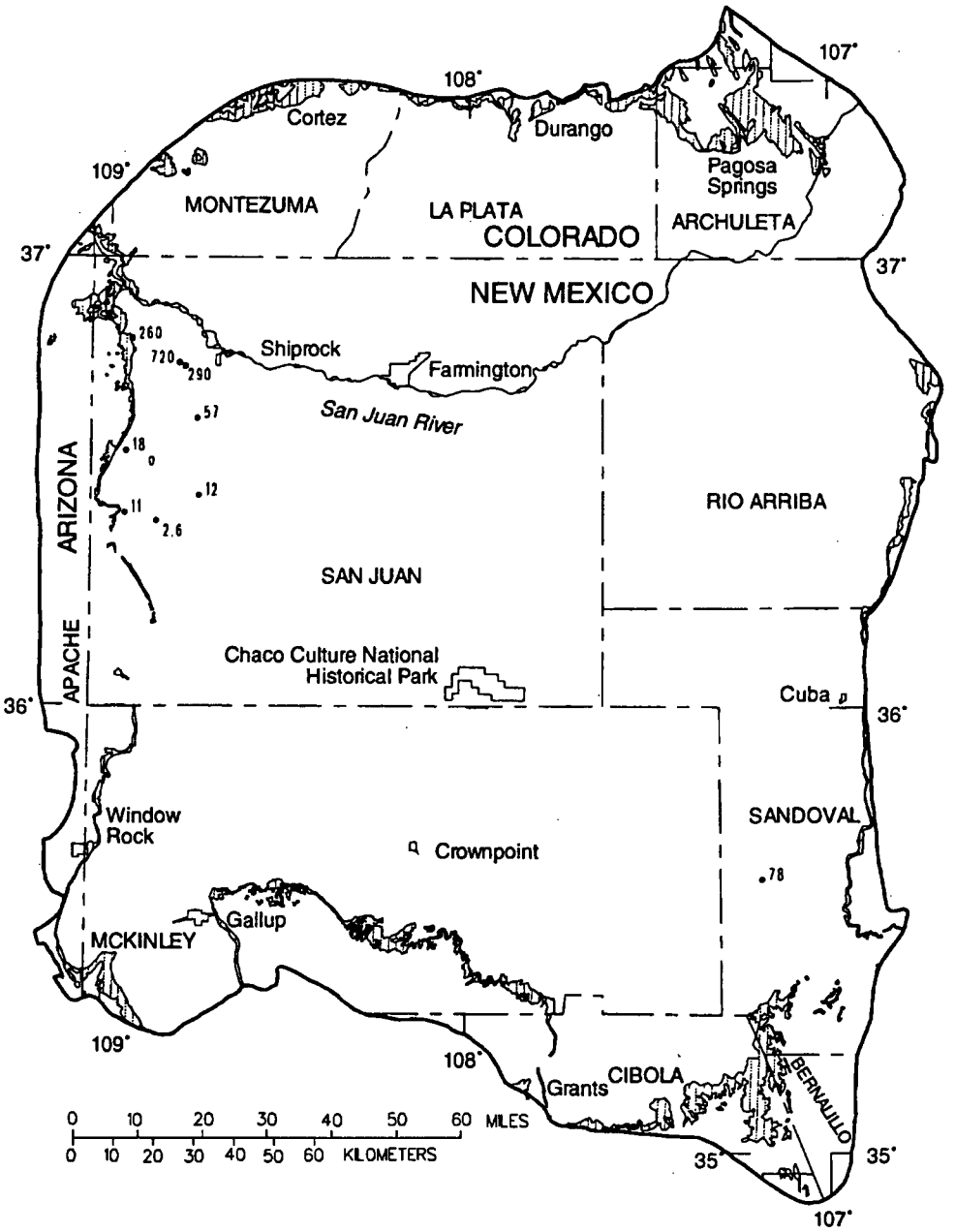

EXPLANATION

OUTCROP OF DAKOTA AQUIFER, MANCOS SHALE, AND BURRO CANYON FORMATION--From Dane and Bachman, 1965; Wilson and others, 1969; and Tweto, 1979

BOUNDARY OF STUDY AREA

•78 WATER WELL--Number is concentration of chloride, in milligrams per liter

Figure 22.--Concentration of chloride in water from water wells completed in the Dakota aquifer.

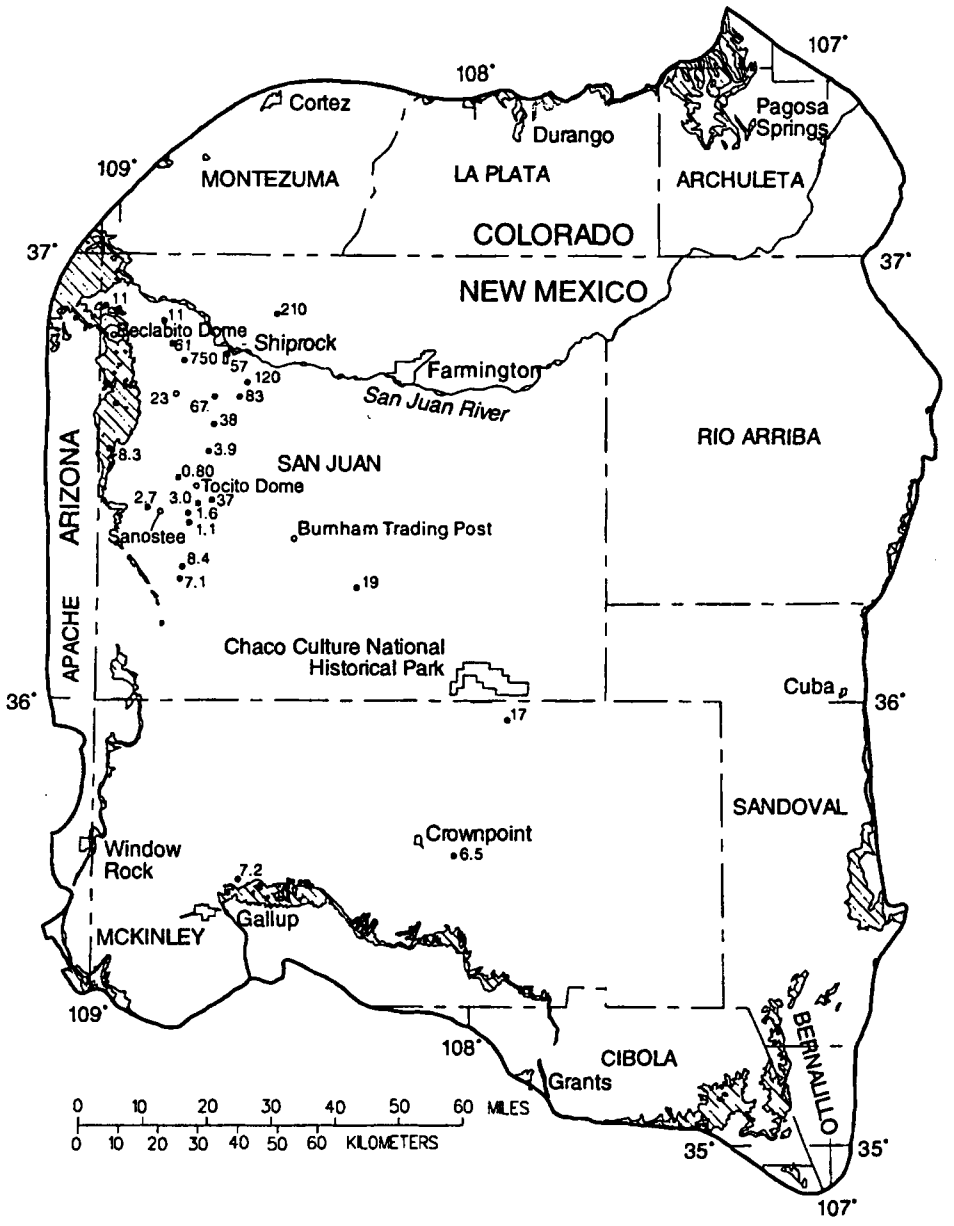

EXPLANATION

OUTCROP OF MORRISON AQUIFER, JURASSIC ROCKS, UNDIVIDED; WANAKAH FORMATION; ENTRADA SANDSTONE; AND SAN RAFAEL GROUP--From Dane and Bachman, 1965; Wilson and others, 1969; Tweto, 1979; and Hintze, 1981

BOUNDARY OF STUDY AREA

• 6.5 WATER WELL--Number is concentration of chloride, in milligrams per liter

Figure 23.--Concentration of chloride in water from water wells completed in the Morrison aquifer.

Concentrations of silica ranged from 8.5 to 35 mg/L in the three aquifers (tables 2-4). Median SiO_2^0 concentrations in samples from the Gallup, Dakota, and Morrison aquifers were 13, 9.8, and 17 mg/L, respectively.

Data for dissolved nutrients and dissolved organic carbon in the three aquifers are shown in table 5. Nitrate was detected in samples from only four wells. Two wells located in the outcrop area of the Morrison aquifer contained NO_3^- concentrations greater than 0.2 mg/L. Ammonium was not detected in samples near outcrops, but a concentration of 0.520 mg/L was measured in well 20 in the Morrison aquifer south of Shiprock.

Trace-constituent data for samples collected from the three aquifers are presented in table 6. Constituent concentrations generally found to be below the minimum reporting level were Al, Be, Cd, Cr, Co, Cu, Pb, Hg, Mo, Ni, Se, Ag, and V. Trace-element concentrations generally found to be above the minimum reporting level included As, Ba, B, Fe, Li, Mn, and Sr. The minimum reporting levels differ for some elements due to the requested level of detection.

Twenty-three samples were filtered with both a 0.10-µm filter and a 0.45-µm filter (table 6). Of these 23 samples, 11 in which the 0.45-µm filter was used were larger or equal in concentration to the samples in which the 0.10-µm filter was used. This suggests that some Fe colloids passing through a 0.45-µm filter are removed with a 0.10-µm filter as described by Kennedy and others (1974). Iron concentrations in the 0.10-µm filtered samples that were greater than concentrations in the 0.45-µm filtered samples (12 of 23) may be caused by analytical uncertainties or field-collection techniques. There are no apparent systematic areal patterns of Fe concentrations in the Gallup aquifer. Iron concentrations in samples from the Dakota aquifer indicate a general increase in the direction of ground-water flow to the north. Iron concentrations in the Morrison aquifer were generally less than 12 µg/L in the recharge area and increased to a maximum value of 980 µg/L in a sample from a well near the San Juan River discharge area.

Arsenic concentration was less than 1 µg/L in 12 of 14 samples collected from the Gallup and Dakota aquifers, but was less than 1 µg/L in only 4 of 23 samples from the Morrison aquifer (table 6).

Concentrations of Li generally were larger in the Morrison aquifer than in the other two aquifers and increased in the direction of ground-water flow. Lithium concentrations in the Morrison aquifer increased from less than 50 µg/L in samples collected from wells in the recharge area to 540 µg/L in a sample collected from well 20 near the San Juan River.

Strontium concentrations in samples generally increased in the direction of ground-water flow in the three aquifers. In the Gallup aquifer, Sr^{2+} concentrations were 360 µg/L or less except for one concentration that was 920 µg/L (table 6). In the Dakota aquifer, Sr^{2+} concentrations were variable both spatially and in samples from the same well. Strontium concentrations ranged from 140 to 3,300 µg/L in four samples from three wells completed in the Dakota aquifer. Water from well 13 on two different dates contained Sr^{2+} concentrations of 350 and 3,300 µg/L, suggesting a problem in reproducibility and a need for additional sampling to verify Sr^{2+} concentrations. Strontium concentrations in the Morrison aquifer ranged from 38 to 12,000 µg/L and were substantially larger than in the other two aquifers.

Table 5.--Concentrations of dissolved nutrients and dissolved organic carbon in water from the Gallup, Dakota, and Morrison aquifers

[See figures 8-10 for location of wells. Wells 1-10 are completed in the Gallup aquifer, wells 11 and 13 in the Dakota aquifer, and wells 14-38 in the Morrison aquifer. Concentrations in milligrams per liter; --, not reported; <, less than detection limit]

Well number	Date of sample	Nitrite, as N	Nitrite plus nitrate, as N	Nitrogen ammonia, as N	Nitrogen ammonia plus organic, as N	Phosphorus, as P	Phosphorus ortho-phosphate, as P	Organic carbon
1	07-01-88	<0.010	<0.100	0.220	0.40	0.010	<0.010	--
2	04-22-86	--	--	--	--	--	--	1.3
	10-21-87	<0.010	<.100	.460	2.2	<.010	.021	.6
3	04-21-86	--	--	--	--	--	--	1.1
4	07-15-88	--	--	--	--	--	--	1.6
5	06-30-87	<.010	<.100	.041	1.9	.010	.010	.9
6	06-30-88	<.010	<.100	.180	.50	.021	.021	--
7	06-28-88	.021	.130	.041	.20	.021	.030	--
8	12-03-87	<.010	<.100	.060	<.20	.010	<.010	.8
9	04-29-86	--	--	--	--	--	--	1.1
	08-11-87	<.010	<.100	.030	<.20	.021	.010	--
10	06-30-88	<.010	<.100	.070	.30	.120	.120	.8
11	07-23-87	<.010	<.100	.120	.40	.010	<.010	--
13	04-29-86	--	--	--	--	--	--	1.0
	12-03-87	<.010	<.100	.730	.80	.010	<.010	--
14	06-10-88	.010	<.100	.041	<.20	<.010	<.010	--
15	06-24-86	--	--	--	--	--	--	.4
	07-21-87	<.010	<.100	.760	1.0	.010	<.010	1.8
17	07-02-86	--	--	--	--	--	--	.1
18	06-16-86	--	--	--	--	--	--	.2
	06-09-87	<.010	<.100	.540	1.3	.010	<.010	--
19	06-19-86	--	--	--	--	--	--	.2
	07-14-87	<.010	<.100	.140	.80	.010	<.010	1.8
20	06-10-87	<.010	<.100	.520	1.1	.010	<0.010	--
21	06-18-86	--	--	--	--	--	--	0.1
22	06-19-86	--	--	--	--	--	--	.2
	06-10-87	<.010	<.100	.450	1.3	.010	<.010	--
23	06-10-88	.021	.230	.010	<.20	.010	<.010	--
24	07-01-86	--	--	--	--	--	--	.6
25	06-09-88	<.010	.220	.010	<.20	<.010	<.010	.6
26	07-22-87	<.010	<.100	<.010	.90	<.010	<.010	--
	06-17-86	--	--	--	--	--	--	.2
27	06-18-86	--	--	--	--	--	--	.2
28	06-30-86	--	--	--	--	--	--	.2
	07-17-87	<.100	<.100	.021	.60	.010	<.010	--
30	07-23-87	<.010	<.100	<.010	.50	<.010	<.010	1.7
32	06-24-86	--	--	--	--	--	--	.2
	07-15-87	.021	.110	<.010	.20	.041	.021	--
33	07-15-87	<.010	<.100	<.010	.40	.030	.030	1.9
34	07-16-87	<.010	<.100	<.010	.30	.010	<.010	1.7
35	06-11-87	<.010	<.100	.110	.50	.010	<.010	4.1
36	04-24-86	--	--	--	--	--	--	.5
	10-22-87	<.010	<.100	.021	<.20	<.010	.021	.3
37	10-02-87	<.010	<.100	.090	.30	.010	.021	--
	07-01-87	<.010	<.100	.110	.30	.010	<.010	1.1
38	07-01-87	<.010	<.100	.110	.30	.010	<.010	1.1

Table 6.--Concentration of dissolved trace constituents in water from the Gallup, Dakota, and Morrison aquifers

[See figure 8-10 for location of wells; wells 1-10 are completed in the Gallup aquifer, wells 11-13 in the Dakota aquifer, and wells 14-38 in the Morrison aquifer; concentrations in micrograms per liter; --, not reported; <, concentration less than detection limit; samples filtered with a 0.45-micron filter except Al.1, Fe.1, and Mn.1 where a 0.10-micron filter was used]

Well number	Date of sample	Aluminum (Al)	Aluminum (Al.1)	Arsenic (As)	Barium (Ba)	Beryllium (Be)	Boron B	Cadmium (Cd)	Chromium (Cr)	Cobalt (Co)	Copper (Cu)	Iron (Fe)	Iron (Fe.1)
1	07-01-88	<10	--	2	33	<.05	--	<1	<1	<3	<1	330	--
2	04-22-86	<10	<10	<1	17	<17	--	<3	<1	<1	2	309	160
	10-21-87	<10	--	<1	<100	<10	--	<1	<1	2	1	250	--
3	04-21-86	10	10	<1	100	<10	--	<1	<1	<1	1	40	50
4	07-15-88	<10	--	<1	26	<.5	--	<1	<1	<3	2	22	--
5	06-30-87	<10	<20	<1	<34	<.5	--	<1	<1	<10	<10	<21	40
	06-28-88	<10	--	--	--	--	110	--	--	--	--	30	--
6	06-30-88	<10	--	<1	31	<.5	--	<1	2	<3	1	17	--
7	06-28-88	<10	--	<1	38	<.5	--	<1	1	<3	5	16	--
8	12-03-87	<10	--	<1	<100	<10	--	<1	<1	<1	<1	430	--
9	04-29-86	<10	<10	<1	7	<5	--	<1	<1	<3	1	10	10
	08-11-87	<10	--	--	--	--	90	--	--	--	--	<3	--
10	06-30-88	<10	--	<1	14	<.5	--	<1	<1	<3	44	640	--
11	07-23-87	<10	--	<1	10	<.5	--	<1	<1	<3	<1	680	--
12	06-29-88	<10	--	1	24	<.5	--	<1	<1	<3	1	53	--
13	04-29-86	<10	<10	<1	<100	<10	--	<1	<1	1	2	70	30
	12-03-87	<10	--	--	--	--	200	--	--	--	--	17	--
14	06-10-88	<10	--	1	19	<.5	--	<1	3	<3	6	440	--
15	07-21-87	20	10	1	<100	<10	--	<1	<1	<1	<1	300	230
16	06-24-86	<10	20	21	17	<.5	--	<1	<1	<3	<1	7	10
	06-08-88	<10	--	--	--	--	180	--	--	--	--	12	--
17	07-02-86	<10	--	12	<100	<10	--	<1	<1	<1	<1	30	--
18	06-16-86	<10	<10	<1	100	<10	--	<1	<1	<1	<1	170	160
	06-09-87	<10	--	--	--	--	150	--	--	--	--	170	--
19	07-14-87	--	<10	--	--	--	1,600	--	--	--	--	980	1,000
20	06-19-86	<10	--	13	100	<10	--	<1	<1	<1	<1	990	--
	06-10-87	<10	--	--	--	--	300	--	--	--	--	470	--
21	06-18-86	<10	10	1	100	<10	--	<1	<1	<1	1	540	540
22	06-19-86	<10	10	2	100	<10	--	<1	<1	<1	<1	140	150
	06-10-87	<10	--	--	--	--	150	--	--	--	--	240	--
23	06-10-88	<10	--	3	26	<0.5	--	<1	1	<3	<1	140	--
24	07-01-86	<10	<10	<1	10	<.5	--	<1	<1	<3	2	159	180
25	06-09-88	<10	--	2	120	<.5	--	<1	1	<3	1	85	--
	04-25-89	<10	--	--	--	--	30	--	--	--	--	180	--
26	06-17-86	20	20	4	36	<.5	--	<1	<1	<3	<1	6	<10
	07-22-87	20	--	--	--	--	30	--	8	--	--	15	--
	07-01-88	10	--	--	--	--	30	--	--	--	--	3	--
27	06-18-86	20	10	3	25	<.5	--	<1	<1	<3	1	<3	<10
	06-11-88	20	--	--	--	--	20	--	--	--	--	7	--
28	06-30-89	10	10	3	15	<.5	--	<1	<1	<3	1	3	<10
	07-17-87	10	6	--	--	--	--	--	--	--	--	--	--
	07-01-88	<10	--	--	--	--	100	--	--	--	--	>3	--
29	06-29-88	20	--	2	9	<.5	--	<1	1	<3	<1	8	--
	11-22-88	20	--	--	--	--	--	--	--	--	--	--	<3
30	07-23-87	<10	<10	11	61	<.5	--	<1	<1	<3	3	11	<10
	01-05-89	<10	--	--	--	--	--	--	--	--	--	--	11
31	01-05-89	10	--	--	--	--	--	--	--	--	--	--	8
32	06-24-86	20	20	2	24	<.5	--	<1	1	<3	1	7	<10
	07-15-87	30	--	--	--	--	10	--	--	--	--	34	--
	06-11-88	30	--	--	--	--	20	--	--	--	--	--	19
33	07-15-87	--	20	--	--	--	--	--	--	--	--	<10	--
	06-29-88	20	--	--	--	--	110	--	--	--	--	6	--
	11-23-88	<10	--	--	--	--	70	--	--	--	--	<3	--
34	07-16-87	<10	10	4	43	.5	--	1	<1	<3	<1	14	<10
	11-22-88	<10	--	--	--	--	--	--	--	--	--	8	--
35	06-11-87	20	20	5	46	<.5	--	<1	<1	<3	<1	140	120
36	04-24-86	<10	<10	6	30	<.5	--	<1	<1	<3	1	159	250
	10-22-87	<10	10	6	42	<.5	--	<1	<1	<3	<1	100	70
37	10-02-87	<10	<10	<1	34	<.5	--	<1	<1	<3	1	14	<10
38	07-01-87	<10	<10	<1	12	<.5	--	<1	<1	<3	<1	680	1,900
	07-14-88	<10	--	--	--	--	120	--	--	--	--	620	--

Table 6.– Concentration of dissolved trace constituents in water from the Gallup, Dakota, and Morrison aquifers–Concluded

Well number	Date of sample	Lead (Pb)	Lithium (Li)	Manganese (Mn)	Manganese (Mn.1)	Mercury (Hg)	Molybdenum (Mo)	Nickel (Ni)	Selenium (Se)	Silver (Ag)	Strontium (Sr)	Vanadium (V)	Zinc (Zn)
1	07-01-88	<5	46	150	--	<0.1	<10	<1	<1	<1	920	<6	31
2	04-22-86	1	98	8	10	<.1	<1	<1	<1	<1	350	1	<9
	10-21-87	<5	120	<10	--	<.1	<1	5	<1	<1	350	<1	<10
3	04-21-86	<1	70	20	20	<.1	<1	1	<1	<1	280	<1	<10
4	07-15-88	<5	14	4	--	<.1	<10	<1	<1	1	97	<6	5
5	06-30-87	<10	<4	<5	<10	.1	<10	1	<1	1	89	<6	<100
	06-28-88	--	--	5	--	--	--	--	--	--	85	--	--
6	06-30-88	<5	12	6	--	.1	<10	1	<1	<1	89	<6	19
7	06-28-88	5	<4	4	--	<.1	<10	4	<1	<1	52	<6	<3
8	12-03-87	<5	100	20	--	.1	3	<1	<1	<1	360	<1	<10
9	04-29-86	<1	23	2	<10	<.1	<10	1	<1	<1	26	<6	<3
	08-11-87	--	--	2	--	--	--	--	--	--	26	--	--
10	06-30-88	<5	10	20	--	<.1	<10	<1	10	<1	18	<6	590
11	07-23-87	<5	140	30	--	.1	<10	<1	<1	<1	930	<6	4
12	06-29-88	<5	24	7	--	<.1	<10	<1	<1	1	140	<6	34
13	04-29-86	1	100	60	10	<.1	<1	<1	<1	<1	350	2	<10
	12-03-87	--	--	<3	--	--	--	--	--	--	3,300	--	--
14	06-10-88	<5	15	61	--	<.1	<10	5	<1	<1	1,100	<6	150
15	07-21-87	<5	840	130	140	<.1	<1	<1	<1	<1	6,700	3	40
16	06-24-86	<5	61	<1	<10	<.1	<10	<1	<1	<1	62	<6	6
	06-08-88	--	--	<1	--	--	--	--	--	--	66	--	--
17	07-02-86	<5	270	70	--	.1	1	<1	<1	<1	7,500	<1	<10
18	06-16-86	<5	300	100	90	<.1	1	<1	<1	<1	12,000	<1	10
	06-09-87	--	--	87	--	--	--	--	--	--	11,000	--	--
19	07-14-87	--	--	30	30	--	--	--	--	--	--	--	--
20	06-19-86	<5	540	110	16	<.1	13	<1	<1	<1	10,000	2	10
	06-10-87	--	--	87	--	--	--	--	--	--	9,000	--	--
21	06-18-86	<5	270	70	70	<.1	2	1	<1	<1	7,500	<1	<10
22	06-19-86	<5	220	160	160	<.1	3	<1	<1	<1	11,000	<1	<10
	06-10-87	--	--	9	--	--	--	--	--	--	9,800	--	--
23	06-10-88	<5	33	3	--	<0.1	<10	6	3	<1	100	<6	27
24	07-01-86	<5	88	3	<10	<.1	<10	1	<1	<1	469	<6	8
25	06-09-88	<1	37	2	--	<.1	<10	5	27	<1	1,100	6	94
	04-25-89	--	--	3	--	--	--	--	--	--	380	--	--
26	06-17-86	<5	20	3	<10	.3	<10	<1	<1	<1	70	<6	9
	07-22-87	--	--	4	--	--	--	--	--	--	63	--	--
	07-01-88	--	--	<1	--	--	--	--	--	--	71	--	--
27	06-18-86	<5	40	<1	<10	<.1	<10	<1	<1	<1	67	<6	7
	06-11-88	--	--	<1	--	--	--	--	--	--	76	--	--
28	06-30-89	<5	38	<1	<10	<.1	<10	<1	<1	<1	260	<6	10
	07-17-87	--	--	2	--	--	--	--	--	--	650	--	--
	07-01-88	--	--	<1	--	--	--	--	--	--	380	--	--
29	06-29-88	<1	15	2	--	<.1	<10	<1	5	<1	47	<6	<3
	11-22-88	--	--	1	--	--	--	--	--	--	56	--	--
30	07-23-87	<5	35	<1	<10	<.1	<10	<1	2	<1	810	14	51
	01-05-89	--	--	2	--	--	--	--	--	--	780	--	--
31	01-05-89	--	--	<1	--	--	--	--	--	--	47	--	--
32	06-24-86	<5	41	3	<10	<.1	<10	<1	2	<1	42	14	10
	07-15-87	--	--	2	--	--	--	--	--	--	39	--	--
	06-11-88	--	--	<1	--	--	--	--	--	--	41	--	--
33	07-15-87	--	--	--	<10	--	--	--	--	--	--	--	--
	06-29-88	--	--	3	--	--	--	--	--	--	45	--	--
	11-23-88	--	--	3	--	--	--	--	--	--	38	--	--
34	07-16-87	<5	42	13	10	.1	<10	<1	<1	<1	130	--	--
	11-22-88	--	--	12	--	--	--	--	--	--	140	--	--
35	06-11-87	6	70	19	20	.1	<10	<1	<1	1	1,100	<6	6
36	04-24-86	1	109	8	20	.1	30	<1	<1	<1	2,400	<6	<3
	10-22-87	<5	110	10	<10	<.1	30	1	<1	<1	2,200	<6	<3
37	10-02-87	<5	33	7	<10	<.1	<10	1	<1	<1	100	<6	5
38	07-01-87	<5	60	140	150	<.1	<10	3	<1	<1	2,000	6	200
	07-14-88	--	--	130	--	--	--	--	--	--	2,100	--	--

Dissolved Gases

Direct measurement of gas composition is useful for correcting pH values of water that loses carbon dioxide gas (Pearson and others, 1978). Results of four gas analyses for the Morrison aquifer are shown in table 7. The samples appear to be representative of dissolved-gas compositions expected from the aquifer.

Table 7.--Concentrations of dissolved gases in water from the Morrison aquifer
[See figures 8-10 for location of wells; concentration in milligrams per liter; nd, not detected]

Well number	Date of sample	Nitrogen (N_2)	Oxygen (O_2)	Argon (Ar)	Carbon dioxide (CO_2)	Methane (CH_4)	Ethane (C_2H_6)
18	06-09-87	1.48	0.004	0.015	0.0007	0.008	nd
20	06-10-87	1.34	.007	.014	.001	.051	0.002
22	06-10-87	1.42	.010	.015	.0007	.018	nd
35	06-11-87	1.08	.009	.014	.003	.001	nd

Stable Isotopes

To evaluate hydrologic and geochemical processes, the stable isotopes of $\delta^{18}O$, δD, $\delta^{13}C$, and $\delta^{34}S$ were determined. Data for the first three isotopes are presented in the text. Stable-isotopic ratios are expressed in units of parts per thousand (per mil, $^0/_{00}$) relative to a standard:

$$\delta_x = \left[\frac{R_x}{R_s} - 1\right] \times 1,000 \qquad (1)$$

where δ is delta;
R is the ratio of heavier to lighter isotope;
x is the sample; and
s is the standard.

For an example of deriving the delta (δ) notation, hydrogen isotopes are the ratio of deuterium (D = ^2H) to hydrogen (H):

$$\delta D = \left[\frac{\frac{D}{H_x}}{\frac{D}{H_{V-SMOW}}} - 1\right] \times 1,000 \qquad (2)$$

where V-SMOW is Vienna-Standard Mean Ocean Water.

Oxygen and hydrogen isotopes can be ideal tracers of water movement because they compose the water. Isotopic variations in precipitation (atmospheric deposition) result from changes in temperature, altitude, and other factors. For example, winter precipitation is depleted in heavy isotopes (D, ^{18}O) relative to summer precipitation. Because high-latitude precipitation is depleted, the isotopic ratio is lighter than low-latitude precipitation. The mixing of recharge water tends to average the isotopic variations of precipitation. At low temperatures (as compared to geothermal regimes) associated with most aquifers, no hydrogen isotopes are exchanged between water and solid phases. Thus, the isotopic composition of water changes only as a function of physical and chemical processes in the aquifer such as evaporation or mineral dissolution.

Isotopic ratios are shown in table 8, and a plot of the δD and $\delta^{18}O$ ratios for 36 samples collected from the Gallup, Dakota, and Morrison aquifers is shown in figure 24. A line defined by Craig (1961) as $\delta D = 8\delta^{18}O + 10$ represents samples collected from various localities in the world. Vuataz and Goff (1986) defined a local meteoric water line for northern New Mexico as $\delta D = 8\delta^{18}O + 12$, which is parallel to and slightly left of the world meteoric line. This local meteoric line was applied to the San Juan Basin study area by Phillips and others (1986b) in their report on the Ojo Alamo aquifer. However, most of the isotopic ratios plot to the right of the world meteoric line in figure 24. This suggests a different local meteoric water line for these samples or evaporation during infiltration of precipitation, which is common in semiarid environments (Phillips and others, 1986b, p. 181).

Phillips and others (1986b, p. 181) calculated the mean isotopic ratio for modern precipitation in the central San Juan Basin as $-12.8\,^{0}/_{00}$ for $\delta^{18}O$ and as $-90\,^{0}/_{00}$ for δD. Recharge water of Pleistocene age averaged $3.0\,^{0}/_{00}$ lighter in $\delta^{18}O$ and $25\,^{0}/_{00}$ lighter in δD than modern recharge water. During the Pleistocene, climatic changes such as a decrease in mean annual temperature and an increase in winter precipitation may have accounted for the shift to lighter isotopic ratios (Phillips and others, 1986b, p. 183).

The areal distribution of δD is shown for the Morrison aquifer in figure 25. Heavier isotopic ratios ($\delta^{18}O = -14.2\,^{0}/_{00}$ and $\delta D = -103.5\,^{0}/_{00}$) were found in samples at well 30 in the recharge area near Sanostee than in samples collected from wells 10 mi downgradient to the east and northeast. Water in an area encompassing four wells in the Morrison aquifer had light values of $\delta^{18}O$ ($-15.0\,^{0}/_{00}$ to $-15.6\,^{0}/_{00}$) and δD ($-114\,^{0}/_{00}$ to $-116\,^{0}/_{00}$). Comparing data for these four wells to modern precipitation calculated by Phillips and others (1986a) indicates a depletion of $2.8\,^{0}/_{00}$ in $\delta^{18}O$ and $26\,^{0}/_{00}$ in δD, which is similar to Pleistocene samples. The data imply that ground water 10 mi from the outcrop area was recharged during the Pleistocene.

Carbon-13/carbon-12 ratio data were collected to examine sources and sinks of carbon as an aid in determining chemical reactions that control the carbon distribution in the aquifers. In general, soil gas CO_2 contains a $\delta^{13}C$ value of $-20\,^{0}/_{00}$ to $-25\,^{0}/_{00}$, and carbonate minerals have $\delta^{13}C$ values close to $0\,^{0}/_{00}$ (Drever, 1982, p. 345). Stable carbon isotopic values typically range from $-10\,^{0}/_{00}$ to $-12.5\,^{0}/_{00}$ in samples, as a result of soil gas CO_2 reacting with carbonate minerals. Chemical reactions will affect $\delta^{13}C$ values in water in different ways: calcite dissolution adds carbon so $\delta^{13}C$ values become heavier; calcite precipitation removes carbon so $\delta^{13}C$ values become lighter; feldspar dissolution does not change $\delta^{13}C$ values in a system closed to CO_2. The oxidation of organic matter adds light carbon ($\delta^{13}C$) to the system.

Table 8.--Isotopic ratios of stable isotopes in water from the Gallup, Dakota, and Morrison aquifers

[See figures 8-10 for location of wells; wells 1-10 are completed in the Gallup aquifer, wells 12-13 in the Dakota aquifer, and wells 14-38 in the Morrison aquifer; values are in per mil ($^0/_{00}$); --, not reported]

Well number	Date of sample	Oxygen ($\delta^{18}O$)	Hydrogen (δD)	Carbon ($\delta^{13}C$)	Sulphur, SO_4^{2-} ($\delta^{34}S$)
1	07-01-88	-13.6	-101	-12.3	-14.0
2	04-22-86	-13.5	-113	--	--
	10-21-87	--	--	-9.8	-6.0
3	04-21-86	-14.3	-110	--	--
4	07-15-88	-14.2	-105	-8.0	15.4
5	06-30-87	-13.9	-98	-26.1	--
	06-28-88	--	--	--	-5.4
6	06-30-88	-14.0	-104	-8.6	-6.1
7	06-28-88	-15.0	-111	-11.2	1.6
8	12-03-87	-13.0	-97	--	--
9	04-29-86	-11.8	-87	--	--
	08-11-87	-11.9	-90	-7.6	-10.4
10	06-30-88	-14.3	-106	-12.2	-1.6
12	06-29-88	-14.4	-106	-13.1	-1.3
13	04-29-86	-13.0	-96	--	--
14	06-10-88	-13.0	-96	-8.6	.5
15	07-21-87	-13.6	-101	-19.0	--
16	06-24-86	-14.6	-107	--	9.4
	06-08-88	--	--	-6.5	--
17	07-02-86	-14.1	-103	--	11.7
18	06-16-86	-14.1	-103	-8.8	10.2
	06-09-87	--	-104	--	--
19	07-14-87	-12.7	-97	-3.7	8.6
20	06-19-86	-13.9	-103	--	10.1
21	06-18-86	-14.1	-103	--	9.0
22	06-19-86	-14.0	-104	-9.2	10.1
23	06-10-88	-15.9	-120	-9.1	3.0
24	07-01-86	-12.5	-94	-10.9	-6.1
25	06-09-88	-13.2	-98	-10.3	3.7
26	06-17-86	-15.6	-114	-10.8	10.1
	07-01-88	--	--	-10.5	11.2

Table 8.--Isotopic ratios of stable isotopes in water from the Gallup, Dakota, and Morrison aquifers--Concluded

Well number	Date of sample	Oxygen ($\delta^{18}O$)	Hydrogen (δD)	Carbon ($\delta^{13}C$)	Sulphur, SO_4^{2-} ($\delta^{34}S$)
27	06-18-86	-15.9	-115	-10.0	10.9
28	06-30-86	-15.7	-114	--	--
	07-01-88	--	--	-10.0	14.0
29	06-29-88	-15.6	-116	-10.5	14.9
30	07-23-87	-14.2	-104	-10.9	--
32	06-24-86	-14.6	-107	-13.4	5.0
	07-15-87	--	--	-12.7	--
33	07-15-87	-15.3	-113	-11.7	--
34	07-16-87	-14.1	-104	-10.7	--
35	06-11-87	-14.0	-104	-11.9	--
36	04-24-86	-14.3	-114	--	--
	10-22-87	-14.4	-108	-11.7	12.8
37	10-02-87	-14.5	-108	-12.2	-18.7
38	07-01-87	-11.0	-82	-13.5	-13.0
	07-14-88	--	--	-13.1	-10.3

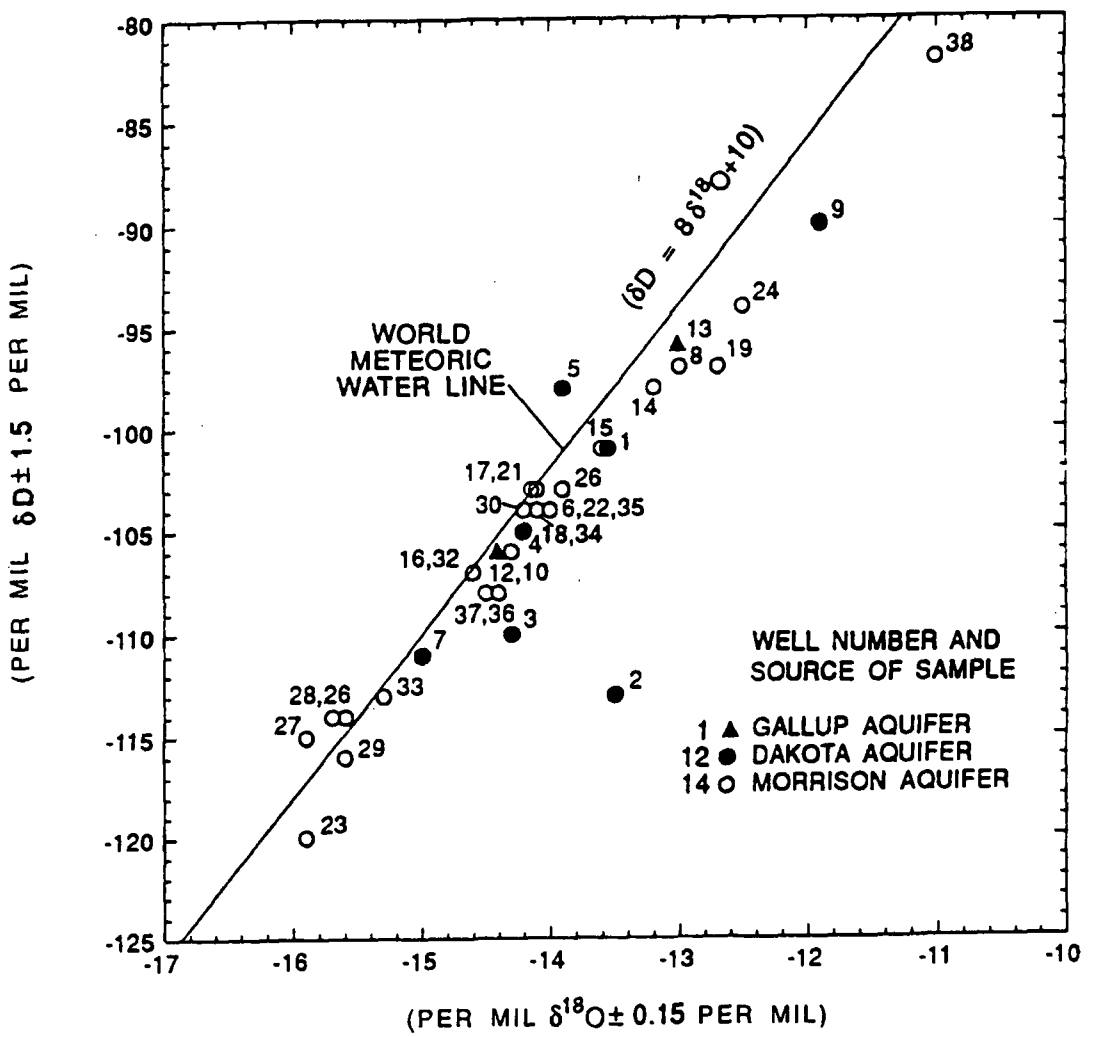

Figure 24.--Oxygen and deuterium isotopic ratios in water from water wells completed in the Gallup, Dakota, and Morrison aquifers. Well locations are shown in figures 8, 9, and 10.

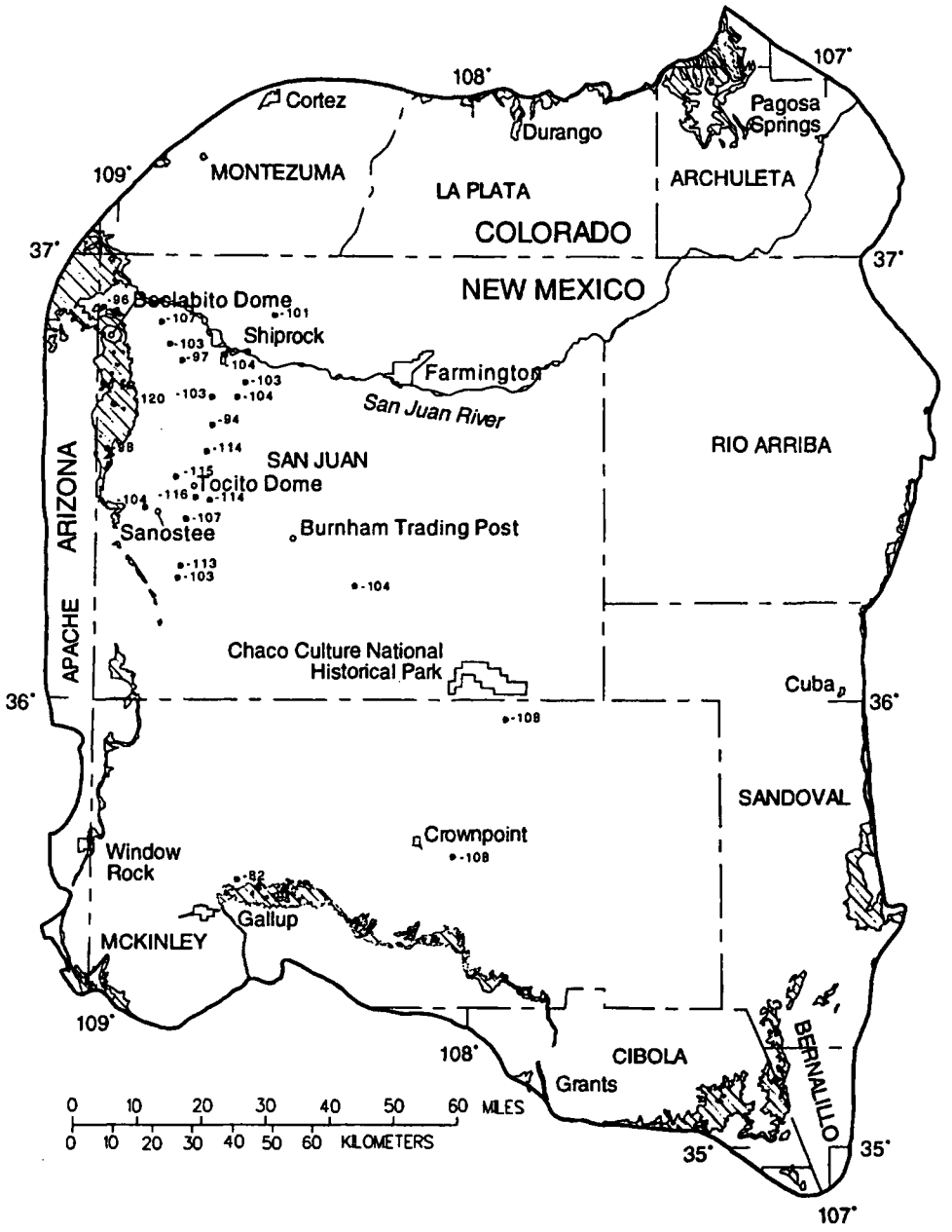

EXPLANATION

OUTCROP OF MORRISON AQUIFER, JURASSIC ROCKS, UNDIVIDED; WANAKAH FORMATION; ENTRADA SANDSTONE; AND SAN RAFAEL GROUP--From Dane and Bachman, 1965; Wilson and others, 1969; Tweto, 1979; and Hintze, 1981

BOUNDARY OF STUDY AREA

•-104 WATER WELL--Number is deuterium isotopic ratio, in per mil relative to Standard Mean Ocean Water (SMOW)

Figure 25.--Deuterium isotopic ratio in water from water wells completed in the Morrison aquifer.

Stable carbon isotopic data ($\delta^{13}C$) are shown in table 8 and in figure 26 for the Gallup aquifer and figure 27 for the Morrison aquifer. Values of $\delta^{13}C$ for the Gallup aquifer generally were consistent with carbonate minerals reacting with soil gas (-7.6 $^{0}/_{00}$ to -12.3 $^{0}/_{00}$) except for one sample that contained very light $\delta^{13}C$ of -26.1 $^{0}/_{00}$ (fig. 26), suggesting an organic carbon source.

Carbon-13/carbon-12 ratio values for samples from the Morrison aquifer ranged from -3.7 $^{0}/_{00}$ to -19.0 $^{0}/_{00}$ (fig. 27). However, 16 of 20 samples had a smaller range of -9.1 $^{0}/_{00}$ to -13.1 $^{0}/_{00}$, which coincides with well locations that are more than 10 mi from the San Juan River (fig. 26). The analytical accuracy of the $\delta^{13}C$ analysis was generally ± 0.3 $^{0}/_{00}$ (Carol Kendall, U.S. Geological Survey, oral commun., 1989). Thus, the minor variability of the $\delta^{13}C$ values in the samples may be due to chemical reactions involving carbon or may be due to analytical accuracy. For example, a value of -10.5 $^{0}/_{00}$ ± 0.3 $^{0}/_{00}$ includes three samples (wells 26 and 29) in the northwestern part of the basin (table 8).

Radioactive Isotopes

The radioactive isotopes ^{3}H, ^{14}C, and ^{36}Cl were used to determine the residence time that water has been isolated from the atmosphere. Residence times are useful for determination of aquifer characteristics and for geochemical analysis of flow paths. The half-lives of the three radioisotopes are: ^{3}H = 12.26 years, ^{14}C = 5,730 years, and ^{36}Cl = 301,000 years. Therefore, applications of age dating with the three radioisotopes are significantly different. Tritium is applicable in detecting modern (post-1952) water in the sample. The isotope ^{14}C is applicable in determining ages to approximately 50,000 years (Durrance, 1986). Because of its slow decay, ^{36}Cl is applicable in age determinations of 100,000 to approximately 1 million years (Bentley and others, 1986). Processes that include mixing and ion filtration can be determined using ^{36}Cl radioisotopes as shown by Phillips and others (1986a).

Activities of ^{3}H in samples from 26 wells generally were less than 1 tritium unit (3.2 pCi/L) as shown in table 9. This indicates that the sampled ground water has not mixed with modern water and has been isolated from the atmosphere at least since 1952.

During the initial collection of radioisotope samples in 1986, samples for ^{14}C analysis were collected from four wells completed in the Morrison aquifer. Of water from wells 18, 22, 26, and 27, only water from well 27, closest to the recharge area, contained measurable ^{14}C (table 9). Therefore, the ^{14}C dating technique could be applied practicably only to water samples near recharge areas in the Morrison aquifer in this part of the study area. Twenty-four ^{14}C samples were analyzed between 1986 and 1989, 12 of which contained detectable ^{14}C.

The ^{14}C technique revealed that samples collected from the Morrison aquifer rapidly increased in apparent age; ^{14}C was not detected downgradient from the recharge areas. Slow flow rates or mixing of modern and ancient waters may have resulted in nondetectable ^{14}C activities. Therefore, in view of the limited application of the ^{14}C data to samples from the Morrison aquifer, Dr. Fred Phillips at New Mexico Institute of Mining and Technology prepared, analyzed, and interpreted results of ^{36}Cl samples. The atmosphere produces ^{36}Cl by cosmic ray spallation of ^{36}Ar and neutron activation of ^{36}Ar (Bentley and others, 1986). Meteroic water contains ^{36}Cl; as precipitation becomes recharge water moving into the subsurface, ^{36}Cl decays exponentially. Chlorine-36 can be added from subsurface sources derived from rock weathering and production of neutrons in uranium radionuclide decay. The application of ^{36}Cl to ground-water hydrology has been demonstrated in two regional aquifers: the Great Artesian Basin in Australia (Bentley and others, 1986) and the Milk River aquifer in Alberta, Canada (Phillips and others, 1986a). Age-dating techniques using ^{36}Cl were substantiated with independent modeling results and provided new insights into hydrochemical processes in the two aquifer systems.

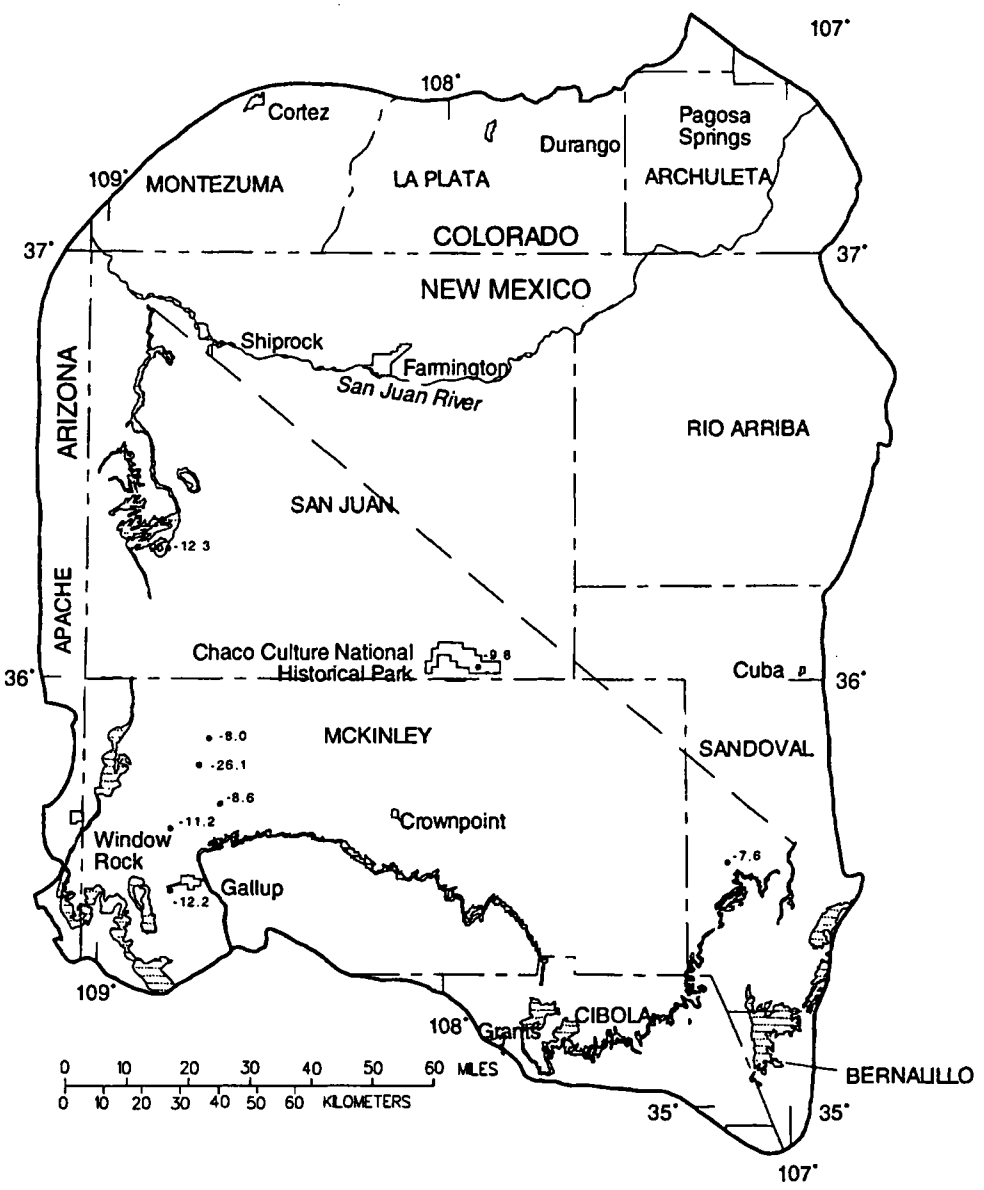

EXPLANATION

OUTCROP OF GALLUP AQUIFER--In Arizona includes Pescado Tongue of Mancos Shale. In the southeastern part of the study area mapped as part of the Mesaverde Group, undivided. From Dane and Bachman, 1965; and Hackman and Olson, 1977

BOUNDARY OF STUDY AREA

APPROXIMATE SUBSURFACE EXTENT OF GALLUP AQUIFER--From Molenaar, 1973

• -8.0 WATER WELL--Number is carbon-13 isotopic ratio, in per mil relative to Peedee belemnite (PDB)

Figure 26.--Carbon-13 isotopic ratio in water from water wells completed in the Gallup aquifer.

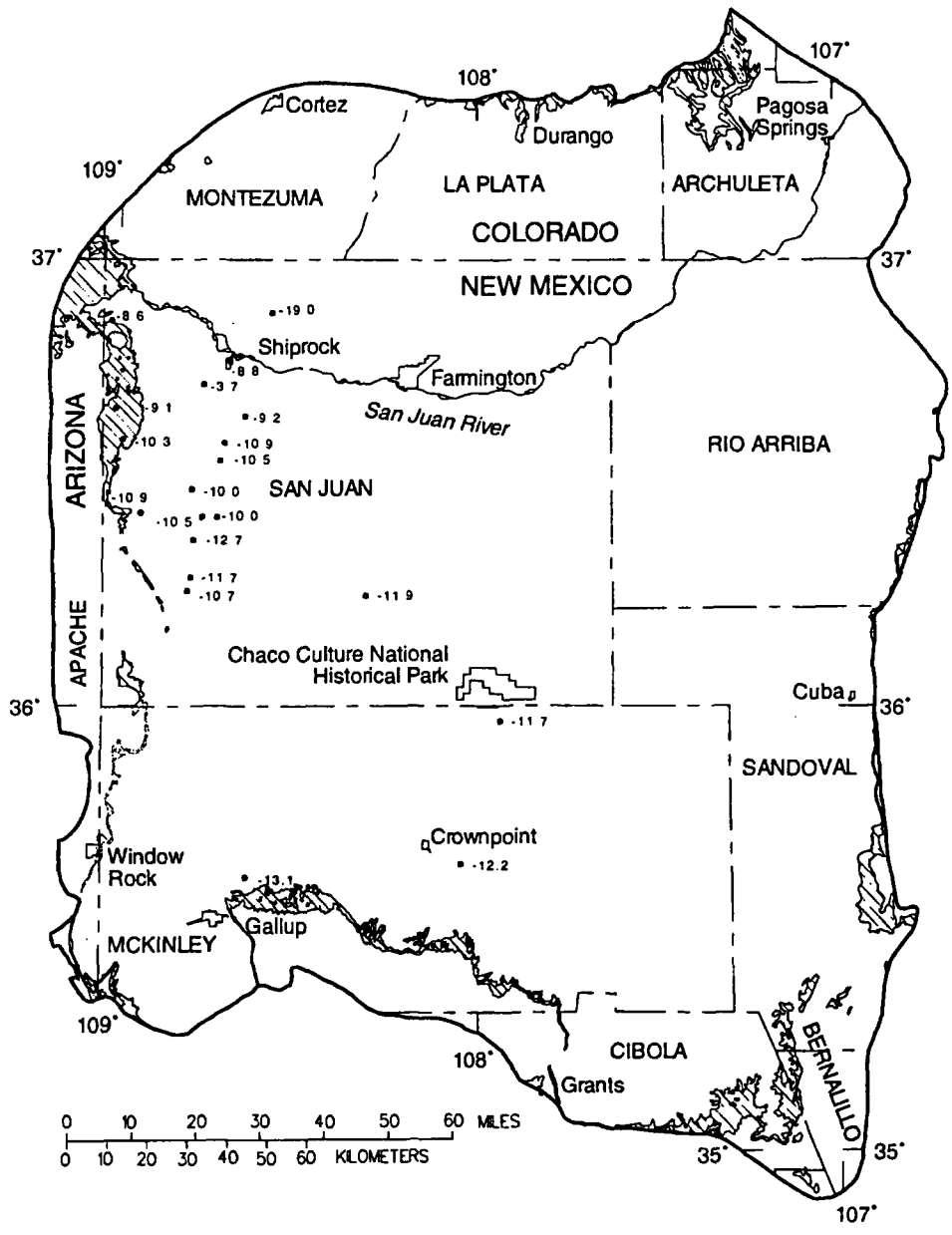

EXPLANATION

OUTCROP OF MORRISON AQUIFER, JURASSIC ROCKS, UNDIVIDED; WANAKAH FORMATION; ENTRADA SANDSTONE; AND SAN RAFAEL GROUP--From Dane and Bachman, 1965; Wilson and others, 1969; Tweto, 1979; and Hintze, 1981

BOUNDARY OF STUDY AREA

• -11.9 WATER WELL--Number is carbon-13 isotopic ratio, in per mil relative to Peedee belemnite (PDB)

Figure 27.--Carbon-13 isotopic ratio in water from water wells completed in the Morrison aquifer.

Water samples from 34 wells were collected to measure ^{36}Cl, as shown in table 9. Analytical error was less than 10 percent. The primary focus of the ^{36}Cl investigation was a detailed examination of the Morrison aquifer. The $^{36}Cl/10^{15}Cl$ values (unitless atomic ratios of ^{36}Cl atoms per 10^{15} chlorine atoms where chloride is the atomic sum of the stable isotopes ^{35}Cl and ^{37}Cl) ranged from 4 to 2,201. Figure 28 displays the areal distribution of $^{36}Cl/10^{15}Cl$ data for the Morrison aquifer. Multiple samples for the same well location are shown where available. The expected recharge input value for the San Juan Basin area was 700 (Jones and Phillips, 1990). Samples obtained near the southern outcrop (well 38) and western outcrop (well 30) contained ratios of 630 and 573, respectively. The simple interpretation of data shown in figure 28 is that values greater than 700 are a result of buildup of ^{36}Cl and values less than 700 are due to radioactive decay of ^{36}Cl. Repeat sampling for ^{36}Cl at four of five wells indicated that $^{36}Cl/10^{15}Cl$ ratios were not reproducible within 10 percent (fig. 28; table 9). Well construction and open-hole completion opposite multiple sandstones within the Morrison aquifer have a similar effect on the ^{36}Cl data as on the previously discussed water-chemistry data.

Comparison of the ^{14}C data with the ^{36}Cl data was not reliable due to collection of the data on different sampling dates. Chemical concentrations and isotope contents varied in several wells over time as previously described.

Collection and analysis of ^{36}Cl radioisotopes, as well as other constituents, clearly indicated that the original assumptions of the ground-water flow system were inadequate. The flow system was re-evaluated to provide a conceptual model, consistent with the chemical data, with which to interpret the sources of solutes.

Table 9.--Activities of tritium, carbon-14, and chlorine-36 isotopes in water from the Gallup, Dakota, and Morrison aquifers

[See figures 8-10 for location of wells; wells 1-2 and 4-10 are completed in the Gallup aquifer, wells 11-13 in the Dakota aquifer, and wells 14-38 in the Morrison aquifer; pCi/L, picocuries per liter; <, less than detection limit; --, no data. A, B, and C refer to repeat sampling of wells as shown in figures 31-33]

Well number	Date of sample	Tritium (^{3}H) (pCi/L)	Carbon-14 (^{14}C) (percent modern)	Chlorine-36 ($^{36}Cl/10^{15}Cl$) (ratio)	Chlorine-36 (^{36}Cl) (atoms/liter)
1	07-01-88	<0.3	--	676	9.0
2	10-21-87	<.3	<0.4	198	16.5
4	07-15-88	<.3	2.2	122	.9
5	06-30-87	<.3	<.4	--	--
	06-28-88	--	--	153	11.7
6	06-30-88	1.5	6.4	22	.2
7	06-28-88	<.3	2.6	569	9.2
8	12-03-87	--	--	537	21.0
9	08-11-87	.4	4.5	--	--
10	06-30-88	<.3	2.8	--	--
11	07-23-87	--	--	169	16.4
12	06-29-88	--	--	730	3.2

Table 9.--Activities of tritium, carbon-14, and chlorine-36 isotopes in water from the Gallup, Dakota, and Morrison aquifers--Concluded

Well number	Date of sample	Tritium (^3H) (pCi/L)	Carbon-14 (^{14}C) (percent modern)	Chlorine-36 ($^{36}Cl/10^{15}Cl$) (ratio)	Chlorine-36 (^{36}Cl) (atoms/liter)
13	12-03-87	--	--	149	19.7
14	06-10-88	--	--	244	4.6
15	07-21-87	<0.3	<1.0	15	5.5
16	06-24-86	4.0	--	--	--
	06-08-88	--	<1.1	44	.8
17	07-02-86	--	--	42	4.4
18	06-16-86	--	<1.2	--	--
	06-09-87	<.4	--	59	5.7
19	07-14-87	<.3	<.4	4	5.1
20	06-10-87	1.2	--	38	7.7
22	06-19-86	3.0	<1.2	--	--
	06-10-87	--	--	42	5.9
23	06-10-88	<.3	10.5	333	13.0
24	07-01-86	<.3	--	213	13.8
25	06-09-88	<.3	31.5	295	5.0
26	06-17-86	2.0	<.8	--	--
	07-01-88	--	--	251	1.7
27	06-18-86	1.0	3.1	--	--
	06-11-88	--	--	36	.1
28	06-30-86A	--	--	163	7.8
	07-17-87B	--	--	15	1.6
29	06-29-88B	--	--	417	2.1
30	07-23-87	<.3	15.6	--	--
	01-05-89	--	--	573	2.6
31	01-05-89	<26	--	2,201	6.0
32	06-24-86	3.0	--	--	--
	07-15-87	<.3	11.2	--	--
	06-11-88	--	--	42	.1
33	07-15-87A	<.3	<1.0	400	29.2
	06-29-88B	--	--	121	2.5
	11-23-88C	--	--	274	3.9
34	07-16-87B	<.3	<1.0	1,857	22.4
	11-22-88A	<26	--	481	6.4
35	06-11-87	<1.0	<.4	290	9.4
36	04-24-86A	--	--	648	15.4
	10-22-87B	<.3	<.4	537	15.5
37	10-02-87	<.3	.8	894	9.9
38	07-01-87	.3	14.4	--	--
	07-14-88	--	--	630	7.7

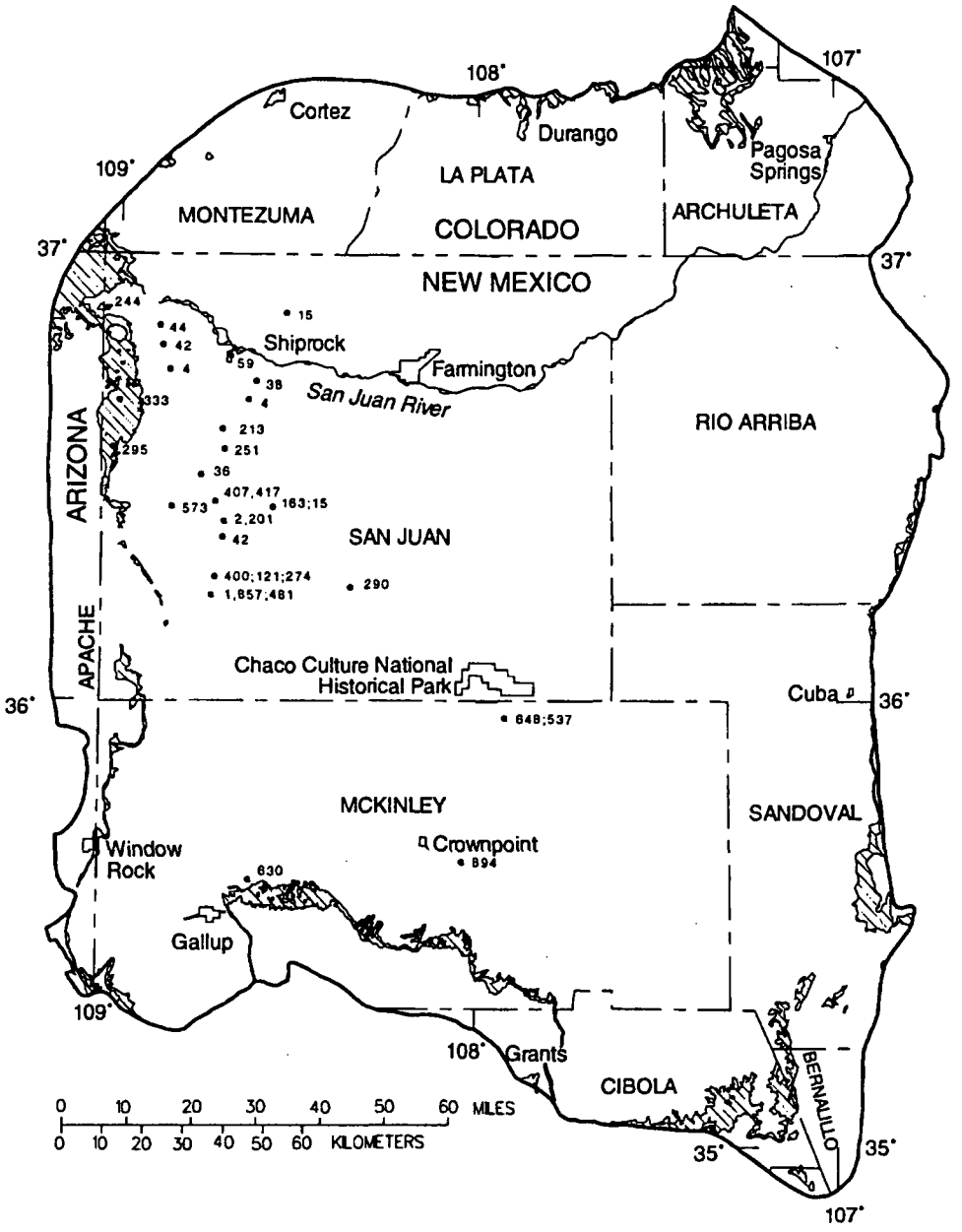

EXPLANATION

OUTCROP OF MORRISON AQUIFER, JURASSIC ROCKS, UNDIVIDED; WANAKAH FORMATION; ENTRADA SANDSTONE; AND SAN RAFAEL GROUP--From Dane and Bachman, 1965; Wilson and others, 1969; Tweto, 1979; and Hintze, 1981

BOUNDARY OF STUDY AREA

• 333 WATER WELL--Number represents ratio of chlorine-36 to stable chlorine isotopes. Multiple ratios for a well are listed in chronological order

Figure 28.--Ratio of chlorine-36 to stable chlorine isotopes in water from water wells completed in the Morrison aquifer.

Physical and Geochemical Processes

Physical processes of the flow system and geochemical processes controlling rock/water/gas interactions affect the observed chemical concentrations and isotopic contents. Physical processes that are examined include ground-water flow, mixing, evaporation, dilution, and ion filtration. Geochemical processes examined include mineral solubility, ion exchange, and oxidation/reduction. The geochemical data were used to examine these physical and geochemical processes.

The fluctuation in ion concentration among water analyses, particularly for wells containing large open intervals, may be due to the lithology of the Morrison aquifer, which is a sequence of sandstones and shales. Heterogeneity in sandstone properties, such as hydraulic conductivity, may result in variability of ion concentrations contained in the individual sandstone layer if the sandstones are confined between shale layers and no mixing occurs within the Morrison aquifer. Thus, a water sample from a well completed in multiple lithologies in the Morrison aquifer may be a mix of different water chemistries. Changes in ion chemistry in samples collected at a well at different times may be due to changes in hydraulic head. A change in hydraulic head may cause the sandstone layers in the aquifer to contribute different amounts of water to the well bore, which would change the mix of different water chemistries. Wells completed in the Morrison aquifer that flowed continuously during the duration of the field sampling caused a lowering of the hydraulic head, resulting in changes in ion chemistry for samples collected at different times. In large regional aquifer systems such as the San Juan Basin, the water chemistry at a particular location commonly has been assumed to have changed little, if any, over short time periods of a few years. The results determined for six wells completed in the Morrison aquifer and one well in the Dakota aquifer suggest that repeated sampling over time is needed to verify reproducibility of ion chemistry.

Decreases in chloride concentrations 10 mi downgradient from the recharge area may be due to factors including mixing of recharge water with more dilute water within the Morrison aquifer; leakage of more dilute water from above or below the Morrison aquifer; or ion filtration. Another potential cause of low chloride concentrations may be changing rates of recharge in the Morrison aquifer. Large rates of recharge during times of high precipitation would dilute chloride concentrations. Conversely, small rates of recharge during dry periods would likely concentrate chloride in the recharge area by evaporation in the vadose zone.

Ion filtration is a process previously proposed as being active in the San Juan Basin (Berry, 1959) and other basins (such as Phillips and others, 1986b). The ion-filtration hypothesis assumes a semipermeable membrane such as a clay layer or shale separating two zones of higher hydraulic conductivity. Electrochemical and pressure factors can result in exclusion of negatively charged ions, such as chloride, and a decrease in salinity on the low-pressure side of the membrane. Dilute water passes through the membrane to increase the pressure on the "filtrate" side. By applying this hypothesis to the Morrison aquifer, saline water from either the Dakota above the Morrison or the Entrada below the Morrison would be filtered by clay or shale layers and result in the observed low chloride concentrations. Clays or shales of the Brushy Basin and Recapture Members within the Morrison aquifer are the most likely semipermeable membranes within the Dakota-Entrada sequence.

As previously described, δD values in samples from four wells completed in the Morrison aquifer were depleted by $26^0/_{00}$ relative to modern precipitation. These lighter isotopic values may indicate that recharge for these four wells occurred during a time period of cooler mean

temperature and wetter conditions than exist today. This would be consistent with average Pleistocene values found for the Ojo Alamo aquifer by Phillips and others (1986b). A second hypothesis explaining the existence of depleted $\delta^{18}O$ and δD values is membrane filtration. The ion filtration process would enrich the heavy isotopes in the residual solution and deplete the heavy isotopes in the solution passing through the shale (Coplen and Hanshaw, 1973).

Increases in chloride concentrations in wells near the San Juan River relative to chloride concentrations in recharge areas may be due to factors including dissolution of halite (NaCl) within the Morrison aquifer; leakage of saline water from above or below the Morrison aquifer; mixing of dilute recharge water with saline, deep-basin water near the discharge area in the Morrison aquifer; or oil-field brine contamination. The large solubility of halite, lack of observed halite, and deposition in a freshwater (nonmarine) environment suggest that NaCl dissolution is an unlikely source of increased chloride concentration. Leakage of saline water into the Morrison aquifer and mixing of dilute and saline water within the aquifer are likely processes controlling chloride concentrations.

Figure 29 compares the ratio for concentrations of Br^-/Cl^- to the concentration of chloride. The log-log plot was developed by Whittemore (1988) to evaluate mixing of brines with dilute water and to differentiate between natural brines and oil-field brines. In general, dilute recharge water has Br^-/Cl^- ratios as low as 10×10^{-4} (concentration ratio). Saline solutions from natural brines increase in chloride and the Br^-/Cl^- ratio decreases. The points plotted in figure 29 represent analyses of water from the three aquifers. The lowest Br^-/Cl^- ratio was for well 19, which contained 750 mg/L Cl^- and 0.05 mg/L Br^-, resulting in a ratio of 0.67×10^{-4} Br^-/Cl^-. By comparison, the lowest Br^-/Cl^- ratio found in a natural salt water was 0.57×10^{-4} (Whittemore, 1988, p. 345). Samples from wells completed in the Morrison aquifer near the San Juan River contain Br^-/Cl^- ratios between values found for recharge-type water and halite brine. This suggests mixing of dilute recharge water with saline water.

To aid in identifying physical processes, sampled wells completed in the Morrison aquifer were grouped by location and sample type by Jones and Phillips (1990). Five groups of wells are shown in figure 30 and were designated as follows: group 1 is wells near the San Juan River with elevated chloride concentrations; group 2 is wells located near the Morrison Formation outcrop; group 3 is wells downgradient from the recharge area; group 4 is wells 33 and 34; and group 5 is wells in the central and southern parts of the basin.

Graphical representation of ^{36}Cl data is useful in delineating processes such as dissolution of radioactively "dead" Cl^-, ion filtration, dilution, evaporation, and decay or buildup of ^{36}Cl from uranium deposits (Bentley and others, 1986; Phillips and others, 1986a; Jones and Phillips, 1990). Figure 31 is a plot of the $^{36}Cl/10^{15}Cl$ ratio data and ^{36}Cl concentrations (in atoms/liter $\times 10^{-7}$) for each sample using the group symbol defined in figure 30. As described in Phillips and others (1986a, p. 2012), the addition of "dead" Cl^- will decrease the $^{36}Cl/10^{15}Cl$ ratio (addition of ^{35}Cl and ^{37}Cl) without changing the ^{36}Cl concentration, resulting in a downward shift of the data points as shown by the diagram in figure 31. Dilution, evaporation, or ion filtration will affect the ^{35}Cl, ^{36}Cl, and ^{37}Cl concentrations; therefore, the $^{36}Cl/10^{15}Cl$ ratio will not change, and points in figure 31 would shift horizontally if these processes occurred. Radioactive decay decreases and buildup increases ^{36}Cl concentrations; these processes are represented by sloped lines in figure 31.

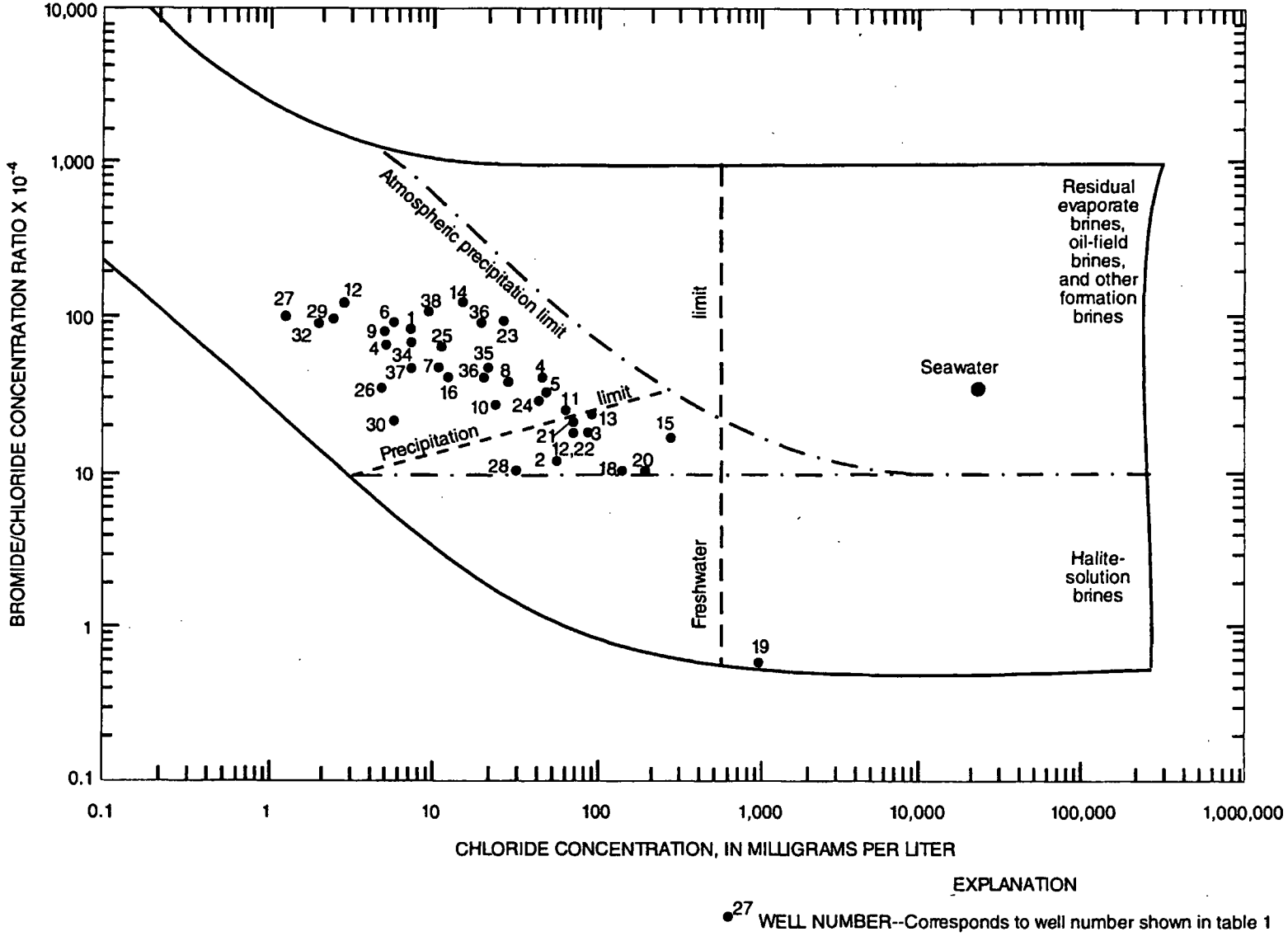

Figure 29.--Ratio of bromide/chloride versus chloride concentrations for water samples from the Gallup, Dakota, and Morrison aquifers.

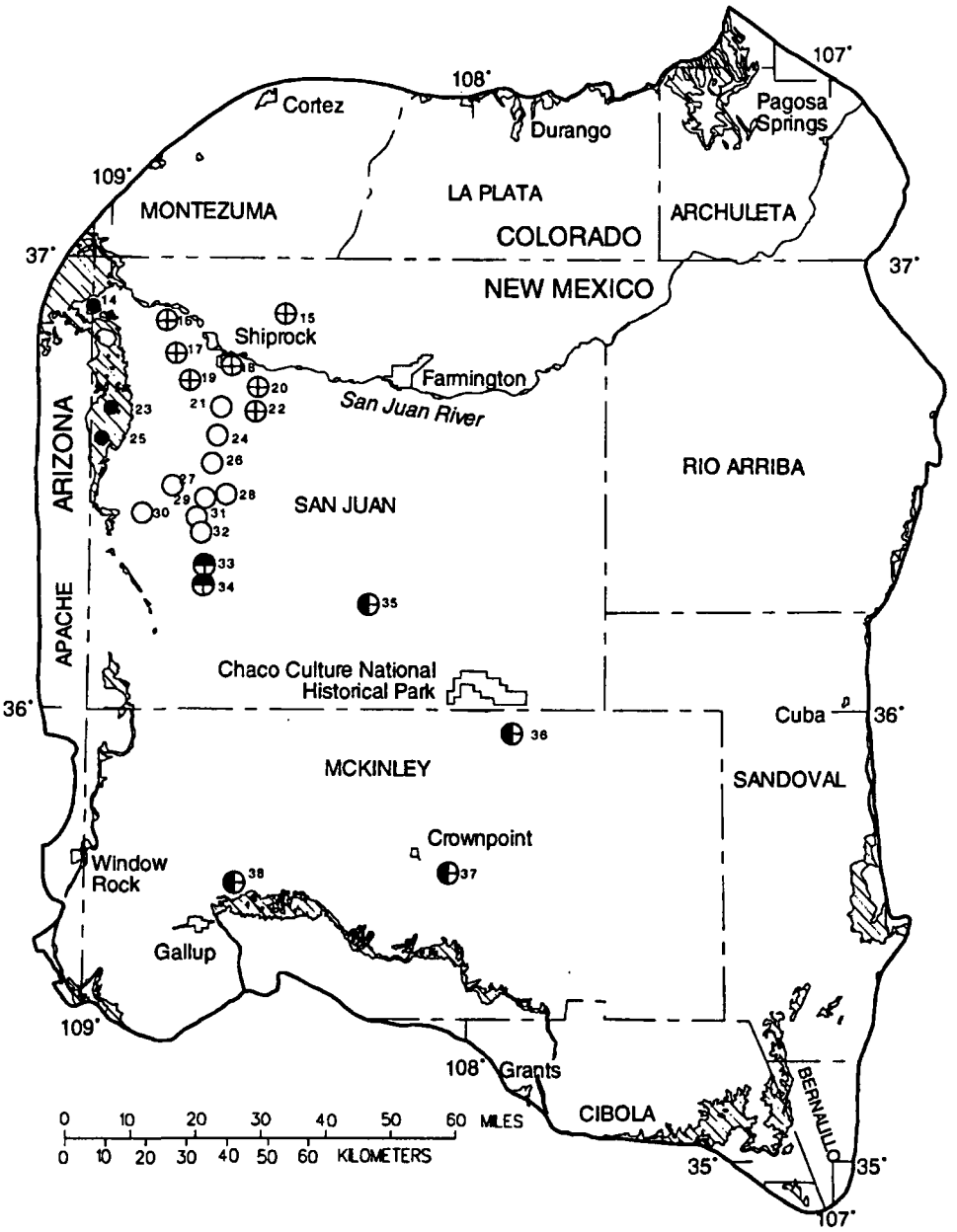

EXPLANATION

OUTCROP OF GALLUP AQUIFER, JURASSIC ROCKS, UNDIVIDED; WANAKAH FORMATION; ENTRADA SANDSTONE; AND SAN RAFAEL GROUP--From Dane and Bachman, 1965; Wilson and others, 1969; Tweto, 1979; and Hintze, 1981

BOUNDARY OF STUDY AREA

⊕ 15 WATER WELL--Symbol represents group 1 wells located near the San Juan River with elevated Cl^- concentrations. Number corresponds to well number shown in table 1

● 23 WATER WELL--Symbol represents group 2 wells located near the outcrop of Morrison Formation. Number corresponds to well number shown in table 1

○ 24 WATER WELL--Symbol represents group 3 wells located downgradient from the recharge area. Number corresponds to well number shown in table 1

⊕ 33 WATER WELL--Symbol represents group 4 wells, wells 33 and 34. Number corresponds to well number shown in table 1

◐ 38 WATER WELL--Symbol represents group 5 wells located in the central and southern parts of the basin. Number corresponds to well number shown in table 1

Figure 30.--Location, well number, and group for water wells completed in the Morrison aquifer used in analysis of chlorine-36 data shown in figures 31-33.

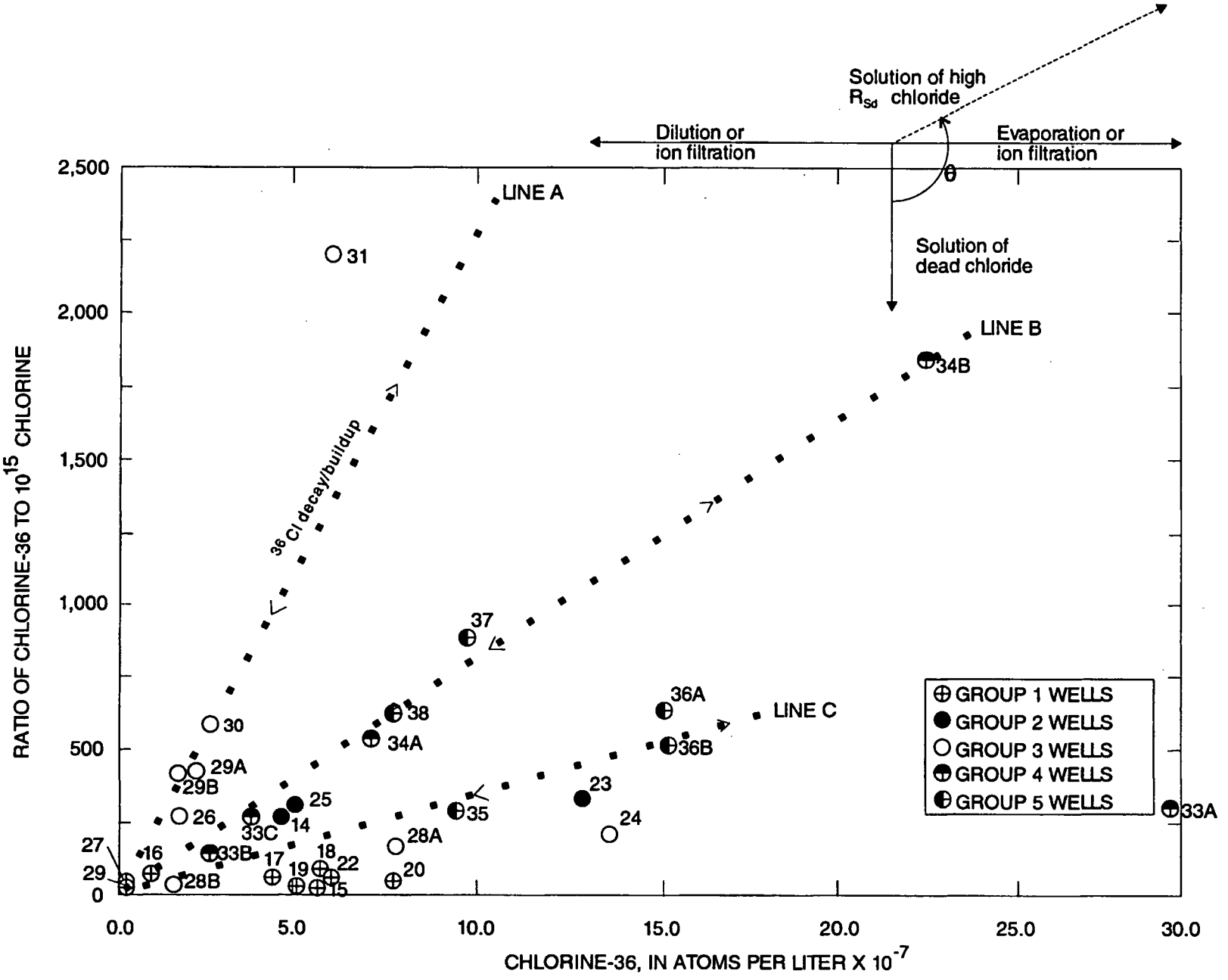

Figure 31.--Chlorine-36/chlorine versus chlorine-36 for water from the Morrison aquifer. The displacement caused by various processes is illustrated (modified from Jones and Phillips, 1990).

Three decay (or buildup) lines were plotted in figure 31 to show samples containing different salinities: line (A) was drawn through sample 30 and the origin for dilute samples; line (B) was drawn through sample 34B and the origin for slightly saline samples; and line (C) was drawn through sample 36B and the origin for saline samples. In general, data points assigned to the well groups defined in figure 30 are described by these three lines. Dilute samples generally followed line A and consisted primarily of group 3 wells: 30, 29, 26, 27, and 31. Samples containing slightly saline values plotted along line B and generally belonged to groups 2 and 5 (outcrop samples and southern San Juan Basin samples). Samples containing saline values plotted along line C and generally consisted of group 5 wells. Wells located near Shiprock and the San Juan River plotted below line C. The buildup of ^{36}Cl due to uranium deposits may have affected samples 31 and 34B (fig. 31).

Chloride mass-balance equations derived by Jones and Phillips (1990) indicate that mixing of waters could be evaluated by plotting the $^{36}Cl/10^{15}Cl$ ratio against the inverse of the chloride concentration in milligrams per liter (figs. 32 and 33). The three lines A, B, and C in figure 31 are shown in figures 32 and 33. Compared to figure 31, lines A, B, and C plot in reverse order in figures 32 and 33 because the chloride concentration decreases away from the origin in figures 32 and 33. Line A represents the ^{36}Cl decay curve and is not affected by other processes such as dilution or ion exchange. Samples that fall on the ^{36}Cl decay curve are 30, 29B, and 26. A decrease in chloride concentration for samples 29A, 32, and 27 results in plots to the right of line A as shown by line D in figure 32. These samples may be the result of dilution or ion filtration of chloride in the Morrison aquifer. Likewise, samples that plotted to the left of line A were concentrated in chloride, possibly due to evaporation or ion filtration on the opposite side of the membrane, as represented by line E.

Dr. Fred Phillips (New Mexico Institute of Mining and Technology, written commun., 1991) compared the $^{36}Cl/Cl$ ratios with Br^-/Cl^- ratio data. The mixing of three end-member sources explains the observed data. The first end member is recharge water having a large $^{36}Cl/Cl$ ratio and large Br^-/Cl^- ratio; chloride concentrations range from 7 to 14 mg/L. The second end member is likely either ion filtrate or very ancient ground water recharged under a more humid climate. This second end member is characterized by a small $^{36}Cl/Cl$ ratio, large Br^-/Cl^- ratio, and is very dilute with chloride concentration less than 5 mg/L. The third end member is upward-leaking deep-basin brine containing small ratios of $^{36}Cl/Cl$ and Br^-/Cl^-; Cl^- concentrations exceed 100 mg/L. Therefore, the mixing of recharge water and an ion filtrate or ancient dilute recharge water with upward-leaking brine dominates the flow regime in the northwestern part of the San Juan Basin. This mixing of ground water affects ion constituent concentrations and precluded quantitative mass-balance calculations of geochemical reactions affecting water chemistry.

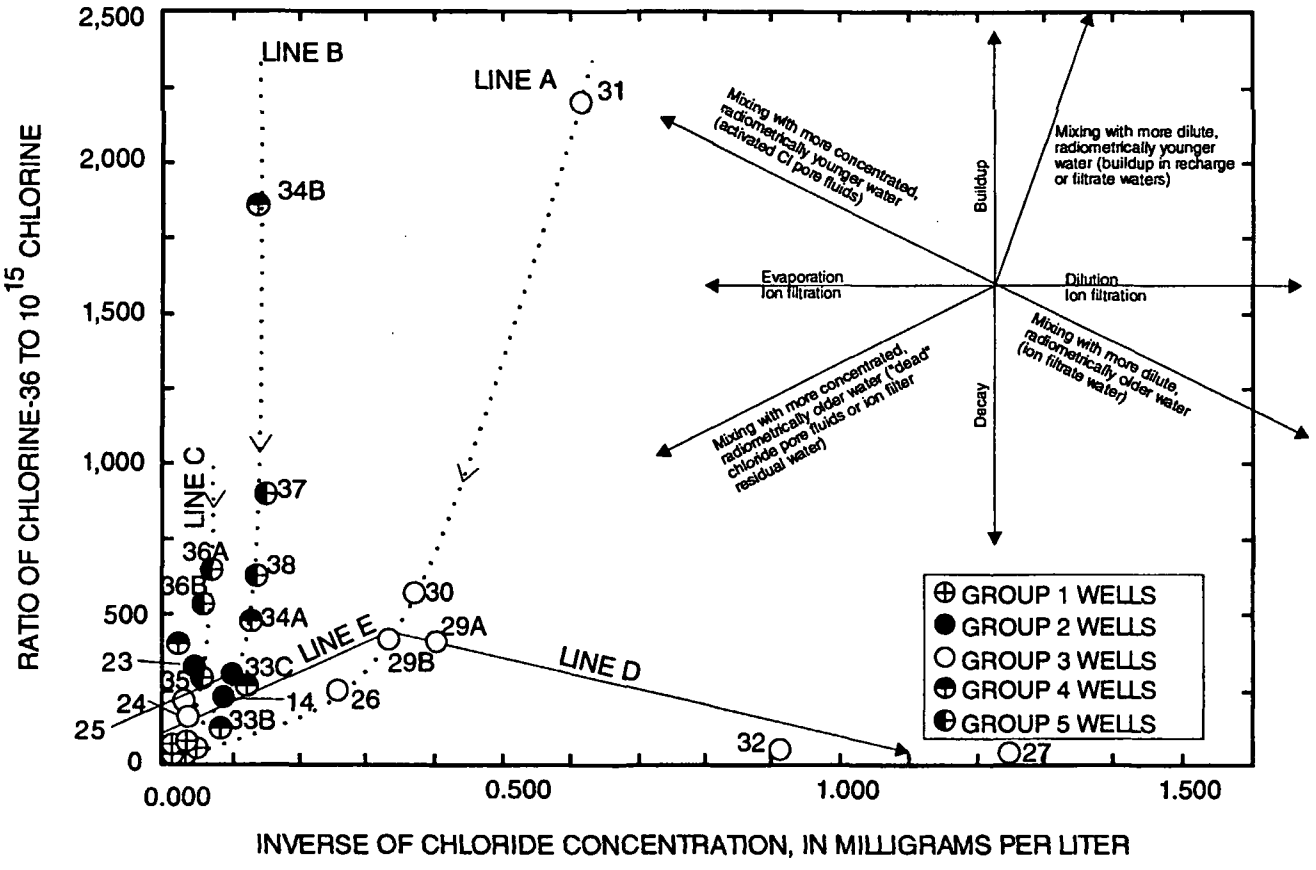

Figure 32.--Chlorine-36/chlorine versus inverse of chloride concentration for water from the Morrison aquifer. Figure 33 provides additional details (modified from Jones and Phillips, 1990).

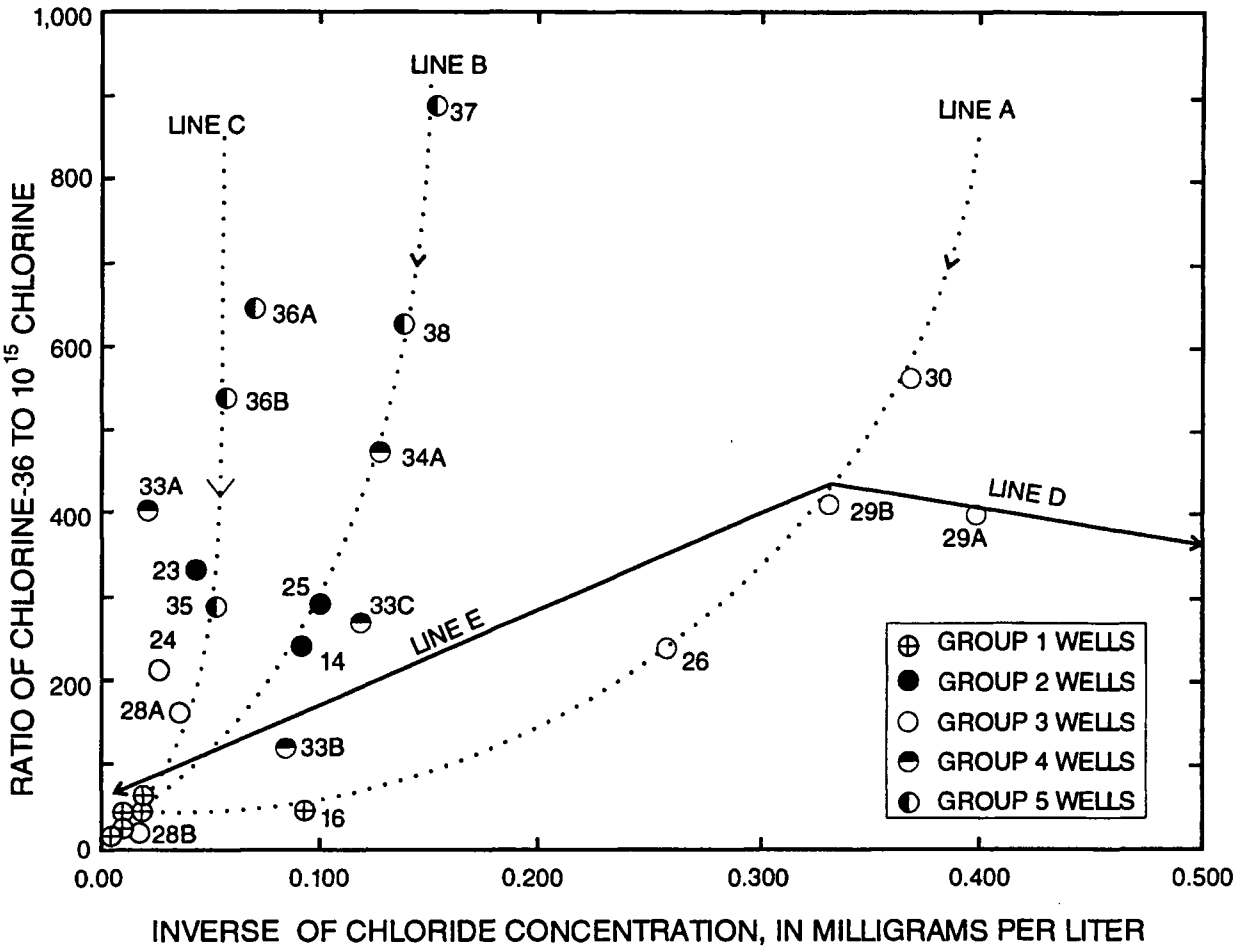

Figure 33.--Chlorine-36/chlorine versus inverse of chloride concentration for water from the Morrison aquifer--expanded scale. Expanded scale shows part of figure 32 in more detail (modified from Jones and Phillips, 1990).

To examine further the possibility of upward leakage into the Morrison aquifer, water-quality analyses were retrieved from the NWIS data base. Single-completion wells in the Wanakah Formation were not available. Chemical analyses for two samples from wells completed in the Entrada Sandstone are shown in table 10. Well Je1 is located on the northwest side of the basin approximately 8 mi west of Morrison well 21, and well Je2 is located approximately 8 mi east of Morrison well 36 (table 10). Sodium, sulfate, and chloride are the predominant major ions in both samples from the Entrada Sandstone. Chloride concentrations are significantly larger in water from the Entrada than in water from the Morrison aquifer. The chloride concentration is 1,100 mg/L in water from well Je1 compared with a chloride concentration of 67 mg/L (table 4) in well 21 from the Morrison aquifer. The chloride concentration is 810 mg/L in water from Entrada well Je2 compared with a chloride concentration of 17 mg/L (table 4) in well 36 from the Morrison. Vertical leakage of water into the Morrison through fractures or other areas of large permeability would increase chloride concentrations in the Morrison aquifer. This finding is generally consistent for samples from wells that have multiple completions in the Morrison and Wanakah Formations. Water from two wells, 26 and 24, completed in the Morrison aquifer, contain chloride concentrations of 3.9 and 38 mg/L (table 4). Well 26 is completed in the Recapture Member and well 24 is completed in the Recapture and Salt Wash Members and in the Wanakah Formation.

Table 10.--Two chemical analyses of water from the Entrada Sandstone
[Concentration in milligrams per liter except where otherwise indicated. --, no data]

	Well identification	
	Je1	Je2
Latitude	364838	360344
Longitude	1085154	1075156
Sample date	09-17-69	03-28-78
Specific conductance (microsiemens per centimeter at 25 degrees Celsius)	9,320	10,000
pH (standard units)	8.20	8.30
Alkalinity (as $CaCO_3$)	410	470
Bicarbonate	570	--
Carbonate	10	2
Calcium	72	70
Manganese	28	8.3
Sodium	2,200	2,800
Potassium	9.0	15
Chloride	1,100	810
Sulfate	2,800	4,300
Fluoride	3.6	5.3
Dissolved solids	6,600	8,300

Physical processes, predominantly leakage and mixing, account for some of the sources and distribution of solutes and isotopes in the three aquifers. Other sources and mechanisms for addition and removal of solutes are controlled by geochemical processes.

Magnesium concentrations were larger in water samples from the Gallup aquifer than from the other two aquifers. This suggests a mineral source of Mg^{2+} in the Gallup aquifer that was not present in the other two aquifers or a sink for Mg^{2+} in the other two aquifers. Dissolution of calcite would contribute Ca^{2+} ions and dissolution of dolomite contributes Ca^{2+} and Mg^{2+} ions as shown in reactions 3 and 4:

$$CaCO_{3(c)} + H^+ = Ca^{2+} + HCO_3^- \quad (3)$$

$$CaMg(CO_3)_{2\,(c)} + 2H^+ = Ca^{2+} + Mg^{2+} + 2HCO_3^- \quad (4)$$

Dolomite, but not calcite, was observed in the Gallup aquifer by Kaharoeddin (1971), suggesting that the source of Ca^{2+} and Mg^{2+} is likely dolomite dissolution reactions.

The small Ca^{2+} and Mg^{2+} concentrations in the Dakota aquifer indicate that either dolomite dissolution is not a major process, cation exchange occurs, or the available data were not representative of the Dakota aquifer. Calcium and magnesium concentrations were also small in the Morrison aquifer. Dolomite minerals have not been observed in the Morrison, and calcite minerals are present but in small amounts (less than 10 percent calcite from two outcrop locations in the northwestern part of the basin according to Hansley, 1990).

The removal of Ca^{2+} and Mg^{2+} and the increase in Na^+ in the Gallup aquifer in the direction of ground-water flow are indicative of ion-exchange reactions with clay minerals (reaction 5):

$$Ca^{2+} + Na_2X = 2Na^+ + CaX; \quad (5)$$

where X = ion-exchange site.

Chlorite and glauconite clay minerals were observed by Kaharoeddin (1971) in the Gallup aquifer. Chlorite has a very low cation-exchange capacity of less than 10 meq/100 g (Drever, 1982, p. 82). Glauconite, an iron-rich variety of illite, has a higher cation-exchange capacity of 10 to 40 meq/100 g (Drever, 1982, p. 74 and 82). This suggests that glauconite rather than chlorite would be more effective in the exchange of the divalent cations (Ca^{2+}, Mg^{2+}) for the monovalent Na^+ cation in the Gallup aquifer.

The presence of small concentrations of Ca^{2+} and Mg^{2+} in samples from the Dakota and Morrison aquifers may be a result of sampling where dissolution of carbonates and cation exchange both occur in the recharge area, possibly in the soil zone or unsaturated zone, prior to reaching the location of the sampled wells. Another possible explanation is that dissolution of carbonates was not a significant process and that silicate hydrolysis was the major process resulting in Na^+ concentrations. The dissolution of albite ($NaAlSi_3O_8$) releases Na^+ as shown in reactions 6 and 7. Albite altering to kaolinite ($Al_2Si_2O_5(OH)_4$) has been observed in core and outcrop samples from the Morrison aquifer (Hansley, 1990).

$$NaAlSi_3O_{8\,(c)} + 8H_2O = Na^+ + Al(OH)_4^- + 3H_4SiO_4^0 \quad (6)$$

$$2NaAlSi_3O_8 + 2CO_2 + 11H_2O = 2Na^+ + Al_2Si_2O_5(OH)_{4\,(c)} + 4H_4SiO_4^0 + 2HCO_3^- \quad (7)$$

Sources of bicarbonate include carbonate dissolution (reactions 3 and 4) and silicate hydrolysis (reaction 7). Dissolution of the carbonate mineral dolomite is a likely source of HCO_3^- in the Gallup aquifer (reaction 6). Silicates hydrolyzing in the presence of CO_2 gas contribute HCO_3^- (reaction 7). Silicate minerals observed in all three aquifers include potassium feldspar, plagioclase feldspar (such as albite), and several clay minerals.

Sources of sulfate include dissolution of sulfate-bearing minerals and oxidation of sulfide minerals. However, for the Gallup aquifer, no sulfate or sulfide minerals were observed by Williams (1956) or Kaharoeddin (1971). The large concentrations of SO_4^{2-} in water analyses shown in table 2 suggest that there is a source of SO_4^{2-} and that the mineralogical data may not be complete for the Gallup aquifer. The Mancos Shale confines the Gallup aquifer and may be a source of SO_4^{2-}.

Sulfate concentrations in the Dakota aquifer do not increase uniformly but rather form two groups of small and large concentrations. No sources of SO_4^{2-} were studied by Walters and others (1987), who were concerned primarily with trace-element concentrations.

Sulfate concentrations increase downgradient in the Morrison aquifer toward Shiprock. Sources of SO_4^{2-} in water from the Morrison aquifer include dissolution of sulfate minerals or oxidation of sulfide minerals. Anhydrite ($CaSO_4$) and pyrite (FeS_2) have been observed in the Morrison aquifer (Hansley, 1990). A dissolution reaction for anhydrite producing SO_4^{2-} is shown in reaction 8. Oxidation of 1 mole of pyrite can release 2 moles of SO_4^{2-} (reaction 9).

$$CaSO_{4(c)} = Ca^{2+} + SO_4^{2-} \quad (8)$$

$$FeS_{2(c)} + 4O_{2\,(g)} + 2H_2O = FeO(OH) + 2SO_4^{2-} + 4H^+ \quad (9)$$

$(Silica)_T$ is the total sum of three ions: $H_4SiO_4^0$, $H_3SiO_4^-$, and $H_2SiO_4^{2-}$. Below a pH of 9, most dissolved $(SiO_2)_T$ exists as $H_4SiO_4^0$. As pH rises above 9, $H_3SiO_4^-$ becomes an important species (Drever, 1982, p. 91-92), followed by $H_2SiO_4^{2-}$ above a pH of 12. Dissolved $(SiO_2)_T$ concentrations would be expected to increase with increasing pH above 9 because both $H_2SiO_4^{2-}$ and $H_3SiO_4^-$ would be in solution. Dissolved $(SiO_2)_T$ is plotted against field pH in figure 34 for water from the Morrison aquifer. No correlation exists for all points; however, a cluster of $(SiO_2)_T$ samples plot in the range of 18 to 20 mg/L with pH values between 9.2 and 9.5. Another control on $(SiO_2)_T$ concentration is temperature (Krauskopf, 1979, p. 169-170). The effects of water temperature on dissolved $(SiO_2)_T$ appear to be significant for values greater than 25 °C (fig. 34). The maximum $(SiO_2)_T$ concentration of 35 mg/L was associated with the warmest water of 51.8 °C.

An oxidation-reduction (redox) reaction controls nitrogen speciation. The denitrification process (reaction10) is shown below:

$$NO_3^- + 2CH_2O + 2H^+ = NH_4^+ + 2CO_{2(g)} + H_2O; \quad (10)$$

where CH_2O = organic matter.

Microbes use the oxygen in nitrate ions to oxidize organic matter to CO_2. The denitrification process in the aquifer probably occurs after oxygen is consumed by the oxygen-reducing microbes.

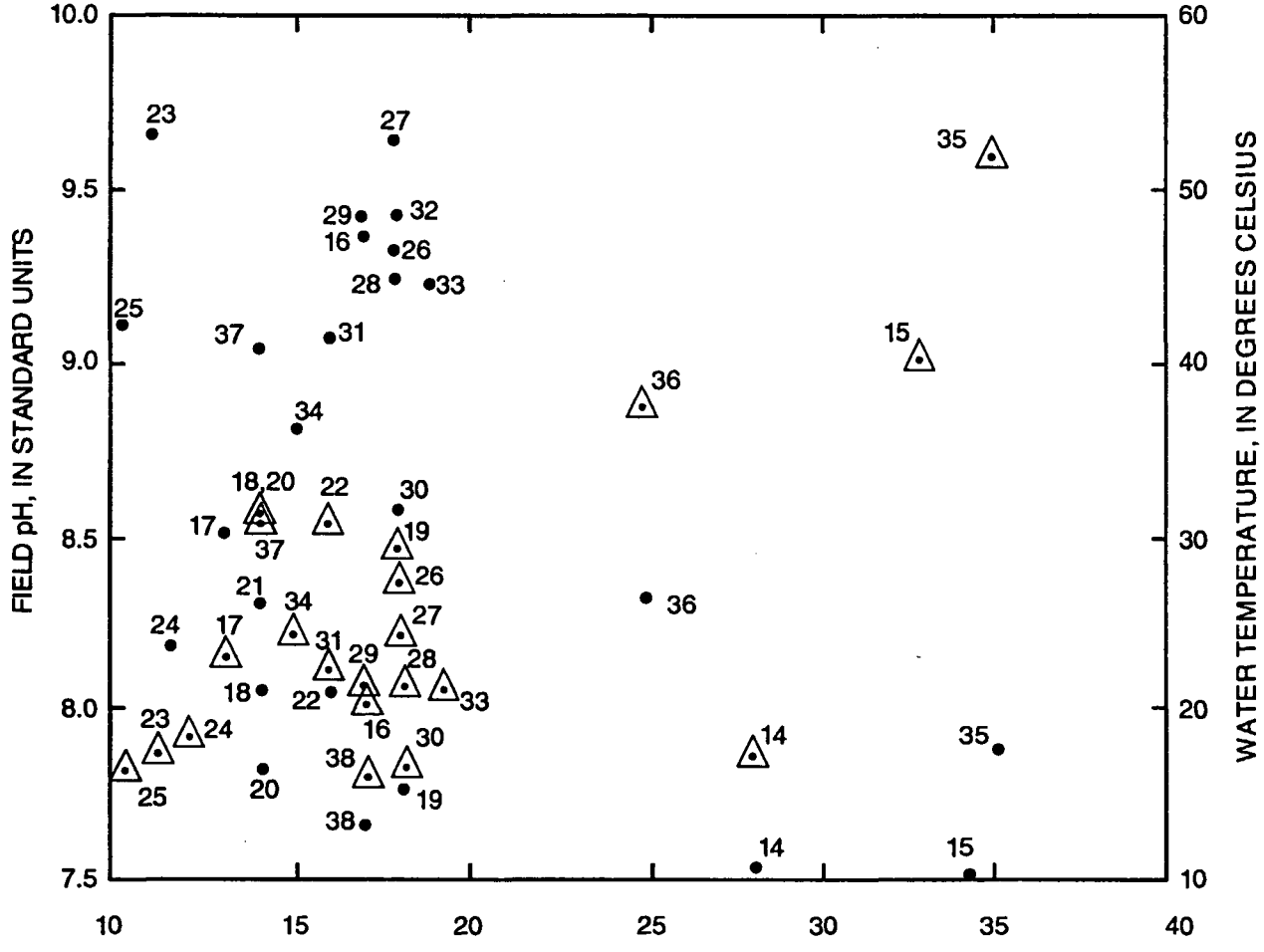

Figure 34.--Concentration of dissolved silica versus field pH and temperature of water samples from the Morrison aquifer.

Degrees of mineral saturation were computed with the computer code WATEQF (Plummer and others, 1976) to identify areas where minerals are likely to dissolve, precipitate, or be in thermodynamic equilibrium with the water. Requirements for input into the code include data on the major ions, pH, temperature, SiO_2, Fe, PO_4, Sr, and F. Analytical data for Al and $(SiO_2)_T$ are required for calculating states of saturation for aluminosilicate minerals. A value of 10 µg/L for Al was assumed for values less than the detection limit of 10 µg/L. Redox calculations were made using dissolved oxygen (where detected) or the SO_4/H_2S ratio (H_2S was converted from total sulfide data).

WATEQF modeling provides an estimate of the mineral saturation index (SI) for a suite of minerals for each sample. The definition of SI is:

$$SI = \log \frac{IAP}{K_T} \qquad (11)$$

where IAP is ion activity product; and
K is equilibrium constant at temperature T, in degrees Kelvin.

If SI is negative, the solution is undersaturated with respect to the mineral. Conversely, a positive SI indicates supersaturation with respect to the mineral. Where IAP equals K_T, thermodynamic equilibrium is indicated.

Results from WATEQF modeling indicate various states of saturation for minerals in the three sandstone aquifers. Albite, amorphous silica, and gypsum were found to be undersaturated in all samples collected from the three aquifers, suggesting that these minerals would dissolve in ground water where they are present in the aquifer. Values of SI for calcite in the Gallup and Dakota aquifers generally are positive, suggesting conditions suitable for calcite precipitation.

Values of SI for calcite in samples from the Morrison aquifer ranged from positive to negative, indicating both precipitation and dissolution of calcite minerals in some parts of the aquifer. Most samples were supersaturated with respect to calcite, indicating that calcite would precipitate. Several samples, particularly near the San Juan River in the vicinity of Shiprock, were undersaturated with respect to calcite, indicating that calcite would dissolve where present.

Values of SI calculated for dolomite ($CaMg(CO_3)_2$) for samples in the three aquifers have similar patterns to the SI data for calcite. Notable exceptions are three samples from the Gallup aquifer in the central part of the basin that are supersaturated with respect to calcite and undersaturated with respect to dolomite. The difference in SI values for dolomite relative to calcite may be the presence of small Mg^{2+} concentrations detected in several samples from the Gallup aquifer.

SI values were computed for clay minerals including chlorite, kaolinite, illite, and the smectite group of montmorillonite minerals. SI values for chlorite samples from the Gallup aquifer ranged from highly positive (5.0) to highly negative (-4.3). Highly positive SI values indicate that precipitation of chlorite may consume 0.5 mole/liter of Mg from the water. SI values for chlorite in the Morrison aquifer ranged from 3.7 to -6.2. No discernible trends in SI values for chlorite were evident.

Kaolinite minerals were observed in the Dakota and Morrison aquifers. Values of SI for both aquifers show general trends of undersaturation (suggesting dissolution) with respect to kaolinite near the recharge areas and supersaturation (suggesting precipitation) downgradient.

WATEQF calculations for illite minerals indicate predominant undersaturation of the minerals in samples collected from the three aquifers. Exceptions were two samples obtained from wells located in the outcrop area of the Morrison aquifer. Illite has been observed in the Dakota and Morrison aquifers, suggesting the potential for dissolution reactions that would release Mg^{2+}, Al hydroxides, and silicic acid.

Smectite minerals were observed in the Dakota and Morrison aquifers. The thermodynamic data for smectite minerals are not well constrained, creating large uncertainties in the SI calculations. Smectite was found to be supersaturated for all samples from the two aquifers.

SUMMARY AND CONCLUSIONS

Geochemical data were obtained for 38 wells completed in the Gallup, Dakota, and Morrison aquifers to examine sources of solutes and hydrologic controls that affect the concentration and distribution of solutes in the San Juan Basin. The scope was constrained primarily to the northwestern part of the basin because of well availability and disturbances to the natural ground-water system by uranium mining in the southern part of the basin. Although the Gallup, Dakota, and Morrison aquifers were examined, 25 of the 38 wells were completed in the Morrison aquifer, which had the most available wells completed in single aquifers.

Based on a series of samples collected along ground-water flow paths, chemical concentrations were variable depending on vertical sampling interval, well location, and sampling date. Several sandstone units contributed water to wells completed in the Morrison aquifer, suggesting that the Morrison aquifer is not a simple two-dimensional flow system. The data presented in this report indicate an upward component of flow into the Morrison aquifer. The entire section above and below the Morrison aquifer appears to be controlled by a three-dimensional flow regime where saline brine leaks upward near the San Juan River discharge area. Temporal changes in ion constituent concentrations may be a result of changes in hydraulic head in individual sandstone layers that contributed water to the well. The assumption that water chemistry in wells does not change over short periods in a large regional aquifer cannot be made as has been done commonly in previous investigations.

Predominant ions found in the three aquifers were generally Ca^{2+}, Na^{+}, HCO_3^{-}, and SO_4^{2-}. The Gallup aquifer contained Ca^{2+}-HCO_3^{-} in recharge areas and Na^{+}-SO_4^{2-} downgradient. The Dakota Sandstone contained Na^{+}-HCO_3^{-} in recharge areas with the addition of SO_4^{2-} downgradient. Predominant ions in the Morrison aquifer were Na^{+}-HCO_3^{-} in recharge areas and Na^{+}-SO_4^{2-} downgradient.

Maximum chloride concentrations found in the Gallup, Dakota, and Morrison aquifers were 240, 720, and 750 mg/L, respectively. Median chloride concentrations were 20, 57, and 11 mg/L, respectively. Detectable trace-element concentrations included As, Ba, B, Fe, Li, Mn, and Sr.

Radioactive isotopes were useful in distinguishing sources of water to the Morrison aquifer. The absence of ^{3}H activities confirmed that ground water from all wells sampled has not mixed with modern water and has been isolated from the atmosphere since at least 1952. Of 24 samples analyzed, ^{14}C activities were detected in 12. Age dating with ^{14}C was not meaningful given the different sources of water in the aquifer. The ^{36}Cl radioisotopic data proved most useful in differentiating the sources of water in the Morrison aquifer. Comparing Br^-/Cl^- concentration ratios to $^{36}Cl/Cl$ ratios indicates three major end members of water resulting from different sources. Recharge water had a large $^{36}Cl/Cl$ ratio and small Br^-/Cl^- ratio. Chloride concentrations were between 7 and 14 mg/L. A second end member of water contained small ^{36}Cl ratios, large Br^-/Cl^- ratios, was very dilute, and contained chloride concentrations below 5 mg/L. These results suggest that water may have filtered into the Morrison through zones that trap dissolved solids by the ion-filtration process. A second hypothesis is that this water is very ancient water that was recharged during a humid climatic period. The third end member of water is characterized by upward-leaking, deep-basin brine containing small ratios of $^{36}Cl/Cl$ and Br^-/Cl^- and large chloride concentrations exceeding 100 mg/L.

Chemical and radioisotopic data indicate that water from overlying and underlying units mixes with recharge water in the Morrison aquifer. Recharge water contained a large $^{36}Cl/Cl$ ratio and a small Br^-/Cl^- ratio. Approximately 10 mi downgradient, however, samples from four wells completed in the Morrison aquifer were considerably different in composition compared to recharge samples. Oxygen stable isotopes decreased by 2.8 $^{0}/_{00}$ and deuterium decreased 26 $^{0}/_{00}$, relative to recharge. Carbon-14 radioisotope activities were not detectable. Chlorine-36/Cl ratios were small and Br^-/Cl^- ratios were large. These results suggest two potentially viable processes: ion filtration or trapping of ancient dilute water recharged under a humid climate. For water samples near the San Juan River, pH decreased to about 8.0, Cl^- concentrations increased to more than 100 mg/L, and $^{36}Cl/Cl$ ratios and Br^-/Cl^- ratios were small. Leakage of deep basin brine into the fresher water of the Morrison aquifer appears to control ion constituent concentrations.

The mixing of recharge water and an ion filtrate or ancient dilute recharge water with upward-leaking brine dominates the flow regime in the northwestern part of the San Juan Basin. This mixing of ground water controls ion constituent concentrations and precluded quantitative mass-balance calculations of geochemical reactions controlling water chemistry. Geochemical reactions involve dissolution of carbonate, silicate, and sulfate minerals present in the three aquifers, ion-exchange reactions, and oxidation reduction.

REFERENCES CITED

Bennett, G.D., 1979, Regional ground-water systems analyses: Water Spectrum, v. 11, no. 4, p. 36-42.

Bentley, H.W., Phillips, F.M., Davis, S.N., Habermehlz, M.A., Airey, P.L., Calf, G.E., Elmore, David, Gove, H.E., and Torgersen, Thomas, 1986, Chlorine-36 dating of very old groundwater, 1. The Great Artesian Basin, Australia: Water Resources Research, v. 22, no. 13, p. 1991-2001.

Berry, F.A.F., 1959, Hydrodynamics and geochemistry of the Jurassic and Cretaceous systems in the San Juan Basin, northwestern New Mexico and southwestern Colorado: Palo Alto, Stanford University, unpublished Ph.D. dissertation, 213 p.

Cadigan, R.A., 1967, Petrology of the Morrison Formation in the Colorado Plateau region: U.S. Geological Survey Professional Paper 556, 113 p.

Claassen, H.C., 1982, Guidelines and techniques for obtaining water samples that accurately represent the water chemistry of an aquifer: U.S. Geological Survey Open-File Report 82-1024, 49 p.

Condon, S.M., and Peterson, Fred, 1986, Stratigraphy of Middle and Upper Jurassic rocks of the San Juan Basin--Historical perspective, current ideas, and remaining problems, *in* Turner-Peterson, C.E., Santos, E.S., and Fishman, N.S., eds., A basin analysis case study--The Morrison Formation, Grants uranium region, New Mexico: American Association of Petroleum Geologists Studies in Geology, no. 22, p. 7-26.

Coplen, T.B., and Hanshaw, B.B., 1973, Ultrafiltration by a compacted clay membrane--I. Oxygen and hydrogen isotopic fractionation: Geochimica et Cosmochimica Acta, v. 37, p. 2295-2310.

Craig, Harmon, 1961, Isotopic variations in meteoric waters: Science, v. 133, p. 1702-1703.

Craig, L.C., Holmes, C.N., Cadigan, R.A., Freeman, V.L., Mullens, T.E., and Weir, G.W., 1955, Stratigraphy of the Morrison and related formations, Colorado Plateau region--A preliminary report: U.S. Geological Survey Bulletin 1009-E, p. 125-168.

Craigg, S.D., Dam, W.L., Kernodle, J.M., and Levings, G.W., 1989, Hydrogeology of the Dakota Sandstone in the San Juan structural basin, New Mexico, Colorado, Arizona, and Utah: U.S. Geological Survey Hydrologic Investigations Atlas HA-720-I, 2 sheets.

Craigg, S.D., Dam, W.L., Kernodle, J.M., Thorn, C.R., and Levings, G.W., 1990, Hydrogeology of the Point Lookout Sandstone in the San Juan structural basin, New Mexico, Colorado, Arizona, and Utah: U.S. Geological Survey Hydrologic Investigations Atlas HA-720-G, 2 sheets.

Crossey, L.J., 1989, Clay mineral diagenesis in Westwater Canyon Sandstone Member of Morrison Formation, San Juan Basin, New Mexico (abs.): American Association of Petroleum Geologists, Rocky Mountain Section Meeting, Albuquerque, N. Mex., October 1-4, 1989, p. 41.

Dam, W.L., 1988, Methods and preliminary results of geochemical sampling, San Juan Basin, New Mexico, Colorado, Arizona, and Utah, *in* McLean, J.S., and Johnson, A.I., eds., Aquifers of the Western Mountain area: American Water Resources Association Monograph Series 14, p. 203-217.

Dam, W.L., Kernodle, J.M., Levings, G.W., and Craigg, S.D., 1990a, Hydrogeology of the Morrison Formation in the San Juan structural basin, New Mexico, Colorado, Arizona, and Utah: U.S. Geological Survey Hydrologic Investigations Atlas HA-720-J, 2 sheets.

REFERENCES CITED--Continued

Dam, W.L., Kernodle, J.M., Thorn, C.R., Levings, G.W., and Craigg, S.D., 1990b, Hydrogeology of the Pictured Cliffs Sandstone in the San Juan structural basin, New Mexico, Colorado, Arizona, and Utah: U.S. Geological Survey Hydrologic Investigations Atlas HA-720-D, 2 sheets.

Dane, C.H., and Bachman, G.O., 1965, Geologic map of New Mexico: U.S. Geological Survey, 2 sheets, scale 1:500,000.

Dane, C.H., Bachman, G.O., and Reeside, J.B., Jr., 1957, The Gallup Sandstone, its age and stratigraphic relationships south and east of the type locality, *in* Little, C.J., and Gill, J.J., eds., Guidebook to geology of southwestern San Juan Basin: Four Corners Geological Society, Second Field Conference, p. 99-113.

Drever, J.I., 1982, The geochemistry of natural waters: Englewood Cliffs, N.J., Prentice-Hall, 388 p.

Durrance, E.M., 1986, Radioactivity in geology, principles and applications: West Sussex, England, Ellis Horwood Ltd., 441 p.

Fassett, J.E., 1977, Cretaceous and Tertiary rocks of the eastern San Juan Basin, New Mexico and Colorado, *in* Siemers, C.T., ed., Guidebook of Ghost Ranch, central-northern New Mexico: New Mexico Geological Society, 25th Field Conference, p. 225-230.

Fassett, J.E., and Hinds, J.S., 1971, Geology and fuel resources of the Fruitland Formation and Kirtland Shale of the San Juan Basin, New Mexico and Colorado: U.S. Geological Survey Professional Paper 676, 76 p.

Frenzel, P.F., and Lyford, F.P., 1982, Estimates of vertical hydraulic conductivity and regional ground-water flow rates in rocks of Jurassic and Cretaceous age, San Juan Basin, New Mexico and Colorado: U.S. Geological Survey Water-Resources Investigations 82-4015, 59 p.

Green, M.W., and Pierson, C.T., 1977, A summary of the stratigraphy and depositional environments of Jurassic and related rocks in the San Juan Basin, Arizona, Colorado, and New Mexico, *in* Fassett, J.E., ed., Guidebook of San Juan Basin III--Northwestern New Mexico: New Mexico Geological Society, 28th Field Conference, p. 147-152.

Gregory, H.E., 1938, The San Juan Country--A geographic and geologic reconnaissance of southeastern Utah, *with contributions by* M.R. Thorpe and H.D. Miser: U.S. Geological Survey Professional Paper 188, 123 p.

Hackman, R.J., and Olson, A.B., 1977, Geology, structure, and uranium deposits of the Gallup 1° by 2° quadrangle, New Mexico and Arizona: U.S. Geological Survey Miscellaneous Geologic Investigations Map I-981, 2 sheets, scale 1:250,000.

Hansley, P.L., 1986, Regional diagenetic trends and uranium mineralization in the Morrison Formation across the Grants Uranium Region, *in* Turner-Peterson, C.E., Santos, E.S., and Fishman, N.S., eds., A basin analysis case study--The Morrison Formation, Grants uranium region, New Mexico: American Association of Petroleum Geologists Studies in Geology 22, p. 277-301.

_____1990, Regional diagenesis of sandstones in the Upper Jurassic Morrison Formation, San Juan Basin--Geologic, chemical, and kinetic constraints: U.S. Geological Survey Bulletin 1808-H, 35 p.

Hintze, L.F., 1981, Geologic map of Utah: Utah Geological and Mineral Survey, 1 sheet, scale 1:500,000.

REFERENCES CITED--Continued

Jones, B.G., and Phillips, F.M., 1990, A ^{36}Cl investigation of groundwater flow in the Morrison Formation of the San Juan Basin, New Mexico: Socorro, New Mexico Institute of Mining and Technology Hydrology Program Report H90-5, 97 p.

Kaharoeddin, F.A., 1971, Regressive and transgressive phenomena in the Gallup Sandstone in the northwestern part of San Juan County, New Mexico: Albuquerque, University of New Mexico, unpublished M.S. thesis, 81 p.

Kelley, V.C., 1951, Tectonics of the San Juan Basin, *in* Guidebook of the south and west sides of the San Juan Basin, New Mexico and Arizona: New Mexico Geological Society, Second Field Conference, p. 124-131.

Kelly, T.E., 1977, Geohydrology of the Westwater Canyon Member, Morrison Formation, of the southern San Juan Basin, New Mexico, *in* Guidebook of San Juan Basin III--Northwestern New Mexico: New Mexico Geological Society, 28th Field Conference, p. 285-290.

Kennedy, V.C., Zellweger, G.W., and Jones, B.F., 1974, Filter pore-size effects on the analysis of Al, Fe, Mn, and Ti in water: Water Resources Research, v. 10, no. 4, p. 785-790.

Kernodle, J.M., Levings, G.W., Craigg, S.D., and Dam, W.L., 1989, Hydrogeology of the Gallup Sandstone in the San Juan structural basin, New Mexico, Colorado, Arizona, and Utah: U.S. Geological Survey Hydrologic Investigations Atlas HA-720-H, 2 sheets.

Kernodle, J.M., Thorn, C.R., Levings, G.W., Craigg, S.D., and Dam, W.L., 1990, Hydrogeology of the Kirtland Shale and Fruitland Formation in the San Juan structural basin, New Mexico, Colorado, Arizona, and Utah: U.S. Geological Survey Hydrologic Investigations Atlas HA-720-C, 2 sheets.

Knapton, J.R., 1985, Field guidelines for collection, treatment, and analysis of water samples, Montana District: U.S. Geological Survey Open-File Report 85-409, 86 p.

Knight, R.L., and Cooper, J.C., 1955, Suggested changes in Devonian terminology of the Four Corners area, *in* Guidebook to Four Corners: Four Corners Geological Society Guidebook, First Field Conference, p. 56-58.

Krauskopf, K.B., 1979, Introduction to geochemistry (2d ed.): New York, McGraw-Hill, 617 p.

Lawton, D.R., Goodenkauf, O.L., Hanson, B.V., and Smith, F.A., 1984, Dakota aquifers in eastern Nebraska--Aspects of water quality and use, *in* Jorgensen, D.G., and Signor, D.C., eds., Geohydrology of the Dakota aquifer: National Water Well Association, C.V. Theis Conference on Geohydrology, Lincoln, Nebr., October 5-6, 1982, Proceedings, p. 221-228.

Levings, G.W., Craigg, S.D., Dam, W.L., Kernodle, J.M., and Thorn, C.R., 1990a, Hydrogeology of the Menefee Formation in the San Juan structural basin, New Mexico, Colorado, Arizona, and Utah: U.S. Geological Survey Hydrologic Investigations Atlas HA-720-F, 2 sheets.

_____1990b, Hydrogeology of the San Jose, Nacimiento, and Animas Formations in the San Juan structural basin, New Mexico, Colorado, Arizona, and Utah: U.S. Geological Survey Hydrologic Investigations Atlas HA-720-A, 2 sheets.

Merrick, M.A., 1980, Geology of the eastern part of the Regina quadrangle, Sandoval and Rio Arriba Counties, New Mexico: Albuquerque, University of New Mexico, unpublished M.S. thesis, 91 p.

REFERENCES CITED--Continued

Molenaar, C.M., 1973, Sedimentary facies and correlation of the Gallup Sandstone and associated formations, northwestern New Mexico, *in* Fassett, J.E., ed., Cretaceous and Tertiary rocks of the southern Colorado Plateau: Four Corners Geological Society Memoir, p. 85-110.

_____1974, Correlation of the Gallup Sandstone and associated formations, Upper Cretaceous, eastern San Juan and Acoma Basins, New Mexico, *in* Siemers, C.T., ed., Guidebook of Ghost Ranch, central-northern New Mexico: New Mexico Geological Society, 25th Field Conference, p. 251-258.

_____1977a, San Juan Basin time-stratigraphic nomenclature chart, *in* Guidebook of San Juan Basin III: New Mexico Geological Society, 28th Field Conference, p. xii.

_____1977b, Stratigraphy and depositional history of Upper Cretaceous rocks of the San Juan Basin area, New Mexico and Colorado, *with a note on* Economic resources, *in* Guidebook of San Juan Basin III: New Mexico Geological Society, 28th Field Conference, p. 159-166.

_____1989, San Juan Basin stratigraphic correlation chart, *in* Finch, W.I., Huffman, A.C., Jr., and Fassett, J.E., eds., Coal, uranium, and oil and gas in Mesozoic rocks of the San Juan Basin--Anatomy of a giant energy-rich basin: 28th International Geological Congress, Washington, D.C., American Geophysical Union, Guidebook for Field Trip T120, p. xi.

Owen, D.E., 1973, Depositional history of the Dakota Sandstone, San Juan Basin area, New Mexico, *in* Fassett, J.E., ed., Cretaceous and Tertiary rocks of the southern Colorado Plateau: Four Corners Geological Society Memoir, p. 37-51.

_____1984, The Jackpile Sandstone Member of the Morrison Formation in west-central New Mexico--A formal definition: New Mexico Geology, v. 6, no. 3, p. 45-52.

Pearson, F.J., Fisher, D.W., and Plummer, L.N., 1978, Correction of ground-water chemistry and carbon isotopic composition for effects of CO_2 outgassing: Geochimica et Cosmochimica Acta, v. 42, p. 1799-1807.

Phillips, F.M., Bentley, H.W., Davis, S.N., Elmore, D., and Swanick, G.B., 1986a, Chlorine-36 dating of very old groundwater, 2. Milk River aquifer, Alberta, Canada: Water Resources Research, v. 22, p. 2003-2016.

Phillips, F.M., Peeters, L.A., Tansey, M.K., and Davis, S.N., 1986b, Paleoclimatic inferences from an isotopic investigation of groundwater in the central San Juan Basin, New Mexico: Quaternary Research 26, p. 179-193.

Piper, A.M., 1944, A graphic procedure in the geochemical interpretation of water analyses: American Geophysical Union Transactions, v. 25, p. 914-923.

Plummer, L.N., Jones, B.F., and Truesdell, A.H., 1976 (1984 rev.), WATEQF--A Fortran IV version of WATEQ, a computer program for calculating chemical equilibrium of natural waters: U.S. Geological Survey Water-Resources Investigations 76-13, 70 p.

Sears, J.D., 1925, Geology and coal resources of the Gallup-Zuni Basin, New Mexico: U.S. Geological Survey Bulletin 767, 53 p.

Stiff, H.A., Jr., 1951, The interpretation of chemical water analysis by means of patterns: Journal of Petroleum Technology, v. 3, no. 10, p. 15-17.

Stone, W.J., Lyford, F.P., Frenzel, P.F., Mizell, N.H., and Padgett, E.T., 1983, Hydrogeology and water resources of San Juan Basin, New Mexico: Socorro, New Mexico Bureau of Mines and Mineral Resources Hydrologic Report 6, 70 p.

REFERENCES CITED--Concluded

Stumm, Werner, and Morgan, J.J., 1981, Aquatic chemistry (2d ed.): New York, John Wiley and Sons, 583 p.

Thorn, C.R., Levings, G.W., Craigg, S.D., Dam, W.L., and Kernodle, J.M., 1990a, Hydrogeology of the Cliff House Sandstone in the San Juan structural basin, New Mexico, Colorado, Arizona, and Utah: U.S. Geological Survey Hydrologic Investigations Atlas HA-720-E, 2 sheets.

_____1990b, Hydrogeology of the Ojo Alamo Sandstone in the San Juan structural basin, New Mexico, Colorado, Arizona, and Utah: U.S. Geological Survey Hydrologic Investigations Atlas HA-720-B, 2 sheets.

Turner-Peterson, C.E., and Fishman, N.S., 1989, Late Jurassic weather forecast, Four Corners area--Dry, hot, and partly sunny (abs.): American Association of Petroleum Geologists, Rocky Mountain Section Meeting, Albuquerque, N. Mex., October 1-4, 1989, p. 96.

Turner-Peterson, C.E., Santos, E.S., and Fishman, N.S., eds., 1986, A basin analysis case study--The Morrison Formation, Grants uranium region, New Mexico: American Association of Petroleum Geologists Studies in Geology, no. 22, 391 p.

Tweto, Ogden, 1979, Geologic map of Colorado: U.S. Geological Survey, 2 sheets, scale 1:500,000.

U.S. Environmental Protection Agency, 1986, Maximum contaminant levels (subpart B of part 141, National interim primary drinking-water regulations): U.S. Code of Federal Regulations, Title 40, Parts 100 to 149, revised as of July 1, 1986, p. 524-528.

Vuataz, F.D., and Goff, Fraser, 1986, Isotope geochemistry of thermal and nonthermal waters in the Valles Caldera, Jemez Mountains, northern New Mexico: Journal of Geophysical Research, v. 91, no. B2, p. 1835-1853.

Walters, L.J., Jr., Owen, D.E., Henley, A.L., Winsten, M.S., and Valek, K.W., 1987, Depositional environments of the Dakota Sandstone and adjacent units in the San Juan Basin utilizing discriminant analysis of trace elements in shales: Journal of Sedimentary Petrology, v. 57, no. 2, p. 265-277.

Wengerd, S.A., and Matheny, M.L., 1958, Pennsylvanian System of Four Corners Region: American Association of Petroleum Geologists Bulletin, v. 42, no. 9, p. 2048-2106.

Whitney, Gene, and Northrop, H.R., 1987, Diagenesis and fluid flow in the San Juan Basin, New Mexico--Regional zonation in the mineralogy and stable isotope composition of clay minerals in sandstone: American Journal of Science, v. 287, p. 353-382.

Whittemore, D.O., 1988, Bromide as a tracer in ground-water studies--Geochemistry and analytical determination, *in* Ground-Water Geochemistry Conference: National Water Well Association, Denver, Colo., February 16-18, 1988, Proceedings, p. 339-360.

Williams, J.R., 1956, A petrographic study of the subsurface Gallup Sandstone of San Juan County, New Mexico: Lubbock, Texas Tech University, unpublished thesis.

Wilson, E.D., Moore, R.T., and Cooper, J.R., 1969, Geologic map of Arizona: Arizona Bureau of Mines and U.S. Geological Survey, 1 sheet, scale 1:500,000.

Woodward, L.A., and Schumacher, O.L., 1973, Morrison Formation of southeastern San Juan Basin, New Mexico: Socorro, New Mexico State Bureau of Mines and Mineral Resources Circular 129, 7 p.

•U.S. GOVERNMENT PRINTING OFFICE: 1995-774-409/45001

HYDROGEOLOGY AND STEADY-STATE SIMULATION OF GROUND-WATER FLOW IN THE SAN JUAN BASIN, NEW MEXICO, COLORADO, ARIZONA, AND UTAH

By John Michael Kernodle

U.S. GEOLOGICAL SURVEY
Water-Resources Investigations Report 95-4187

REGIONAL AQUIFER-SYSTEM ANALYSIS

Albuquerque, New Mexico
1996

U.S. DEPARTMENT OF THE INTERIOR
BRUCE BABBITT, Secretary

U.S. GEOLOGICAL SURVEY
Gordon P. Eaton, Director

For additional information write to:

District Chief
U.S. Geological Survey
Water Resources Division
4501 Indian School Road NE, Suite 200
Albuquerque, NM 87110-3929

Copies of this report can be purchased from:

U.S. Geological Survey
Branch of Information Services
Box 25286
Denver, CO 80225-0286

CONTENTS

	Page
Abstract	1
Introduction	1
Purpose and scope	3
Description of the study area	3
Population and economy	3
Previous investigations	5
Reports related to the investigation	5
Geohydrologic setting	7
Geology	7
Climate	12
Surface water	16
Ground water	16
Hydrostratigraphic units	18
Alluvium and other Quaternary deposits	19
Lithology	19
Hydraulic properties	19
Chuska Sandstone	21
Lithology	21
Hydraulic properties	21
San Jose Formation	21
Geometry and lithology	21
Hydraulic properties	22
Animas and Nacimiento Formations	22
Geometry and lithology	24
Hydraulic properties	26
Ojo Alamo Sandstone	26
Geometry and lithology	28
Hydraulic properties	28
Kirtland Shale and Fruitland Formation	28
Geometry and lithology	29
Hydraulic properties	29
Pictured Cliffs Sandstone	32
Geometry and lithology	32
Hydraulic properties	34
Lewis Shale	34
Geometry and lithology	34
Hydraulic properties	34

CONTENTS--Continued

	Page
Cliff House Sandstone	36
Geometry and lithology	36
Hydraulic properties	38
Menefee Formation	38
Geometry and lithology	40
Hydraulic properties	40
Point Lookout Sandstone	40
Geometry and lithology	41
Hydraulic properties	41
Crevasse Canyon Formation	41
Geometry and lithology	43
Hydraulic properties	43
Gallup Sandstone	43
Geometry and lithology	43
Hydraulic properties	44
Dakota Sandstone	44
Geometry and lithology	46
Hydraulic properties	46
Morrison Formation	48
Geometry and lithology	48
Hydraulic properties	51
Wanakah Formation	54
Geometry and lithology	54
Hydraulic properties	54
Entrada Sandstone	56
Geometry and lithology	56
Hydraulic properties	56
Natural boundaries of the ground-water-flow system	57
Geologic boundaries	57
Outcrop area boundaries	59
Surface-water boundaries	59
Recharge from precipitation	59
Evapotranspiration	65
Subcrop boundaries	66
Oil-water and gas-water interfaces	66
Density contrasts	68

CONTENTS--Concluded

Page

Description of the model 68
Flow equation, assumed conditions, and computer programs 69
Representation of boundaries 70
Distributed recharge from precipitation 74
Stream-aquifer interaction 74
Internal geometric boundaries 75
Subcrop boundaries 75
Simulated hydraulic properties 79
Model calibration and sensitivity analysis 89
Preconditioned hydraulic-head distribution 91
Model refinements and sensitivity to changes in simulated aquifer properties 91
Discussion of simulation analyses 92
Summary and conclusions 107
Selected references 108

FIGURES

Figures 1-4. Maps showing:
1. Location of the Regional Aquifer-System Analysis areas of investigation 2
2. Location of Colorado Plateau, San Juan structural basin, and study area 4
3. Estimated 1985 population density in the San Juan Basin 6
4. Structural elements of the San Juan Basin and adjacent areas 8
5. Diagram showing time- and rock-stratigraphic framework and nomenclature 9
6. Generalized hydrogeologic section of San Juan Basin showing major aquifers, confining beds, and direction of ground-water flow 10
7-14. Maps showing:
7. Major faults in the San Juan Basin 11
8. Mean annual precipitation for the period 1931-60 13
9. Mean winter precipitation for the period 1931-60 14
10. Potential mean annual evaporation 15
11. Location of streams simulated in the model 17
12. Distribution of Quaternary deposits 20
13. Approximate altitude and configuration of the base of the Animas and Nacimiento Formations 23
14. Approximate thickness of the San Jose, Animas, and Nacimiento Formations 25

FIGURES--Continued

Page

Figures 15-34. Maps showing:

15. Approximate altitude and configuration of the top of the Ojo Alamo Sandstone 27
16. Approximate thickness of the combined Kirtland Shale and Fruitland Formation 30
17. Approximate altitude and configuration of the top of the Kirtland Shale 31
18. Approximate altitude and configuration of the top of the Pictured Cliffs Sandstone 33
19. Approximate altitude and configuration of the top of the Lewis Shale 35
20. Approximate altitude and configuration of the top of the Cliff House Sandstone 37
21. Approximate altitude and configuration of the top of the Menefee Formation 39
22. Approximate altitude and configuration of the top of the Point Lookout Sandstone 42
23. Approximate altitude and configuration of the top of the Gallup Sandstone 45
24. Approximate altitude and configuration of the top of the Dakota Sandstone 47
25. Approximate altitude and configuration of the top of the Morrison Formation 49
26. Approximate thickness of the Morrison Formation 50
27. Location of uranium extraction sites in the Grants uranium belt 52
28. Approximate altitude and configuration of the top of the Wanakah Formation 55
29. Location of major dikes in the San Juan Basin 58
30. Location of drainage basins used to determine the rainfall-altitude-runoff relation for the San Juan Mountains 61
31. Surface-water drainage basins and the division of the San Juan Basin into three rainfall-runoff regimes 62
32. Range of estimated direct recharge 63
33. Location of oil, gas, and water wells completed in the Gallup Sandstone and Tocito Sandstone Lentil 67
34. Finite-difference model grid and locations of hydrogeologic sections shown in figures 37 and 38 71
35. Perspective view of the finite-difference model grid 72
36. Diagram showing correlation of geologic units and model layers 73

FIGURES--Continued

Page

Figure 37. West to east sections showing the vertical layers used in the model:

A. West to east section along 35 degrees 30 minutes latitude 76
B. West to east section along 35 degrees 45 minutes latitude 77
C. West to east section along 36 degrees latitude 77
D. West to east section along 36 degrees 15 minutes latitude 77
E. West to east section along 36 degrees 30 minutes latitude 78
F. West to east section along 36 degrees 45 minutes latitude 78
G. West to east section along 37 degrees latitude 78
H. West to east section along 37 degrees 15 minutes latitude 79

38. South to north sections showing the vertical layers used in the model:

A. South to north section along 107 degrees longitude 80
B. South to north section along 107 degrees 15 minutes longitude 81
C. South to north section along 107 degrees 30 minutes longitude 81
D. South to north section along 107 degrees 45 minutes longitude 81
E. South to north section along 108 degrees longitude 82
F. South to north section along 108 degrees 15 minutes longitude 82
G. South to north section along 108 degrees 30 minutes longitude 82

39. Map showing location of the general-head boundary used to simulate the downward movement of water from the Chuska Sandstone, Deza Formation, and landslide deposits into the regional aquifers 83

40. Maps showing simulated horizontal and vertical hydraulic conductivities for the:

A. San Jose Formation 84
B. Animas and Nacimiento Formations 84
C. Combined Ojo Alamo Sandstone, Kirtland Shale, and Fruitland Formation (vertical only) 85
D. Pictured Cliffs Sandstone 85
E. Lewis Shale 85
F. Cliff House Sandstone 85
G. Menefee Formation 86
H. Point Lookout Sandstone, Hosta Tongue, and Crevasse Canyon Formation 86
I. Gallup Sandstone and Mancos Shale 86
J. Dakota Sandstone 86
K. Morrison Formation 87

41. Map showing simulated horizontal hydraulic conductivity for the combined Ojo Alamo Sandstone, Kirtland Shale, and Fruitland Formation 88

42. Map showing simulated horizontal transmissivity and upward vertical hydraulic conductivity for the Entrada Sandstone 90

FIGURES--Concluded

Page

Figures 43-53. Maps showing computed steady-state head in the:
- 43. San Jose Formation 93
- 44. Animas and Nacimiento Formations 94
- 45. Combined Ojo Alamo Sandstone, Kirtland Shale, and Fruitland Formation 95
- 46. Pictured Cliffs Sandstone 96
- 47. Cliff House Sandstone 97
- 48. Menefee Formation 98
- 49. Point Lookout Sandstone 99
- 50. Gallup Sandstone 100
- 51. Dakota Sandstone 101
- 52. Morrison Formation 102
- 53. Entrada Sandstone 103

54. Maps showing vertical flow directions between selected adjacent hydrostratigraphic units in the San Juan Basin:
- A. San Jose Formation and the Animas and Nacimiento Formations 104
- B. Animas and Nacimiento Formations and the combined Ojo Alamo Sandstone, Kirtland Shale, and Fruitland Formation 104
- C. Combined Ojo Alamo Sandstone, Kirtland Shale, and Fruitland Formation and the Pictured Cliffs Sandstone 105
- D. Pictured Cliffs Sandstone and the Cliff House Sandstone 105
- E. Cliff House Sandstone and the Point Lookout Sandstone 105
- F. Point Lookout Sandstone and the Gallup Sandstone 105
- G. Gallup Sandstone and the Dakota Sandstone 106
- H. Dakota Sandstone and the Morrison Formation 106
- I. Morrison Formation and the Entrada Sandstone 106

CONVERSION FACTORS AND VERTICAL DATUM

Multiply	By	To obtain
LENGTH		
inch	0.02540	meter
foot	0.3048	meter
mile	1.609	kilometer
foot per day	0.3048	meter per day
AREA		
square mile	2.590	square kilometer
	43,560.	square foot
foot squared per day	0.09290	meter squared per day
VOLUME		
cubic foot	0.02832	cubic meter
	7.48	gallon
acre-foot	1,233	cubic meter
	43,560	cubic foot
cubic foot per second	0.02832	cubic meter per second
	448.8	gallon per minute
gallon per minute	0.00006309	cubic meter per second
gallon per minute per foot	0.2070	liter per second per meter
gallon per day per foot squared	0.04075	meter per day

Temperature in degrees Celsius (°C) can be converted to degrees Fahrenheit (°F) as follows:

$$°F = 9/5\ (°C) + 32$$

Sea level: In this report, "sea level" refers to the National Geodetic Vertical Datum of 1929 --a geodetic datum derived from a general adjustment of the first-order level nets of the United States and Canada, formerly called Sea Level Datum of 1929.

HYDROGEOLOGY AND STEADY-STATE SIMULATION OF GROUND-WATER FLOW IN THE SAN JUAN BASIN, NEW MEXICO, COLORADO, ARIZONA, AND UTAH

By John Michael Kernodle

ABSTRACT

As part of a multidisciplinary regional aquifer-system analysis, a three-dimensional steady-state ground-water-flow model was constructed for the San Juan Basin in parts of New Mexico, Colorado, Arizona, and Utah. The model simulated ground-water flow in 12 hydrostratigraphic units representing all of the major sources of ground water from aquifers of Jurassic and younger age.

Ten map reports in the U.S. Geological Survey Hydrologic Investigations Atlas 720 series were prepared in conjunction with this investigation. The units that were described in the atlases were the San Jose, Nacimiento, and Animas Formations; Ojo Alamo Sandstone; Kirtland Shale and Fruitland Formation; Pictured Cliffs Sandstone; Cliff House Sandstone; Menefee Formation; Point Lookout Sandstone; Gallup Sandstone; Dakota Sandstone; and Morrison Formation. Additional descriptions of the alluvial and landslide deposits, Chuska and Crevasse Canyon Sandstones, Lewis and Mancos Shales, Wanakah Formation, and Entrada Sandstone are included in this report. Much of the information in the HA-720 series was generated from digital computer data bases that were directly usable by the computer for compilation of input data for the model. In essence, the major components of the ground-water-flow model were described and documented in the series of hydrologic atlases.

The primary finding resulting from the ground-water-flow simulation was that boundary conditions and internal geometry of the aquifers are the major controls of steady-state ground-water flow and hydraulic heads in the San Juan Basin. Another significant finding was that the computed steady-state ground-water flux is a very minor component (about 1 percent) of the total water budget of the basin.

INTRODUCTION

This report is one in a series resulting from the U.S. Geological Survey's Regional Aquifer-System Analysis (RASA) program (Sun, 1986). The program began in 1978 with a study of the Northern Great Plains Basin (fig. 1) and has expanded to include 28 regional aquifer systems nationwide that have been or were planned to be investigated.

The study of the San Juan structural basin began in October 1984. Although the San Juan Basin geologically is a part of the Colorado Plateau and is partly in the Colorado River drainage, which defined the area of a preceding RASA, it was excluded from that study because the ground-water-flow system in the San Juan Basin remains regional in scale and is a classical example of an artesian ground-water-flow system. The isolation of the San Juan Basin as a separate investigation within the Colorado Plateau thus provided the opportunity to derive and focus on information that could be compared with other classical artesian basins.

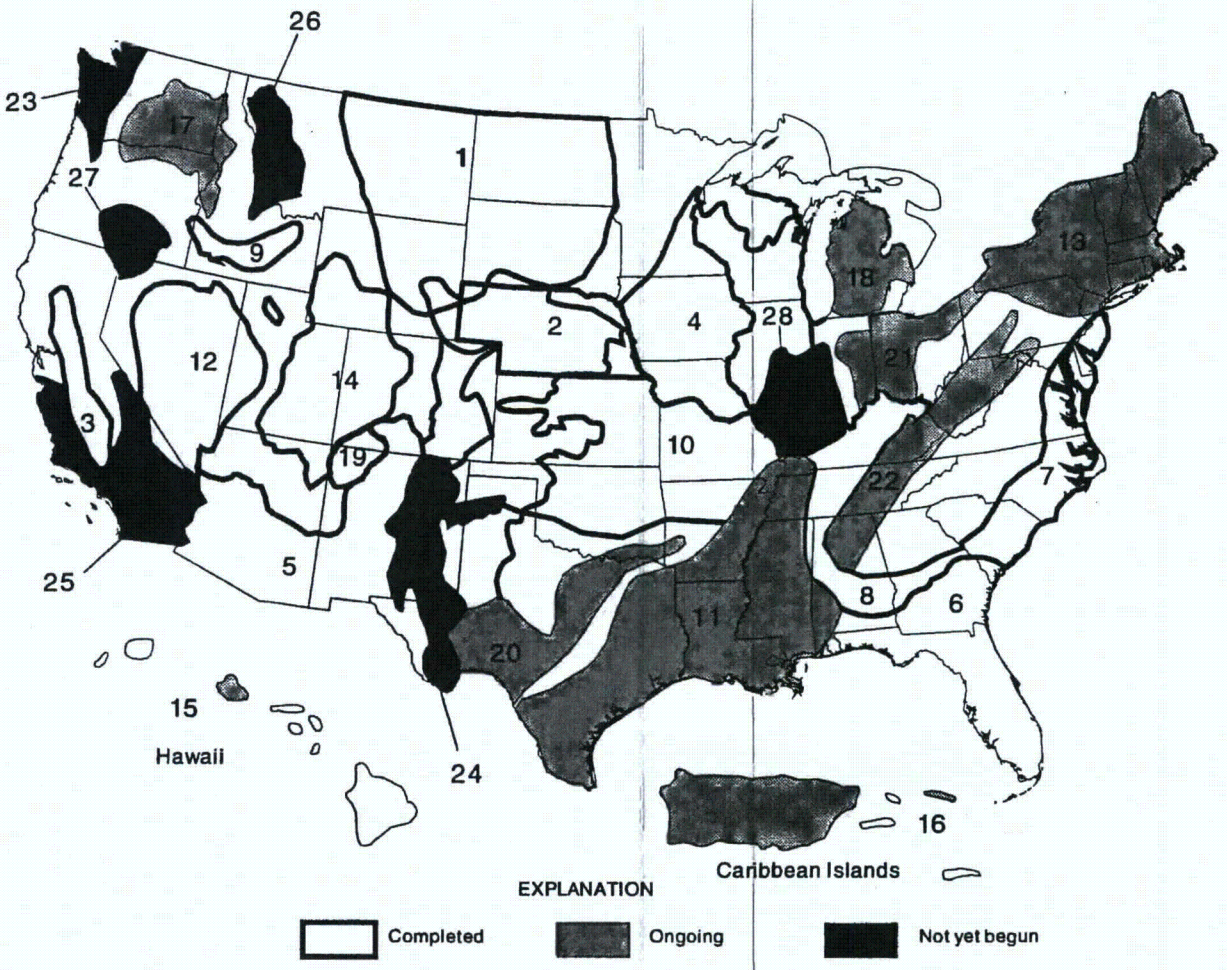

1. Northern Great Plains
2. High Plains
3. Central Valley California
4. Northern Midwest
5. Southwest alluvial basins
6. Floridian aquifer
7. Northern Atlantic Coastal Plain
8. Southeastern Coastal Plain
9. Snake River Plain
10. Central Midwest
11. Gulf Coastal Plain
12. Great Basin
13. Northeast glacial valleys
14. Upper Colorado River Basin
15. Oahu Island, Hawaii
16. Caribbean Islands
17. Columbia Plateau
18. Michigan Basin
19. San Juan Basin
20. Edwards-Trinity aquifer
21. Ohio/Indiana carbonates and glacial deposits
22. Appalachian Valleys and Piedmont
23. Puget-Willamette Trough
24. Pecos River Basin
25. Southern California alluvial basins
26. Northern Rockies Intermontane Basin
27. Alluvial basins, Oregon, Calif., Nev.
28. Illinois Basin

Figure 1.--Location of the Regional Aquifer-System Analysis areas of investigation.

Purpose and Scope

The purposes of the San Juan Basin RASA (Welder, 1986) are to: (1) define and characterize the aquifer system; (2) assess the effects of past, present, and potential ground-water use on aquifers and streams; and (3) determine the availability and quality of ground water. These broad objectives were reduced to four specific tasks: (1) the geologic framework was described; (2) the geochemical processes in a selected part of the flow system were investigated and described; (3) the flow system was simulated and described (this report); and (4) a summary of the investigation was prepared. This report describes the geohydrology and presents the results of three-dimensional steady-state ground-water-flow simulations of the major aquifers in the San Juan Basin.

Information on the major water-yielding units in the basin presented in the Hydrologic Investigations Atlas 720 Series and additional unpublished information on non-water-yielding units and minor aquifers were used to describe the geohydrology of the basin and to construct the ground-water-flow model. Existing literature and well-completion records provided information on aquifer properties, water levels, potentiometric heads, and well yields. The completed model was used to give an integrated description of the aquifer-system components and their relation to and interaction with surface recharge and discharge.

Description of the Study Area

The San Juan structural basin is located in New Mexico, Colorado, Arizona, and Utah, and has an area of about 21,600 square miles (fig. 2). The structural basin is about 140 miles wide and about 200 miles long. The study area is that part of the structural basin that contains rocks of Triassic and younger age; therefore, the study area is less extensive than the structural basin. Triassic through Tertiary sedimentary rocks are emphasized in this study because these units are the major aquifers in the basin. The study area is about 140 miles wide (about the same as the structural basin), 180 miles long, and has an area of about 19,380 square miles. The study area represents 15,550 square miles in New Mexico, 3,100 square miles in Colorado, 720 square miles in Arizona, and 11 square miles in Utah.

Land-surface altitudes in the study area range from about 4,500 feet above sea level in southeastern Utah to about 11,300 feet in the southeastern part of the basin. The area-weighted mean altitude is about 6,700 feet. Annual precipitation in the high mountainous areas along the north and east margins of the basin is as much as 40 inches, whereas annual precipitation in the lower altitude central basin is generally less than 8 inches. Mean annual area-weighted precipitation in the study area is about 12 inches.

Population and Economy

Data obtained from documents published by the U.S. Bureau of the Census (1980 and 1985) were used to calculate the population of the study area. The population in 1970 was calculated to be about 134,000. The population increased to about 194,000 in 1980, 212,000 in 1982, 221,000 in 1984, and then decreased to about 210,000 in 1985. The economy of the basin is supported by exploration for and development of natural gas, petroleum, coal, and uranium resources; urban enterprise; farming and ranching; tourism; and recreation. The rise and fall in population were related to changes in the economic strength of the minerals, oil, and gas industries and support services. Uranium-mining and -milling activities underwent rapid growth from the 1950's until the late 1970's and early 1980's when most uranium-mining activity came to an abrupt end. Likewise, the oil and gas industry prospered until about 1983 and then declined rapidly.

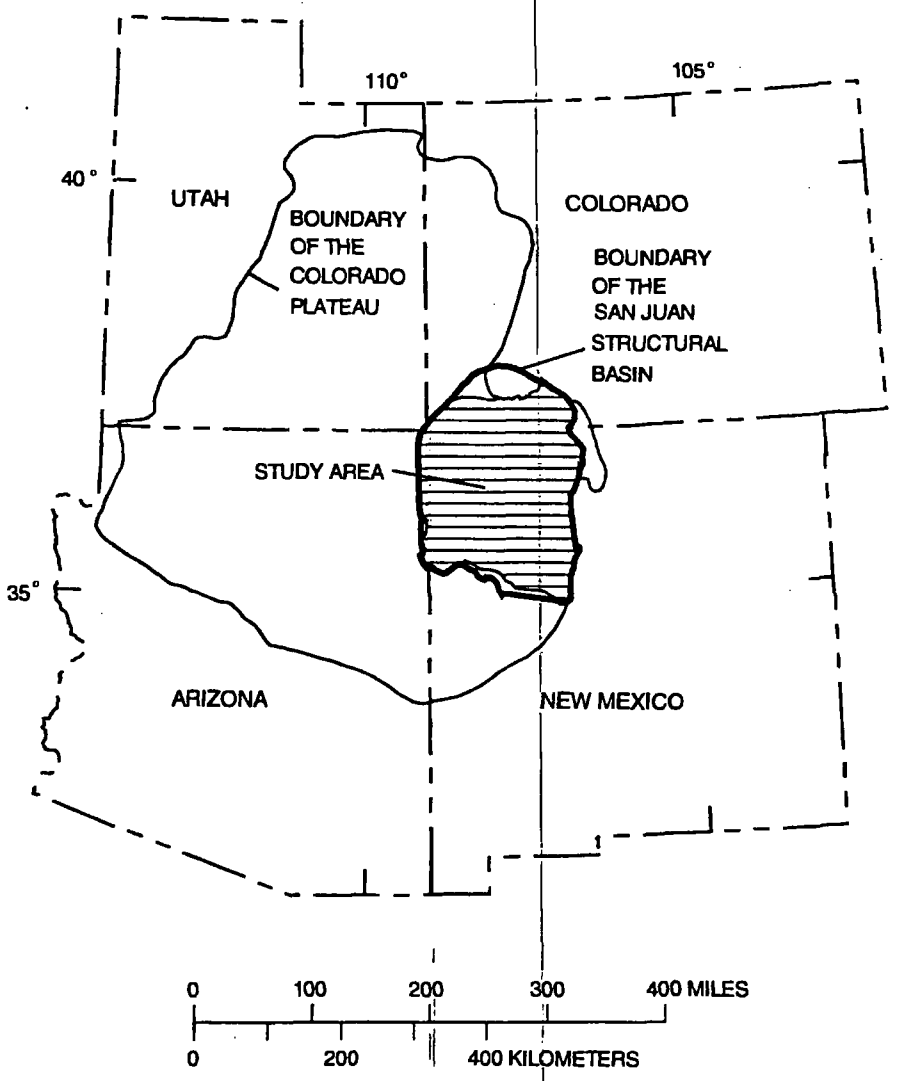

Figure 2.--Location of Colorado Plateau, San Juan structural basin, and study area.

Population density governs the amount of water that is required for private-domestic or municipal supplies. Population density also reflects the distribution or concentration of commercial and industrial facilities that also have water needs. Ranges in estimated population density in the San Juan Basin for 1985 are shown in figure 3.

Previous Investigations

Wright (1979) prepared a bibliographic reference for papers and reports that pertain to geologic and geohydrologic subjects for the San Juan Basin. Her publication listed more than 2,500 manuscripts, including many private consultants' reports. Many other hydrogeologic documents have been published since the release of her compilation, including the citations listed in the next paragraph. In addition, a vast number of archeological, climatic, paleoclimatic, and surface-water reports have information relevant to a study of the ground-water basin.

Stone and others (1983) compiled a fairly comprehensive summary of the hydrogeology of the New Mexico part of the San Juan Basin. That report describes the geohydrologic properties of the Wanakah Formation (later terminology) and younger hydrostratigraphic units. Frenzel (1982) completed a three-dimensional steady-state ground-water-flow model of the San Juan Basin in New Mexico and Colorado. Later (1983), he prepared an uncalibrated transient version of the model to investigate possible effects related to proposed development of Federal coal leases. Other models prepared by the U.S. Geological Survey include those by Hearne (1977) and McLean (1980) of aquifers in the vicinity of Gallup, New Mexico. A three-dimensional steady-state model of the Morrison-Dakota-Gallup aquifer subsystem was completed by Kernodle and Philip (1988). One of the most recent models is of the aquifers in Mesozoic rocks in the Four Corners area (Thomas, 1989). Many other reports and papers are cited in the following sections.

Reports Related to the Investigation

Sun (1986) compiled a summary of RASA investigations. That summary contains detailed information on the overall purpose of the RASA program and the scope and status of the individual investigations, including the San Juan Basin RASA.

A series of Hydrologic Atlases was published in conjunction with this investigation that describe the hydrology, geology, and geochemistry of the major water-yielding hydrostratigraphic units in the study area. Reports in this series describe the hydrogeology of the Dakota Sandstone (Craigg and others, 1989); Gallup Sandstone (Kernodle and others, 1989); Point Lookout Sandstone (Craigg and others, 1990); Morrison Formation (Dam and others, 1990a); Pictured Cliffs Sandstone (Dam and others, 1990b); Kirtland Shale and Fruitland Formation (Kernodle and others, 1990); Menefee Formation (Levings and others, 1990a); San Jose, Nacimiento, and Animas Formations (Levings and others, 1990b); Cliff House Sandstone (Thorn and others, 1990a); and Ojo Alamo Sandstone (Thorn and others, 1990b) in the San Juan structural basin.

The series of atlases was intended to provide information upon which subsequent investigative reports such as this could rely for basic reference material. This report describes a three-dimensional ground-water-flow model of Jurassic and younger hydrostratigraphic units. Levings and others (1996) provided a coherent overview of the multidisciplinary facets of the investigation. The hydrogeochemistry of the Morrison, Dakota, and Gallup aquifers in the northwestern part of the basin was described by Dam (1995). Craigg (in press) describes the geologic framework of the San Juan Basin.

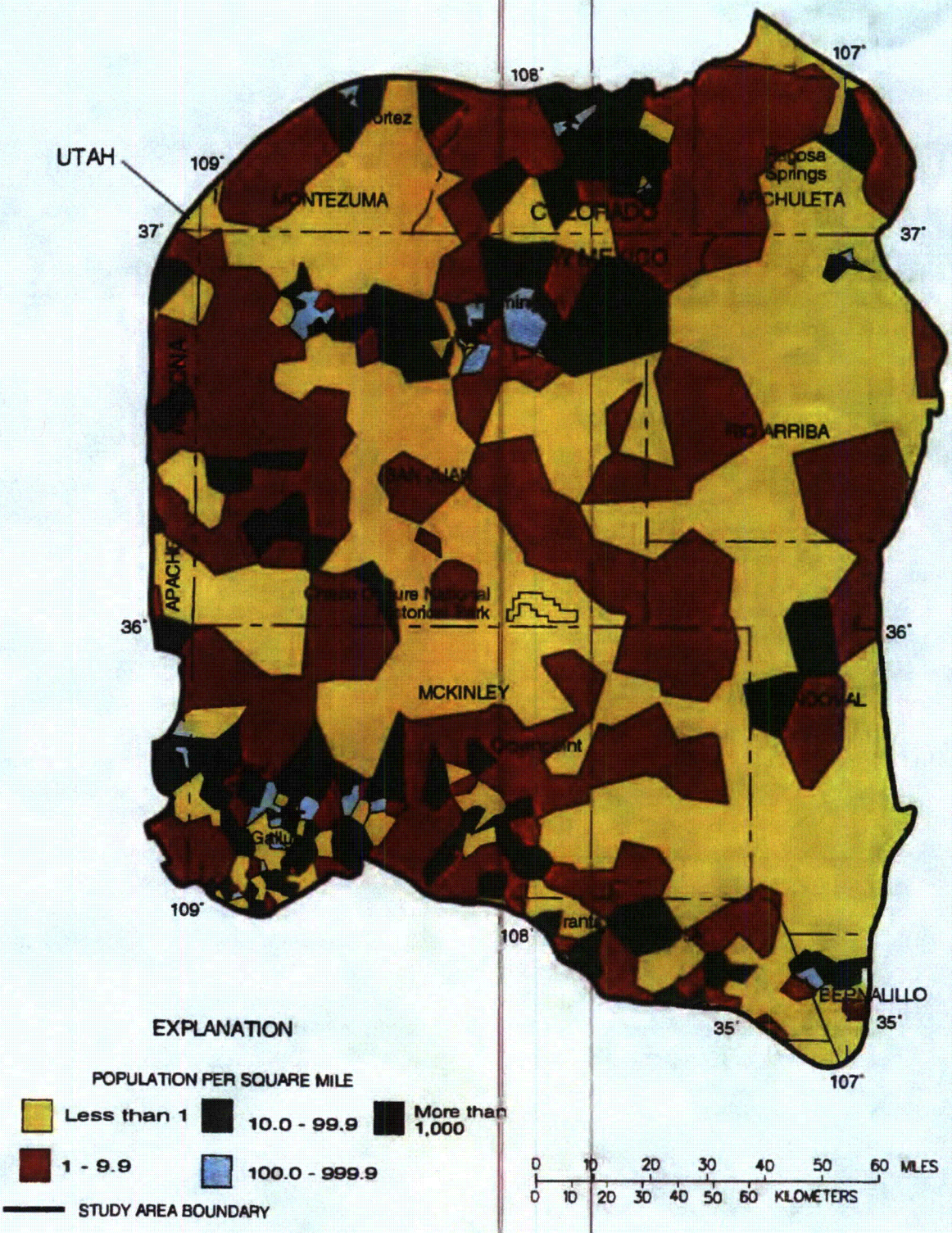

Figure 3.--Estimated 1985 population density in the San Juan Basin (from U.S. Bureau of the Census, 1980 and 1985).

GEOHYDROLOGIC SETTING

Geology

The San Juan structural basin (fig. 4), formed during the Laramide Orogeny (Late Cretaceous-early Tertiary), is an asymmetric syncline that deepens to the northeast. The limits of the basin generally are clearly delineated by faults, uplifts, or monoclines. The clearest example of a fault determining the basin boundary is along the eastern side of the basin where Precambrian granite has been uplifted east of the Nacimiento Fault. The Defiance and Nutria Monoclines also are good examples of basin-bounding features. In some areas, however, the boundary is indistinct and the basin merges across structural saddles with adjacent basins or embayments. Examples of this indistinct boundary between basins are found in the Gallup and Acoma Sags and the Four Corners Platform.

The San Juan structural basin contains a thick sequence of sedimentary rocks ranging in age from Cambrian through Tertiary (fig. 5), but principally from Pennsylvanian through Tertiary. The maximum thickness of the sequence of rocks is about 14,000 feet (Fassett and Hinds, 1971, p. 4). These sedimentary rocks dip basinward from the basin margins toward the troughlike structural center (deepest part of the basin) except where locally interrupted by intrabasinal folds, faults, and domes. Older sedimentary rocks crop out around the basin margins and are successively overlain by younger rocks toward the center of the structural basin (fig. 6). Volcanic rocks of Tertiary age and various deposits of Quaternary age also are present in the basin.

Faulting is common, especially around the northeastern, eastern, and southeastern perimeter of the basin (fig. 7). Faults along the northeastern and eastern perimeter generally are on the platform areas outside the Hogback Monocline. Displacement along these faults is as much as several hundred feet, and along Nacimiento Fault is several thousand feet. Displacement along individual faults in the Puerco Fault Zone in the southeastern part of the basin typically ranges from several tens to a few hundred feet. The basinward side of faults is usually the downthrown side in the Puerco Fault Zone. Fault orientation and displacement in the Crownpoint-Grants, New Mexico, area (also known as the Grants uranium belt) are more disheveled than elsewhere, often leading to some remarkable structures as in the area just south of Crownpoint. When fault displacement and synclinal structure are combined, the maximum structural relief in the basin is about 10,000 feet (Kelley, 1951, p. 126). The present structural elements of the basin largely had developed by middle Tertiary time (Kelley, 1951, p. 130).

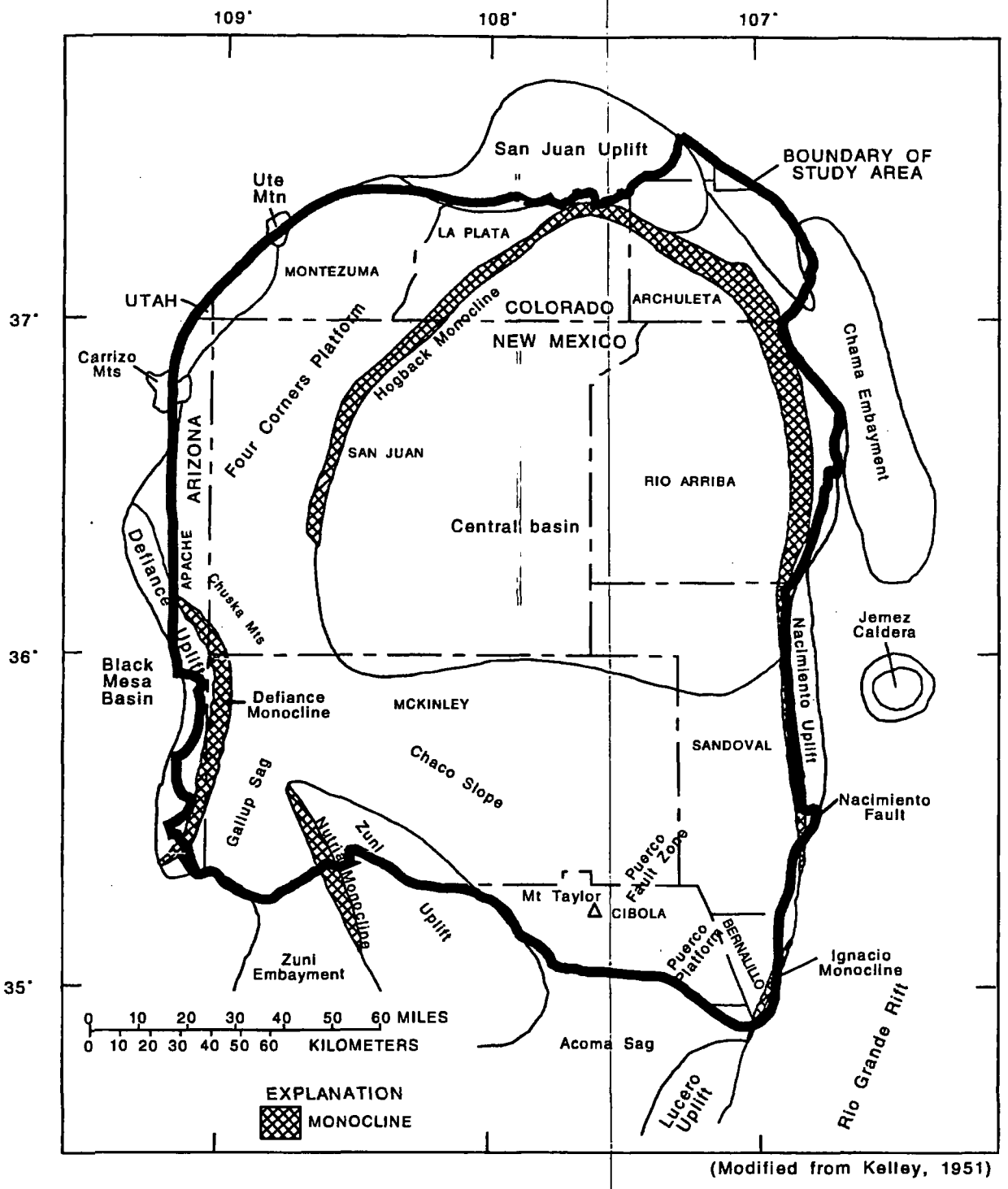

Figure 4.--Structural elements of the San Juan Basin and adjacent areas.

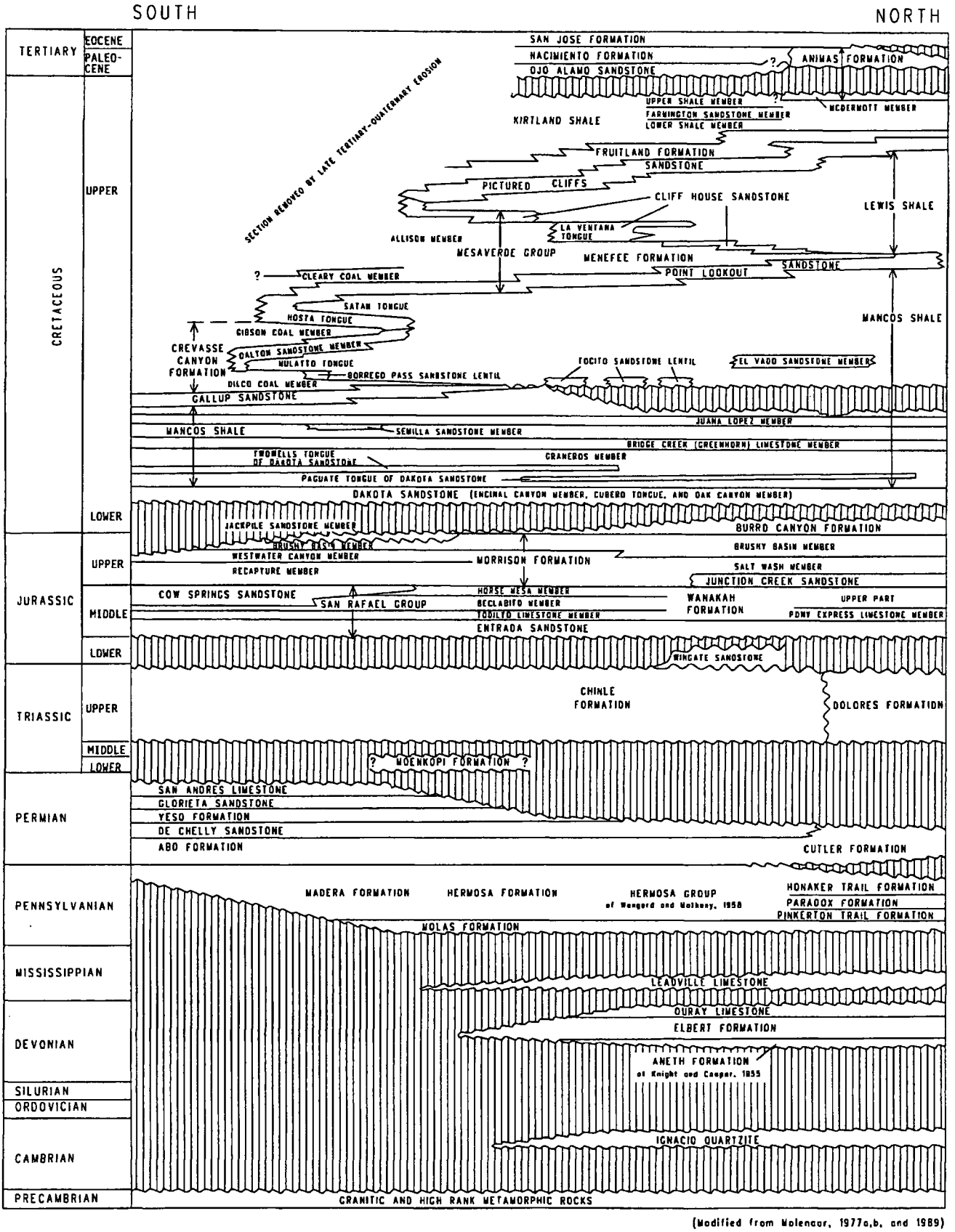

(Modified from Molenaar, 1977a,b, and 1989)

Figure 5.--Time- and rock-stratigraphic framework and nomenclature.

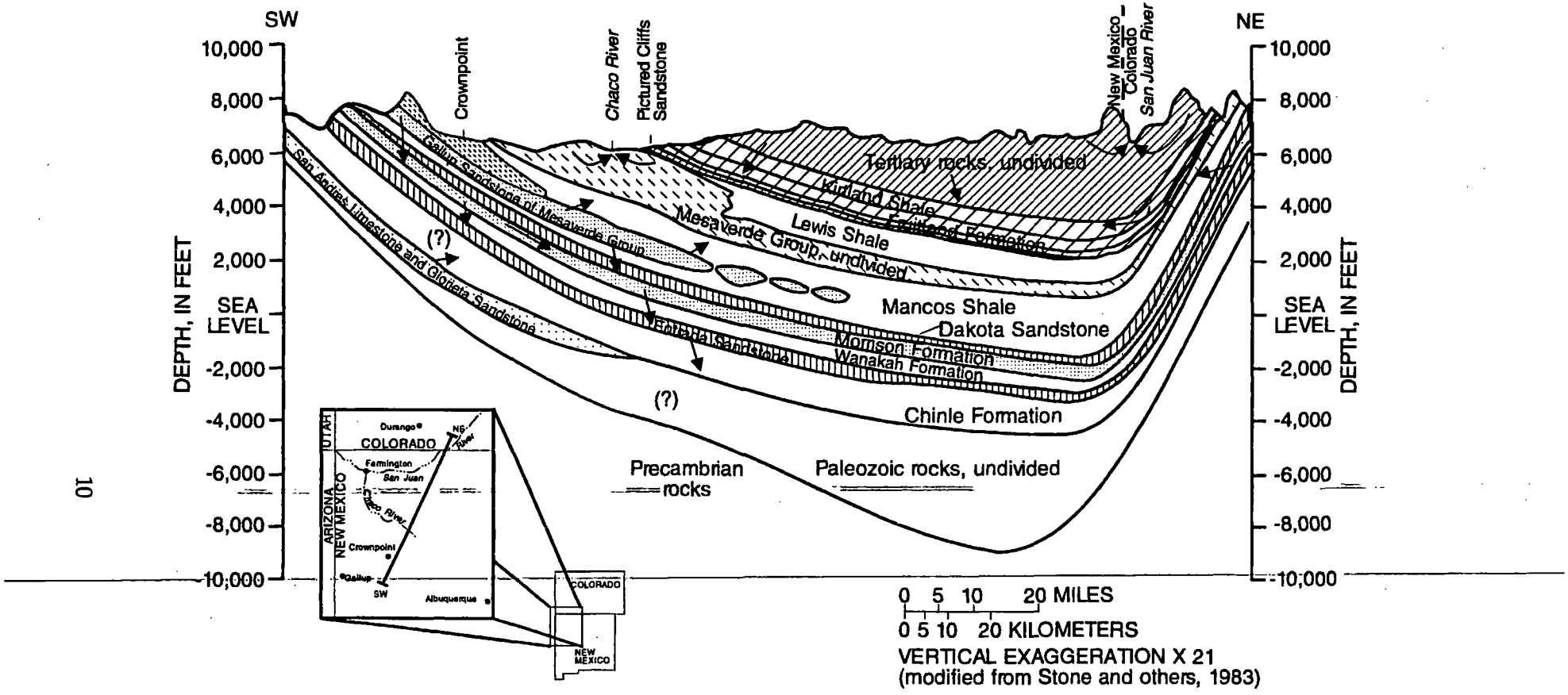

Figure 6.--Generalized hydrogeologic section of San Juan Basin showing major aquifers (stippled), confining beds (blank), and direction of ground-water flow (arrows).

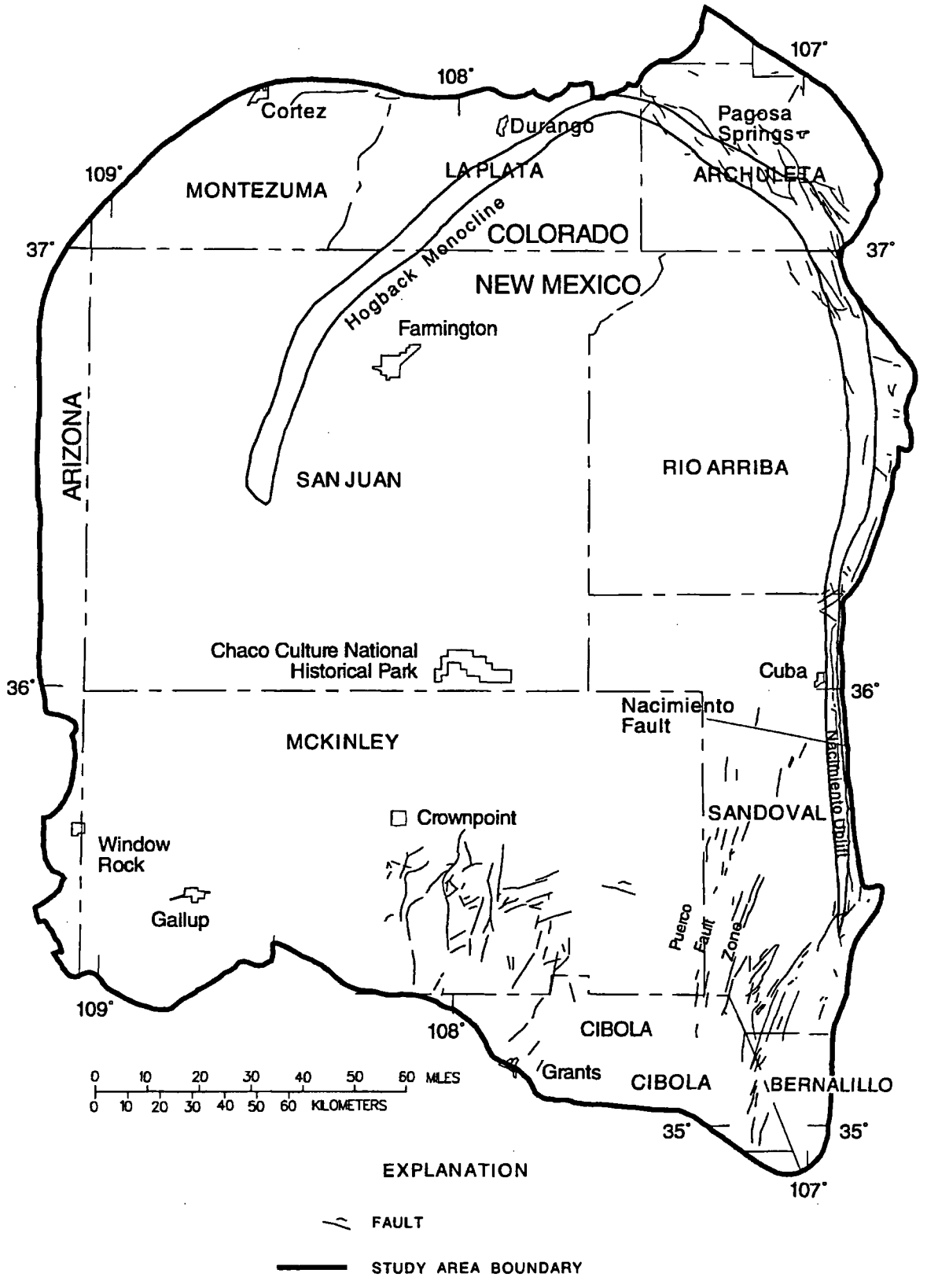

Figure 7.--Major faults in the San Juan Basin.

Climate

The San Juan Basin is located in the arid Southwestern United States and therefore typically has mild winters with periodic cold-front storms; hot, dry, and windy springs and early summers; warm and monsoonal late summers; and cool, clear autumns. However, within the San Juan Basin a wide range of climatic conditions are determined primarily by topographic altitude and somewhat by slope aspect. The low-altitude central and northwestern part of the basin has the warmest temperatures and the least amount of precipitation (upper Sonoran climate). The mountainous regions around most of the northern and eastern perimeter of the basin have the coolest temperatures and receive the most precipitation (Canadian climate zone).

Figures 8 and 9 are maps of mean annual and mean winter precipitation for the period 1931-60. As stated earlier, amounts of annual precipitation range from almost 40 inches in the northeastern part of the study area to less than 8 inches in the lower altitude central basin (U.S. Department of Commerce, no date). Most winter precipitation occurs as snowfall, especially in the higher mountain areas where snowpack typically exceeds 100 inches. Spring runoff from melting mountain snowpacks accounts for most surface water in the basin. Convective summer thunderstorms locally may result in considerable amounts of water in a very brief period, often causing severe and dangerous flash floods.

Potential mean annual evaporation (fig. 10) ranges from a low of less than 40 inches in the northeastern to more than 60 inches in the northwestern part of the study area (National Oceanic and Atmospheric Administration, no date). In only a very small part of the study area does annual precipitation exceed potential evaporation, and throughout most of the area potential evaporation greatly exceeds precipitation. With additional losses due to transpiration, the potential annual water deficit is large throughout most of the area. Because of the timing of rain and snowfall, however, water periodically is available for runoff and ground-water recharge regardless of the annual potential deficit.

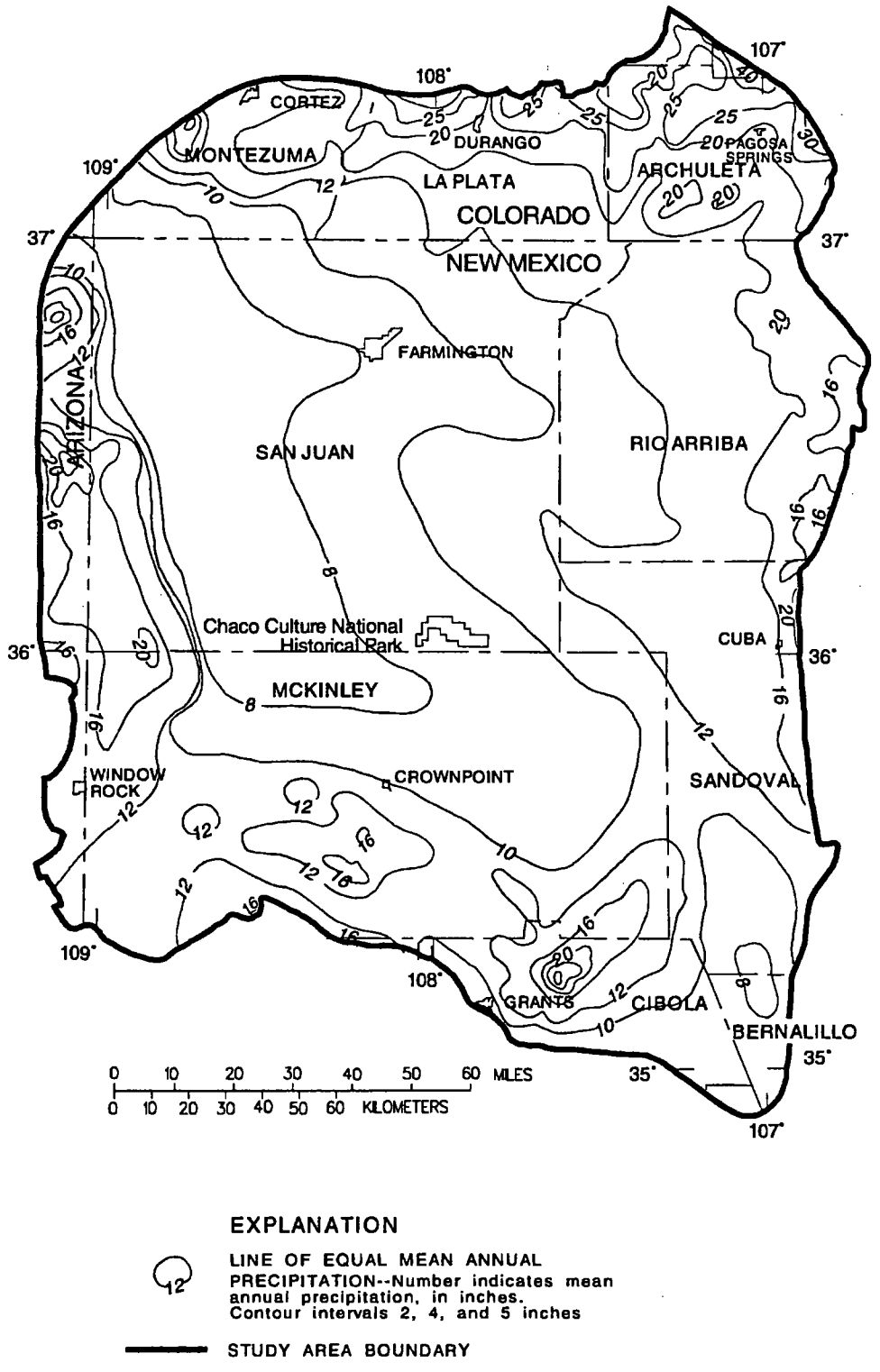

Figure 8.--Mean annual precipitation for the period 1931-60 (from U.S. Department of Commerce, no date).

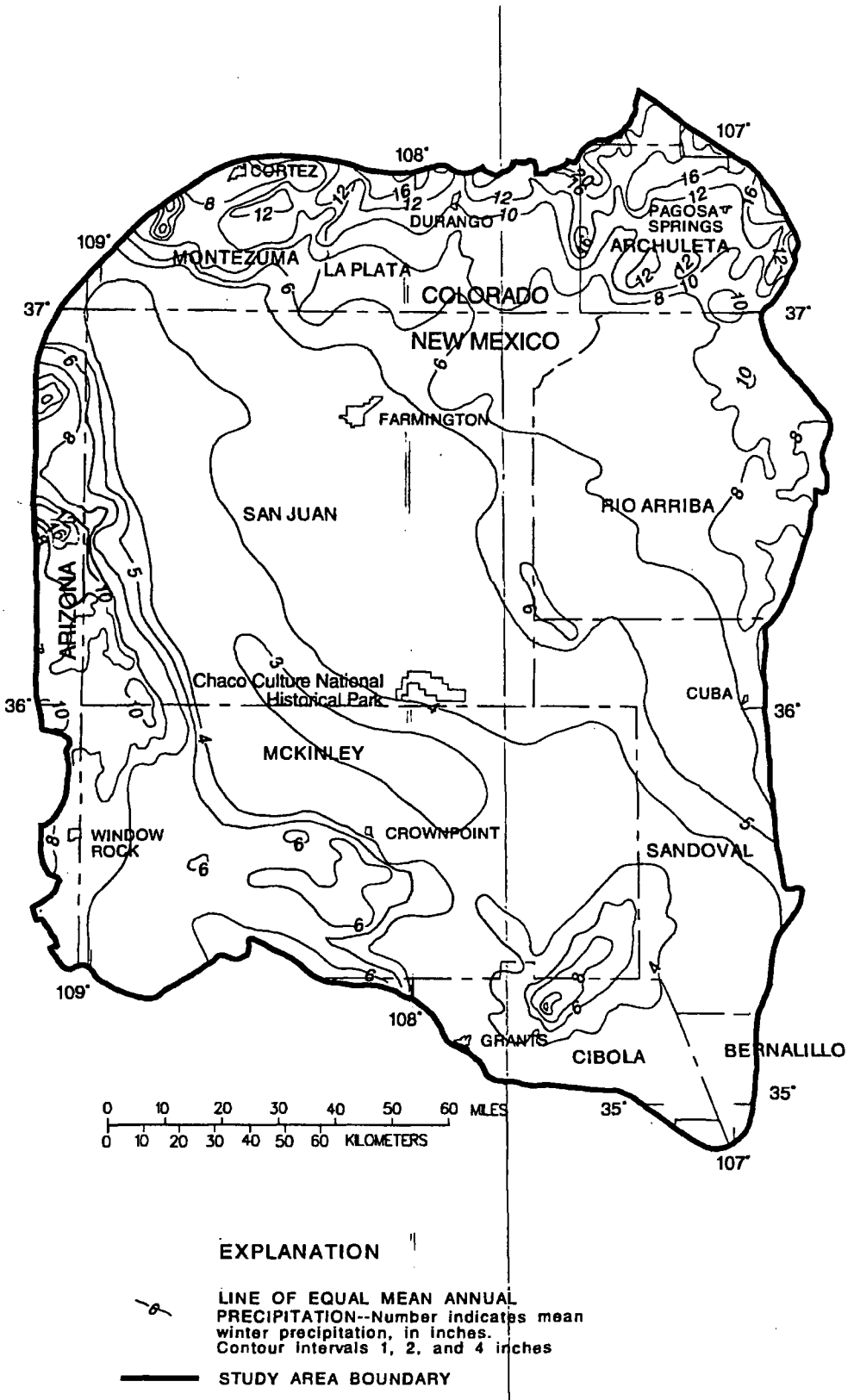

Figure 9.--Mean winter precipitation for the period 1931-60 (from U.S. Department of Commerce, no date).

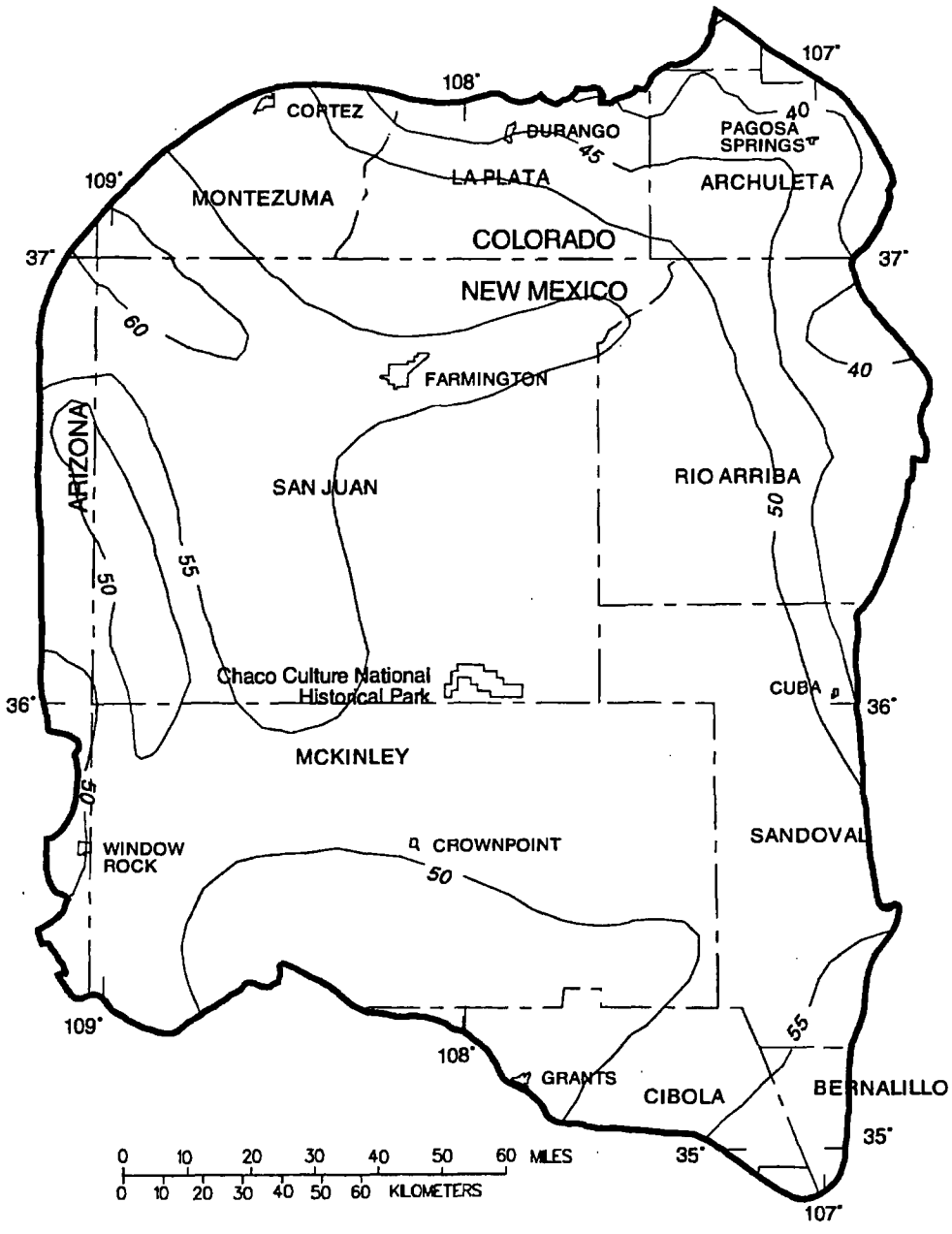

EXPLANATION

50 — LINE OF EQUAL POTENTIAL MEAN ANNUAL EVAPORATION--Number indicates potential evaporation, in inches per year. Contour interval 5 inches

STUDY AREA BOUNDARY

Figure 10.--Potential mean annual evaporation (from National Oceanic and Atmospheric Administration, no date).

Surface Water

The study area is drained mainly by the San Juan River and its tributaries (fig. 11). The San Juan River is a tributary to the Colorado River. The Puerco River and its tributaries in the southwestern part of the study area are also part of the Colorado River system. East of the Continental Divide the Rio Chama, Rio Salado, Rio Puerco, and Rio San Jose drain to the Rio Grande. A diversion from the headwaters of the San Juan River transfers about 100,000 acre-feet of water per year to the headwaters of the Rio Chama.

Only the San Juan River and its major northern tributaries are naturally perennial in the study area. Portions of some streams are perennial for short reaches downstream from spring or well discharges or discharges of treated municipal wastewater. Other streams are ephemeral or seasonal and many only flow immediately after storms.

Several large reservoirs are in the study area. The largest of these, Navajo Reservoir on the San Juan River, is used for irrigation and municipal water supplies. Water stored in or passed through two other reservoirs in the study area, Heron Lake and El Vado Reservoir on the Rio Chama in New Mexico, is allocated for municipal use by the City of Albuquerque, New Mexico, although much of this water is leased from the City for agricultural use downstream from Albuquerque. Bluewater Lake on the Rio San Jose is used to supply water for irrigation. Lemon and Vallecito Reservoirs, in Colorado just outside the study area, provide flood control and supply water for irrigation within the San Juan Basin. All of these reservoirs offer excellent recreational opportunities.

Ground Water

In a simplified conceptual model of the ground-water-flow system in the San Juan Basin, water enters the ground-water-flow system from precipitation on aquifer outcrops and from stream-channel loss as streams cross the outcrops. Recharge from direct precipitation occurs only after the near-surface demands for moisture are met by the water that does not run off and a residual amount of water is able to reach the zone of saturation in the aquifer. These near-surface demands include evaporation, transpiration, and sublimation.

Once water is in the ground-water-flow system it moves downgradient to areas of natural or artificial discharge, in accordance with Darcy's law (Darcy, 1856) whereby the flow is equal to the ground-water gradient times the aquifer's hydraulic conductivity times the cross-sectional area of the aquifer perpendicular to the direction of flow. Areas of natural discharge include springs and seeps in topographically low parts of the outcrop, discharge from the aquifer outcrop to stream channels, and upward movement across confining units to the surface along fault planes, fractures, and, to a modest extent, along intrusive dikes. Striking examples of spring discharge along fault planes and fractures are at the southern end of the Nacimiento Uplift in the southeastern part of the study area.

Another important mechanism of natural discharge is water moving from one aquifer across a less permeable unit to another aquifer that has relatively lower hydraulic head. Water might also move across a less permeable unit directly to land surface where it would contribute to soil moisture and hence to evaporation or transpiration. Both forms of vertical ground-water movement may be significant in the San Juan Basin.

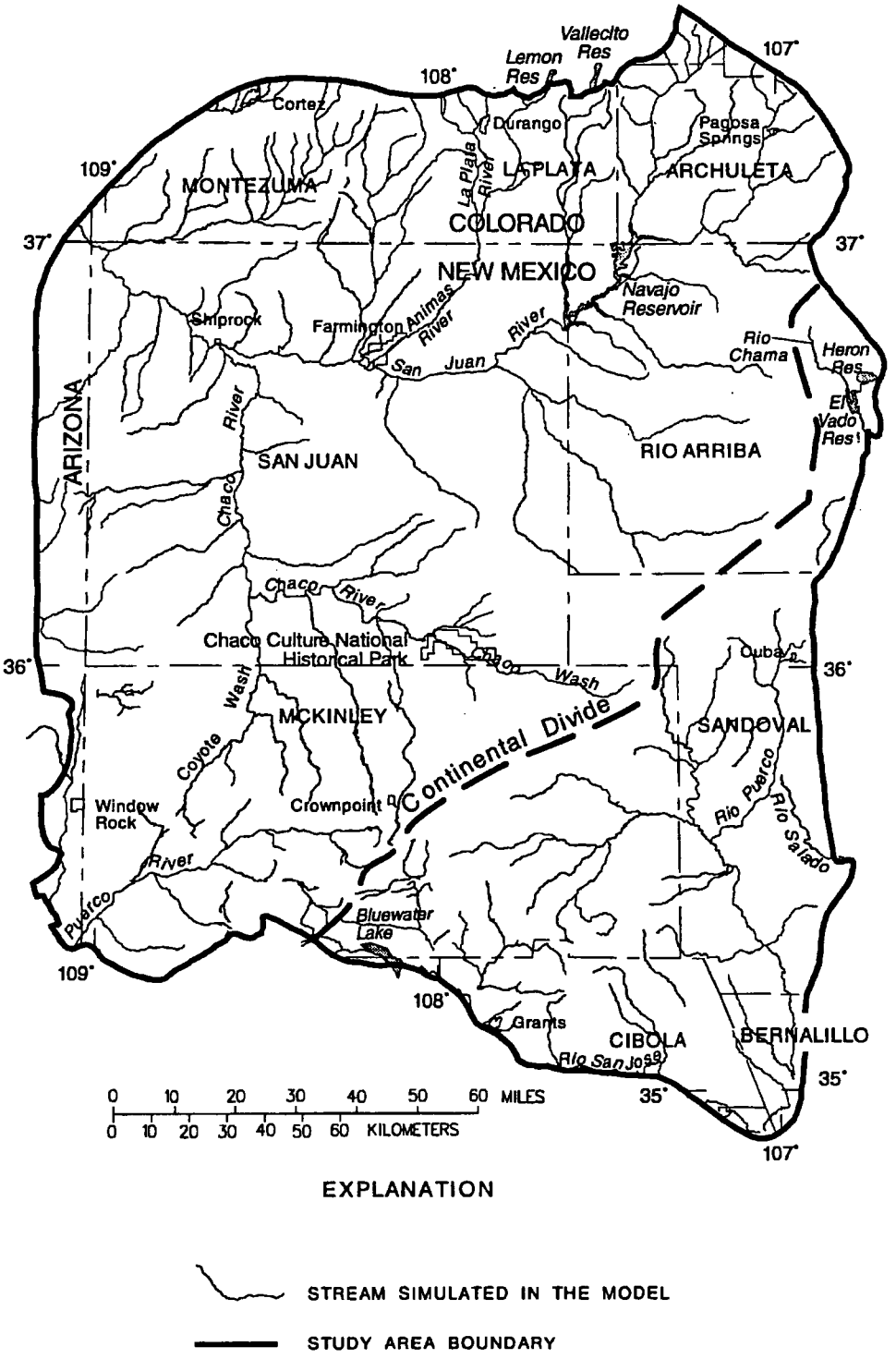

Figure 11.--Location of streams simulated in the model.

Artificial discharge occurs at flowing or pumped wells or in conjunction with open-pit or subsurface mining operations. Free-flowing wells are commonplace in the basin and most of those are completed in multiple aquifers so the percentage of water contributed by each aquifer is unknown. Pumped wells or controlled flowing wells also are common and supply water to satisfy municipal, small-community, private-domestic, and livestock needs. The majority of these wells are windmill powered and small yielding, but some yield large quantities of water. Mine dewatering operations have been a major source of ground-water discharge in the south-central part of the basin. Some mines required the removal of as much as 3 cubic feet per second of ground water to keep the mine from flooding. All of the mines presently are closed, the dewatering has ceased, and ground-water levels are now recovering from head reductions that commonly exceeded 1,000 feet.

Complexities in the flow system arise because of non-uniformity in the aquifers. The aquifers may thin or pinch out, or the composition and hydraulic properties may vary in space. Aquifers also may have preferred directions of ground-water flow that are controlled by the orientation of fracture systems or by a persistent orientation of the aquifer's matrix of sedimentary materials. Other pore-filling liquids or gases may create barriers to the movement of water, or water in parts of an aquifer may be saline enough to create a density barrier to movement of freshwater. All of these conditions are present to some degree in the San Juan Basin.

HYDROSTRATIGRAPHIC UNITS

The San Juan Basin has many hydrostratigraphic units that function either as aquifers or confining units. Other units, such as thin alluvial deposits, may not be hydrologically extensive enough to be classified as major aquifers but potentially are very important in the role they serve in capturing precipitation that eventually becomes recharge to underlying units. Much of the following description of the major hydrostratigraphic units in the San Juan Basin was taken directly from U.S. Geological Survey Hydrologic Investigations Atlases in the HA-720 series (Craigg and others, 1989, 1990; Dam and others, 1990a, b; Kernodle and others, 1989, 1990; Levings and others, 1990a, b; and Thorn and others, 1990a, b).

The structure-contour maps presented in this section are derived from computer-generated and human-edited continuous-surface representations of the tops of the major hydrostratigraphic units. These continuous-surface data layers were generated from the control points shown in the HA-720 series of Hydrologic Investigations Atlases and geographic information system (GIS)-generated outcrop altitudes. The representations were imported into the GIS, which was then used to produce the figures in the atlases and in this report. Much of the information in those atlases also was used directly by the computer for compilation of input data for the model, as described later. In essence, the major components of the ground-water-flow model were documented in the series of hydrologic atlases. In the following section the hydrostratigraphic units are discussed in order of uppermost (youngest) to lowermost (oldest) occurrence.

Alluvium and Other Quaternary Deposits

Quaternary and recent deposits in the San Juan Basin include stream-deposited alluvium and older terrace deposits, landslide deposits, and eolian sand. The areal distribution of these sediments are shown in figure 12. Most Quaternary and younger deposits are unconsolidated and form a thin covering over older bedrock sediments.

Lithology

Stream-deposited alluvium and older terrace deposits are associated with major streams and rivers in the San Juan Basin. The alluvium consists of unconsolidated sediments that range from silt to cobbles in size but predominantly are sand and gravel. Along major streams the alluvium is varied in composition, depending on the mix of material from the various erosional source areas. Alluvial deposits also occur as a thin veneer of fine-grained sediments in the valleys of intermittent streams.

Landslide deposits are mapped on the northeastern flank of the Chuska Mountains and locally in the San Juan Mountains in the northeastern part of the study area. These colluvial deposits consist of material derived from the topographically higher source areas. The landslide material on the flank of the Chuska Mountains consists of reworked sand from the Chuska Sandstone; the deposits in the San Juan Mountains primarily are derived from volcanic or volcaniclastic sources.

Unconsolidated wind-blown deposits are common in the central part of the basin, although they generally are not mapped on small-scale geologic maps. Typically, these deposits are very thin, but local dunes near dry washes, which are excellent sources of fine-grained material, may reach heights of 20 feet. These recent eolian deposits are not known to yield water to wells.

Hydraulic Properties

In the absence of other sources of water, alluvial deposits, where present, commonly are relied upon as a source of water for domestic and livestock use. Along the major rivers and streams, wells are of conventional vertical design, whereas in the valleys of intermittent streams, where the hydraulic conductivities and saturated thickness generally are small, most wells are constructed as galleries of horizontal drains feeding to a central collector. Reported well yields range from less than 1 gallon per minute to as much as 1,100 gallons per minute. The median yield of 48 wells is 15 gallons per minute. The largest reported yields are from wells completed in the alluvium in the Rio San Jose Valley (fig. 11) in the vicinity of Grants, New Mexico. The smaller yields are from gallery wells completed in the alluvium of minor stream valleys.

Hydraulic conductivities of sand and gravel can vary from 10 to 1,000,000 gallons per day per foot squared (roughly 1 to 100,000 feet per day) (Freeze and Cherry, 1979, table 2.2), but a more typical range is from 15 feet per day for fine sand to about 1,000 feet per day for coarse gravel (Lohman, 1972, table 17). Tests along the San Juan River (fig. 11) upstream from Farmington indicate that the hydraulic conductivity of alluvium ranges from 0.006 to 220 feet per day (Peter and others, 1987, p. 29). The thickness of alluvium at this site was reported to range from about 14 to 61 feet, and the saturated thickness was less than 25 feet in all 13 test holes. Water occurs in the alluvium under unconfined conditions. No tests have been made where the storage coefficient of the alluvium was determined. However, a typical specific yield for moderately to well-sorted unconsolidated sediments would be in the range of 0.1 to 0.25.

No known hydraulic data exist for the landslide and recent eolian deposits in the basin. No instances are known where these deposits are used as a source of water.

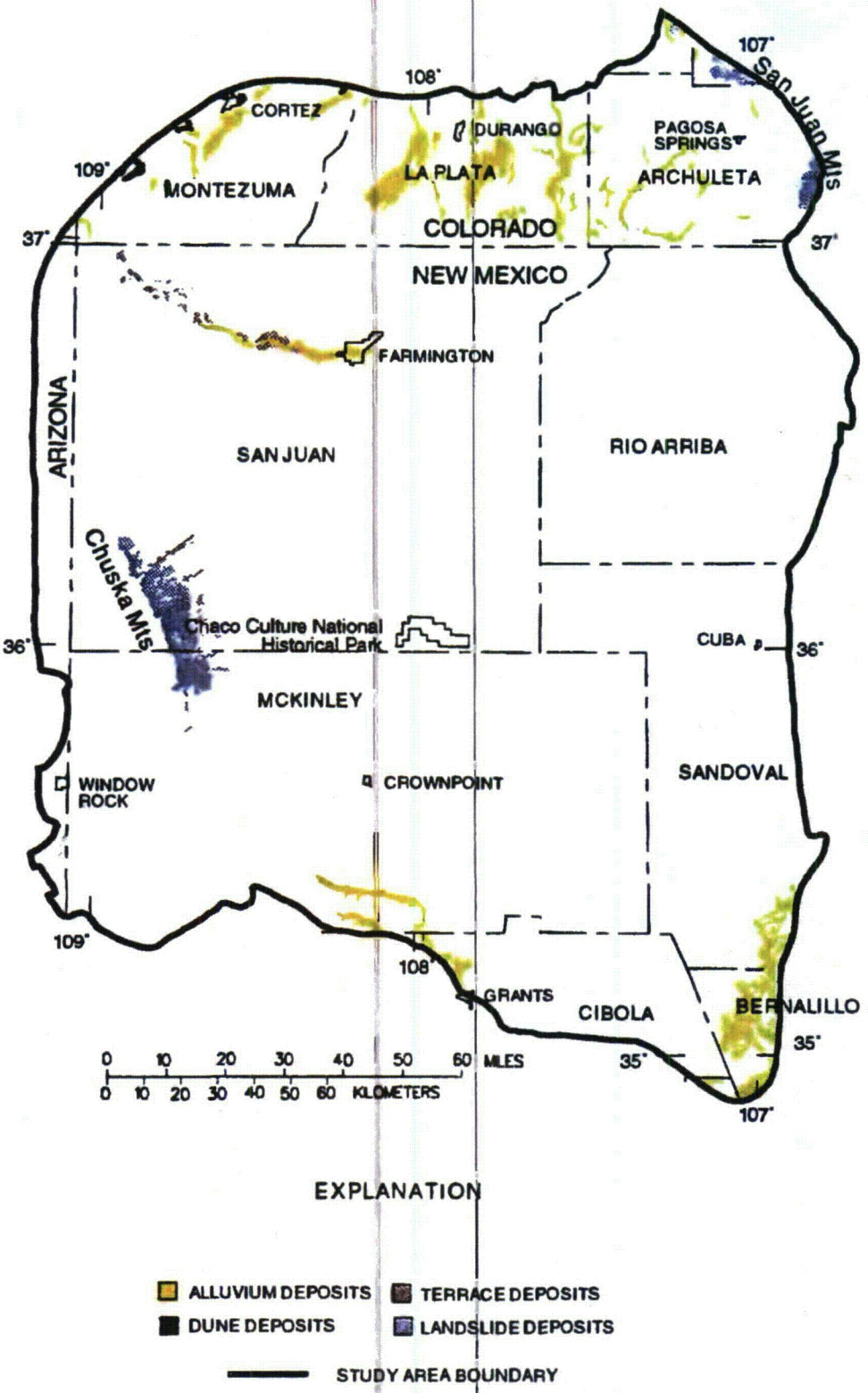

Figure 12.--Distribution of Quaternary deposits.

Chuska Sandstone

The Chuska Mountains (fig. 12) in the western part of the basin primarily are formed from the Chuska Sandstone, a consolidated, windblown sand of Tertiary age that was deposited on upturned and eroded Cretaceous and older sediments. Several moderate-sized intrusive mafic necks form a spine along the ridge of the mountains and, together with associated horizontal lava flows, may have provided the erosional resistance necessary to protect the sandstone from weathering away, as has happened toward its source area to the south-southwest.

Lithology

The Chuska Sandstone is a fine-grained, moderately well sorted sandstone (Harshbarger and Repenning, 1954, p. 6). Cross-bed units typically range from 5 to 15 feet in thickness. Thick zones of silicic cement form resistant ledges at and near the top of the unit, but overall the sandstone is weakly cemented. Cementation is more complete to the southwest, allowing conventional headward erosion of streams. The poorly cemented sand on the northeastern flank of the Chuska Mountains has allowed piping and massive slump failure during pluvial periods in the Pleistocene Epoch. The average thickness of the Chuska Sandstone is about 1,000 feet and the maximum preserved thickness is 1,750 feet (Wright, 1956, p. 416). The Chuska Sandstone conformably overlies a horizontally bedded fluvial sandstone and shale about 250 feet in thickness (the Deza Formation of Wright, 1954).

Hydraulic Properties

No measurements are known of the hydraulic properties of the Chuska Sandstone. However, the unit is water yielding and springs are abundant around the flanks of the Chuska Mountains, usually at the base of the Chuska Sandstone. Most of the springs are undeveloped, but some serve as domestic water supplies. The sandstone is recharged by leakage from the numerous lakes and potholes along the top of the mountains. In addition to the discharge from springs, the sandstone loses water to the underlying Cretaceous and older sediments.

San Jose Formation

The San Jose Formation of Eocene age was defined by Simpson (1948a, b). The San Jose Formation occurs in New Mexico and Colorado, and its outcrop forms the land surface over much of the eastern half of the central basin (fig. 4). It overlies the Nacimiento Formation in the area generally south of the Colorado-New Mexico State line and overlies the Animas Formation in the area generally north of the State line (Fassett, 1974, p. 229). The basal contact of the San Jose varies with location in the basin. This contact is a disconformity along the basin margins and an angular unconformity along the Nacimiento Uplift; the contact is conformable in the central basin (Baltz, 1967, p. 54; Fassett, 1974, p. 229).

Geometry and Lithology

The San Jose Formation was deposited in various fluvial-type environments (Baltz, 1967, p. 44-55). In general, the unit consists of an interbedded sequence of sandstone, siltstone, and variegated shale. The sandstones are buff to yellow and rusty colored, crossbedded, very fine to

coarse-grained arkose, which are locally conglomeratic and contain abundant silicified wood (Baltz, 1967, p. 46; Fassett, 1974, p. 229; Anderholm, 1979, p. 23).

Baltz (1967, p. 45) recognized four formal members of the San Jose Formation in the east-central part of the basin; he also identified, but did not name, a fifth member in the northeastern part of the basin. The members and their principal lithology in descending order are Tapicitos Member (shale), Llaves Member (sandstone), Regina Member (shale), and Cuba Mesa Member (sandstone). The stratigraphic relation and subsequent mapability of these members are complicated by extensive intertonguing and pinch-outs (Fassett, 1974, p. 229; Anderholm, 1979, p. 23; Stone and others, 1983, p. 25), and whether the members can be identified throughout the basin has been the subject of some discussion.

Thickness of the San Jose Formation generally increases from west to east. Fassett (1974, p. 229) reported a maximum thickness of 2,400 feet in the east-central part of the basin, and Stone and others (1983, p. 25) reported a range from about 200 feet in the west and south to almost 2,700 feet in the center of the structural basin.

Hydraulic Properties

Transmissivity data for the San Jose Formation are minimal. Values of 40 and 120 feet squared per day were determined from two aquifer tests (Stone and others, 1983, table 5).

The reported or measured discharge from 46 water wells completed in the San Jose Formation ranges from 0.15 to 61 gallons per minute and the median is 5 gallons per minute. Most of the wells provide water for livestock and domestic use, but a few provide cooling water for natural gas compression and transmission plants.

The San Jose Formation is a very suitable unit for recharge from precipitation because soils that form on the unit are sandy and highly permeable and therefore readily adsorb precipitation. However, low annual precipitation, relatively high transpiration and evaporation rates, and deep dissection of the San Jose Formation by the San Juan River and its tributaries all tend to reduce the effective recharge to the unit.

Animas and Nacimiento Formations

Most of the Animas Formation is of Paleocene age, but the lower part of the formation is of latest Late Cretaceous age (Barnes and others, 1954). It crops out principally inside the northern margin of the central basin (fig. 4). The Animas is present in only about the northern one-third of the basin, mainly in Colorado; it does not occur south of a line that extends from Dulce, New Mexico, to the La Plata River Valley (fig. 11) near the Colorado-New Mexico State line (fig. 13). Along this line the Animas Formation grades laterally into the Nacimiento Formation (Fassett and Hinds, 1971, p. 33; Fassett, 1974, p. 229), which occupies the same stratigraphic interval (fig. 5). In the north the Animas Formation conformably overlies the Kirtland Shale of Late Cretaceous age; farther south, near the New Mexico-Colorado State line, the unit may unconformably overlie the Ojo Alamo Sandstone of Tertiary age (Fassett and Hinds, 1971, p. 34).

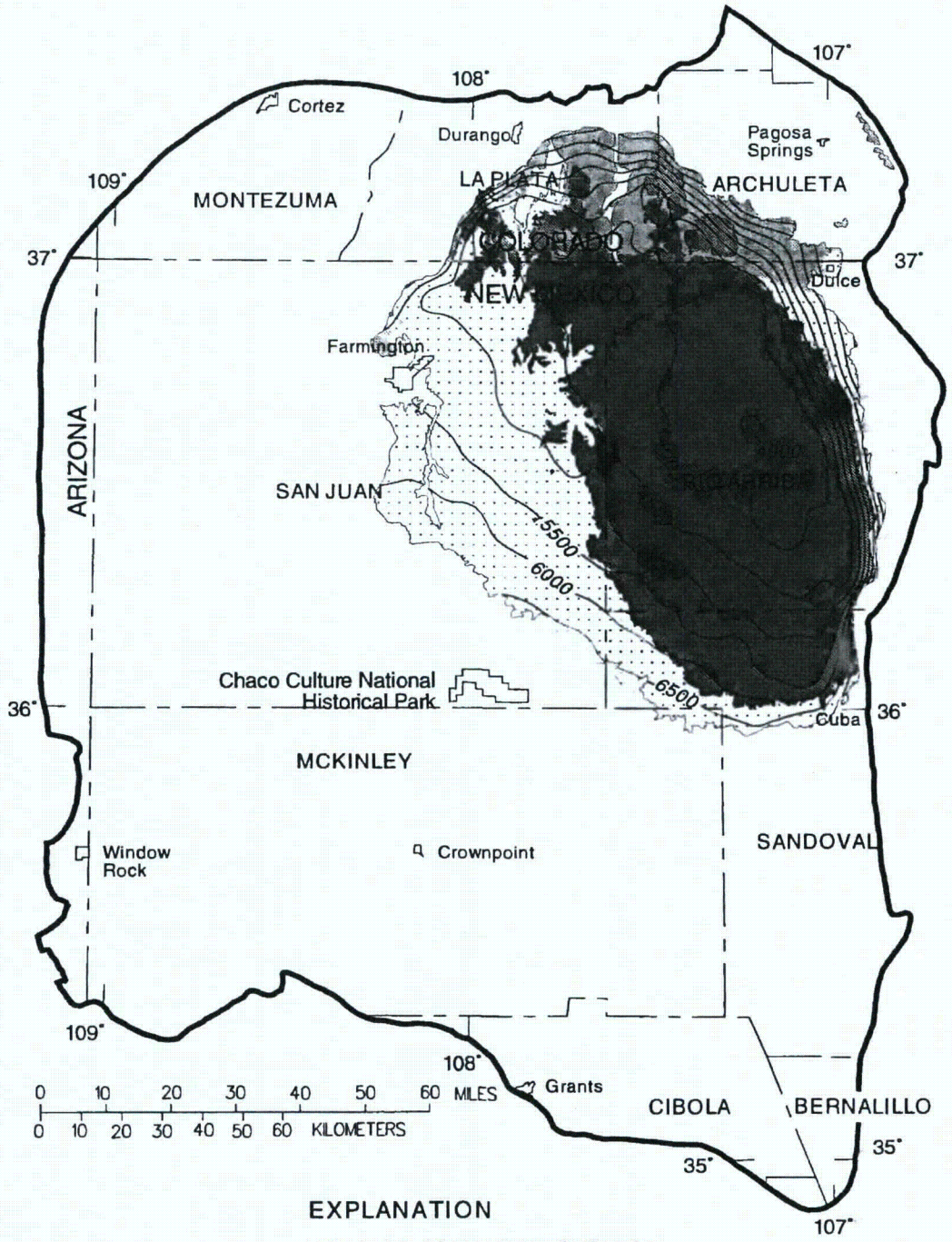

Figure 13.--Approximate altitude and configuration of the base of the Animas and Nacimiento Formations.

Geometry and Lithology

The Animas Formation consists of two members: the unnamed upper member of Paleocene age (Barnes and others, 1954) and the lower McDermott Member of latest Late Cretaceous age. The unnamed upper member disconformably overlies the McDermott Member; this unconformity represents a time gap of about 6 million years (Fassett, 1977). The Animas Formation consists mainly of volcaniclastic deposits; the diagnostic characteristic of the Animas Formation as a whole is the presence of macroscopic volcanic material (Fassett and Hinds, 1971, p. 33). The unnamed upper member consists of varicolored and interbedded tuffaceous sandstone, conglomerate, and shale (Fassett, 1974, p. 229). The McDermott Member consists of varicolored (dominantly purple) tuffaceous sandstone and conglomerate with minor variegated shale (Reeside, 1924, p. 25). Thickness of the Animas Formation ranges from about 230 feet at the type section along the Animas River (fig. 11) at Durango, Colorado (Barnes and others, 1954), to about 2,700 feet near the La Plata-Archuleta County line in Colorado (fig. 14) (Fassett and Hinds, 1971, p. 33).

The Nacimiento Formation is of Paleocene age (Baltz, 1967, p. 35). It crops out in a broad band inside the southern and western margins of the central basin and in a narrow band along the west face of the Nacimiento Uplift (fig. 4). The Nacimiento is a nonresistant unit and typically erodes to low, rounded hills or forms badlands topography.

The Nacimiento Formation occurs in approximately only the southern two-thirds of the basin where it conformably overlies and intertongues with the Ojo Alamo Sandstone (Baltz, 1967, p. 41; Fassett, 1974, p. 229). The Nacimiento Formation grades laterally into the main part of the Animas Formation (Fassett and Hinds, 1971, p. 34; Fassett, 1974, p. 229); thus, in this area the two formations occupy the same stratigraphic interval (fig. 5). The altitude of the base of the Animas and Nacimiento Formations is shown in figure 13.

Strata of the Nacimiento Formation mainly were deposited in lakebeds in the central basin area with lesser deposition in stream channels (Brimhall, 1973, p. 201; Fassett, 1974, p. 229). In general, the Nacimiento consists of drab, interbedded black and gray shale with discontinuous, white, medium- to very coarse grained arkosic sandstone (Fassett, 1974, p. 229; Stone and others, 1983, p. 30). Baltz (1967, p. 39) stated that the percentage of sandstone increases northward. Stone and others (1983, p. 30) indicated that the formation may contain more sandstone than commonly has been reported because some investigators assume the slope-forming strata in the unit are shales, whereas in many places the strata actually are poorly consolidated sandstones.

Total thickness of the Nacimiento Formation ranges from about 500 to 1,300 feet (Molenaar, 1977a). The unit generally thickens from the basin margins toward the basin center (Baltz, 1967, p. 38; Steven and others, 1974; Stone and others, 1983). The sandstone deposits within the Nacimiento Formation are much thinner than the total thickness of the formation because their environment of deposition was localized stream channels (Brimhall, 1973, p. 201). The combined thickness of the combined San Jose, Animas, and Nacimiento Formations ranges from 500 to more than 3,500 feet (fig. 14).

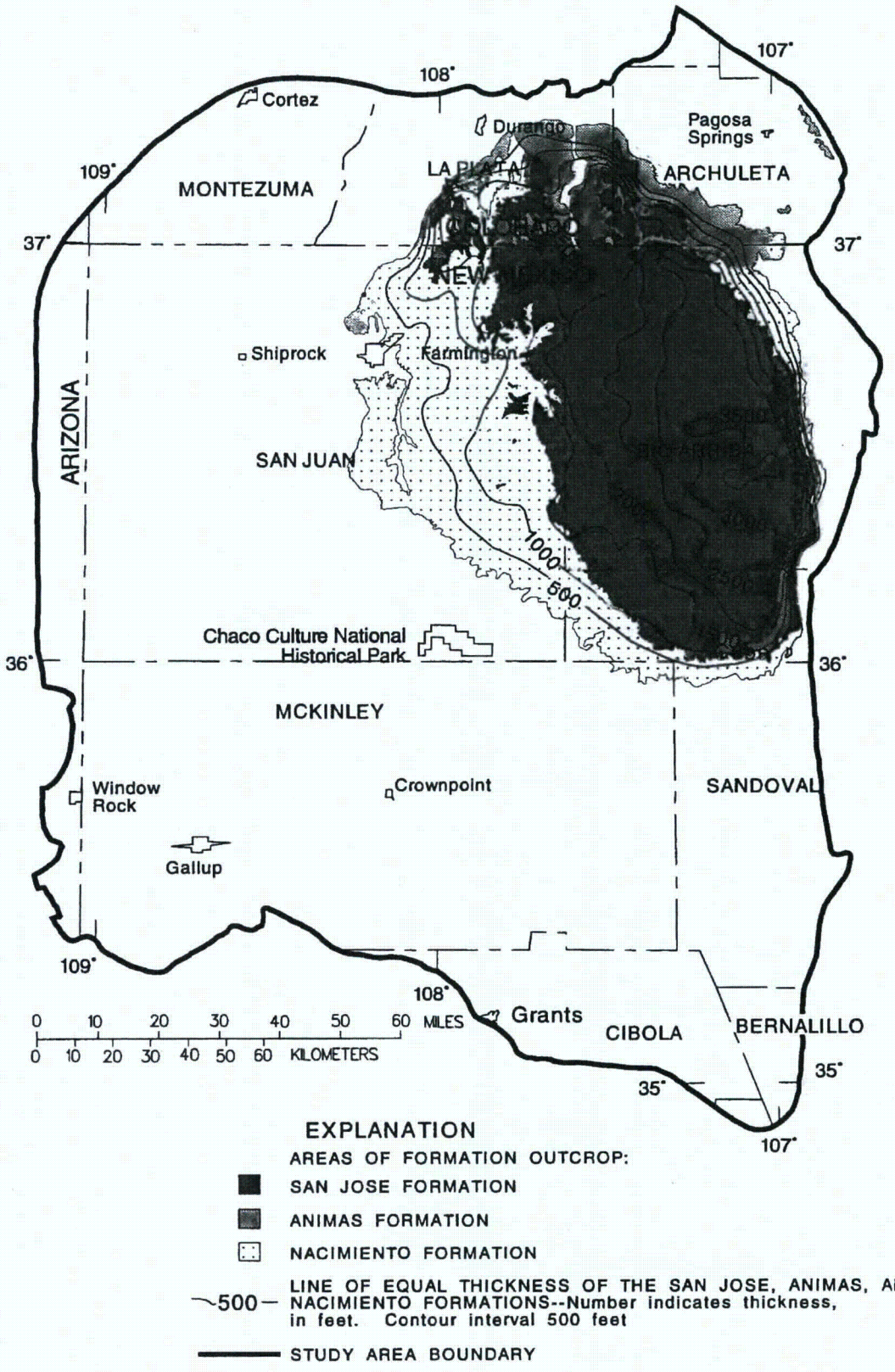

Figure 14.--Approximate thickness of the San Jose, Animas, and Nacimiento Formations.

Hydraulic Properties

Reported well yields for 53 wells completed in either the Animas or Nacimiento Formations range from 2 to 90 gallons per minute and the median yield is 7.5 gallons per minute. The primary use of water from the Nacimiento and Animas Formations is domestic and livestock supplies. There are no known aquifer tests for the Animas or Nacimiento Formations, but specific capacities reported for six wells range from 0.24 to 2.30 gallons per minute per foot of drawdown (Levings and others, 1990b).

The Animas and Nacimiento Formations are in many ways hydrologically similar to the San Jose Formation because sands in both units produce approximately the same quantities of water. However, the greater percentage of fine material in the Animas and Nacimiento Formations may restrict downward vertical leakage to the Ojo Alamo Sandstone or Kirtland Shale. The poorly cemented fine material is highly erodible, forms a badlands terrain, and supports only spotty vegetation. These conditions are more conducive to runoff than to retention of precipitation.

Ojo Alamo Sandstone

The Ojo Alamo Sandstone is of early Tertiary (Paleocene) age. It crops out inside the central basin and typically forms cliffs and dip slopes or caps low mesas and forms rounded hills. The majority of Ojo Alamo rocks are in New Mexico (fig. 15). The unit pinches out in the northwest about halfway between Farmington, New Mexico, and the Colorado State line west of the La Plata River (fig. 11). In the northeast, Ojo Alamo outcrops extend into Colorado, where they pinch out a few miles north of the State line, south of Pagosa Springs, Colorado (Fassett, 1974, p. 228). Subsurface studies by Fassett and Hinds (1971, fig. 9 and p. 29) indicate that the Ojo Alamo is not present north of a line connecting the northernmost limits of the Ojo Alamo outcrops (fig. 15).

The Ojo Alamo Sandstone disconformably overlies the Kirtland Shale throughout most of the basin. On the east side, however, the Kirtland Shale has been removed by pre-Ojo Alamo erosion, and the Ojo Alamo disconformably overlies the Fruitland Formation; locally in places where the Fruitland Formation has been removed, the Ojo Alamo rests directly on the Lewis Shale (Fassett, 1974, p. 228). The contact of the Ojo Alamo with underlying rocks has been described by O'Sullivan and others (1972, p. 56) as "a sharp wavy surface of erosion." Fassett and Hinds (1971, p. 28) reported large-scale channeling at the base of the Ojo Alamo and stated that some of these channels cut 50 feet or more into the underlying shales or sandstones of the Kirtland Shale or Fruitland Formation. The Ojo Alamo is conformably overlain by the Nacimiento Formation throughout most of the basin, and intertonguing at the contact is common (Fassett and Hinds, 1971, p. 29).

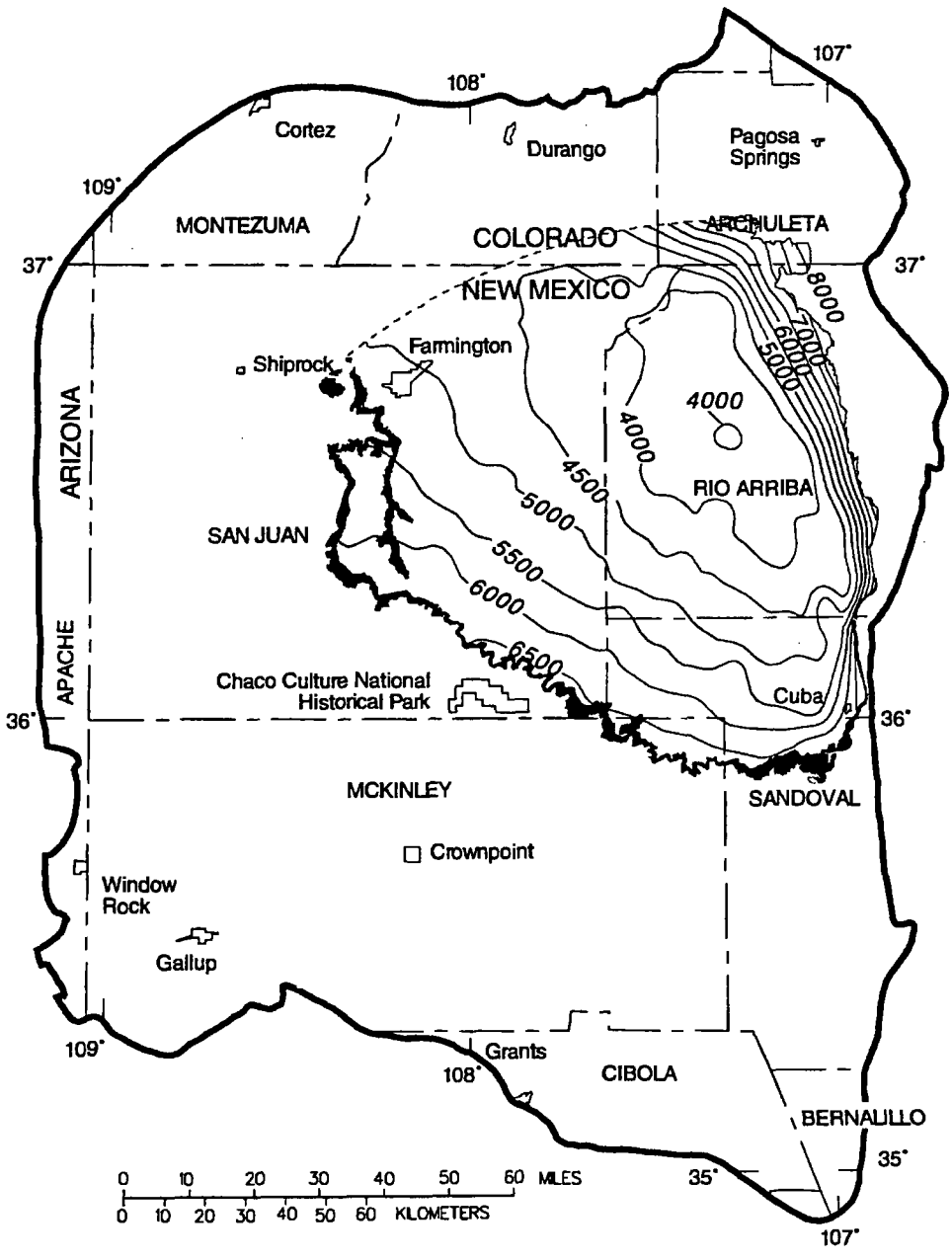

EXPLANATION

OUTCROP OF OJO ALAMO SANDSTONE

APPROXIMATE NORTHERN SUBSURFACE EXTENT OF THE OJO ALAMO SANDSTONE

6500 LINE OF EQUAL ALTITUDE OF THE TOP OF THE OJO ALAMO SANDSTONE--Number indicates altitude, in feet. Contour interval 500 feet. Datum is sea level

STUDY AREA BOUNDARY

Figure 15.--Approximate altitude and configuration of the top of the Ojo Alamo Sandstone.

Geometry and Lithology

In general, the Ojo Alamo Sandstone consists of overlapping sheetlike sequences of conglomeratic sandstones and sandstones, which locally contain interbedded shale lenses. The sandstones are arkosic, light brown to rusty brown, or buff and tan, and contain abundant silicified wood. The sandstones are medium to very coarse grained and often conglomeratic, containing pebbles of various compositions that decrease in size and quantity from west to east across the basin (Baltz and West, 1967, p. 17; Fassett and Hinds, 1971, p. 28).

Thickness of the Ojo Alamo Sandstone is variable. Baltz (1967, p. 32) reported that thickness ranges from 70 feet to a maximum of 200 feet. O'Sullivan and others (1972, p. 57) also reported a maximum thickness of 200 feet. Stone and others (1983, p. 31) reported a range of about 70 to 300 feet. In a basinwide study, Fassett and Hinds (1971, p. 28, 29) reported that thickness of the Ojo Alamo varies from about 20 to 400 feet but that a range of 50 to 150 feet is most common. Fassett and Hinds (1971, p. 28) stated that thickness varies according to the number of sandstone beds that constitute the unit at any given location.

The altitude of the top of the Ojo Alamo Sandstone is shown in figure 15. The top of the Ojo Alamo decreases from a maximum altitude of about 8,000 feet along the northeastern basin margin to about 4,000 feet in the east-central part of the study area.

Hydraulic Properties

The transmissivity of the Ojo Alamo Sandstone ranges from 57 to 164 feet squared per day; the median value is 104 feet squared per day for 10 aquifer tests (Brimhall, 1973, p. 206; Anderholm, 1979, p. 29; Stone and others, 1983, table 5). These data represent wells that are on or near the outcrop and are less than 1,100 feet deep. Data are available for three aquifer tests performed on two test wells more than 4,000 feet deep near the center of the basin; transmissivity for these tests ranges from 0.05 to 0.39 foot squared per day and the median value is 0.35 foot squared per day (Mercer, 1969).

Reported or measured discharges from 19 water wells completed in the Ojo Alamo Sandstone range from 1.2 to 112 gallons per minute, and the median is 12 gallons per minute. The specific capacity of nine of these wells ranges from 0.01 to 2.04 gallons per minute per foot of drawdown and the median is 0.26 gallon per minute per foot of drawdown.

The Ojo Alamo is resistant to erosion, and the outcrop generally forms a prominent ridge or cliff or caps mesas. In the outcrop the Ojo Alamo is deeply fractured at wide intervals of as much as 15 feet. Soil cover on the outcrop usually is thin and sandy. In contrast to the overlying Animas and Nacimiento Formations, the Ojo Alamo usually supports a modest stand of conifers in areas where there is sufficient precipitation, indicating capture and retention of moisture. Although the unit is relatively thin it is a dependable source of generally good quality water.

Kirtland Shale and Fruitland Formation

The combined Kirtland Shale and Fruitland Formation, of Late Cretaceous age (Baltz, 1967; Fassett and Hinds, 1971), crops out inside the margins of the central basin. Topography formed on the unit typically varies from rolling to rough, and badlands commonly are developed. Erosion-resistant sandstones commonly cap isolated buttes and hillocks, whereas softer shaley units form

slopes and broad valleys or flats. The upper part of the Kirtland Shale generally forms steep slopes below mesas or buttes that are capped by the overlying erosion-resistant Ojo Alamo Sandstone.

The Kirtland Shale and Fruitland Formation were named by Bauer (1916) for exposures along the San Juan River (fig. 11) west of Farmington, New Mexico. The Ojo Alamo Sandstone of Tertiary age and the McDermott Member of the Animas Formation of Late Cretaceous age (Baltz, 1967; Fassett and Hinds, 1971; Molenaar, 1977b) unconformably overlie the Kirtland Shale. The Kirtland Shale conformably overlies the Fruitland Formation. The Fruitland Formation conformably overlies the Pictured Cliffs Sandstone, and intertonguing locally occurs at the contact.

Geometry and Lithology

In general, the combined Kirtland Shale and Fruitland Formation consists of various thicknesses of interbedded and repetitive sequences of nonmarine channel sandstone, siltstone, shale, and claystone. Coal beds and carbonaceous shales are common in the Fruitland Formation. The Kirtland Shale does not contain coal and has been divided into three members, which in descending order are the upper shale member, Farmington Sandstone Member, and lower shale member (fig. 5; Bauer, 1916).

Thickness of the combined Kirtland Shale and Fruitland Formation ranges from zero on the east side of the basin, because of pre-Ojo Alamo Sandstone erosion, to a maximum of about 2,000 feet in the northwestern part of the basin (Fassett and Hinds, 1971, p. 22, 26; Molenaar, 1977b, p. 165). A basinwide thickness map of the combined Kirtland Shale and Fruitland Formation is shown in figure 16. Thickness of the Kirtland Shale ranges from zero in the east to about 1,500 feet in the northwest; the upper shale member, Farmington Sandstone Member, and lower shale member each are as much as 500 feet thick (Fassett and Hinds, 1971, p. 26; Molenaar, 1977b, p. 165; Stone and others, 1983, p. 31). The Fruitland Formation ranges in thickness from zero in the east to about 500 feet in the northwest (Fassett and Hinds, 1971, p. 23) and averages about 300 to 350 feet thick (Molenaar, 1977b, p. 165).

The overall structural pattern of that part of the San Juan Basin underlain by the Kirtland Shale and Fruitland Formation is shown in figure 17. The top of the Kirtland Shale and Fruitland Formation decreases from a maximum altitude of about 8,000 feet along the northeastern basin margin to about 3,500 feet in the east-central part of the structural basin.

Hydraulic Properties

Reported transmissivity and hydraulic-conductivity data for the Kirtland Shale and Fruitland Formation are limited to aquifer tests conducted on five wells. The transmissivity determined from these tests ranges from 0.6 to 130 feet squared per day (Stone and others, 1983, table 5). The only hydraulic conductivity calculated from the tests is 0.00001 foot per day.

The reported or measured discharge from 12 water wells completed in the Kirtland Shale and Fruitland Formation ranges from 1 to 12 gallons per minute and the median is 3 gallons per minute. The specific capacity of six of these wells ranges from 0.01 to 0.42 gallon per minute per foot of drawdown and the median is 0.03 gallon per minute per foot of drawdown. These tests are most probably of wells that produce drinking water from the Farmington Sandstone Member of the Kirtland Shale.

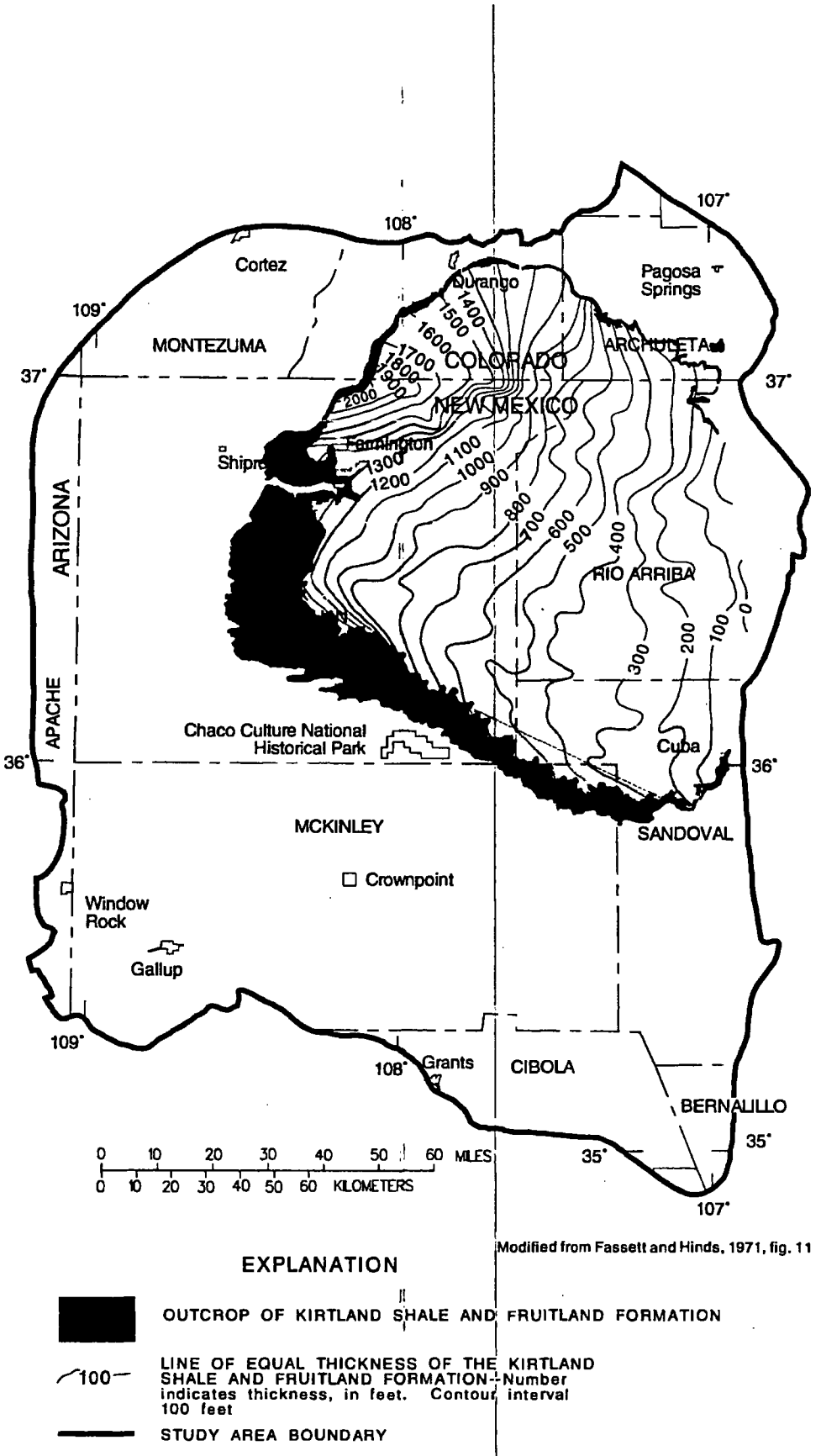

Figure 16.--Approximate thickness of the combined Kirtland Shale and Fruitland Formation.

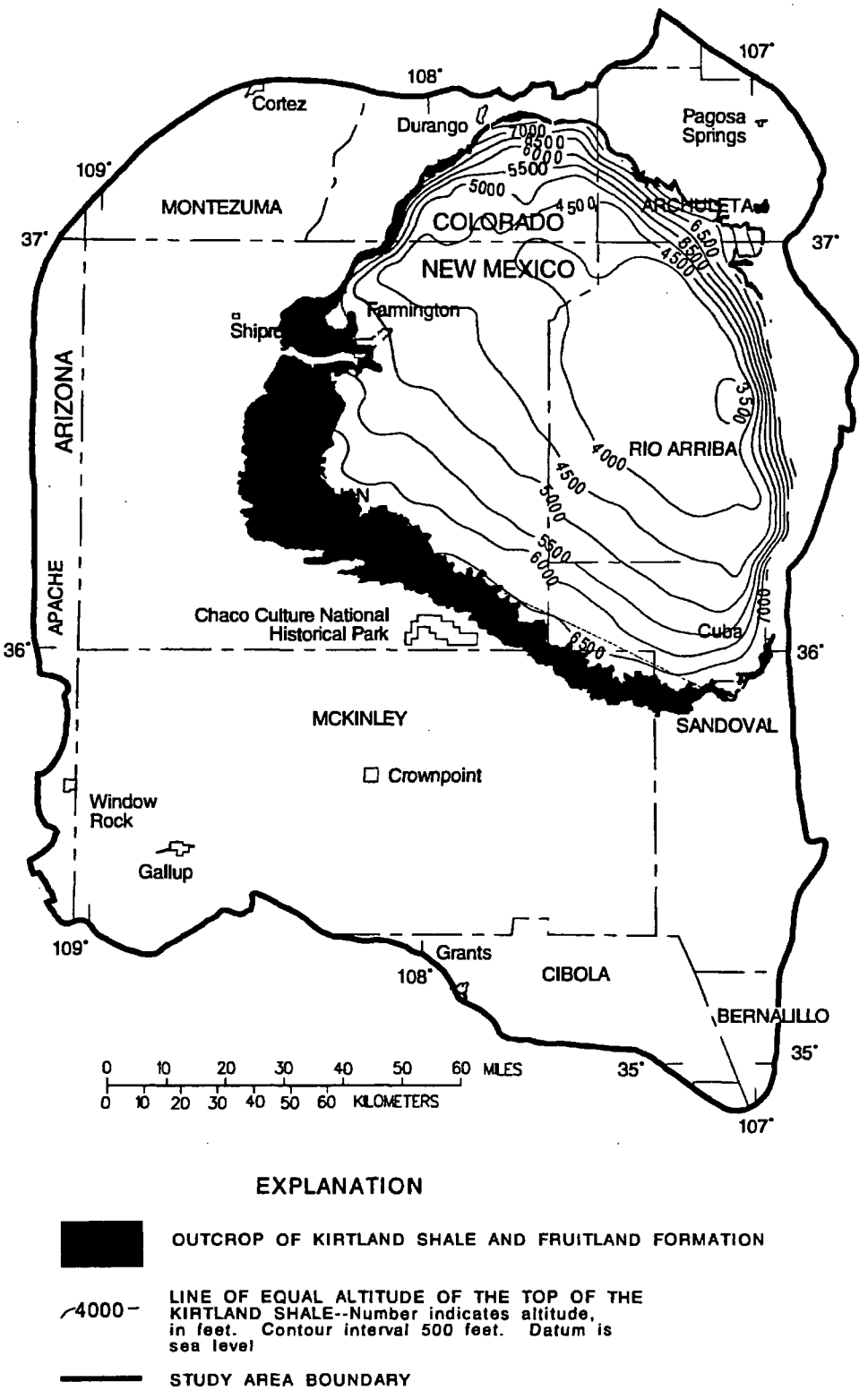

Figure 17.--Approximate altitude and configuration of the top of the Kirtland Shale.

Recently, there has been extensive exploration for methane gas resources from coal beds in the Fruitland Formation. The gas resource in the coal beds had largely been ignored because initial production from most wells was large quantities of poor-quality water and the gas-producing potential was not recognized. The current production practice is to complete the well and pump out water to reduce the pressure at the coal bed. Gradually, gas production increases as water production decreases (Fassett, 1989). Because of the poor-quality water and the identification of over-pressured (greater than hydrostatic pressure) areas in the center of the basin at the Colorado-New Mexico State line, a current question among coal geologists is whether the water is connate (trapped in the coal at the time of deposition) or meteoric (originated from recharge on the outcrop).

Some gas and water production is thought to be from both coal in the Fruitland Formation and sandstone in the underlying Pictured Cliffs Sandstone. Water-quality analyses for these two units also show more similarity with each other than with analyses from the overlying Ojo Alamo Sandstone or the underlying Cliff House Sandstone aquifers.

Pictured Cliffs Sandstone

The Pictured Cliffs Sandstone is of Late Cretaceous age. It crops out inside the margins of the central basin where it caps mesas and buttes or forms erosion-resistant dip slopes. The Pictured Cliffs Sandstone typically is a cliff former, except along the southern outcrop belt where commonly the only way to determine its presence is by drilling. The Pictured Cliffs Sandstone was named by Holmes (1877, p. 248) for exposures having carved petroglyphs near the San Juan River between Shiprock and Farmington, New Mexico.

The Pictured Cliffs Sandstone is a regressive marine coastal-barrier deposit (Molenaar, 1977b, p. 165). It conformably overlies the Lewis Shale (fig. 5). The contact is characterized by a distinct offshore marine transition zone consisting of interbedded thin sandstones, siltstones, and shales (Reeside, 1924, p. 19; Fassett and Hinds, 1971, p. 8). The Fruitland Formation (Late Cretaceous) conformably overlies the Pictured Cliffs, and these two units locally intertongue (Fassett and Hinds, 1971, p. 8).

Geometry and Lithology

The Pictured Cliffs Sandstone generally consists of an upward-coarsening sequence of thick- to very thick bedded, very fine to medium-grained, locally crossbedded and bioturbated sandstone. Thin interbeds of dark marine shale also are present, especially in the lower part of the unit (Baltz, 1967, p. 17-18; Fassett and Hinds, 1971, p. 8). The Pictured Cliffs is tightly cemented in the northern part of the basin, decreasing to poor or no cementation in the southern part.

Thickness of the Pictured Cliffs Sandstone is variable. Molenaar (1977a) reported a maximum thickness of 400 feet, but also reported (1977b, p. 165) that the average thickness is much less. Fassett and Hinds (1971, p. 17) stated that thickness ranges from 0 feet in the east side of the San Juan structural basin to about 400 feet in the north-central part of the basin. Stone and others (1983, p. 33) reported a range in thickness of 25 to 280 feet in New Mexico.

The configuration of the top of the Pictured Cliffs Sandstone is shown on the structure-contour map (fig. 18). The top of the Pictured Cliffs Sandstone decreases from a maximum altitude of about 8,000 feet along the north-central basin margin to about 3,000 feet in the northeastern part of the study area.

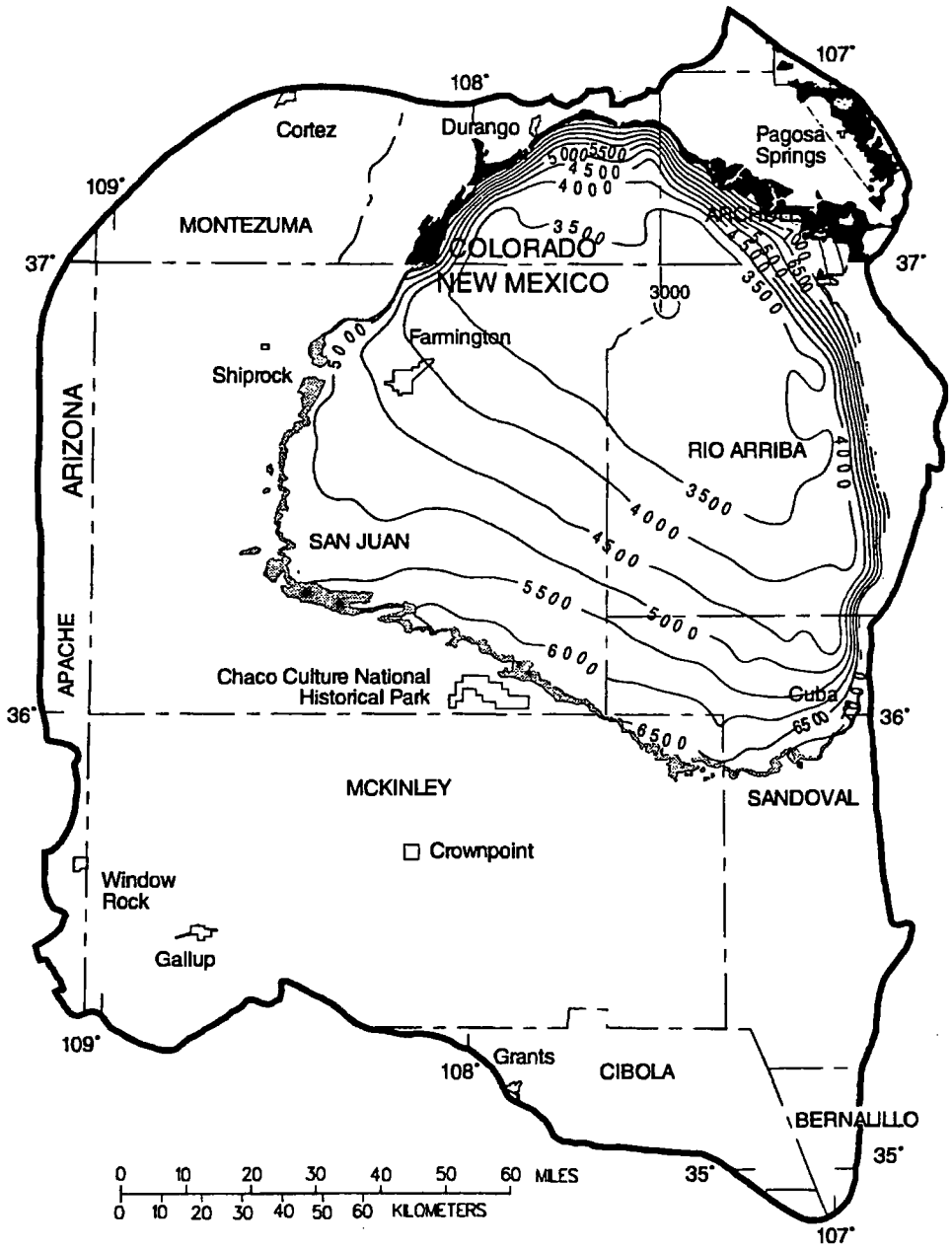

EXPLANATION

AREAS OF FORMATION OUTCROP:

PICTURED CLIFFS SANDSTONE

PICTURED CLIFFS SANDSTONE AND LEWIS SHALE, UNDIVIDED

–6500– LINE OF EQUAL ALTITUDE OF THE TOP OF THE PICTURED CLIFFS SANDSTONE--Number indicates altitude, in feet. Contour interval 500 feet. *Datum is sea level*

STUDY AREA BOUNDARY

Figure 18.--Approximate altitude and configuration of the top of the Pictured Cliffs Sandstone.

Hydraulic Properties

Reported transmissivity and hydraulic-conductivity data for the Pictured Cliffs Sandstone are minimal. Transmissivity from five tests ranges from 0.001 to 3 feet squared per day (Stone and others, 1983, table 5). Hydraulic-conductivity values calculated from drill-stem tests in oil and gas wells in deeper parts of the basin average 0.007 foot per day (Reneau and Harris, 1957).

The reported or measured discharge from 12 water wells completed in the Pictured Cliffs Sandstone ranges from 2 to 73 gallons per minute and the median is 21 gallons per minute. The specific capacity of seven of these wells ranges from less than 0.01 to 0.70 gallon per minute per foot of drawdown and the median is 0.01 gallon per minute per foot of drawdown.

Few water wells are completed in the Pictured Cliffs Sandstone because of the generally poor quality water found in the unit. In the northern part of the basin the source of water to wells is predominantly from fractures and joints, whereas in the southern part it is from interstitial porosity.

Lewis Shale

The Lewis Shale, of Late Cretaceous age (fig. 5), crops out around the margins of the central basin. Topography formed on the unit generally is rolling, and badlands landscapes are common. The type area for the Lewis Shale is in the northwestern San Juan Basin.

The Lewis Shale is conformably overlain by the Pictured Cliffs or, in the northeastern part of the San Juan Basin, may be unconformably overlain by the Fruitland Formation, Kirtland Shale, or Ojo Alamo Sandstone. The Lewis conformably overlies and intertongues with the Cliff House Sandstone. In some areas where Cliff House tongues pinch out, the Lewis Shale may directly overlie the Menefee Formation (Stone and others, 1983, p. 33).

Geometry and Lithology

The Lewis Shale is a gray to dark-gray transgressive marine shale that thins to the west and southwest. In the western part of the basin the Lewis wedges out and the Pictured Cliffs Sandstone rests on the Cliff House Sandstone. The Lewis contains several bentonitic horizons, of which the most widely noted is the Huerfanito Bentonite Bed. The Huerfanito Bentonite Bed is frequently used as a geologic time marker.

The configuration of the top of the Lewis Shale is shown on the structure-contour map (fig. 19). The top of the Lewis Shale decreases from a maximum altitude of about 8,000 feet along the northeastern basin margin to about 3,000 feet in the northeastern part of the central basin.

Hydraulic Properties

The Lewis Shale is not recognized as an aquifer and there are no known tests to determine the hydraulic properties of the unit. Water wells are reported to be completed in the unit, but these actually may be completed in sandstone tongues of the underlying Cliff House Sandstone.

The Lewis Shale serves as a confining unit that hydraulically separates the overlying Pictured Cliffs Sandstone and underlying Cliff House Sandstone aquifers. The low-permeability shale also rejects recharge from precipitation.

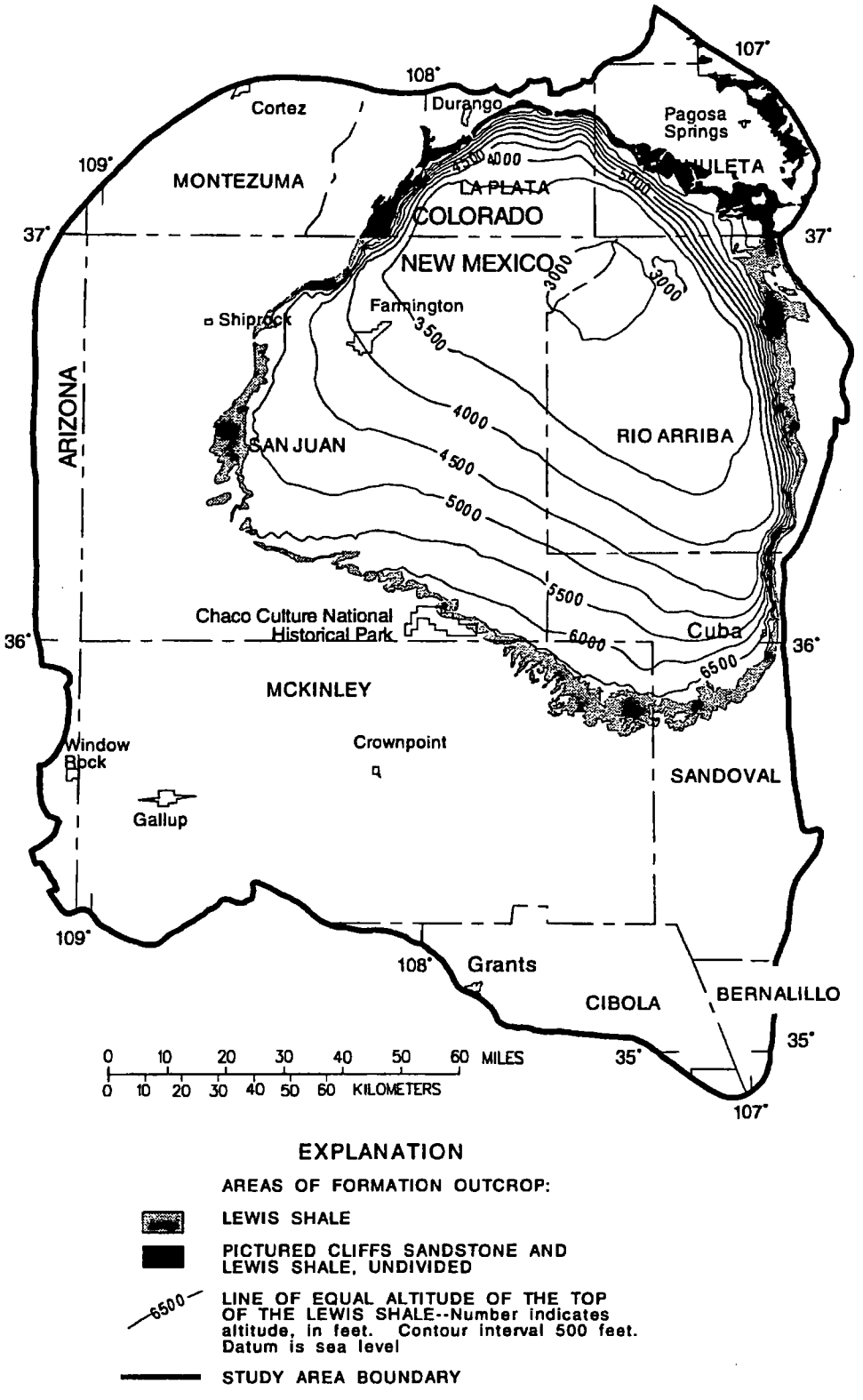

Figure 19.--Approximate altitude and configuration of the top of the Lewis Shale.

Cliff House Sandstone

The Cliff House Sandstone is of Late Cretaceous age (fig. 5). It crops out around the margins of the central basin and typically caps mesas (as in the Chaco Canyon area at Chaco Culture National Historical Park) and southwest of Cuba, New Mexico) and forms erosion-resistant dip slopes and hogbacks (as on the Hogback Monocline) (fig. 4). The Cliff House Sandstone, named by Collier (1919) for exposures on Mesa Verde in southwestern Colorado (fig. 20), is the uppermost formation of the classical three-part Mesaverde Group of the San Juan Basin (Cliff House Sandstone, Menefee Formation, and Point Lookout Sandstone).

The Cliff House Sandstone is conformably overlain by and intertongues with the Lewis Shale; both of these units conformably and unconformably overlie the Menefee Formation, with which they locally intertongue (Molenaar, 1977b, p. 164; Craigg, 1980, p. 7). In some areas where Cliff House tongues pinch out, the Lewis Shale may directly overlie the Menefee Formation (Stone and others, 1983, p. 33). In the western part of the basin, near the confluence of Coyote Wash and the Chaco River (fig. 11), the Cliff House merges with the Pictured Cliffs Sandstone, wedging out the Lewis Shale (fig. 5). The Cliff House Sandstone strata consist of several thick sandstone tongues that represent marine shorezone deposits of an overall transgressing shallow sea. Molenaar (1977b, p. 164) noted that these sandstone bodies actually are offlap or regressive deposits formed during stillstands and minor regressions of the shoreline.

Geometry and Lithology

Stratigraphy of the Cliff House Sandstone is complex. Nomenclature problems and differing interpretations tend to complicate regional correlations. The unit consists of two major sandstone tongues–the Chacra Tongue (Molenaar, 1977b, p. 164) and La Ventana Tongue. Several other minor sandstone tongues of considerably less thickness and areal extent are common (Molenaar, 1977b, p. 164; Stone and others, 1983, sheets 2-4), but pinch out to the northeast.

The Chacra Tongue occurs stratigraphically above and is not physically connected to La Ventana Tongue (Fassett, 1977, p. 196). The Chacra Tongue is the major buildup of the Cliff House Sandstone found at the type section on Mesa Verde, at Chaco Canyon, and at the Hogback Monocline and it forms the margins of the central basin (fig. 4). The unit is about 400 feet thick at its type section on Mesa Verde (fig. 20) (Collier, 1919, p. 297). Molenaar (1977b, p. 164) reported a range of about 150 to 300 feet in thickness, and Stone and others (1983, p. 33) reported a range of 0 to 250 feet in thickness of the Chacra Tongue throughout most of its extent in New Mexico.

The major buildup of La Ventana Tongue crops out in the southeastern part of the basin at La Ventana south of Cuba and, according to some authors, can be traced in the subsurface across the basin to outcrops on Hogback Mountain (fig. 20) south of the San Juan River (Fassett, 1977; Molenaar, 1977b, p. 164). Other authors report that La Ventana Tongue is a more localized buildup in the southeastern part of the basin, representing deposition in a deltaic environment rather than a marine beach environment (Mannhard, 1976; Fuchs-Parker, 1977). Maximum thickness of La Ventana Tongue, according to Molenaar (1977b, p. 164), is about 800 feet. However, Mannhard (1976, p. 39) and Fuchs-Parker (1977, p. 199) reported a maximum thickness of about 1,000 feet in outcrops along State Highway 44 south of Cuba. Mannhard (1976), Fuchs-Parker (1977), and Tabet and Frost (1979) showed La Ventana Tongue to pinch out about 15 to 20 miles west of these outcrops.

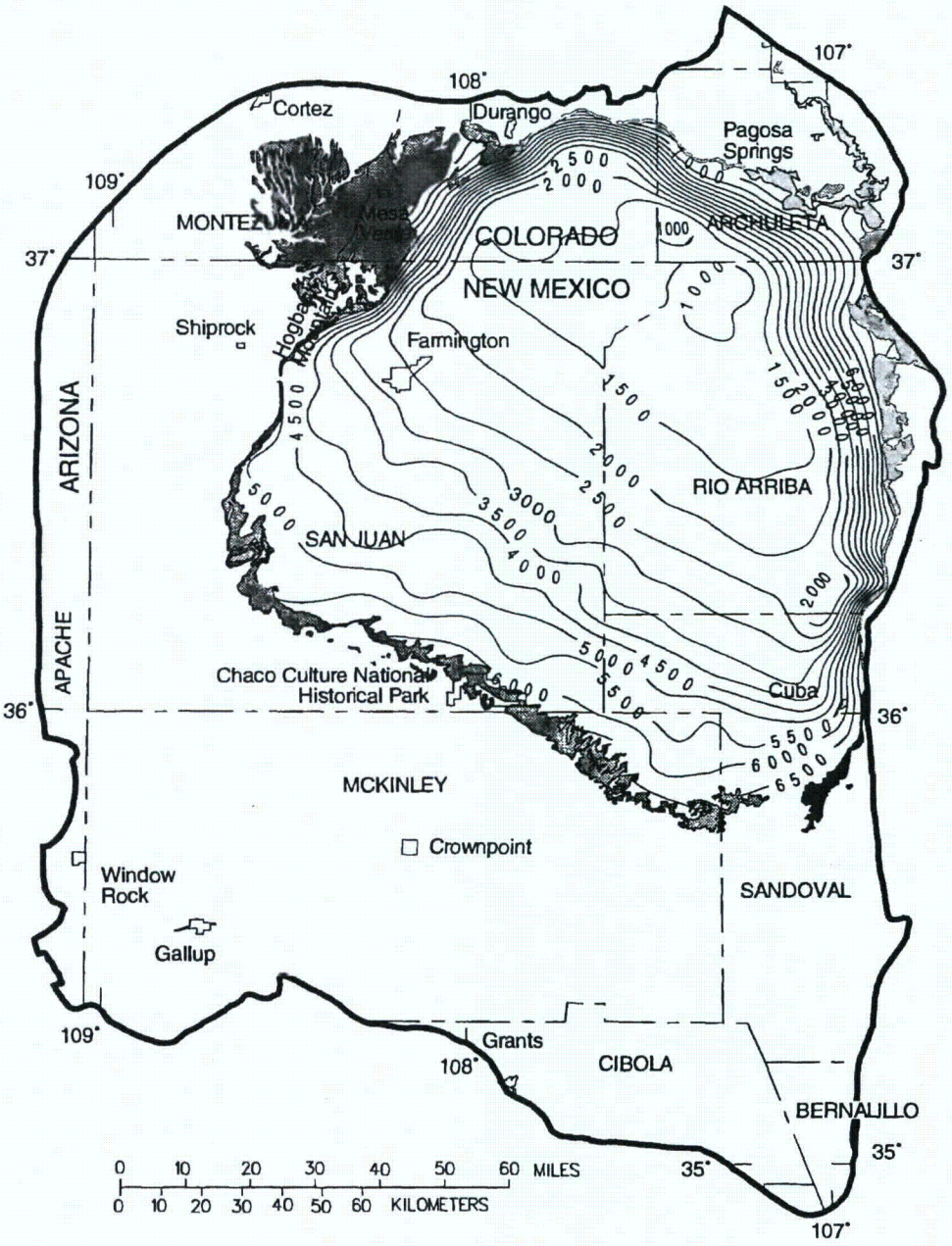

EXPLANATION

AREAS OF FORMATION OUTCROP:

CLIFF HOUSE SANDSTONE

LA VENTANA TONGUE OF CLIFF HOUSE SANDSTONE

MESAVERDE GROUP, UNDIVIDED--Includes Cliff House Sandstone

6500 LINE OF EQUAL ALTITUDE OF THE TOP OF THE CLIFF HOUSE SANDSTONE, LA VENTANA TONGUE, AND MESAVERDE GROUP--Number indicates altitude, in feet. Contour interval 500 feet. Datum is sea level

STUDY AREA BOUNDARY

Figure 20.--Approximate altitude and configuration of the top of the Cliff House Sandstone.

Several other minor tongues of the Cliff House Sandstone of limited areal extent occur in the Lewis Shale northeast of the two major sandstone bodies, Chacra Tongue and La Ventana Tongue. Molenaar (1977b, p. 164) reported that the aggregate thickness of these localized bodies is about 300 feet.

The Cliff House Sandstone generally consists of thick- to very thick bedded and locally crossbedded sandstone with calcite or silica cement and clay matrix. Grain size ranges from very fine to fine and the sandstones are well- to very well sorted (Stone and others, 1983, p. 28, 33). Interbeds of gray shale and silty shale are common (O'Sullivan and Beikman, 1963; Haynes and others, 1972; Craigg, 1980).

The configuration of the top of the Cliff House Sandstone is shown on the structure-contour map (fig. 20). The top of the Cliff House Sandstone decreases from a maximum altitude of about 8,000 feet along the northern rim of the central basin to about 1,000 feet near the structural center of the basin. The dip of the Cliff House Sandstone is steepest near the basin margins (where contours are closely spaced), and less steep on the marginal platforms and near the basin center.

Hydraulic Properties

Transmissivity and hydraulic-conductivity data for the Cliff House Sandstone are extremely limited. A recovery test on a water well in 1961 indicated a transmissivity of 2 feet squared per day (Stone and others, 1983). The average hydraulic conductivity calculated from drill-stem tests in oil and gas wells in deeper parts of the basin is 0.0015 foot per day (Reneau and Harris, 1957).

The reported or measured discharge from 27 water wells completed in the Cliff House Sandstone ranges from 1 to 40 gallons per minute and the median is 8.5 gallons per minute. The specific capacity of 14 of these wells ranges from 0.01 to 0.15 gallon per minute per foot of drawdown and the median is 0.06 gallon per minute per foot of drawdown.

The exposed dip slope of the Cliff House Sandstone offers good recharge potential. The recharge potential is excellent in the northern and northeastern part of the basin where streams cross the outcrop. One of the more probable areas of natural discharge is where the San Juan River crosses the Hogback Monocline (fig. 4) between Farmington and Shiprock, New Mexico.

Menefee Formation

The Menefee Formation (fig. 21) is of Late Cretaceous age (fig. 5) and crops out beyond the margins of the central basin. Erosion-resistant sandstones in the Menefee commonly cap isolated buttes and hillocks, whereas softer shale units form slopes and broad valleys or flats. Topography formed on the Menefee typically is rolling to rough, broken and steep, and generally has a badlands appearance. The upper part of the Menefee Formation commonly forms steep slopes below mesas or buttes capped by the erosion-resistant Cliff House Sandstone.

The Menefee Formation, named by Collier (1919) for exposures on Menefee Mountain near Mesa Verde in southwestern Colorado, is the middle unit of the classical three-part Mesaverde Group of the San Juan Basin. The Menefee Formation conformably or disconformably overlies the Point Lookout Sandstone and is conformably or disconformably overlain by the Cliff House Sandstone; intertonguing locally occurs at both contacts (Tabet and Frost, 1979; Craigg, 1980; Stone and others, 1983). Some authors have reported the Menefee to be conformably overlain by the Lewis Shale in the southeastern part of the basin (Dane, 1936; Beaumont and others, 1956). South of the pinch-out of the Point Lookout Sandstone in the vicinity of Gallup, New Mexico, the Menefee conformably overlies the Crevasse Canyon Formation (fig. 5).

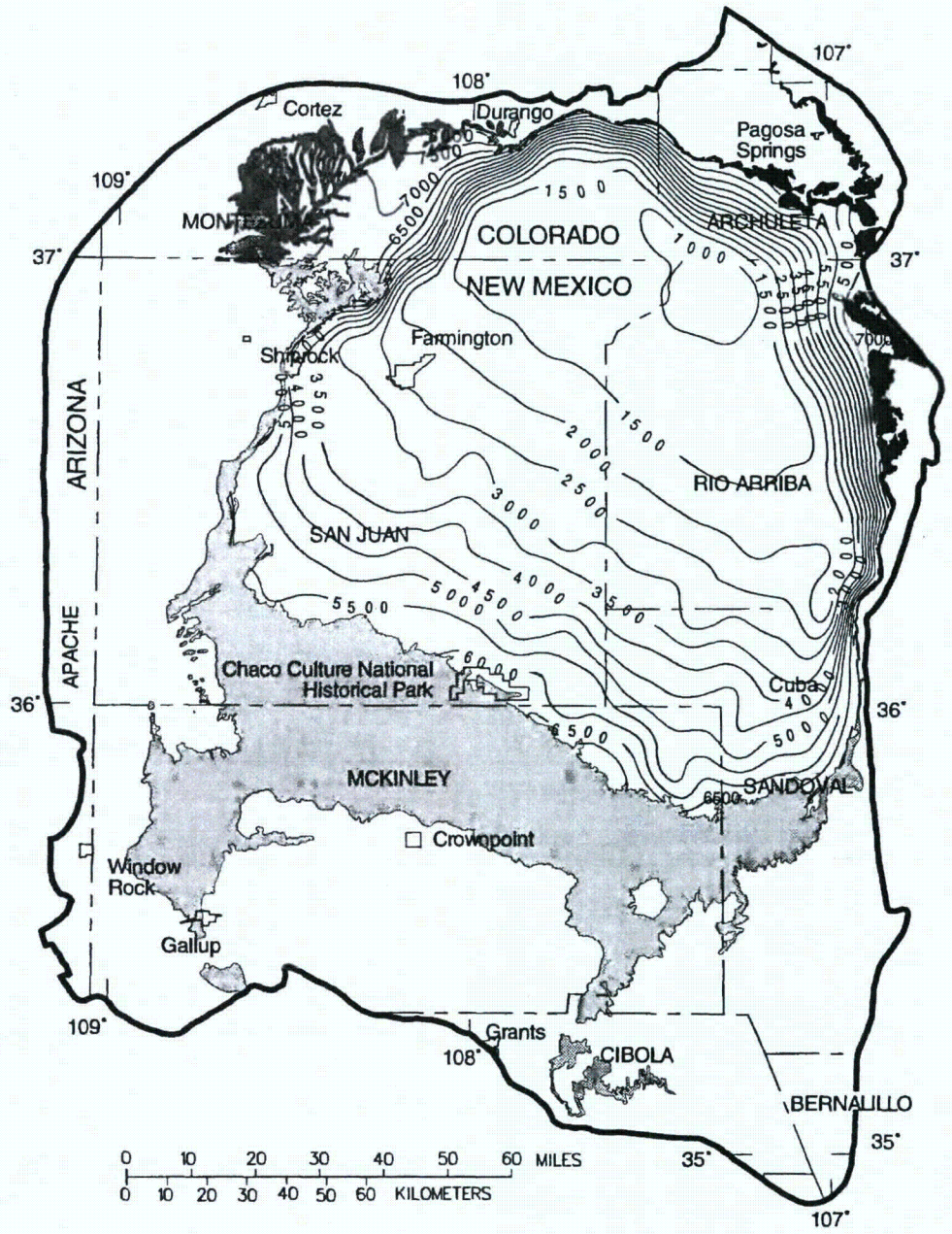

EXPLANATION

AREAS OF FORMATION OUTCROP:

MENEFEE FORMATION

MENEFEE FORMATION AND POINT LOOKOUT SANDSTONE

MESAVERDE GROUP, UNDIVIDED--Includes Menefee Formation

6500 LINE OF EQUAL ALTITUDE OF THE TOP OF THE MENEFEE FORMATION, POINT LOOKOUT SANDSTONE, AND MESAVERDE GROUP--Number indicates altitude, in feet. Contour interval 500 feet. Datum is sea level

STUDY AREA BOUNDARY

Figure 21.--Approximate altitude and configuration of the top of the Menefee Formation.

Geometry and Lithology

In general, the Menefee Formation consists of interbedded and repetitive sequences of differing thicknesses of sandstone, siltstone, shale and claystone, carbonaceous shale, and coal beds of differing thicknesses (Collier, 1919; Sears and others, 1936; Mannhard, 1976; Tabet and Frost, 1979; Craigg, 1980). Typically the sandstones are lenticular, light brown to gray, thick to very thick bedded, and fine to medium grained, with clay matrix and various types of cement. The siltstones commonly are tabular, gray, and thin to thick bedded; shales and claystones typically are light-brownish gray and thick to very thick bedded (Mannhard, 1976; Tabet and Frost, 1979; Craigg, 1980).

The Menefee Formation increases in thickness from north to south. Thickness ranges from zero where the unit pinches out between the Point Lookout and Cliff House Sandstones in Colorado to about 2,000 feet along its southern outcrop area (Molenaar, 1977b, p. 164; Tabet and Frost, 1979).

The configuration of the top of the Menefee Formation is shown on the structure-contour map (fig. 21). The top of the Menefee Formation decreases from a maximum altitude of about 8,000 feet along the north-central basin margin to about 1,000 feet in the northeastern part of the study area.

Hydraulic Properties

The transmissivity of the Menefee Formation depends on the thickness of sandstone lenses penetrated. Transmissivity values reported for nine aquifer tests (Stone and others, 1983) range from 2.7 to 112 feet squared per day and the median value is 10 feet squared per day. Hydraulic conductivity calculated from drill-stem tests in oil and gas wells in deeper parts of the basin averages 0.017 foot per day (Reneau and Harris, 1957).

The reported or measured discharge from 83 water wells and seven springs completed in the Menefee Formation ranges from 2 to 308 gallons per minute and the median is 10 gallons per minute. The specific capacity of 37 of these wells ranges from 0.02 to 0.57 gallon per minute per foot of drawdown and the median is 0.11 gallon per minute per foot of drawdown.

Water from the Menefee Formation is used for livestock watering and domestic purposes. Until a deep well to the Gallup Sandstone was drilled in 1973, the Menefee, supplemented by water from shallow alluvial deposits along Chaco Wash (fig. 11), also was used for the water supply at Chaco Culture National Historical Park. Most wells completed in the Menefee are designed for a low but steady yield of water because the ultimate rate of yield is limited by the rate of leakage of water from shales and silt that encase the lenses of sandstone. Because of the extensive area of the outcrop and the lenticular occurrence of water-yielding sandstones in a clay matrix, the Menefee Formation is both one of the most widely used aquifers and one of the most regionally effective confining units in the basin.

Point Lookout Sandstone

The Point Lookout Sandstone is of Late Cretaceous age (fig. 5) and crops out beyond the margins of the central basin (fig. 4). The outcrops typically form cliffs, cap mesas and buttes, or form erosion-resistant dip slopes and hogbacks (as along the base of the Hogback Monocline in fig. 4). The Point Lookout Sandstone, named by Collier (1919) for exposures on Mesa Verde in southwestern Colorado, is the lowermost formation of the Mesaverde Group of the San Juan structural basin. It conformably overlies the Mancos Shale throughout the basin, and the contact is characterized by a distinct offshore marine transition zone consisting of interbedded thin sandstones, siltstones, and shales (Shetiwy, 1978; Craigg, 1980; Wright, 1984). The Menefee Formation conformably or disconformably overlies the Point Lookout, and the two units locally intertongue at the contact (Tabet and Frost, 1979).

In the southern part of the San Juan Basin, the Point Lookout Sandstone is separated into two units by the Satan Tongue of the Mancos Shale (fig. 5). The upper unit is the main body, or by common usage, the Point Lookout Sandstone. The lower unit is the Hosta Tongue, which is a transgressive marine beach sandstone. The main body and Hosta Tongue merge along the southern margin of the basin (fig. 5) into a combined unit about 250 feet thick (Sears and others, 1941; Beaumont and others, 1956, p. 2154). The Hosta Tongue is of limited areal extent, pinching out 30 miles northeast of its outcrop (Beaumont, 1971, p. 22; Craigg, 1980), and attains a maximum thickness of about 160 feet (Beaumont and others, 1956, p. 2155).

Geometry and Lithology

The Point Lookout Sandstone generally consists of a sequence of thick- to very thick bedded, very fine to medium-grained, locally crossbedded sandstone (Shetiwy, 1978; Craigg, 1980; Wright, 1984). Thin interbeds of dark marine shale also occur, especially in the lower part of the unit.

Thickness of the Point Lookout Sandstone is variable. Beaumont (1971, p. 22) reported thickness to range irregularly from about 100 feet in the southern part of the basin to about 350 feet near the Colorado-New Mexico State line. Molenaar (1977a) reported a maximum thickness of 300 feet. Stone and others (1983, p. 34) reported a range from 40 to 415 feet in New Mexico.

The configuration of the top of the Point Lookout Sandstone is shown on the structure-contour map (fig. 22). The top of the Point Lookout Sandstone decreases from a maximum altitude of about 8,000 feet along the north-central and southeastern basin margins to about 500 feet in the northeastern part of the study area.

Hydraulic Properties

Reported transmissivity of the Point Lookout Sandstone ranges from 0.4 foot squared per day (Craigg, 1980) to 236 feet squared per day (Dames and Moore, 1977; Stone and others, 1983). Dames and Moore reported a storage coefficient of 0.000041 that was based on an analysis of drawdown in an observation well. The average hydraulic conductivity calculated from drill-stem tests in oil and gas wells in the deeper parts of the basin is 0.0058 foot per day (Reneau and Harris, 1957).

The reported or measured discharge from 22 water wells completed in the Point Lookout Sandstone ranges from 1 to 360 gallons per minute and the median is 20 gallons per minute. The specific capacity of six of these wells ranges from 0.02 to 1.67 gallons per minute per foot of drawdown and the median is 0.25 gallon per minute per foot of drawdown.

Crevasse Canyon Formation

The Crevasse Canyon Formation is of Late Cretaceous age (fig. 5). It crops out only in the southern part of the basin. In the western part of the basin the Gibson Coal Member of the Crevasse Canyon forms a rolling, hilly topography in the outcrop. Farther east, the Dalton Sandstone Member commonly is found in cliff-side exposures.

Figure 22.--Approximate altitude and configuration of the top of the Point Lookout Sandstone.

Geometry and Lithology

The Crevasse Canyon Formation, named by Allen and Balk (1954), consists of three members (fig. 5): the transgressive Dilco Coal Member, the regressive Dalton Sandstone Member, and the transgressive Gibson Coal Member. The thickest occurrence of the Dalton Sandstone is in the vicinity of Mount Taylor (fig. 4) where it has a cliff-side exposure beneath the basalt-capped Mesa Chivato. The Gibson Coal Member is thickest in the southwest part of the basin where it is extensively mined at the surface for its coal resources. The Gibson Coal Member thins to the east as the Dalton Sandstone thickens. The Crevasse Canyon Formation underlies the Hosta Tongue of the Point Lookout Sandstone. South of the pinch-out of the Point Lookout Sandstone in the vicinity of Gallup, New Mexico, the Menefee conformably overlies the Crevasse Canyon Formation (fig. 5). The Crevasse Canyon Formation conformably overlies the Gallup Sandstone. The Crevasse Canyon Formation thins rapidly to the northeast and pinches out about 30 miles northeast of its outcrop.

Hydraulic Properties

The Dalton Sandstone Member is the primary water-yielding unit of the Crevasse Canyon Formation. Because of its limited extent, however, it is not a major aquifer in the basin. Stone and others (1983) reported a probable transmissivity of less than 50 feet squared per day for sandstones in the Crevasse Canyon Formation.

Gallup Sandstone

The Gallup Sandstone is of Late Cretaceous age (fig. 5). The unit has a smaller areal extent than the other major Upper Cretaceous marine sandstones in the San Juan structural basin and occurs only in New Mexico and a small part of Arizona. The Gallup Sandstone crops out in an arcuate pattern around the margins of the southwest half of the basin where it typically forms erosion-resistant cliffs and dip slopes.

As originally defined by Sears (1925) and discussed in detail by Dane and others (1957), the Gallup Sandstone consists of various rocks including sandstone (the predominant rock type), conglomerate, shale, carbonaceous shale, and coal. The Gallup Sandstone represents the first major regression of the Upper Cretaceous sea in the San Juan structural basin area and also represents deposition in various marine and nonmarine environments.

Geometry and Lithology

From its outcrops, the Gallup Sandstone dips toward a northwest-trending cutoff line that extends from the southeastern part of the basin, through the central part of the basin, to near Shiprock, New Mexico, in the northwestern part of the basin. The orientation of this cutoff line is about north 50 degrees west. The Gallup Sandstone is not present northeast of this cutoff line because it has been truncated by a pre-Niobrara erosion surface (Pentilla, 1964; Molenaar, 1973, 1974). Thickness of the Gallup Sandstone decreases from about 600 feet near the outcrops along the southern margin of the basin to zero along the northwest-trending pre-Niobrara cutoff line.

Isolated, lenticular sandstone bodies known as Tocito Sandstone Lentils are found in the transgressive Mulatto Tongue of the Mancos Shale northeast of the cutoff line. These isolated sandstone lenses have been referred to by various informal names such as "Basal Niobrara sandstone," "Tocito sandstone," "Transgressive Gallup," and "Stray sandstone" and have been misidentified as parts of the main body of the Gallup Sandstone. Although many of these isolated sandstone bodies are found at stratigraphic horizons that suggest the presence of the Gallup Sandstone, they are not connected to nor are genetically related to the main body of the Gallup Sandstone (Molenaar, 1973, 1974).

The approximate altitude and configuration of the top of the Gallup Sandstone are shown on the structure-contour map (fig. 23). The altitude of the top of the Gallup Sandstone decreases from a maximum of about 7,500 feet in the western part of the basin to about 1,500 feet in the west-central part of the basin.

Hydraulic Properties

Transmissivity and storage-coefficient data for the Gallup Sandstone are available from analysis of drawdown and recovery data for aquifer tests conducted at 17 wells in the study area (Stone and others, 1983, table 5; McLean, 1980; U.S. Geological Survey files, Albuquerque, New Mexico). Values of transmissivity range from 15 to 390 feet squared per day; the median is 123 feet squared per day. Values of storage coefficient calculated from aquifer tests at four wells range from 0.000002 to 0.000033.

The reported or measured discharge from 49 water wells completed in the Gallup Sandstone ranges from less than 1 to 645 gallons per minute and the median is 42 gallons per minute. The specific capacity of 13 of these wells ranges from 0.12 to 2.10 gallons per minute per foot of drawdown and the median is 0.46 gallon per minute per foot of drawdown.

The Gallup Sandstone is a major source of potable or treatable water and serves as the main water supply for the City of Gallup, Chaco Culture National Historical Park, and many small public-distribution systems in the southern part of the basin. It is also a major source of water for livestock use, especially in the southeastern part of the basin. The Gallup Sandstone is a source of water containing dissolved-solids concentrations less than 2,000 milligrams per liter throughout the extent of the main body of the sandstone.

Dakota Sandstone

The Dakota Sandstone generally is thought to be of earliest Late Cretaceous age, although the lowermost part may be of latest Early Cretaceous age (Fassett, 1977, p. 225). The Dakota Sandstone crops out around the basin margins where it typically caps mesas and forms erosion-resistant dip slopes and hogbacks.

The Dakota Sandstone in the San Juan structural basin and vicinity was deposited on a regional erosion surface; the strata represent a transition from continental alluvial-plain deposition in the lower part of the formation to marine shorezone deposition in the upper part. Owen (1973, p. 39-50) presented a comprehensive depositional model for the Dakota Sandstone in the area of the San Juan structural basin.

The Dakota Sandstone unconformably overlies the Brushy Basin Member of the Morrison Formation (Late Jurassic age) throughout much of the basin. However, the Dakota overlies the Westwater Canyon Member of the Morrison in the southwest and the Burro Canyon Formation (Early Cretaceous) in the north (fig. 5). The upper contact of the Dakota is conformable with the Mancos Shale, and intertonguing of these two units is common near the contact.

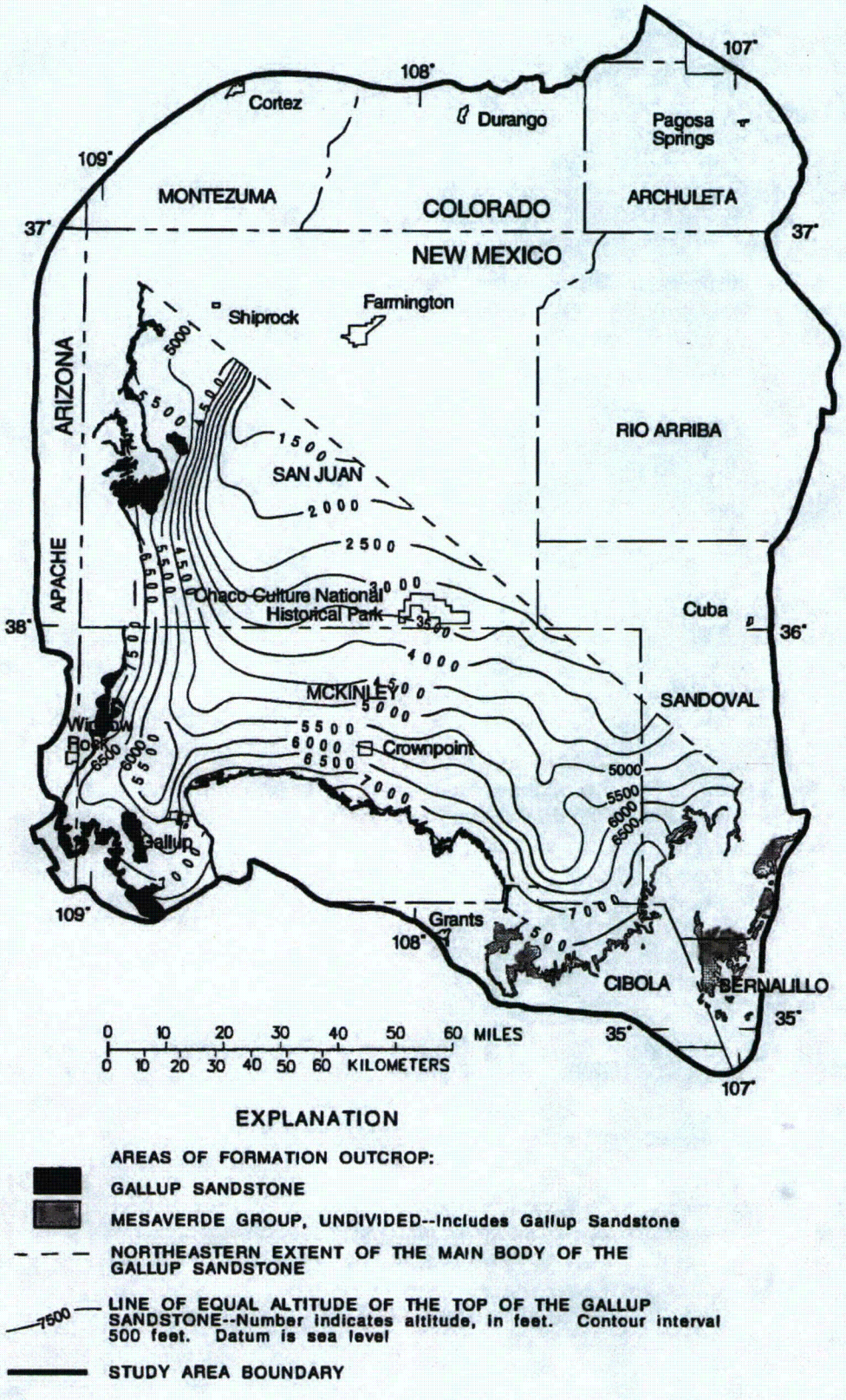

Figure 23.--Approximate altitude and configuration of the top of the Gallup Sandstone.

Geometry and Lithology

Stratigraphy of the Dakota Sandstone is complex. The unit consists of a main sandstone body in the north from which various members and tongues extend depending on location in the San Juan structural basin. The Dakota consists of four members (Landis and others, 1973; Owen, 1973), which, in descending order, are the Twowells Tongue, Paguate Tongue, Cubero Tongue, and Oak Canyon Member (fig. 5). The two upper sandstone members intertongue with the Graneros Member of the Mancos Shale. Owen and Siemers (1977) and Noon (1980) have attempted to extend these members in the east part of the basin. Petroleum geologists have applied informal terminology to some of the tongues of the Dakota Sandstone, such as "Dakota A" for the Twowells Tongue and "Dakota B" for the Paguate Tongue (fig. 5).

The Dakota Sandstone contains three principal lithologies. It typically consists of a sequence of buff to brown, crossbedded, poorly sorted, coarse-grained conglomeratic sandstone and moderately sorted, medium-grained sandstone in the lower part; dark-gray carbonaceous shale with brown siltstone and lenticular sandstone beds in the middle part; and yellowish-tan, fine-grained sandstone interbedded with gray shale in the upper part (fig. 5; Owen, 1973, p. 39-48; Merrick, 1980, p. 45-47).

Thickness of the Dakota Sandstone generally ranges from a few tens of feet to about 500 feet; Stone and others (1983, p. 37) reported that 200 to 300 feet probably is a more common range. Data reported by Stone and others (1983, fig. 66) and Molenaar (1977b, p. 160-161) and data obtained from Petroleum Information Corporation indicate that the thickness of the Dakota generally increases from the west, northwest, and north margins of the basin toward the east, southeast, and south margins.

The altitude and configuration of the top of the Dakota Sandstone are shown on the structure-contour map (fig. 24). The top of the Dakota Sandstone decreases from a maximum altitude of about 9,500 feet above sea level along the northern basin margin to about 1,500 feet below sea level in the northeastern part of the study area.

Hydraulic Properties

Transmissivity and hydraulic-conductivity data for the Dakota Sandstone are few. Transmissivity values of 44 and 85 feet squared per day were reported for aquifer tests conducted northeast of Crownpoint, New Mexico (Dames and Moore, 1977, pls. 4 and 5). An aquifer test conducted east of Grants indicated a transmissivity of 2,000 feet squared per day (Risser and Lyford, 1983, p. 166). Hydraulic-conductivity values calculated from drill-stem tests in oil wells in deeper parts of the basin average 0.03 foot per day (Reneau and Harris, 1957, p. 43).

The reported or measured discharge from 30 water wells completed in the Dakota Sandstone ranges from 1 to 75 gallons per minute and the median is 12 gallons per minute. The specific capacity of 13 of these wells ranges from 0.03 to 3.67 gallons per minute per foot of drawdown and the median is 0.06 gallon per minute per foot of drawdown.

In only a few instances is the Dakota Sandstone the sole source of water to a well. The quality of water generally is not as good as that of water from the underlying Westwater Canyon Member of the Morrison Formation (Craigg and others, 1989; Dam and others, 1990a), and most well drillers opt to extend wells into the Westwater Canyon Member.

The Dakota Sandstone has been mined for uranium ore in the southern part of the basin. Also, the Twowells Tongue and upper Paguate Tongue sandstone members that intertongue with the Graneros Member of the Mancos Shale produce oil and gas in the basin. Similar to the transgressive sands of the Gallup Sandstone, these tongues are hydraulically isolated from the ground-water-flow system.

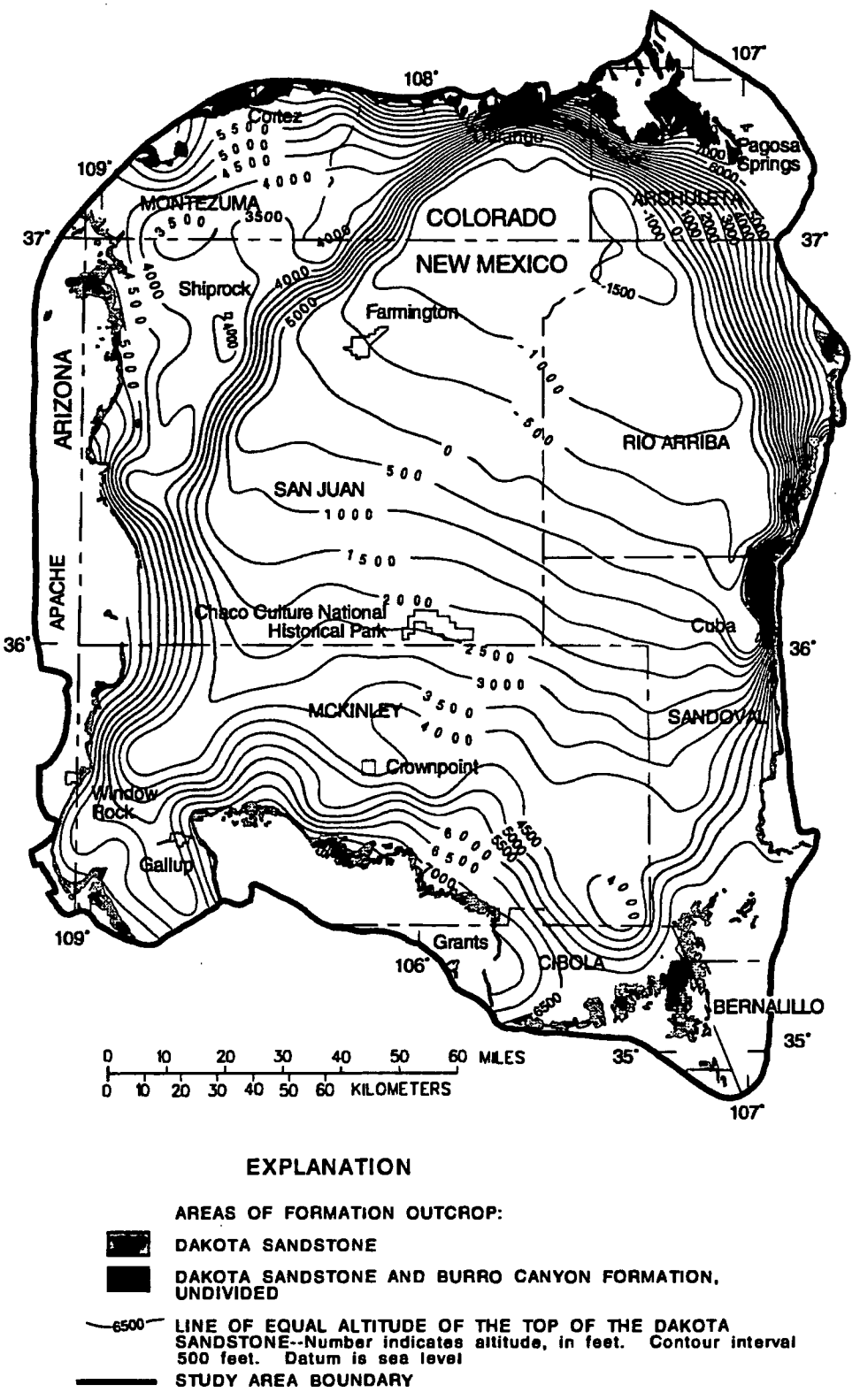

Figure 24.--Approximate altitude and configuration of the top of the Dakota Sandstone.

Morrison Formation

The Morrison Formation is of Late Jurassic age (fig. 5; Cadigan, 1967, p. 6) and crops out around the basin margins. Major sandstones in the Morrison Formation typically form erosion-resistant cliffs and dip slopes, whereas shale units form topographic saddles and dip slopes.

The Morrison Formation is present throughout the San Juan structural basin (Green and Pierson, 1977, p. 151). It conformably overlies the upper part of the Wanakah Formation or Cow Springs Sandstone of Late Jurassic age (Condon and Peterson, 1986, p. 24). In the north part of the basin, the Morrison Formation conformably overlies and probably intertongues with the Junction Creek Sandstone of Late Jurassic age (fig. 5). The Morrison Formation is unconformably overlain by the Dakota Sandstone of Late Cretaceous age throughout most of the San Juan Basin; however, it is conformably overlain by the Burro Canyon Formation of Early Cretaceous age in the northern part of the basin (fig. 5; Green and Pierson, 1977, p. 151).

Geometry and Lithology

The Morrison Formation generally consists of yellowish-tan to pink, fine- to coarse-grained, locally conglomeratic sandstones, which are interbedded with sandy siltstones and green to reddish-brown shales and claystones; minor limestone beds also occur in the formation (Woodward and Schumacher, 1973, p. 3-5; Green and Pierson, 1977, p. 151; Stone and others, 1983, p. 38). These strata were deposited in various continental environments including stream channels, flood plains, and lakes (Green and Pierson, 1977, p. 151).

In the San Juan structural basin the Morrison Formation consists of five members (Gregory, 1938; Craig and others, 1955; Cadigan, 1967; Green and Pierson, 1977; Owen, 1984). These members in descending order are the Salt Wash Member, Recapture Member, Westwater Canyon Member, Brushy Basin Member, and Jackpile Sandstone Member. Recently the Zuni Sandstone was assigned to the Morrison Formation as an eolian facies of the Recapture Member (Condon, 1989).

Because of its geologic characteristics the Westwater Canyon Member is the most important hydrologic unit of the Morrison Formation. Kelly (1977) described the hydrogeology of this member in the south part of the basin. The Westwater Canyon Member is composed of yellowish-gray to tan, pink or light-brown, fine- to coarse-grained locally conglomeratic sandstone, interbedded with shale or claystone (Craig and others, 1955, p. 153; Woodward and Schumacher, 1973, p. 3). Grains increase in size toward the west-central part of the basin until the member consists wholly of conglomeratic sandstone (Craig and others, 1955, p. 154). Thickness of the Westwater Canyon Member increases from about 100 feet on the north, east, and south sides of the San Juan Basin to about 300 feet in the west-central part of the basin (Craig and others, 1955, p. 154).

The altitude and configuration of the top of the Morrison Formation are shown on the structure-contour map (fig. 25). The top of the Morrison Formation decreases from a maximum altitude of about 10,000 feet above sea level along the northern basin margin to about 1,500 feet below sea level in the northeastern part of the basin.

The composite thickness of all members of the Morrison Formation is shown in figure 26. The composite thickness generally correlates with the thickness of the Westwater Canyon Member.

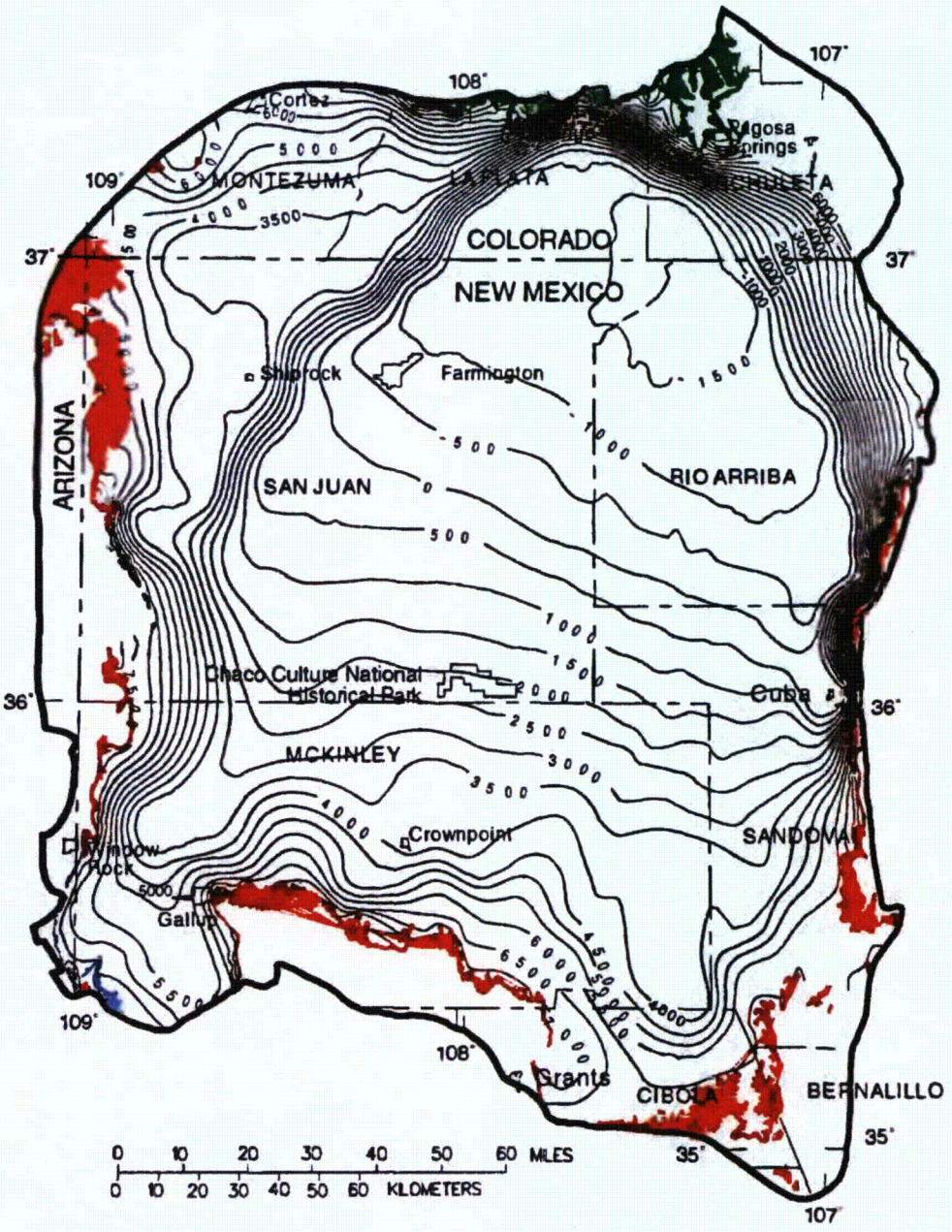

EXPLANATION

AREAS OF FORMATION OUTCROP:

- MORRISON FORMATION
- ZUNI SANDSTONE, OF FORMER USAGE
- SAN RAFAEL GROUP
- MORRISON AND WANAKAH FORMATIONS AND ENTRADA SANDSTONE, UNDIVIDED
- JURASSIC ROCKS, UNDIVIDED
- 5500 — LINE OF EQUAL ALTITUDE OF THE TOP OF THE MORRISON FORMATION--Number indicates altitude, in feet. Contour interval 500 feet. Datum is sea level
- STUDY AREA BOUNDARY

Figure 25.--Approximate altitude and configuration of the top of the Morrison Formation.

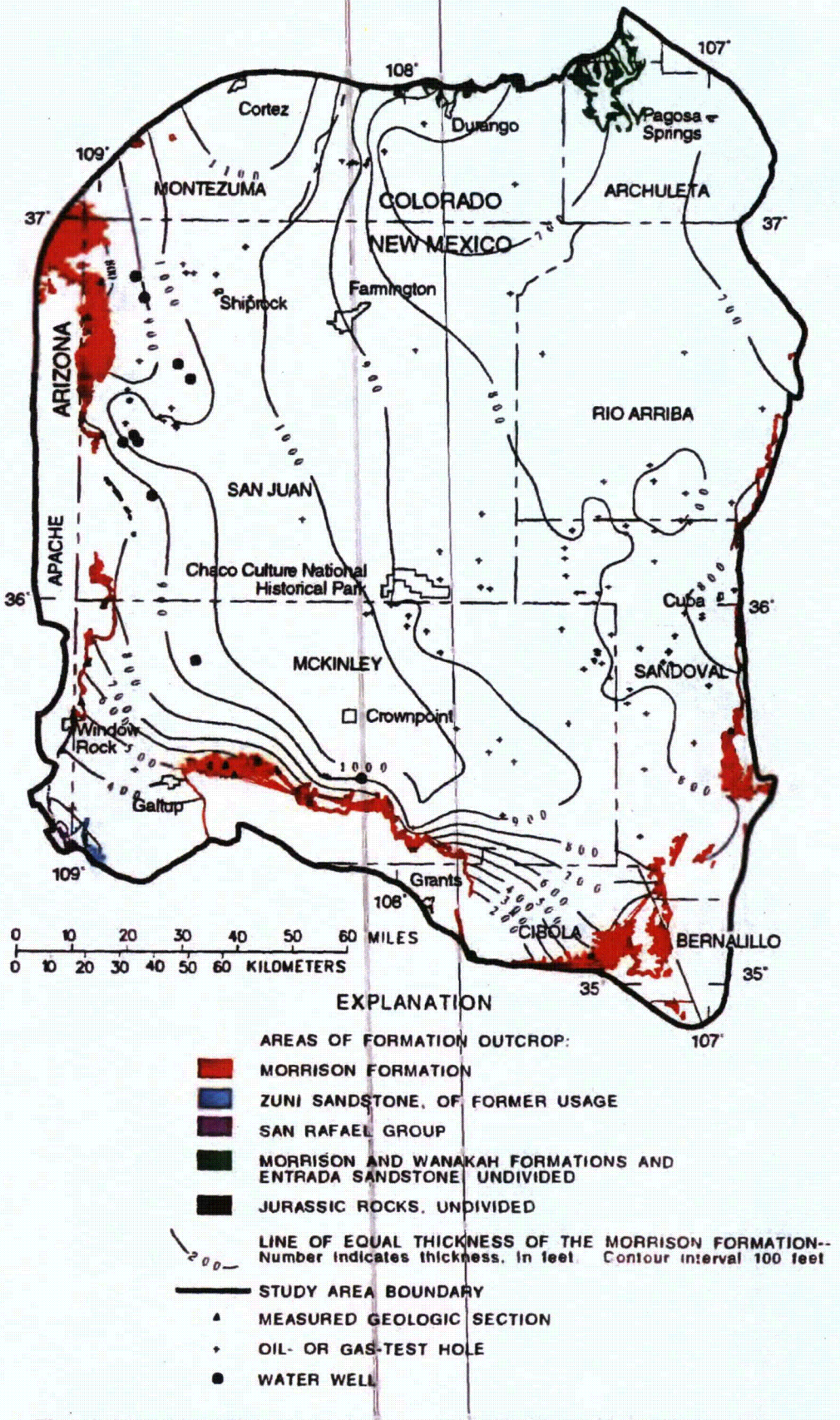

Figure 26.--Approximate thickness of the Morrison Formation.

Hydraulic Properties

Transmissivity, storage coefficient, and hydraulic-conductivity data for the Morrison Formation are available from drawdown and recovery aquifer tests conducted at 31 wells in the study area (Stone and others, 1983, table 5; Risser and others, 1984, p. 23). The transmissivity ranges from 2 to 480 feet squared per day and the median value is 115 feet squared per day. The storage coefficients calculated from aquifer tests at nine wells range from 0.00002 to 0.0002. Hydraulic-conductivity values for three wells range from 0.025 to 0.39 foot per day. A U.S. Department of the Interior report (1986) listed a hydraulic conductivity of 0.3 foot per day for the Jackpile Sandstone and sandstone lenses in the Brushy Basin Member. For a ground-water-flow model of the Westwater Canyon Member northeast of Gallup, New Mexico, Hearne (1977) simulated the aquifer as having a transmissivity of 300 feet squared per day, a confined storage coefficient of 0.0002, and an unconfined storage coefficient of 0.10.

The reported or measured discharge from 83 water wells completed in the Morrison Formation ranges from 1 to 2,250 gallons per minute; the median discharge is 30 gallons per minute. The specific capacity at 32 of these wells ranges from 0.01 to 3.98 gallons per minute per foot of drawdown and the median is 0.42 gallon per minute per foot of drawdown.

One of the major influences on water levels in the Morrison Formation has been aquifer dewatering associated with uranium mining. The location and approximate extent of selected uranium mines in the study area are shown in figure 27. Uranium mining had a modest beginning in the late 1940's, but the industry was well established by the early 1950's. Ore production increased in the mid-1960's and overall mining activity peaked in the late 1970's. By 1981-82, low demand and low prices forced the closure of some mines (primarily the open-pit and underground operations). By 1986 all but one mine had ceased operation. Ground-water levels in the Morrison declined as a result of increased mine dewatering and ore leaching during the growth years of the industry. Later, as mining activity decreased and eventually came to an end in 1991, ground-water levels began to recover.

All wells in the southern part of the study area for which water-level hydrographs have been drawn respond to some degree to uranium-mining activities. Operation of the mines requires the removal of ground water from the aquifer; this results in a reduction in potentiometric head in the aquifer. The rate and extent of reduction are less near the outcrop, where water in the aquifer is under water-table conditions, than in confined areas in the interior of the basin where the Morrison Formation is a confined aquifer. The primary uranium ore body is the Jackpile Sandstone Member of the Morrison Formation.

Three methods of ore extraction have been used in the study area. Open-pit mining techniques were used in the area east of Grants, New Mexico (and to a much lesser extent in the discovery area west-northwest of Grants). This mining method commonly uses gravity flow and existing drainages to remove mine seepage. Open-pit mines usually are within or very near the outcrop area of the formation; the effects of dewatering for open-pit mining are buffered by water-table storage coefficients and reduced transmissivity of the water-yielding units (a function of reduced saturated thickness). Also, the regional base elevation for ground-water discharges usually is only slightly altered from preexisting natural conditions.

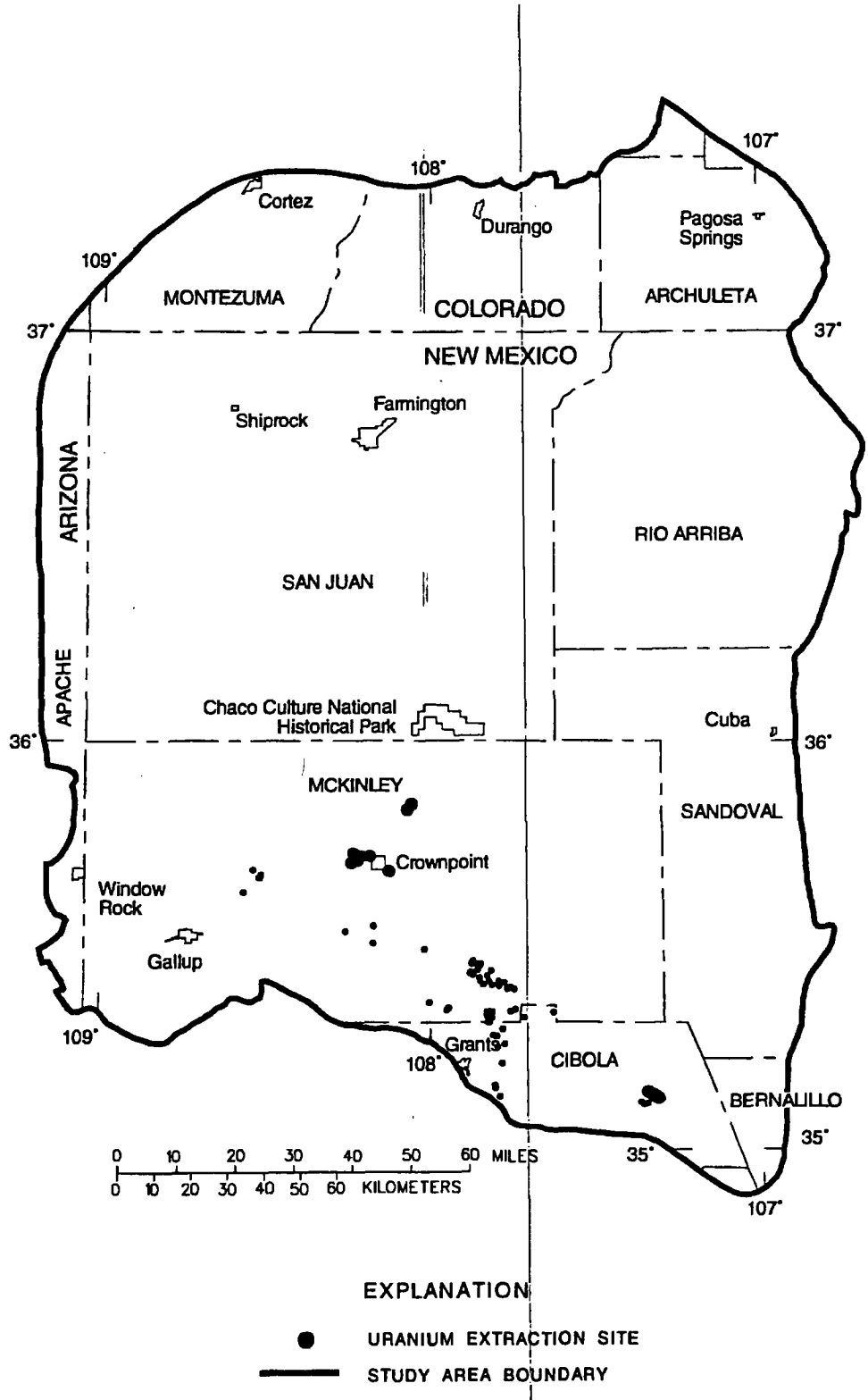

Figure 27.--Location of uranium extraction sites in the Grants uranium belt.

Deep underground mining methods were used east, north, and northwest of Grants, New Mexico, and northeast of Gallup, New Mexico. This mining practice usually has a more immediate and intense effect on regional ground-water levels than open-pit mining because the aquifer is under confined (artesian) conditions rather than unconfined (water-table) conditions. Typically, potentiometric heads will respond two or three orders of magnitude more quickly to a change in withdrawal in the confined part of an aquifer than in the unconfined part. Also, at any specific time after initiation of withdrawal, equal changes in potentiometric head will be measured at distances of at least one order of magnitude greater in the artesian part of the aquifer than in the unconfined part.

In situ leaching techniques were used at several mines in the Crownpoint, New Mexico, area. Commonly, a concentrated oxidant was injected into the mineralized zone in a pattern of wells forming a square. At the center of the square a single well was used to extract the leachate that contained the uranium. In the process, more fluid was extracted than was injected, causing a net decline in pressure head that propagated through the confined aquifer.

Wanakah Formation

The Wanakah Formation, of Jurassic age (fig. 5), crops out at the extreme margins of the basin. Evaporite beds in the Wanakah Formation are moderately resistant to mechanical weathering and form low ridges or crop out in cliff faces under protective caps of younger sandstones of the Dakota Sandstone and Morrison Formation.

The Wanakah Formation is present throughout the San Juan structural basin. It conformably overlies the Entrada Sandstone of Jurassic age. Throughout most of the basin the Wanakah Formation is conformably overlain by the Recapture Member of the Morrison Formation, but in the south it is overlain by the Cow Springs Sandstone and in the north by the Junction Creek Sandstone (fig. 5).

Geometry and Lithology

The Wanakah Formation, as recently redefined (Condon and Huffman, 1988; Condon, 1989), consists of three members. In descending order they are the Horse Mesa, Beclabito, and Todilto Limestone Members. The Horse Mesa and Beclabito Members were previously defined as the Summerville Formation described by Gilluly and Reeside (1928). These members are a massive to planar bedded sandy siltstone and fine-grained silty sandstone as much as 60 feet thick (Green and Pierson, 1977). A basal siltstone grades into limestone and gypsum-anhydrite of the underlying Todilto Limestone Member. The Todilto Limestone Member consists of a basal limestone as much as 30 feet thick. An upper gyspum-anhydrite facies is present in the eastern part of the basin where it reaches a thickness of as much as 90 feet.

The Wanakah Formation is the lowest unit for which a structure-contour map has been prepared for this report (fig. 28). Control for structure maps diminishes very rapidly for lower units and is insufficient for constructing structure maps that do not conflict with maps showing the top of the Wanakah Formation and younger units.

Hydraulic Properties

The Wanakah Formation is usually regarded as a confining unit (Thomas, 1989), although sands in the upper part of the unit might yield small quantities of probably poor quality water. There are no known determinations of hydraulic properties of the Wanakah Formation. Recharge to the unit probably is negligible, but solution openings are known to exist in the gypsum-anhydrite facies in the southeastern part of the basin, indicating some secondary permeability in the unit.

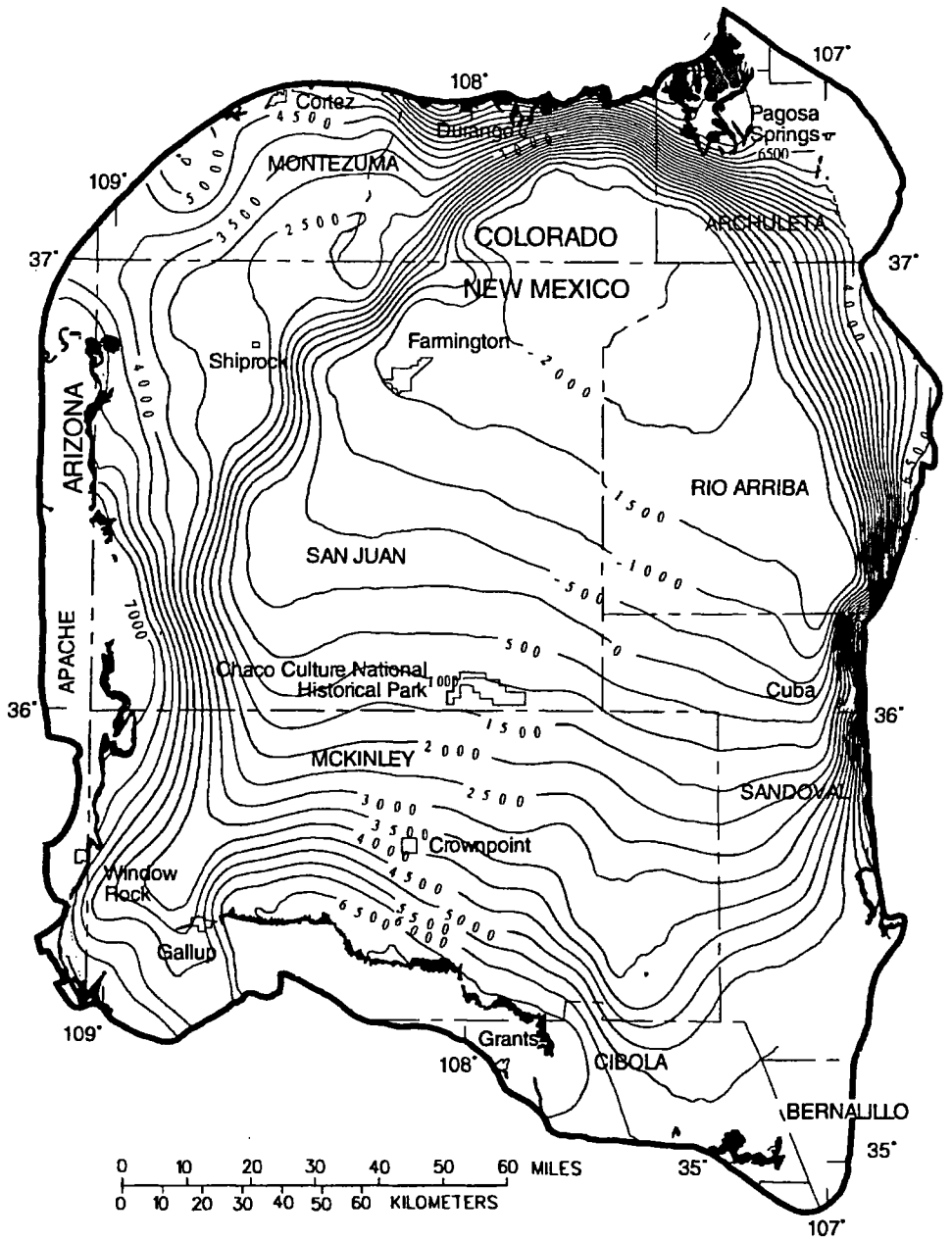

EXPLANATION

OUTCROP OF THE WANAKAH FORMATION AND EQUIVALENT UNITS

6500 — LINE OF EQUAL ALTITUDE OF THE TOP OF THE WANAKAH FORMATION--Number indicates altitude, in feet. Contour interval 500 feet. Datum is sea level

STUDY AREA BOUNDARY

Figure 28.--Approximate altitude and configuration of the top of the Wanakah Formation.

Entrada Sandstone

The Entrada Sandstone is the lowest hydrostratigraphic unit considered in this investigation. The Entrada Sandstone (Gilluly and Reeside, 1928), of Jurassic age (fig. 5), is present throughout the basin and crops out at the perimeter of the basin where it forms cliffs, often capped by the Todilto Limestone Member of the Wanakah Formation, or weathers to rounded hills. The Entrada was formerly misidentified as the Wingate Formation by early investigators (Dutton, 1885).

Geometry and Lithology

In the San Juan Basin the Entrada Sandstone is conformably overlain by the Wanakah Formation and unconformably overlies the Triassic Chinle Formation. The Entrada predominantly is a reddish-orange, massive-bedded, fine- to medium-grained eolian sandstone with some interbedded siltstone. Thickness of the Entrada Sandstone in the San Juan Basin is reported to range from about 60 to 350 feet (Green and Pierson, 1977), but in the southern part of the basin where the unit is used as a water supply it is commonly about 130 feet (Stone and others, 1983).

Hydraulic Properties

Stone and others (1983) reported transmissivity values of less than 50 feet squared per day that were based on the results of several specific-capacity tests. Fassett and others (1977) reported values of hydraulic conductivity ranging from 0.5 to 5 feet per day from drill-stem tests in oil wells.

Wells producing potable water from the Entrada Sandstone generally are completed near the outcrop along the southern basin margin. Reported well yields from six wells completed in the Entrada Sandstone range from 3 to 200 gallons per minute. The average well yield is 40 gallons per minute and the median is about 5 gallons per minute.

In other areas of the basin the Entrada Sandstone produces oil and (or) highly mineralized water. Water that is recovered with oil often is reinjected into the unit. The Entrada also is used for disposal of oil-field brines produced from other units.

NATURAL BOUNDARIES OF THE GROUND-WATER-FLOW SYSTEM

A ground-water-flow boundary is any physical feature or mechanism that alters the movement of water in the ground-water-flow system, or is a sink or source of water to the system. The San Juan Basin, as defined for this investigation, is a virtually self-contained ground-water-flow system whose boundaries generally are clearly defined. These boundaries may be internal or limiting geologic features, surface or subsurface sources or sinks, or contrasts in the properties of the pore-filling liquids.

Geologic Boundaries

Faults, dikes, changes in hydraulic properties, and geometry of the hydrostratigraphic units are examples of geologic boundaries. Boundaries may define the limits of the flow system but, more generally, are internal to the system and cause redirections of ground-water movement within the basin.

Faults (fig. 7) may act as a flow barrier by partly or completely offsetting aquifers and confining units. The Nacimiento Fault along the Nacimiento Uplift, which has a vertical displacement of several thousand feet, places Precambrian granite against the younger sedimentary rocks in the basin, thereby forming a part of the eastern boundary of the ground-water-flow system. Although faulting is common in the Puerco Fault Zone, located in the southeastern part of the study area, most of the faults lack sufficient displacement to completely offset hydrostratigraphic units over a significant distance.

Faulting also can cause nearby fractures in friable rocks, leading to a local increase in permeability and porosity. For example, a well completed in a fracture zone near a fault might have an atypically large yield, or a fracture zone may connect aquifers across a confining unit or with land surface to form springs. The Puerco Fault Zone has probable examples of all these phenomena. Therefore, the net effect of faulting on ground-water movement is sometimes difficult to predict.

Dikes also may have unpredictable effects on the movement of ground water. Numerous dikes are in the basin but most are relatively narrow (2 feet or less) and extend only short distances (a few hundred feet). Most of these dikes are associated with volcanic necks in the Rio Puerco Valley (fig. 11) and Mount Taylor area (fig. 29). These generally have vesicular chill boundaries with the host rock and are highly fractured. Selenite (gypsum) crystals occur at land surface in association with many of these, indicating that the dike is a point of ground-water discharge. In other cases, one or more springs may be associated with the dikes. At depth, these dikes may be a barrier to horizontal ground-water flow but, because of their limited extent, probably are not significant on a regional scale.

Other dikes in the northeastern part of the study area may have a much greater influence on regional ground-water flow. This set of associated dikes (other lesser dikes are present that resemble those in the Rio Puerco Valley) is several feet across and extends as much as 30 miles in a nearly straight north-south direction. These dikes are dense and form erosion-resistant spines supporting north-south ridges. They do not seem to be associated with surface manifestations of ground water, but one dike, near Dulce, produces a seep of oil.

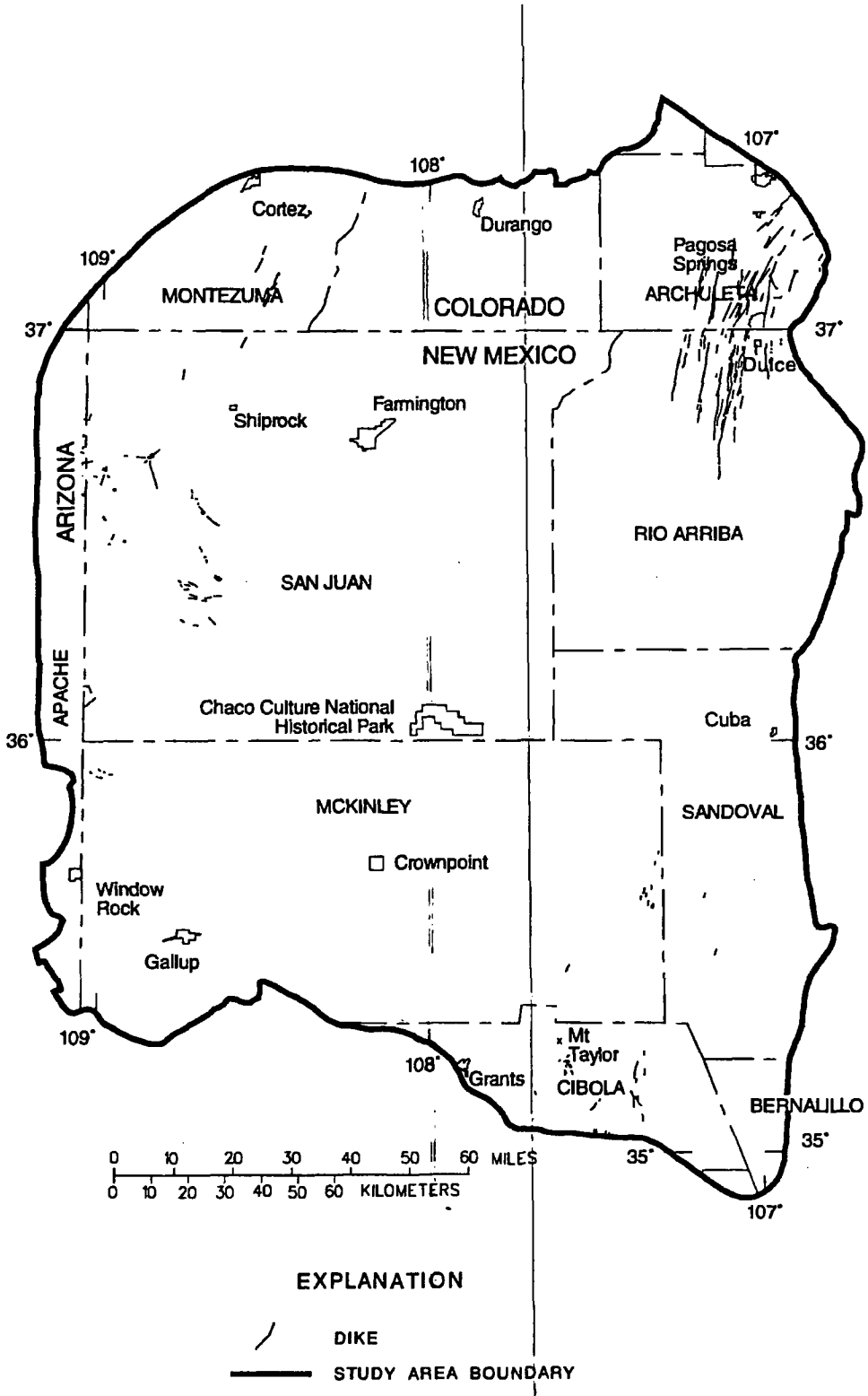

Figure 29.--Location of major dikes in the San Juan Basin.

An aquifer system's internal geometry and the hydraulic contrasts between aquifers and confining units also govern ground-water flow. Hydrogeologic sections, such as that shown in figure 6 (from Stone and others, 1983), illustrate the complex flow patterns that can result from thinning and pinch-outs of units and contrasts in hydraulic conductivity. The geometry of the major hydrostratigraphic units in the basin has previously been discussed.

Outcrop Area Boundaries

Various boundary types exist within the outcrop area of an aquifer. These include aquifer interaction with surface-water bodies and (or) associated alluvial deposits, recharge infiltrating from precipitation, and evapotranspiration. Surface-water interaction at the outcrop may be either a source of water to the aquifer or a discharge from it, depending on the relative difference in hydraulic head.

Surface-Water Boundaries

Surface-water bodies such as streams, lakes, and reservoirs directly influence an aquifer in its outcrop area. Streams and reservoirs may either gain water from or lose water to the aquifer. Generally in the higher altitude parts of the basin streams lose water to aquifers and in the lower altitude parts the streams and valley alluvium gain water. In either gaining or losing situations the quantities of water relative to surface flow usually are too small to detect locally.

Most tributaries to the San Juan River that originate at high altitude (more than 7,500 feet above sea level) have perennial flow. These streams and their tributaries lose water to aquifers in their higher reaches, especially in areas including and northeast of the Hogback Monocline. Other areas where stream-channel recharge might be expected are along the Nutria and Defiance Monoclines and along the northern flank of the Zuni Uplift (fig. 4).

Stream and river reaches that probably gain water from the ground-water system include the lower reaches of the San Juan River and its southern tributaries (Chaco River and Cañon Largo) and parts of the Puerco River, Rio Puerco, and Rio San Jose (fig. 11). Also, although ground water may discharge to the surface in these drainage systems they might not actually contribute to surface-water flow; in many instances the ground-water discharge is entirely consumed by evapotranspiration before it can migrate through valley-fill alluvium to reach the stream channel.

Recharge from Precipitation

Recharge from precipitation is a boundary type that contributes water to the aquifer system. This distributed recharge on the area of aquifer outcrop is the residual from total precipitation after losses to evapotranspiration and surface runoff. Direct ground-water recharge from precipitation was estimated using the approach documented in Hearne and Dewey (1988) and Waltemeyer and Kernodle (1992). The technique uses multiple regression analyses to establish relations between precipitation and selected basin characteristics to predict runoff. An initial assumption is that all net recharge is due exclusively to winter precipitation. Estimated sublimation and evaporation are then subtracted from the difference between total precipitation and total runoff to obtain an estimate of direct recharge on the aquifer outcrop.

Regression equations were developed for three altitude-precipitation regimes in the study area. The first regime includes basins where the area-weighted mean basin altitude is greater than 7,500 feet above sea level. Data from nine instrumented drainage basins in the San Juan Mountains (fig. 30) were used in the regression analysis to determine the rainfall-runoff relation for this regime. Mean winter precipitation and drainage area were found to describe mean winter runoff with a standard error of estimate of 13 percent. The second regime includes basins where area-weighted mean basin altitude is less than 7,500 feet above sea level and area-weighted mean winter precipitation is less than 12 inches. The third regime includes basins where area-weighted mean basin altitude is less than 7,500 feet above sea level and area-weighted mean winter precipitation is greater than 12 inches. Rainfall-runoff relations for the latter two regimes were developed using the basins that Hearne and Dewey (1988, p. 32, 37) used in their rainfall-runoff relations for the Taos Plateau (mean winter precipitation less than 12 inches) and the Sangre de Cristo Mountains (mean winter precipitation greater than 12 inches). Basin area and area-weighted mean winter precipitation were recalculated from the values used by Hearne and Dewey (1988). The study area then was divided into 320 drainage basins and mean winter discharge was computed for each using the equation appropriate for each basin's altitude and amount of precipitation. The areas in the San Juan Basin for which the following equations were developed are shown in figure 31.

For basins having an area-weighted mean basin altitude greater than 7,500 feet above sea level (derived for the San Juan Mountains region), the following equation was derived to define winter runoff:

$$QS = 0.10632 \times AREA^{(0.868)} \times PRECIP^{(0.977)} \quad (1)$$

where QS is mean winter runoff, in cubic feet per second;

AREA is drainage basin area, in square miles; and

PRECIP is area-weighted mean winter precipitation for the period 1931-60, in inches.

For basins having an area-weighted mean basin altitude less than 7,500 feet and an area-weighted mean winter precipitation less than 12 inches (derived for the Taos Plateau region), the regression equation was found to be:

$$QS = 0.00002188 \times AREA^{(1.05)} \times PRECIP^{(4.03)} . \quad (2)$$

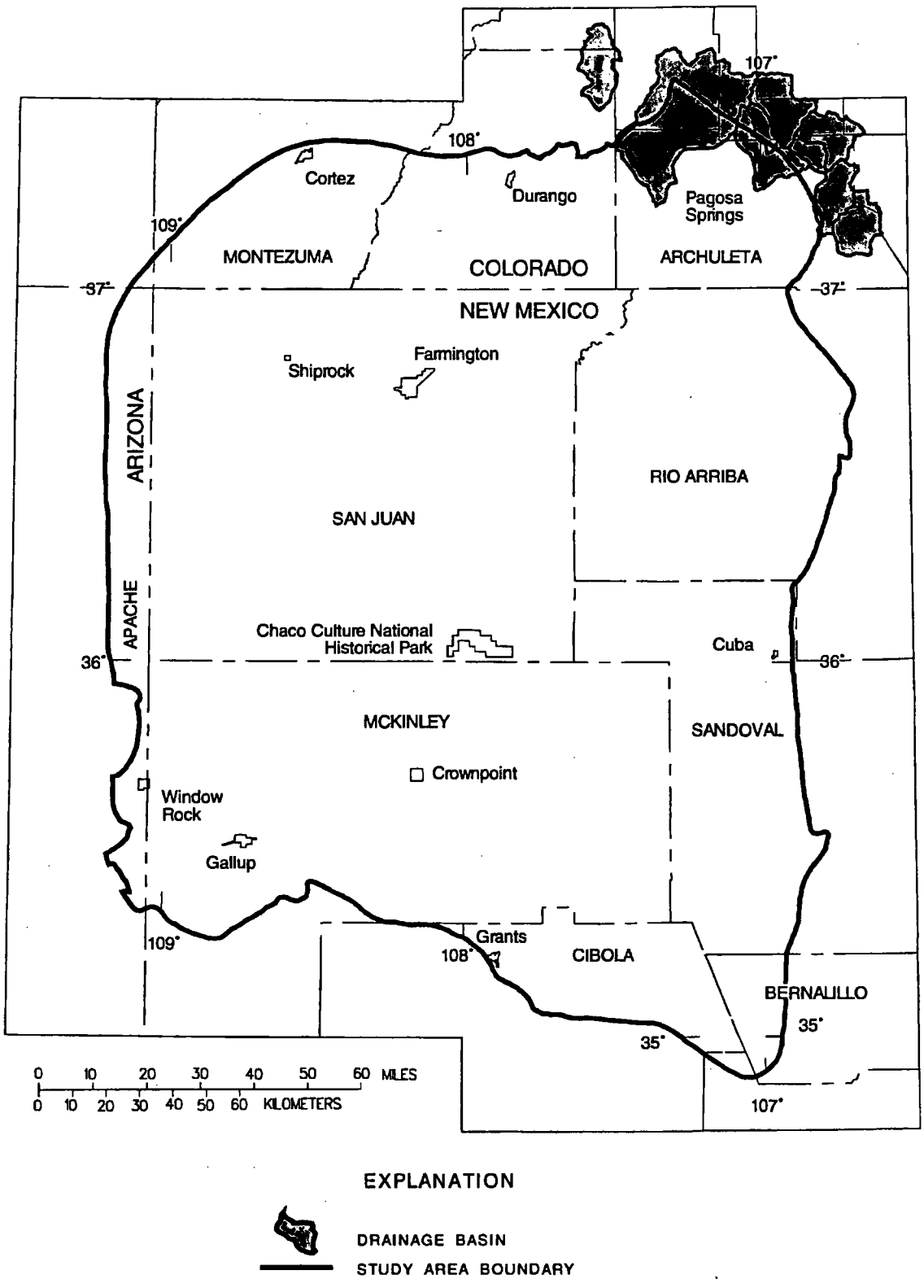

Figure 30.--Location of drainage basins used to determine the rainfall-altitude-runoff relation for the San Juan Mountains.

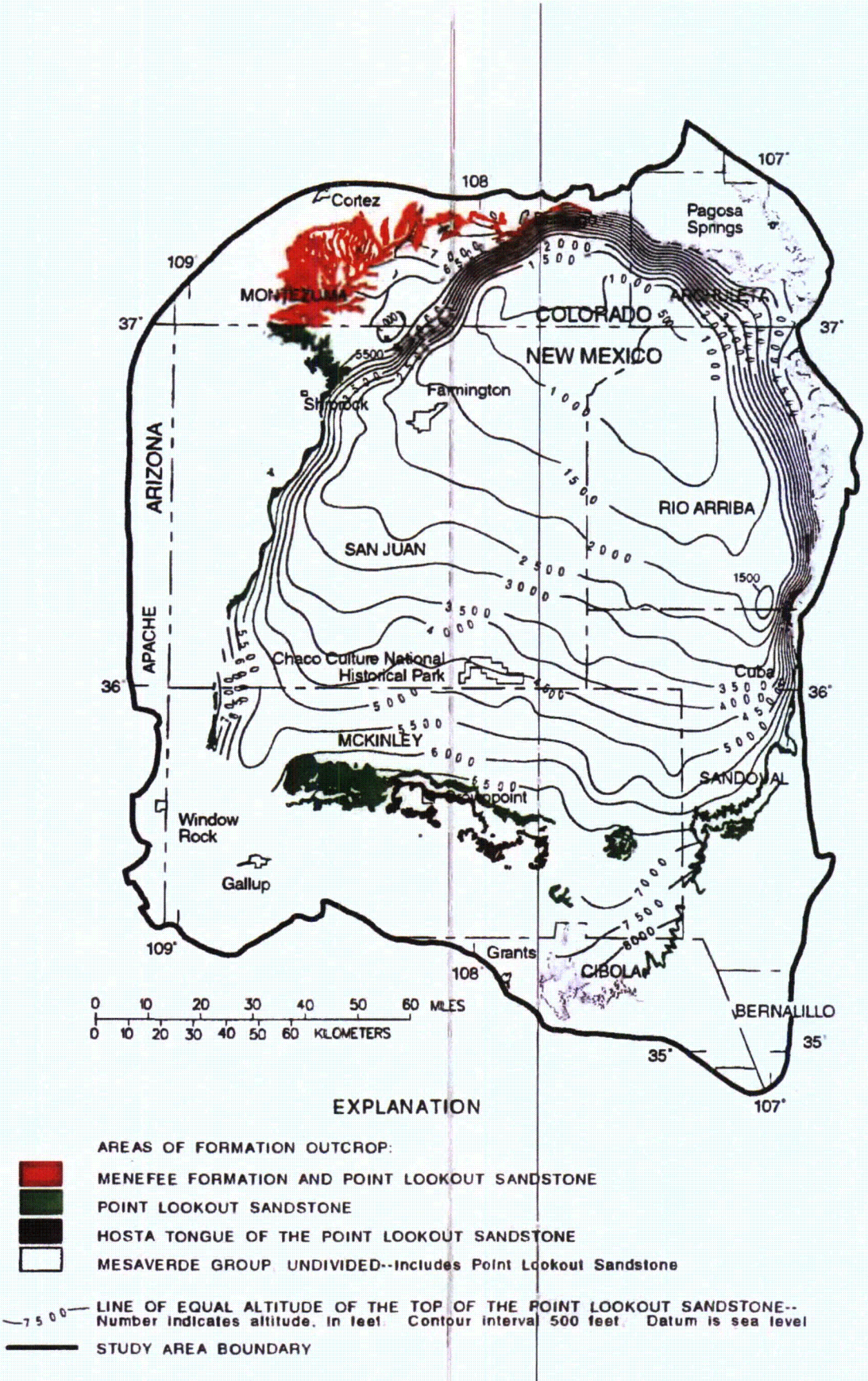

Figure 22.--Approximate altitude and configuration of the top of the Point Lookout Sandstone.

For basins having an area-weighted mean basin altitude less than 7,500 feet and an area-weighted mean winter precipitation more than 12 inches (derived for the Sangre de Cristo Mountains region), the regression equation was found to be:

$$QS = 0.00008318 \times AREA^{(0.972)} \times PRECIP^{(3.57)} . \quad (3)$$

Sublimation and evaporation were then estimated using the equation:

$$QET = 5200500 \times AREA \times ALT^{(-1.89)} \quad (4)$$

where QET is the estimated evaporation and sublimation, in cubic feet per second; and

ALT is the area-weighted mean basin altitude, in feet above sea level.

Finally, estimated direct recharge was computed as the residual of total precipitation minus runoff, sublimation, and evaporation.

Some ranges of estimated direct recharge for the drainage basins are shown in figure 32. The several large areas of virtually no recharge shown in figure 32 coincide with most of the high-altitude areas of the basin. These are areas where the sublimation, evaporation, and runoff components of the surface-water budget are large and the recharge, which is computed as the residual, has the greatest error potential. The estimated rate ranges from 0 to 0.15 inch per year and the area-weighted average for the basin is 0.10 inch per year. A calculated recharge rate of 0.1 inch per year for a drainage basin east of Grants, New Mexico, was reported by the U.S. Department of the Interior (1986, p. 2-53). The combined recharge rate for the entire basin is equivalent to a steady flow of about 150 cubic feet per second.

In the computations, the mechanism of the direct recharge is not restrained. The recharge could be uniformly distributed throughout the drainage basin, concentrated more on the recharge-receptive outcrop areas, or could be channel loss from streams as they cross outcrops. For simulation purposes, however, the recharge was assumed to be restricted to and distributed over the area of outcrop of the aquifers.

The current climate in the basin probably has little influence on the long-term rates of recharge to or discharge from the aquifers in the basin. Preliminary age estimates for water in the Morrison Formation near the center of the basin place the age of the water at about 1.5 million years (Kernodle and Phillip, 1988). Also in the Morrison on the western side of the basin, carbon-14 age dating indicates that water has moved only a short distance (generally less than 20 miles) from the outcrop during the approximately 40,000 years that are dateable by the technique. The water is old enough throughout most of the aquifers in the basin to have been affected by pluvial climatic periods during the Pleistocene Epoch.

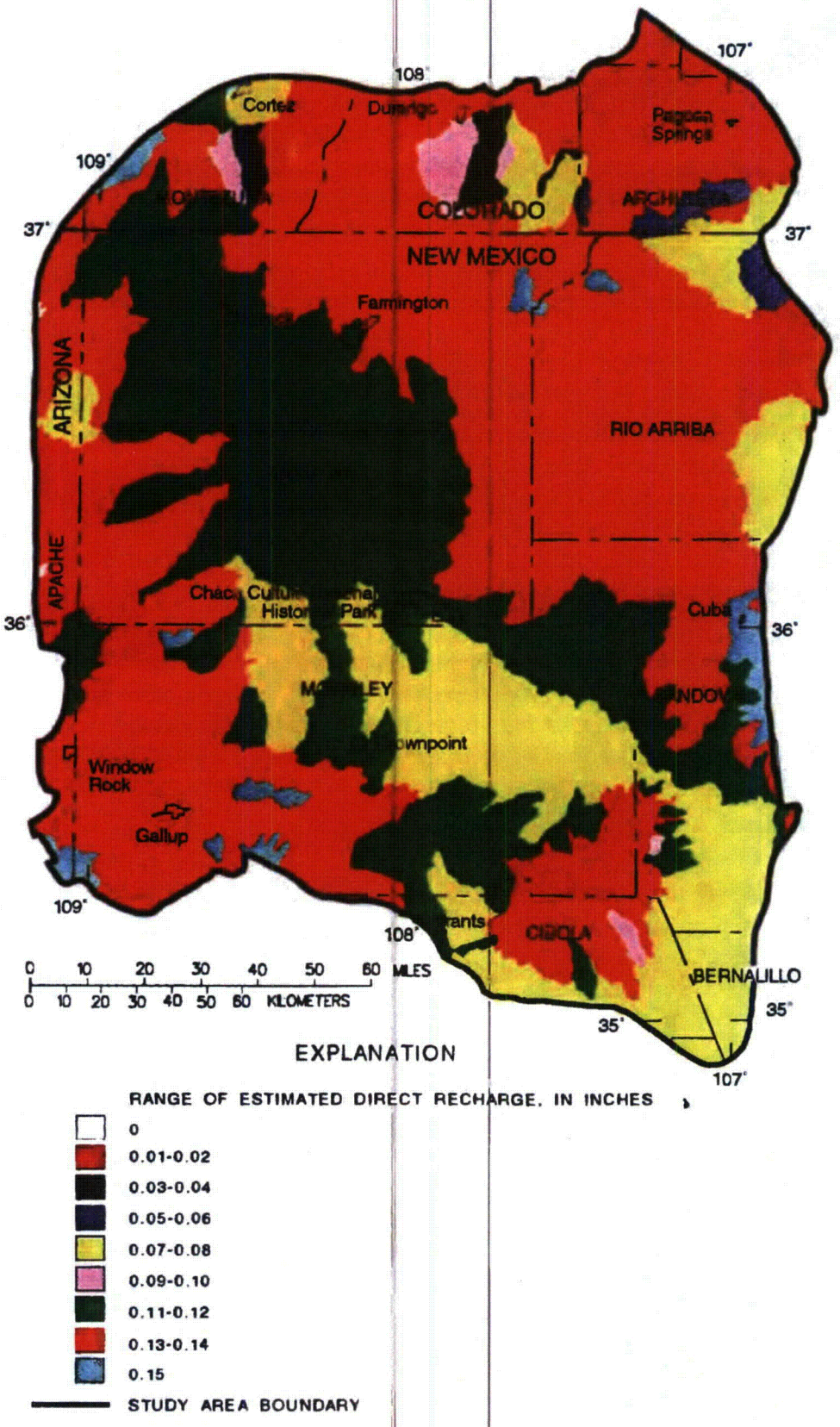

Figure 32.--Range of estimated direct recharge.

Studies have found direct evidence of recharge surges during the Pleistocene (Phillips and others, 1986) or have inferred the surges on the basis of geologic and geomorphic evidence (Watson and Wright, 1963). Phillips and others (1986), using carbon-14 age dating and oxygen-deuterium ratios, found evidence of cooler temperatures and greater effective precipitation for a period prior to 20,000 years before the present and again about 17,000 years before the present. Citing other studies of freshwater ostracoda, Phillips and others (1986) noted another pluvial period about 9,000 years before the present.

Watson and Wright (1963) described landslide development on the east flank of the Chuska Mountains in New Mexico. They attributed the three block glide events that they found to periods of high ground-water levels in the Chuska Sandstone. The higher water levels were postulated to correlate with pluvial periods during the Pleistocene. Periods of high water levels in the Chuska Sandstone are significant because the driving head to the underlying aquifers is thereby increased.

Although much of the water in the aquifers in the basin has been shown to be old and added to the ground-water system during wet climatic cycles, pressure changes in an artesian aquifer propagate much faster than the actual movement of a volume of water. Pressure changes can be shown to adjust quickly to changes in discharge (Dam and others, 1990a), and it is likely that the predevelopment (early 20th century) potentiometric heads reflected current or recent historical climatic conditions, whereas the actual flow paths of water in the aquifers reflect paleorecharge conditions.

Although much of the water now in the ground-water system entered in recharge surges, it is important to note that the system is being recharged under current conditions. Peeters (1983) used carbon-14 and tritium methods to date water in the Ojo Alamo Sandstone. She found that waters of a modern carbon-14 age also had post-atomic age elevated tritium, indicating active modern recharge.

Evapotranspiration

Evapotranspiration acts as a boundary in the ground-water system where water in the zone of saturation is affected by surface processes. This generally happens in areas of ground-water discharge, primarily in the valleys of the gaining streams described previously. Evapotranspiration of ground water is assumed to be zero in areas of great depth to water. As the depth to ground water below land surface decreases, the rate of evapotranspiration of ground water increases (Emery, 1970) until the rate reaches at least the potential annual evaporation (fig. 10). Because this process generally is limited to alluvial-fill stream valleys, however, the contribution of ground water, compared to surface water from the stream, usually cannot be quantitatively determined.

Evapotranspiration is a major component of the overall water budget of the basin. Winter evaporation and sublimation were calculated (eq. 4) to account for 3.4 of the total 6.0 inches of winter precipitation. Basinwide, summer evaporation and transpiration consume virtually all of the remaining 6.3 inches of annual precipitation. Most of this consumptive loss in the basin, in both winter and summer, is by evaporation or sublimation following precipitation and, therefore, is not an element in the ground-water system.

Subcrop Boundaries

A subcrop boundary is a special case of both an internal geometric boundary and an outcrop-area boundary. Areas where this specific boundary type occurs in the San Juan Basin are upturned and eroded aquifers in the Defiance Monocline (fig. 4) that subcrop beneath the Chuska Sandstone and Deza Formation (of Wright, 1954). This boundary type will be illustrated later in the section on internal geometric boundaries. As discussed earlier, the elevated hydraulic head in these overlying units drives water into the underlying regional aquifers.

Oil-Water and Gas-Water Interfaces

Oil and gas are valuable natural resources in the basin, and both are found in abundance in the aquifers described in this report. Several post-Triassic units in the basin produce oil and gas: the Twowells and Paguate Tongues of the Dakota Sandstone, units in the Mesaverde Group, the Pictured Cliffs Sandstone, and coals in the Fruitland Formation.

"Oil and water don't mix" is not totally true in a ground-water system, but the presence of oil or gas in a part of the system does indicate a very stagnant area of ground-water flow. There are two mechanisms of oil entrapment, stratigraphic or structural traps, and an additional mechanism of gas entrapment. The producing oil, gas, and water wells completed in the Gallup Sandstone and transgressive Tocito Sandstone Lentil (fig. 5) are mapped in figure 33, which shows surface expressions of both types of trap. Northeast of the pinch-out of the main body of the Gallup Sandstone (which produces potable water virtually everywhere), the isolated Tocito Sandstone Lentil encapsulated in the Mancos Shale forms stratigraphic traps for oil. The shape of the lenses is clearly outlined by the distribution of producing oil wells. Two clusters of wells producing oil from structural traps are shown (fig. 33) in the southeastern part of the basin. These traps are structural domes where the oil, being lighter than water, rose to displace water and fill the dome.

In both types of traps the presence of oil precludes the flow of freshwater. However, the stratigraphic traps usually are encapsulated in confining units that are very restrictive to any form of fluid flow and the structural traps usually are small in area. A stratigraphic trap is areally restricted to one unit or horizon, whereas a structural trap presents conditions that are favorable for oil or gas production from any suitable unit in the stratigraphic section.

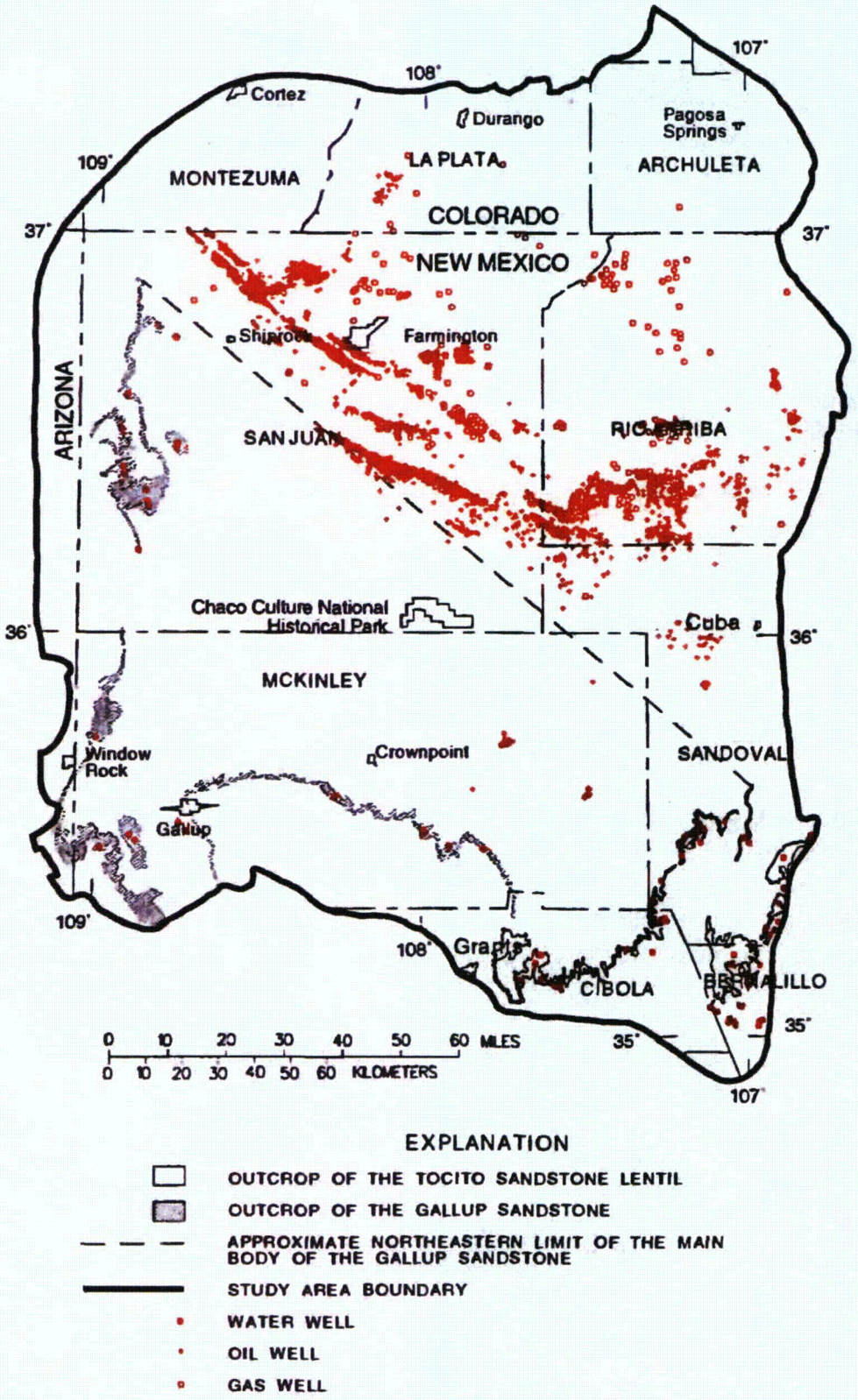

Figure 33.--Location of oil, gas, and water wells completed in the Gallup Sandstone and Tocito Sandstone Lentil.

Gas may be dissolved in water (the third mechanism). In addition, gas will adsorb and absorb on coal, particularly along cleats and microfractures (Fassett, 1989). Gas occurrence of this nature is characteristic of coal beds in the Fruitland Formation, described earlier. In this instance, the presence of gas does not necessarily preclude the movement of water, but other evidence, primarily water-quality data (Dam and others, 1990b; Kernodle and others, 1990), suggests that water in the Fruitland Formation and underlying Pictured Cliffs Sandstone is dissimilar to water in overlying and underlying units (Thorn and others, 1990a, b) and may be at least partially hydraulically isolated from them.

Density Contrasts

Fluid density contrasts, if great enough, can be a barrier to ground-water flow. Density is a function of the quantity of dissolved chemicals in the water and, to a much lesser degree, of the temperature of the water. The highest reported density of water from post-Triassic aquifers in the basin is 1.20 grams per cubic centimeter at 20 degrees Celsius (Dwight's ENERGYDATA, Inc., BRIN data base, Oklahoma City, Oklahoma). This water is from a well completed in the Morrison Formation near the confluence of the La Plata River with the San Juan River (fig. 11), northwest of Farmington, New Mexico. The reported dissolved-solids content of the water was 286,900 milligrams per liter, more than eight times that of sea water (Chow, 1964). All other nearby wells completed in the Morrison Formation, the nearest of which is about 3 miles away, have a reported density of 1.06 grams per cubic centimeter or less, indicating that the anomaly is very localized within the Morrison Formation.

The next highest reported density of water from post-Triassic aquifers is 1.069 grams per cubic centimeter at 20 degrees Celsius (91,500 milligrams per liter dissolved solids) for water from the Dakota Sandstone, within 9 miles of the Morrison well cited above. The density of water in the Dakota Sandstone also rapidly decreases away from this well; each aquifer seems to have its own relatively stagnant zone in the Farmington area.

If the local density gradient is high enough, water of this density will affect the movement of water within the ground-water-flow system (Davies, 1989). It is doubtful that geochemical differences in host-rock and water interactions over the short distance observed here created the sharp density gradients that exist today in the same general area for several different aquifers. Therefore, it is reasonable to assume that conditions of long-term flow stagnation led to the observed density anomalies.

DESCRIPTION OF THE MODEL

The ground-water-flow model completed for this investigation simulated steady-state or predevelopment conditions. Transient simulations were not attempted because of the virtual absence of historical ground-water discharge data. Most urban public-supply systems and mining operations that use or used ground-water supplies were able to provide good withdrawal records. However, the vast majority of ground-water discharges in the basin are from free-flowing, unmetered wells that are often completed in several aquifers. No records exist for changes in discharge from these wells over time. Frenzel (1982) encountered the same lack of ground-water withdrawal data and also limited his model of the basin to a steady-state simulation. Investigators constructing ground-water-flow models of other basins in New Mexico have encountered similar problems and chose to adjust simulated withdrawals until a transient calibration of

potentiometric-head changes was obtained. Examples of these models are documented by O'Brien and Stone (1983), Hearne (1985), and Hearne and Dewey (1988). A summary of the various approaches to modeling, including a choice of parameters to alter during calibration, was compiled for basins in the Rio Grande Rift by Kernodle (1992).

The model of Kernodle and Philip (1988) was a precursor to this effort. That model was used to determine flow paths and times of travel for steady-state flow conditions in the Morrison Formation and Dakota and Gallup Sandstones. This information was then used by Dam (1995) to select appropriate analytical methodologies for isotope age dating of formation water. Travel times determined from the model agree very well with the isotopic age determinations of Dam, and computed potentiometric heads agree well with the results of Frenzel (1982) and of this model.

Flow Equation, Assumed Conditions, and Computer Programs

The computer code used to complete the ground-water-flow model of the San Juan Basin is the modular, three-dimensional, finite-difference code documented by McDonald and Harbaugh (1988). The equation that describes three-dimensional flow (Trescott, 1975; McDonald and Harbaugh, 1988) may be written as:

$$\frac{\partial}{\partial x}\left(K_{xx}\frac{\partial h}{\partial x}\right)+\frac{\partial}{\partial y}\left(K_{yy}\frac{\partial h}{\partial y}\right)+\frac{\partial}{\partial z}\left(K_{zz}\frac{\partial h}{\partial z}\right)-W = S_s\frac{\partial h}{\partial t} \qquad (5)$$

where K_{xx}, K_{yy}, and K_{zz} are values of hydraulic conductivity along the x, y, and z coordinate axes (L/t);

h is the potentiometric head (L);

W is a volumetric flux per unit volume and represents sources and (or) sinks of water (1/t);

S_s is the specific storage of the porous material (1/L); and

t is time (t).

Because the simulation is of steady-state conditions, potentiometric head and storage do not change with time and the right side of equation 5 is equal to zero.

Analytical solutions of equation 5 are possible for only the simplest of hydraulic problems. One approach to obtaining solutions for the typical flow problem is the finite-difference numerical method whereby the area of the aquifer being analyzed is divided into a regular network of horizontal and vertical orthorhombic cells. A set of flow equations is written to describe flow into and out of each cell, then the equations are solved simultaneously by one of several algorithms. The numerical algorithm used in this investigation is the Strongly Implicit Procedure (SIP) documented in McDonald and Harbaugh (1988, chap. 12). The finite-difference numerical method is based on a number of assumed conditions for the flow system: (1) all hydraulic properties of the simulated hydrostratigraphic unit are uniform (homogeneous) within each cell; (2) any anisotropy of hydraulic conductivity is aligned with the principal axes of the finite-difference grid; and (3) the properties of the fluid are uniform in space and constant with time.

A planimetric view of the finite-difference model grid that was used to discretize components of the properties of the simulated aquifers is shown in figure 34. The grid has 100 rows of cells, each 3,000 meters in spacing, and 100 columns of cells, each 3,070 meters in spacing. The entire grid is rotated 46 degrees counterclockwise to conform to a general overall shoreline axis of orientation that prevailed during the transgressions and regressions of the Cretaceous seas.

The planimetric view in figure 34 shows the grid in a Universal Transverse Mercator (zone 12) map projection. The initial orthorhombic grid was projected to this map coordinate system to match the map coordinate rotation and distortion of the spatial data used in the construction of the model. Although the amount of distortion would be relatively minor over a small area it becomes significant (hundreds of feet) for grids that span areas as large as the San Juan Basin. Figure 35 is an oblique areal view of the study area and finite-difference grid as they would appear from a vantage point about 30 miles above the Earth's surface. The figure illustrates the need to form the grid to match the map projection that is used to portray the Earth's surface.

The finite-difference grid is stacked 12 layers deep to represent the major aquifers and confining units in the basin. Figure 36 is a diagram that correlates the previously described hydrostratigraphic units with the finite-difference layers employed in the model. Not all units were explicitly simulated; an entry of "VK" in the diagram indicates that the unit was implicitly simulated using a computed vertical harmonic leakance between finite-difference layers.

A geographic information system (GIS) was used to store, manipulate, analyze, and extract the spatial hydrogeologic data that were used to construct the ground-water-flow model of the San Juan Basin. (The GIS also was used to prepare the map figures in this report.) An introductory explanation of the techniques and procedures of using the GIS in support of the ground-water-flow model may be found in Kernodle and Philip (1988). For readers who would like additional information on the functionality of a GIS, Robinove (1986) authored a concise presentation on the "Principles of logic and the use of digital geographic information systems."

Representation of Boundaries

Distributed recharge from precipitation, stream-aquifer interaction, changes in hydraulic properties, aquifer geometry, and subcrop boundaries were simulated in the steady-state ground-water-flow model of the San Juan Basin. Evapotranspiration, minor faults, dikes, oil-water/gas-water interfaces, and density contrasts were not simulated. Evapotranspiration in areas of aquifer outcrop was incorporated into the computed net rate of recharge and therefore was simulated indirectly. Evapotranspiration in areas of ground-water discharge, coincident with alluvial valleys of major streams, was assumed to be represented by the stream boundary. Minor faults and dikes were not considered to be a significant influence on ground-water flow. Oil and gas were not thought to greatly influence ground-water flow because their occurrence largely is limited to disconnected stratigraphic traps encapsulated in major confining units. Finally, density contrasts were not simulated because the areal extent of high-density water is small, its occurrence coincides with areas of hydraulic stagnation, and the computational resources needed to simulate this boundary condition for only a minor part of the aquifer system could not be justified for this investigation.

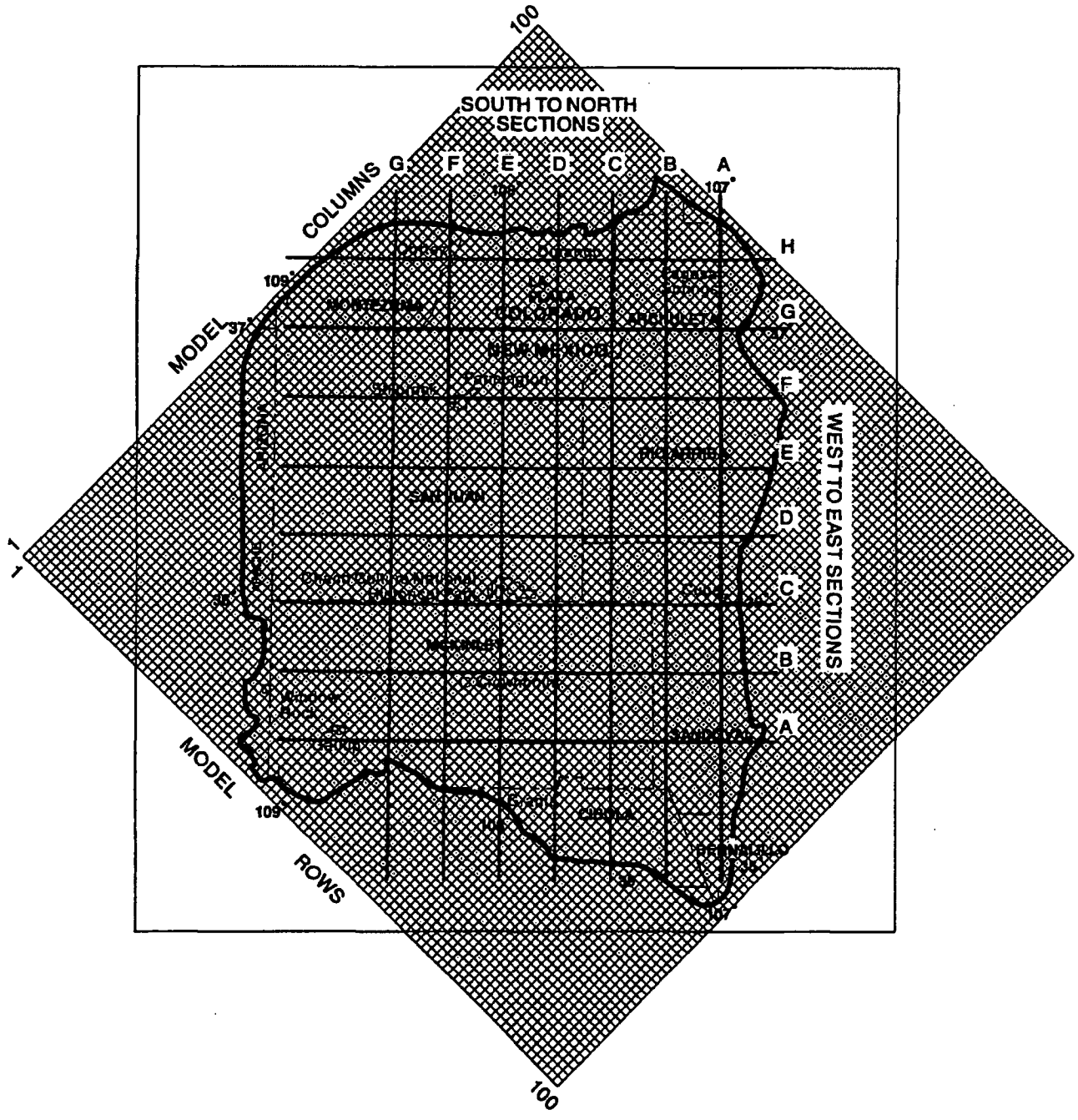

Figure 34.--Finite-difference model grid and locations of hydrogeologic sections shown in figures 37 and 38.

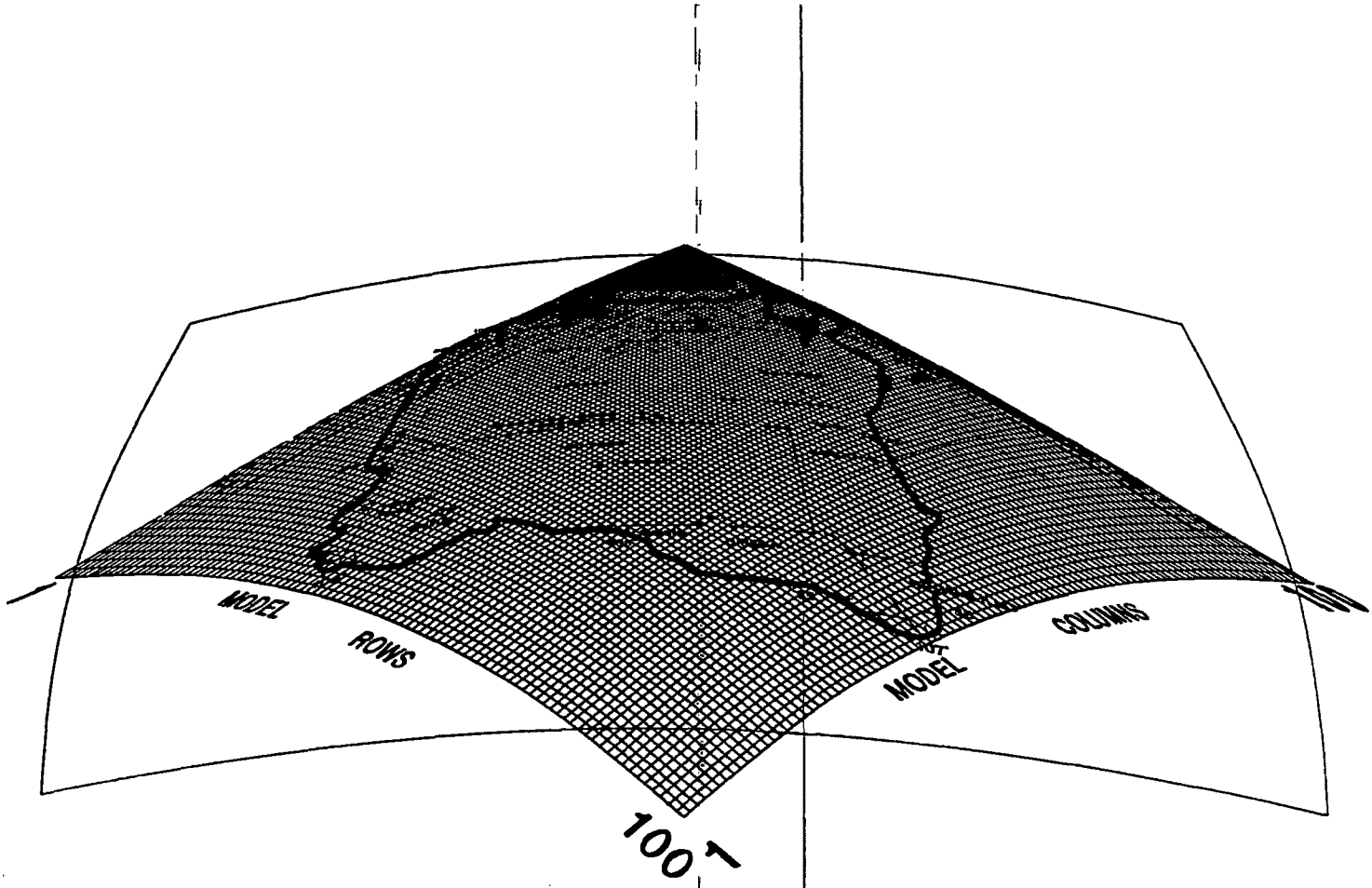

Figure 35.--Perspective view of the finite-difference model grid.

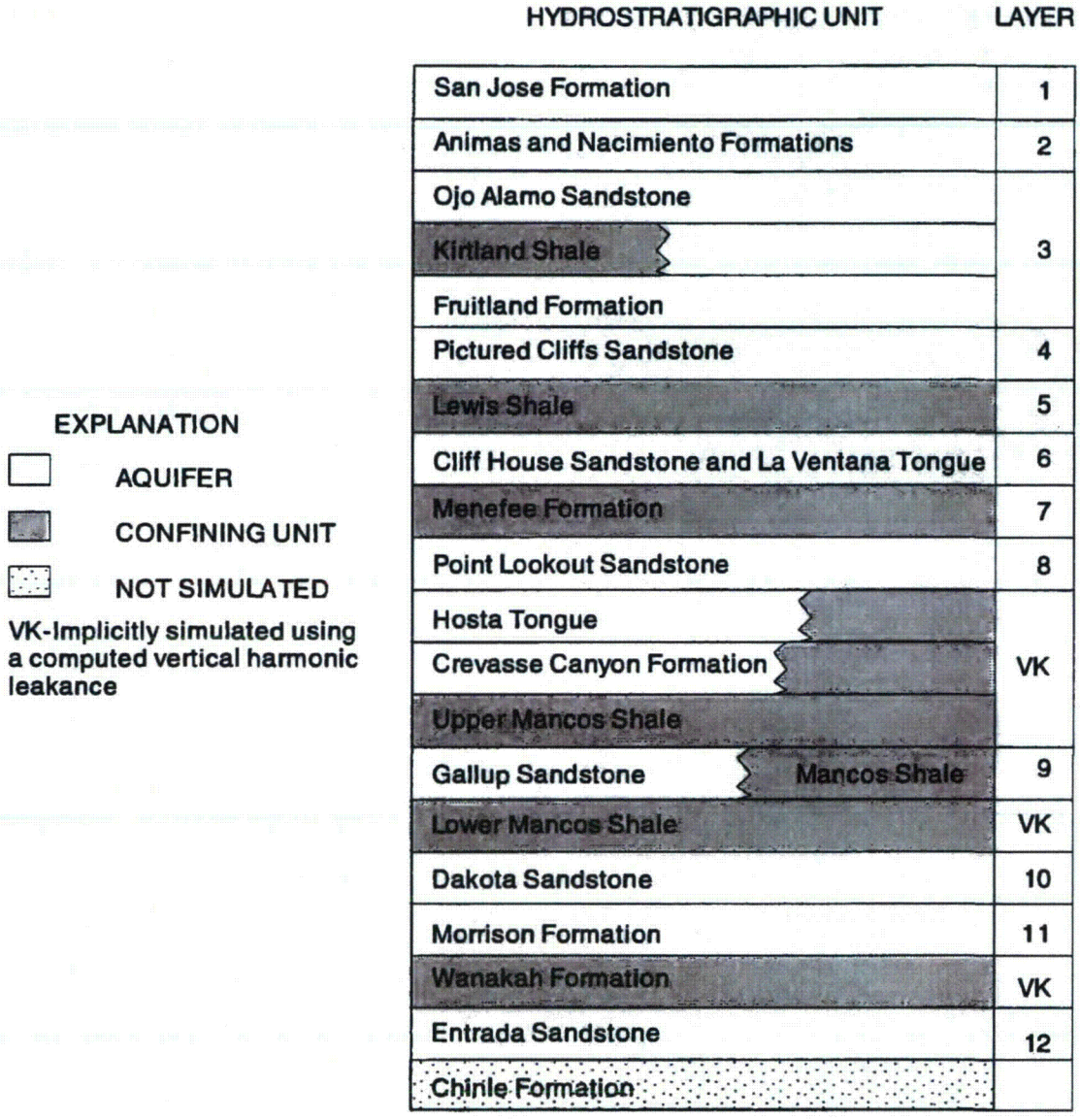

Figure 36.--Correlation of geologic units and model layers.

Distributed Recharge from Precipitation

Distributed recharge from precipitation was simulated as a flux of water introduced to the model cells containing an outcrop of the unit represented by the cell's layer. By using GIS, the model grid was overlaid on a digital map of the aquifer outcrop so that the area of outcrop of each aquifer within each cell could be determined. That information layer was then overlaid on a digital map depicting the rate of recharge so that the rates for each area of outcrop within each model cell could be determined. The net flux to the aquifer for each model cell was then computed as the sum of outcrop areas multiplied by the recharge rate for that area. The entire process was repeated for the outcrop of each of the 12 units represented in the model.

Stream-Aquifer Interaction

The interaction between surface-water bodies and the ground-water system was simulated as a head-dependent flux boundary with limitations placed on the maximum possible surface-water loss (McDonald and Harbaugh, 1988, chap. 6). The flow rate to or from the aquifer is a function of the hydraulic-head difference between the aquifer and the surface-water body, the area (or length times width) of the surface-water body, and the hydraulic conductivity and thickness of the streambed material:

$$QRIV = (HRIV - h)\, K\, L\, W / M \qquad (6)$$

where QRIV is the flux to or from the surface-water body (L^3/t);

HRIV is the representative altitude of the stream surface (L);

h is the model-computed ground-water head (L);

K is the hydraulic conductivity of the streambed material (L/t);

L is the total stream length in a model cell (L);

W is the representative width of streams within a model cell (L); and

M is the thickness of streambed material (L).

The part of the equation that remains constant for each model cell (K L W / M) is referred to as the streambed conductance. Streambed conductance was computed for each cell that contained both aquifer outcrop and a stream segment. The stream network used in the model simulation is the one shown in figure 11. The main stems of the San Juan River, Chaco River, Rio Puerco, and Rio San Jose were assigned a width of 200 feet. All other segments were assigned a width of 100 feet. Some of the larger surface-water features (lakes, reservoirs, and the San Juan River downstream from Navajo Reservoir) were represented as polygon features, eliminating the need to estimate channel width. The bed thickness for all streams was arbitrarily assumed to be 1 foot and the hydraulic conductivity of the bed material was assumed to be 20 feet per day.

In a process similar to the one described for recharge, a series of overlays was performed to arrive at a total stream area for the outcrop of each hydrostratigraphic unit within each model cell. This area was then multiplied by the hydraulic conductivity to determine the streambed conductance for each cell.

The stream-surface altitude (HRIV) was obtained by using the GIS to extract altitude data from a continuous-surface representation of topography for vertices along the lines that define the streams. The altitude data were obtained from 1:250,000-scale digital elevation models that have a vertical accuracy of 30 meters (U.S. Geological Survey, 1987). The altitudes of the vertices were then averaged for the outcrop of each hydrostratigraphic unit within a model cell to obtain a mean channel altitude. The term (HRIV - h) in equation 6 was then limited to a maximum value of 10 feet to place an upper limit on the loss of water from the stream to the aquifer. No limit was placed on ground-water discharge rates to the streams.

Internal Geometric Boundaries

As stated earlier, the structure-contour maps (figs. 13, 15, 17-25, 28) are derived from computer-generated and human-edited continuous-surface representations of the tops of the major hydrostratigraphic units. The maps were then assimilated into the GIS, published as structure-contour maps in the Hydrologic Investigations Atlas 720 series, and became the data base used in this model to define top and bottom altitudes and aquifer (or confining unit) thicknesses.

Other derivative products from the data bases used to produce the hydrologic atlases are possible, including the layer-definition hydrogeologic sections shown in figures 37 and 38. These sections were constructed directly from the digital data layers of the altitudes of land surface and the tops of the hydrostratigraphic units. The sections have been corrected to include the earth's curvature and are vertically exaggerated by a factor of 20. Although these sections represent model layers, they also quantitatively reveal the complex geologic structure of the San Juan Basin from many new vantages not easily obtained without the use of GIS technology.

As stated earlier, these digital data layers were used to define the internal geometry of the 12 hydrostratigraphic units simulated by the model. To do this, an interpolated spot value for the structure altitude of each unit was obtained for the centroid of each model cell.

Subcrop Boundaries

Several regional aquifers are truncated and overlain by the Chuska Sandstone, Deza Formation, and landslide deposits in the vicinity of the Defiance Monocline. The model representation of these hydrostratigraphic units overlain by the Chuska Sandstone is shown in figure 37C, D, and E. The regional aquifers are under hydraulic stress from these overlying units. The rate of downward movement of ground water into the Cretaceous units is governed by the differential hydraulic head, the vertical hydraulic conductivity of the units through which the water must pass, and the thickness of those units. A general-head boundary (McDonald and Harbaugh, 1988, chap. 11) is appropriate for simulation of this hydraulic condition. The equation describing flow to or from this numerical boundary type is identical to the equation for a stream-aquifer boundary (eq. 6) previously described. The difference between the two numerical boundary types is that there is no limit to the amount of water that an aquifer can gain from a general-head boundary.

The location of the general-head boundary used to simulate the downward movement of water from the Chuska Sandstone, Deza Formation, and landslide deposits into the regional aquifers is shown in figure 39. The position and width of the boundary (about one-quarter mile) are intended to be about the same as those of the subcropping aquifers. The boundary simulated a source of water to the Point Lookout, Gallup, and Dakota Sandstones, Morrison Formation, and Entrada Sandstone.

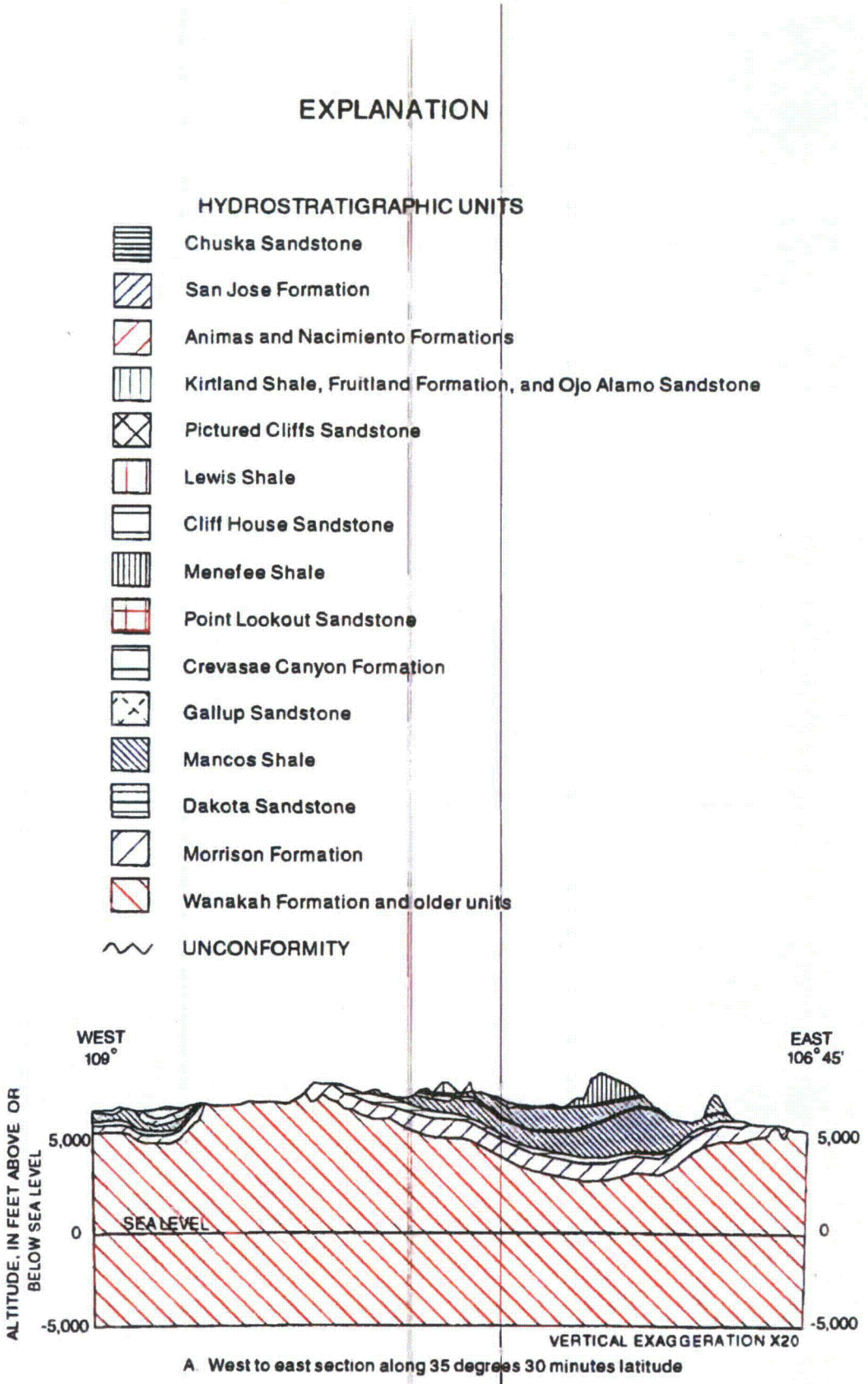

Figure 37.--West to east sections showing the vertical layers used in the model.

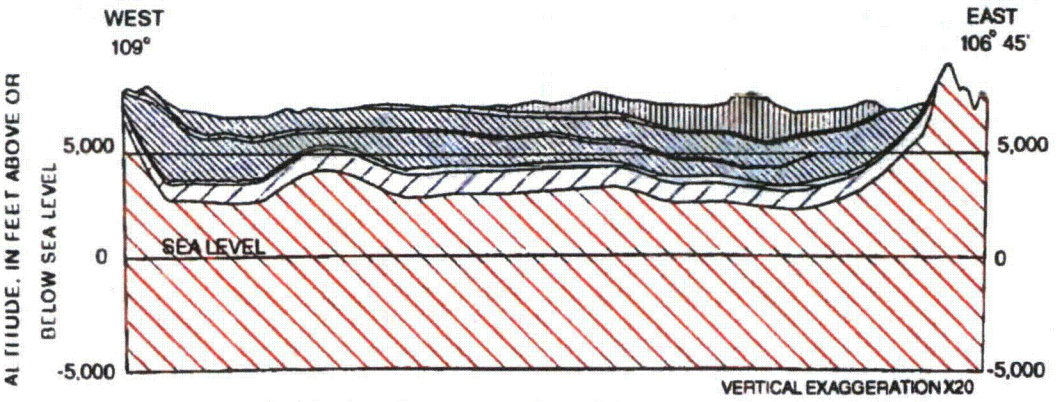

B. West to east section along 35 degrees 45 minutes latitude.

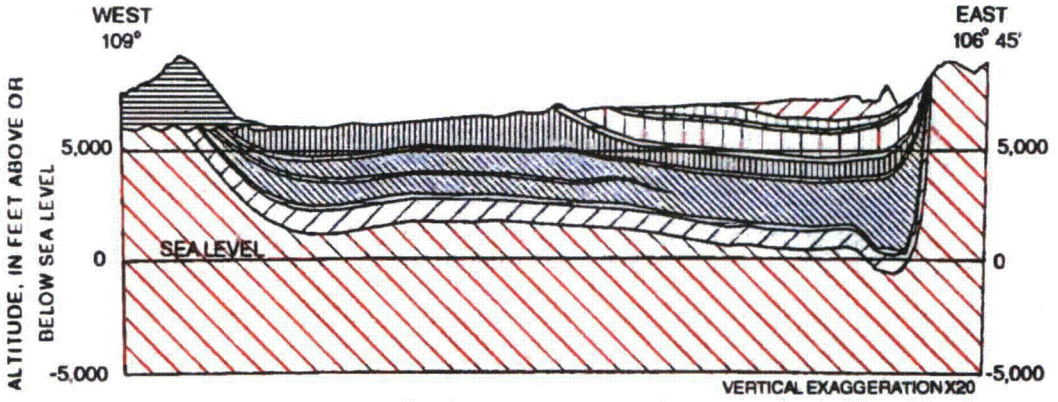

C. West to east section along 36 degrees latitude.

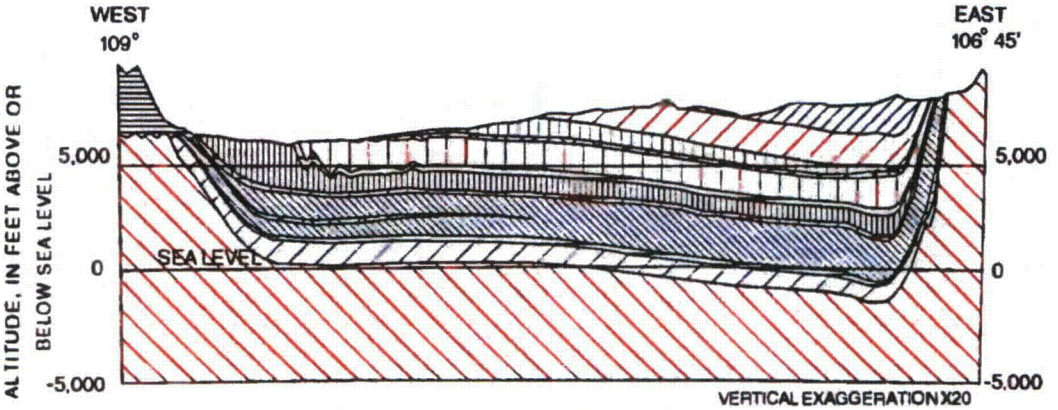

D. West to east section along 36 degrees 15 minutes latitude.

Figure 37.--West to east sections showing the vertical layers used in the model--Continued.

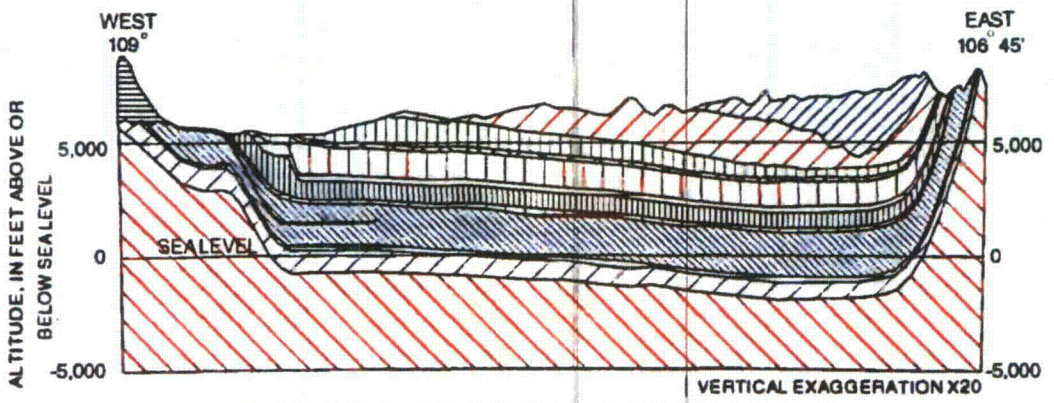

E. West to east section along 36 degrees 15 minutes latitude.

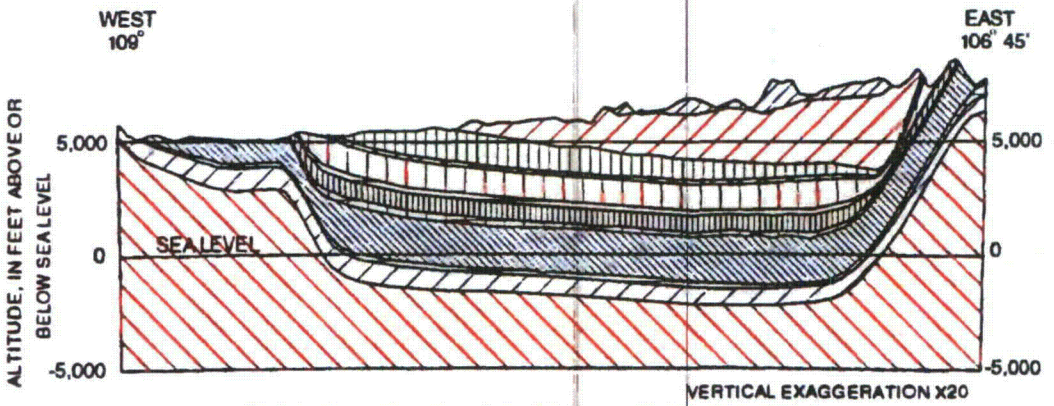

F. West to east section along 36 degrees 30 minutes latitude.

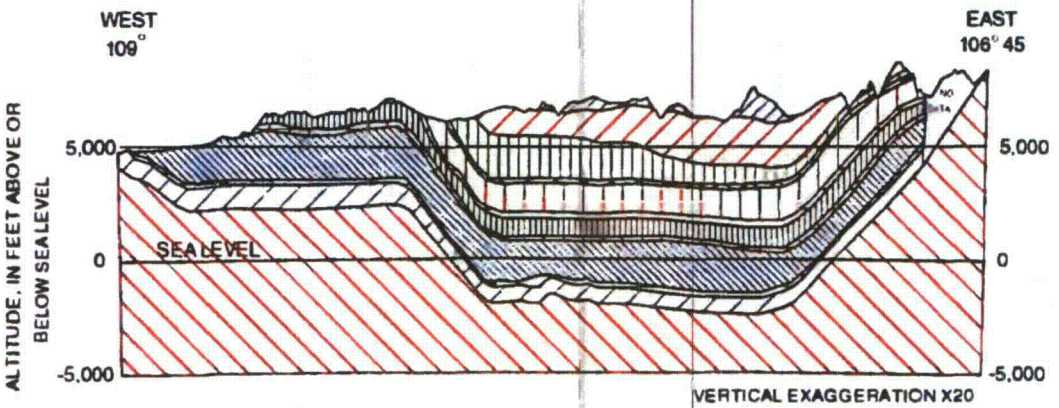

G. West to east section along 36 degrees 45 minutes latitude.

Figure 37.--West to east sections showing the vertical layers used in the model--Continued.

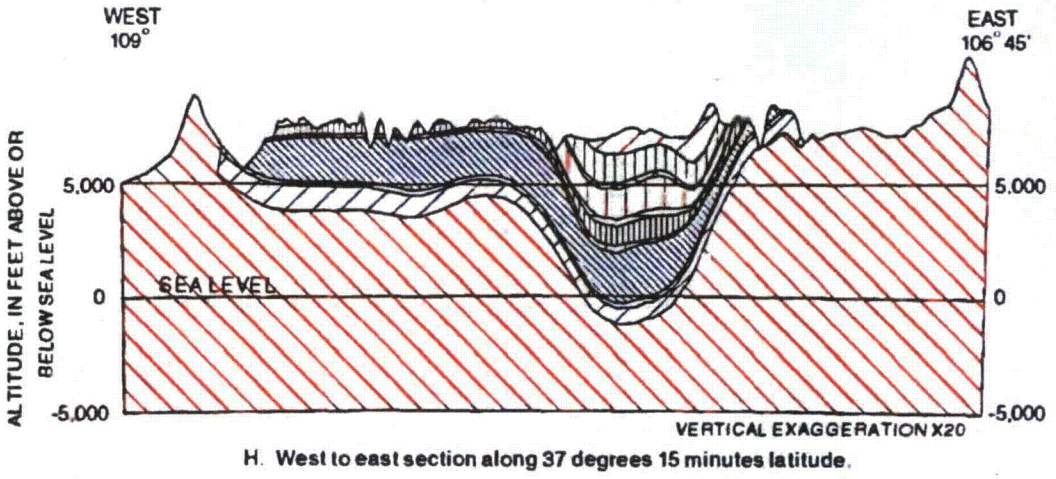

H. West to east section along 37 degrees 15 minutes latitude.

Figure 37.--West to east sections showing the vertical layers used in the model--Concluded.

The eroded surface on which the Chuska Sandstone and Deza Formation rest slopes from about 8,000 feet on the southwest flank to about 7,000 feet on the northeast flank of the Chuska Mountains. The water table in the Chuska Sandstone was assumed to be midway between land surface and this sloping plane. The travel distance (equivalent to M in eq. 6) used to compute the hydraulic conductance was the water-table altitude minus the altitude of the sloping plane. The vertical hydraulic conductivity was simulated as 0.005 foot per day.

Simulated Hydraulic Properties

In addition to the hydraulic properties required to define boundary conditions and aquifer geometry, aquifer anisotropy and horizontal and vertical hydraulic conductivity are required to numerically describe steady-state ground-water flow. The hydrostratigraphic units that were simulated by the ground-water-flow model usually correlated with a single, well-defined geologic unit (fig. 36; fig. 5), making assignment of hydraulic properties relatively simple. For most units a single, areally uniform value for horizontal and another for vertical hydraulic conductivity produced satisfactory simulation results. These values are shown in figure 40. The transmissivity distribution of each unit was obtained by multiplying the unit's horizontal hydraulic conductivity by the thickness of the unit at each model cell. Thicknesses were computed by using the GIS to manipulate the information given earlier regarding thickness and structural altitude of the tops of the hydrostratigraphic units.

The aquifer system was assumed to be anisotropic with the preferred direction of flow being northwest to southeast. The initial assumption was that all units are anisotropic. Final simulations portrayed only the transgressive, regressive units (post-Dakota Sandstone) as anisotropic. The basis for this, discussed earlier, was that the depositional environment of a series of shoreline transgressions and regressions would deposit sands that have a higher permeability in a direction parallel to the shoreline. However, the anisotropy probably is megascopic in origin and scale rather than due to grain orientation. That is, a series of intermeshed bars of sand combine to form a continuous aquifer. The longest unobstructed flow path within each bar is parallel to the shoreline; hence, on a large scale, the preferred direction of flow is in that direction.

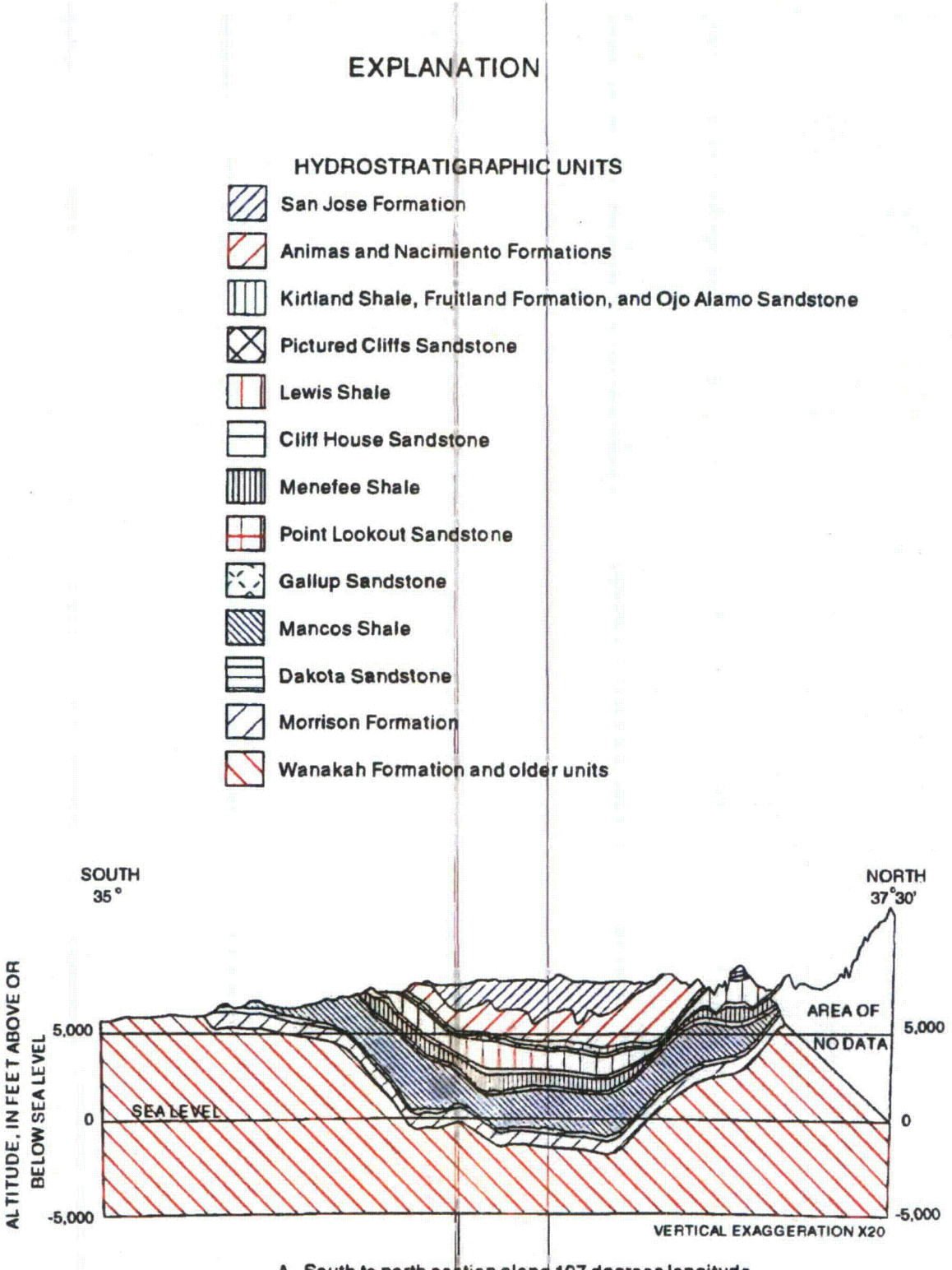

A. South to north section along 107 degrees longitude.

Figure 38.--South to north sections showing the vertical layers used in the model.

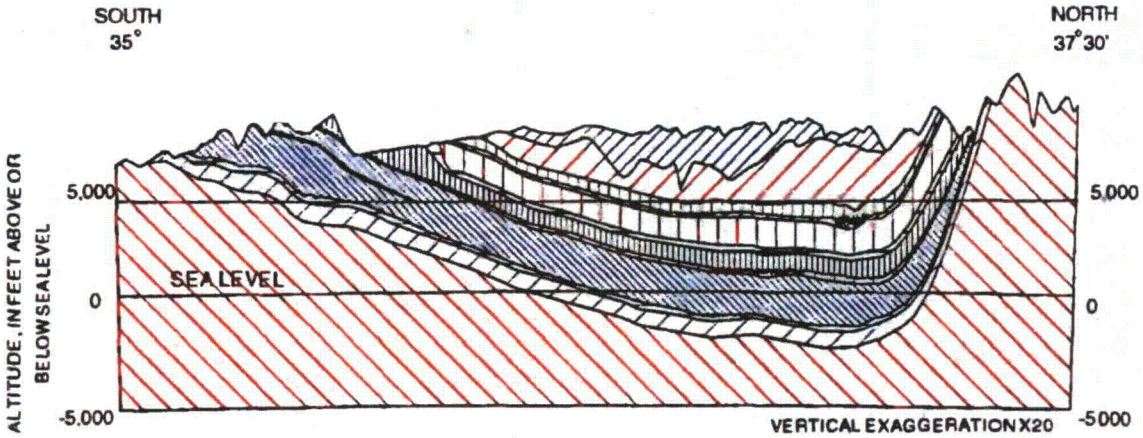

B. South to north section along 107 degrees 15 minutes longitude.

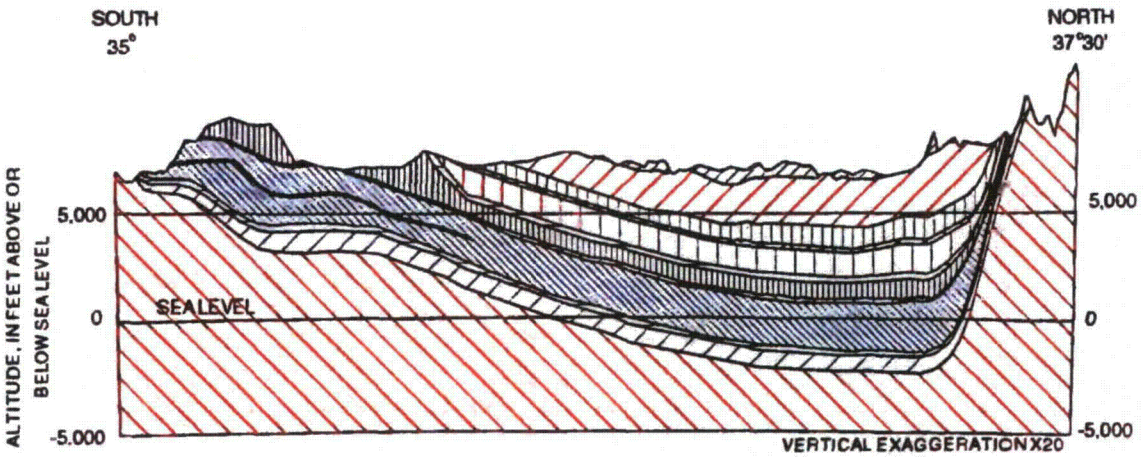

C. South to north section along 107 degrees 30 minutes longitude.

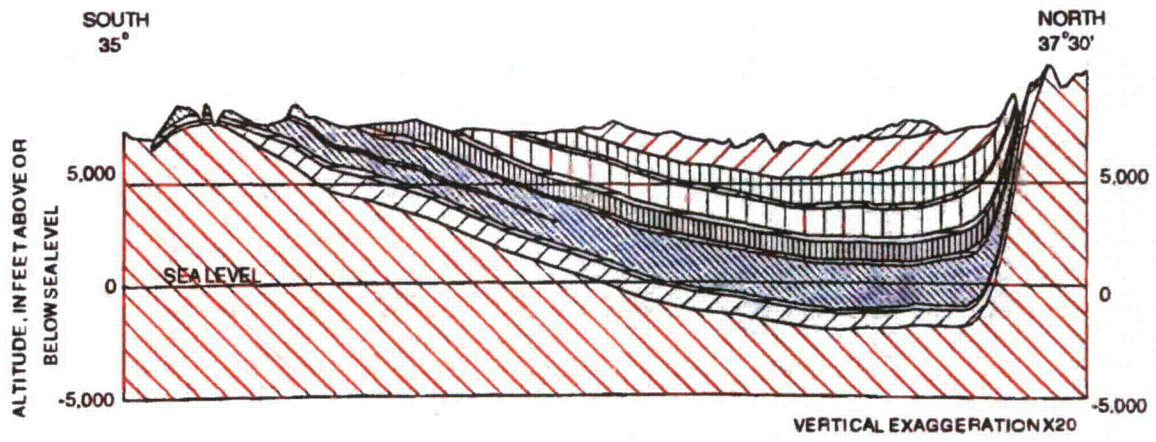

D. South to north section along 107 degrees 45 minutes longitude.

Figure 38.--South to north sections showing the vertical layers used in the model--Continued.

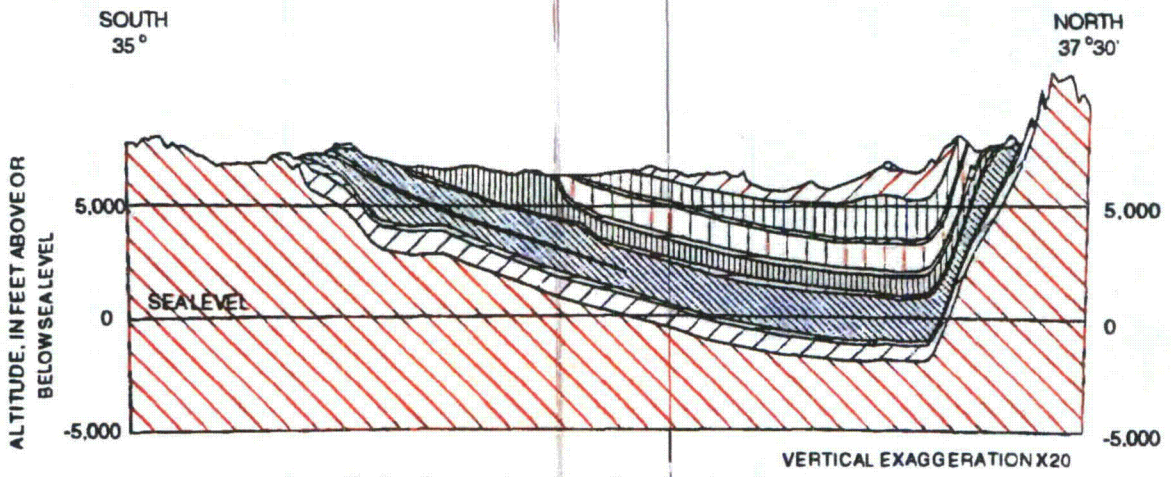

E. South to north section along 108 degrees longitude.

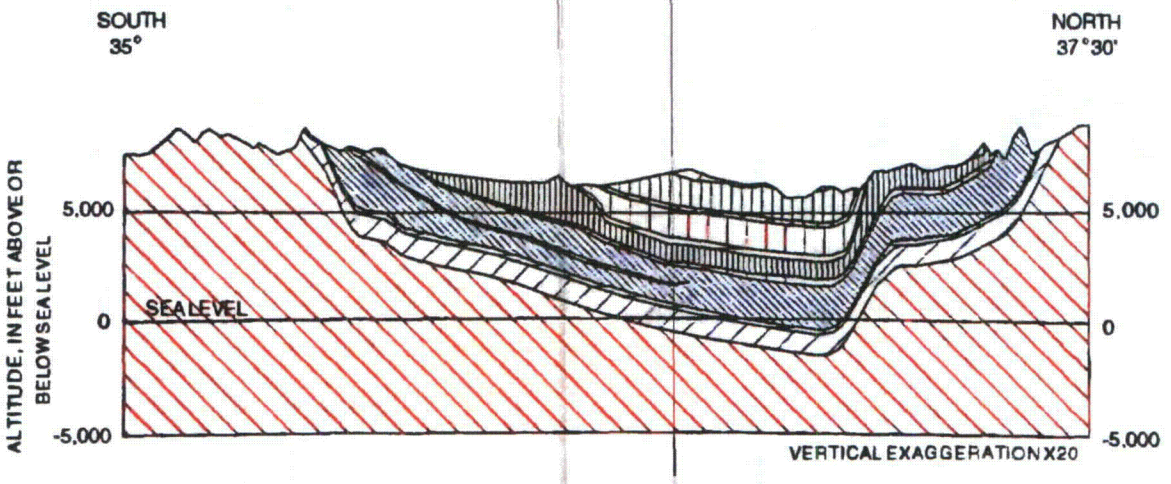

F. South to north section along 108 degrees 15 minutes longitude.

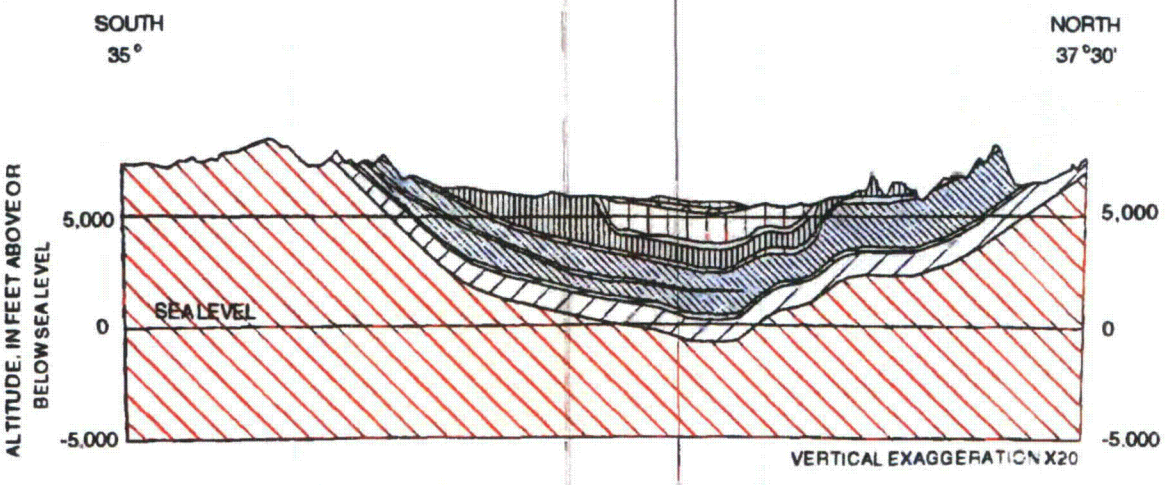

G. South to north section along 108 degrees 30 minutes longitude.

Figure 38.--South to north sections showing the vertical layers used in the model--Concluded.

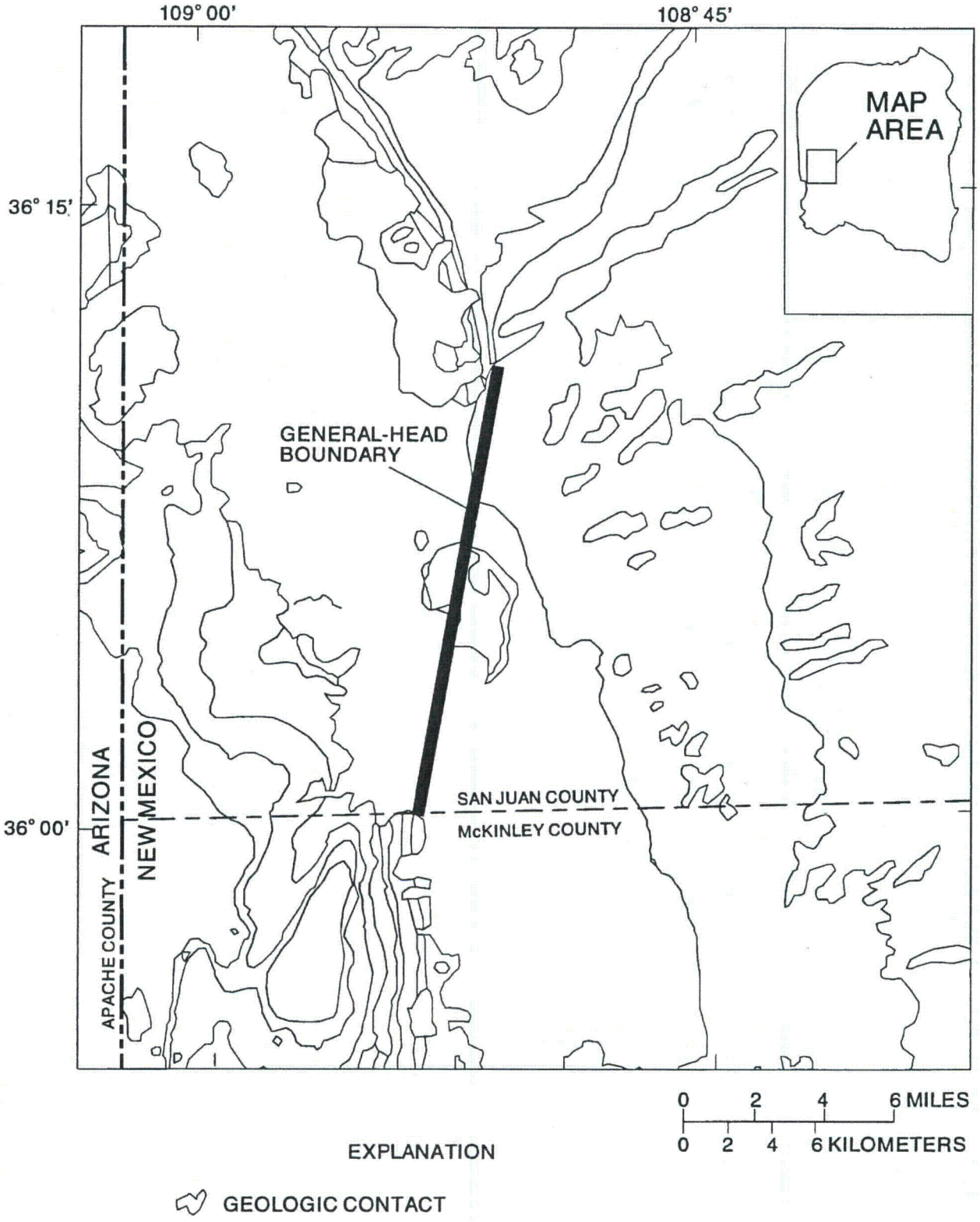

Figure 39.--Location of the general-head boundary used to simulate the downward movement of water from the Chuska Sandstone, Deza Formation, and landslide deposits into the regional aquifers.

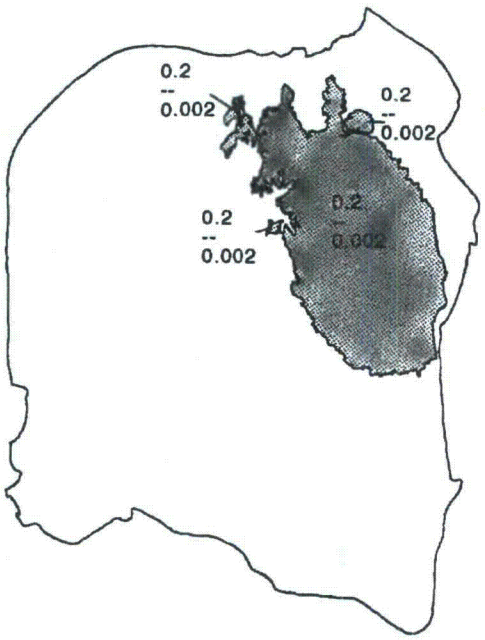

A. Simulated horizontal and vertical hydraulic conductivities for the San Jose Formation.

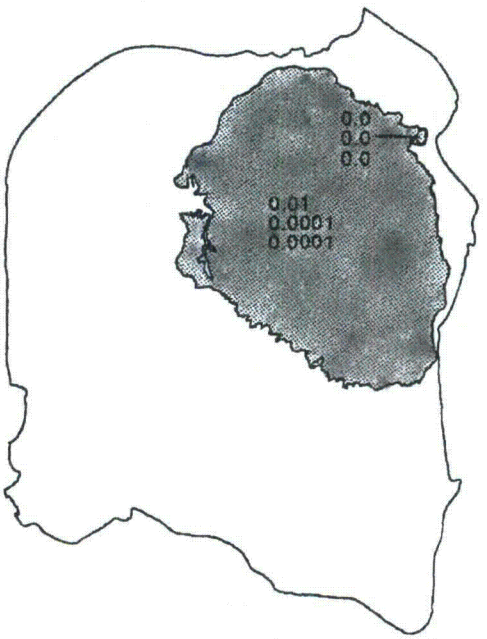

B. Simulated horizontal and vertical hydraulic conductivities for the Animas and Nacimiento Formations.

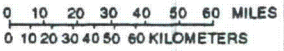

EXPLANATION

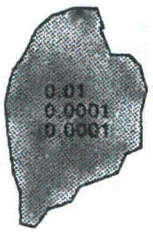

AREA OF HYDRAULIC-CONDUCTIVITY DATA--
Upper number is horizontal, middle number is upper vertical, and lower number is lower vertical hydraulic conductivity, in feet per day. Dashes indicate value not used.

Figure 40.--Simulated horizontal and vertical hydraulic conductivities.

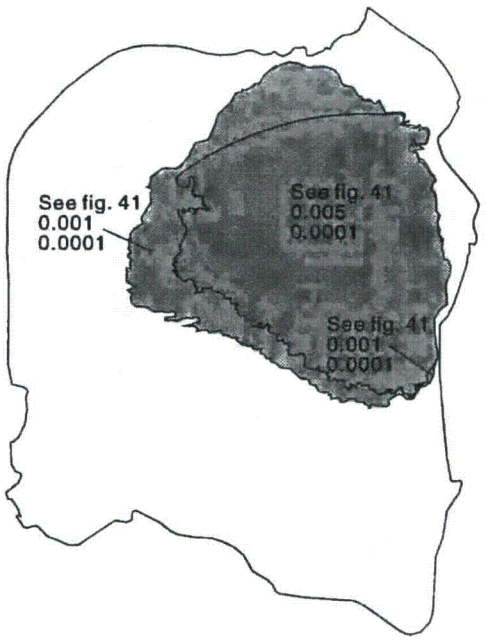

C. Simulated vertical hydraulic conductivities for the combined Ojo Alamo Sandstone, Kirtland Shale, and Fruitland Formation.

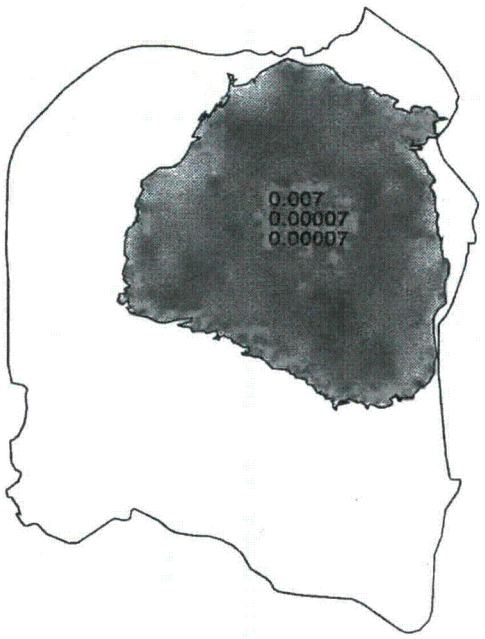

D. Simulated horizontal and vertical hydraulic conductivities for the Pictured Cliffs Sandstone.

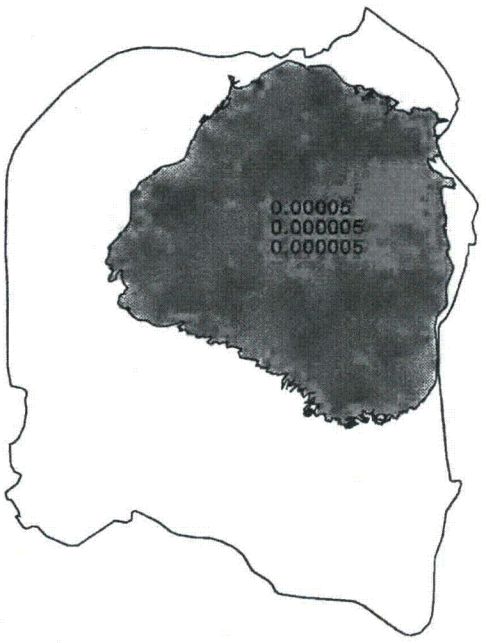

E. Simulated horizontal and vertical hydraulic conductivities for the Lewis Shale.

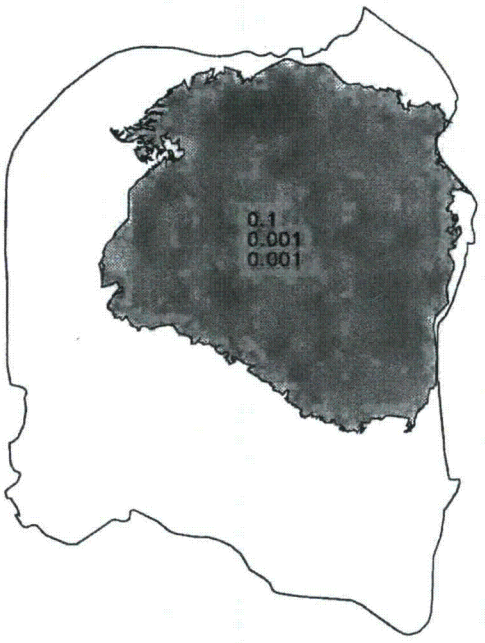

F. Simulated horizontal and vertical hydraulic conductivities for the Cliff House Sandstone.

Figure 40.--Simulated horizontal and vertical hydraulic conductivities--Continued.

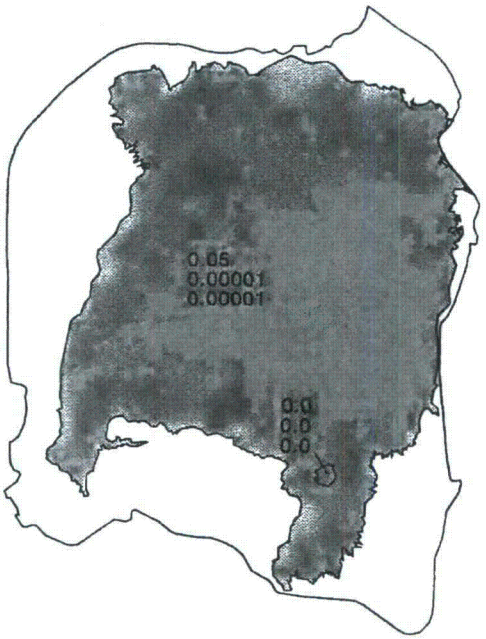

G. Simulated horizontal and vertical hydraulic conductivities for the Menefee Shale.

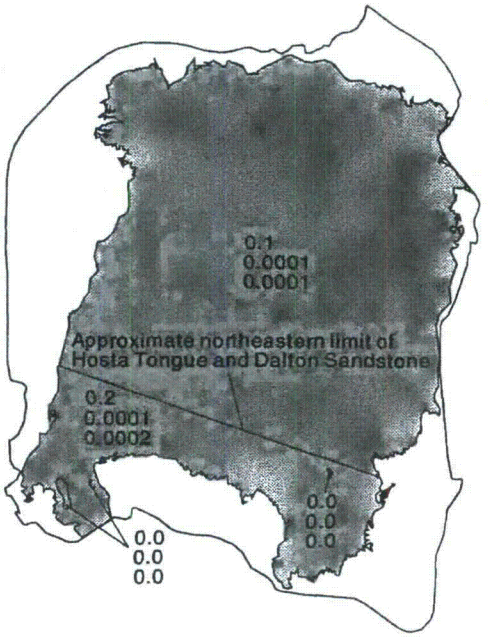

H. Simulated horizontal and vertical hydraulic conductivities for the Point Lookout Sandstone.

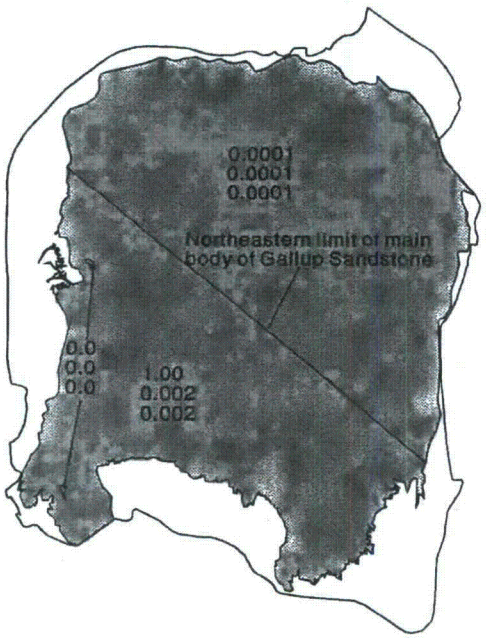

I. Simulated horizontal and vertical hydraulic conductivities for the Gallup Sandstone and Mancos Shale.

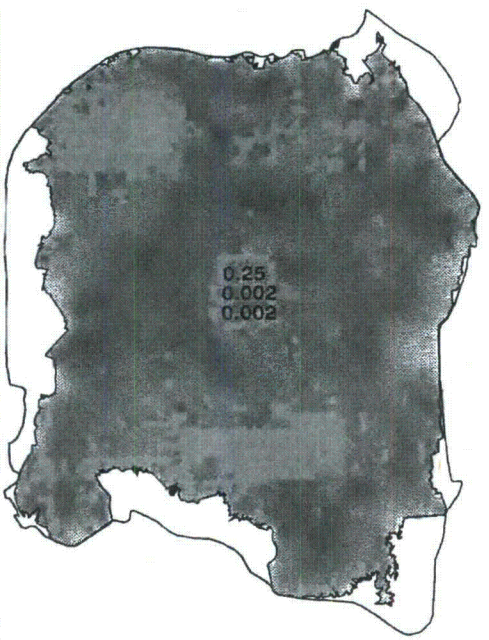

J. Simulated horizontal and vertical hydraulic conductivities for the Dakota Sandstone.

Figure 40.--Simulated horizontal and vertical hydraulic conductivities--Continued.

K. Simulated horizontal and vertical hydraulic conductivities for the Morrison Formation.

Figure 40.--Simulated horizontal and vertical hydraulic conductivities--Concluded.

Most units could be described in simple hydrologic terms; however, the units represented by model layers 3, 8, and 9 were more complex, requiring zoned values of hydraulic conductivity and different values of upward and downward vertical hydraulic conductivity. The units represented by layer 3 are the Ojo Alamo Sandstone, Kirtland Shale, and Fruitland Formation. This combination of units in one layer was formed because information was insufficient to separate the Kirtland and Fruitland into individual hydrostratigraphic units, the Ojo Alamo was thin enough to present serious problems defining tops and bottoms that did not conflict with adjacent units, and the Ojo Alamo pinched out in the subsurface. The solution was to combine the units. The upward vertical hydraulic conductivity is greater than the downward (fig. 40C) to reflect the higher permeability of the Farmington Sandstone Member of the Kirtland Shale and of the Ojo Alamo Sandstone. The horizontal hydraulic conductivity (fig. 41) was computed as the thickness-weighted mean of the conductivities of the Ojo Alamo and Kirtland-Fruitland subunits. In this computation the values of hydraulic conductivity of the Ojo Alamo and Kirtland-Fruitland subunits were assumed to be 1 and 0.01 foot per day, respectively.

The units represented by layer 8 are the main body and Hosta Tongue of the Point Lookout Sandstone and the Crevasse Canyon Formation (primarily the Dalton Sandstone Member). The main body of the Point Lookout Sandstone is persistent and fairly uniform throughout the basin, but the Hosta Tongue and Dalton Sandstone occur only in the south and southwestern part of the basin. At the southern margin of the basin the three units are stacked upon each other with only minor separation by thin tongues of the Mancos Shale and Cleary Coal Member of the Crevasse Canyon. The diagonal line separating conductivity zones in figure 40H is the approximate northeastern limit of the Hosta Tongue and Dalton Sandstone.

The units represented by layer 9 are the main body of the Gallup Sandstone and a thin, arbitrary interval in the middle of the Mancos Shale. The diagonal line in figure 40I (also see fig. 33) represents the northeastern limit of the main body of the Gallup Sandstone. Northeast of this line model layer 9 represents a thin interval of the Mancos Shale with appropriately low horizontal and vertical hydraulic conductivities.

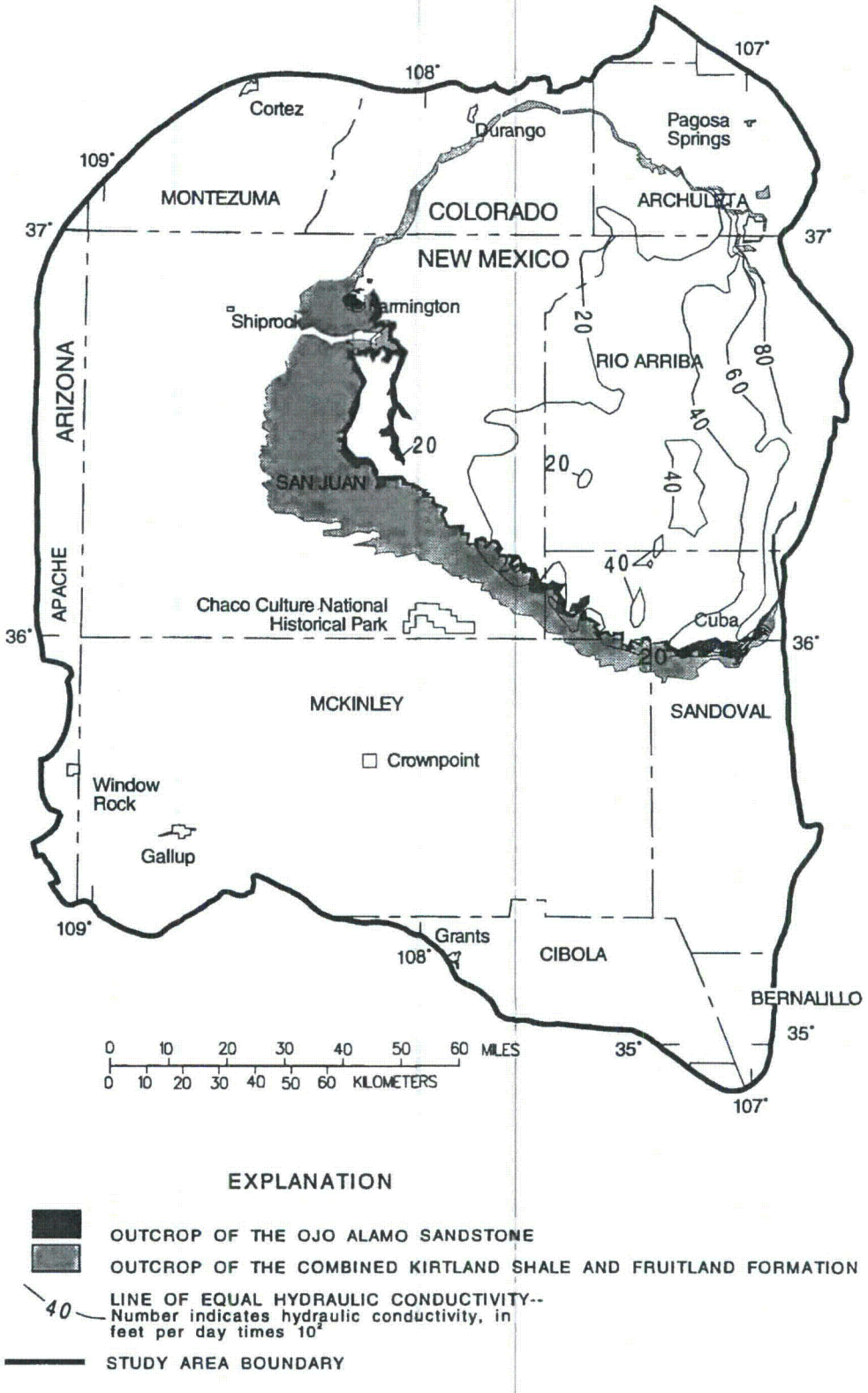

Figure 41.--Simulated horizontal hydraulic conductivity for the combined Ojo Alamo Sandstone, Kirtland Shale, and Fruitland Formation.

The top and bottom of the Entrada Sandstone were not determined because of insufficient control data. Therefore the unit was simulated as being uniformly transmissive (fig. 42). Because the Entrada Sandstone is the basal unit in the simulation there is no downward vertical hydraulic conductivity.

The degree of vertical hydraulic connection between hydrostratigraphic units is a function of the vertical hydraulic conductivity and the thicknesses of the units. Because the conductances (hydraulic conductivity divided by thickness) are in series, the net vertical leakance between units is the harmonic mean of the conductances of the two adjacent units. The model (McDonald and Harbaugh, 1988, chap. 5, p. 11-12) multiplies cell area by vertical leakance to obtain vertical conductance. The equation to determine the vertical leakance between two units (units *a* and *b*) is:

$$VCONT = \frac{1}{\frac{M_a/2}{VK_a} + \frac{M_b/2}{VK_b}} \qquad (7)$$

where $VCONT$ is the vertical leakance (1/t);

M_a, M_b are the thicknesses of units *a* and *b* (L); and

VK_a, VK_b are the vertical hydraulic conductivities of units *a* and *b* (L/t).

By examination of equation 7 one can determine that a low-conductivity unit will have the dominant term in the denominator. In instances where a low hydraulic-conductivity unit is not explicitly simulated (indicated by VK in fig. 36), a third term in the denominator, (M_c / VK_c), usually is vastly dominant over the other two.

MODEL CALIBRATION AND SENSITIVITY ANALYSIS

The steady-state ground-water-flow model of the San Juan Basin did not undergo the typical lengthy process of calibration; the boundary conditions, including internal geometry, were defined and representative values for hydraulic properties were selected on the basis of known aquifer tests and previous reports. The initial model configuration produced generally acceptable results but some refinements, discussed below, were necessary.

The most likely reason that the model needed very little refinement to achieve acceptable calibration is that the dominant controls on the steady-state ground-water-flow system in the San Juan Basin are the boundary conditions, variations in hydraulic properties resulting from different depositional environments, and internal geometry of the aquifer-system components, all described earlier. Because a GIS was used to describe these aquifer-system properties and construct input data for the model, minute details could be portrayed with great accuracy. The accurate portrayal of the boundaries led, in turn, to a quickly calibrated model of the flow system.

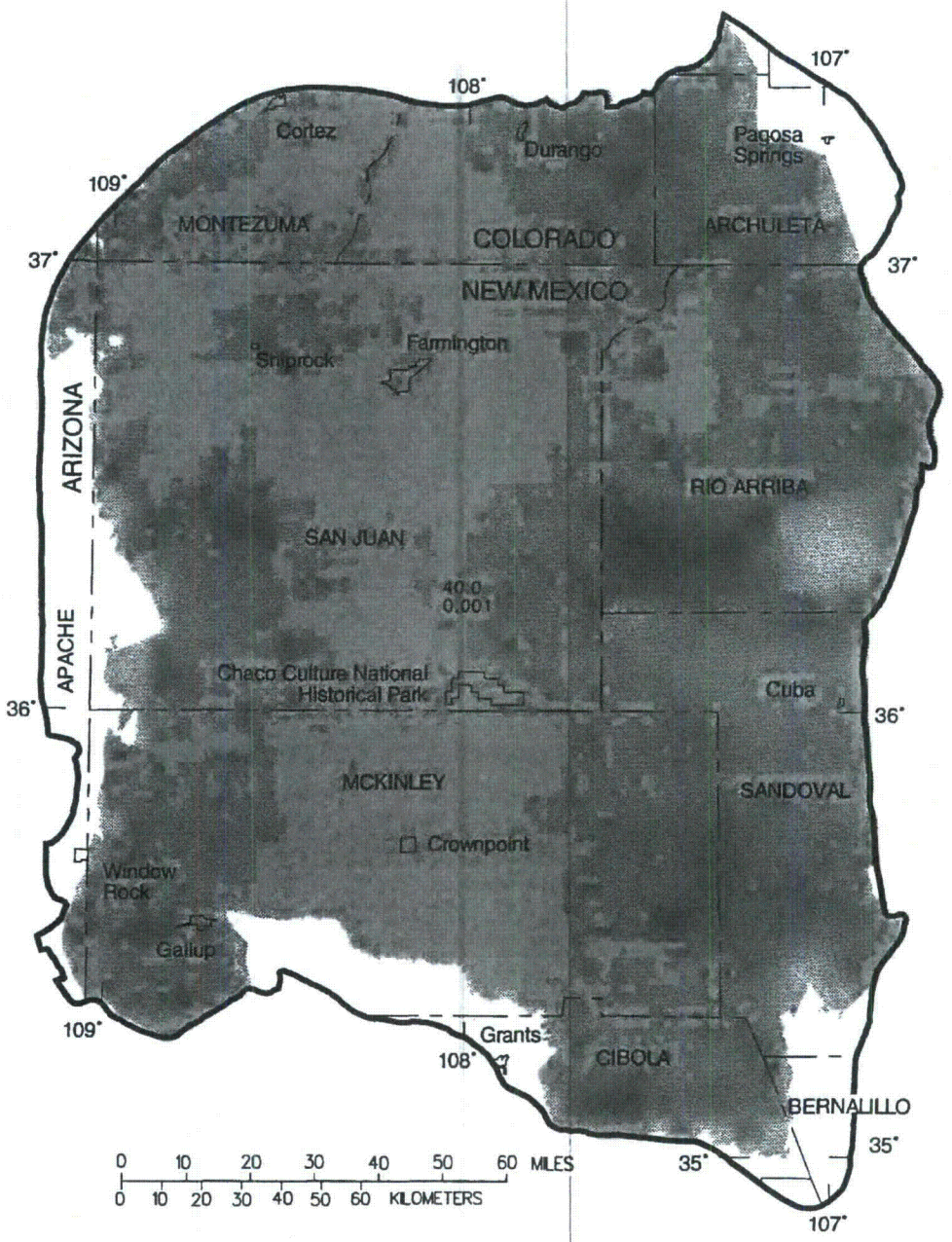

EXPLANATION

40.0
0.001

AREA OF SIMULATED TRANSMISSIVITY AND UPWARD VERTICAL HYDRAULIC CONDUCTIVITY--Upper number is transmissivity, in feet squared per day. Lower number is upward hydraulic conductivity, in feet per day

STUDY AREA BOUNDARY

Figure 42.--Simulated horizontal transmissivity and upward vertical hydraulic conductivity for the Entrada Sandstone.

Calibration of the steady-state ground-water-flow model of the San Juan Basin consisted of matching as closely as possible computed and measured potentiometric heads for a few key wells in the central part of the basin. The selected wells each were completed in a single hydrostratigraphic unit and had measured potentiometric heads that approximated predevelopment conditions. Calibration of the model around the perimeter of the basin was unnecessary because water-level altitudes are closely controlled by recharge and surface-water boundaries. Because the altitudes of the surface-water boundaries were obtained from digital elevation models having a vertical accuracy of 30 meters, computed water-level altitudes in and near the outcrops were not expected to exceed this accuracy. Because the vertical error in land-surface altitude supposedly is not systematic, however, the actual error between computed and measured potentiometric heads in the central part of the basin was expected to be less than 100 feet. For the final steady-state model the average error for control wells completed in the Cliff House and Point Lookout Sandstones and the Morrison Formation was about 50 feet.

Preconditioned Hydraulic-Head Distribution

The hydraulic head used to begin the steady-state simulations was set equal to the altitude at land surface for all model layers. During the first steady-state simulation computed potentiometric heads decayed in the outcrop areas to the level of equilibrium determined by local recharge and surface-water boundaries. In the central part of the basin the potentiometric heads decayed to a level that reflected the hydraulic properties of the aquifers and a distance-weighted average of the potentiometric heads in the outcrop areas. Once a steady-state solution was obtained the heads from that solution were used as initial heads for other simulations, with the exception that land-surface altitude again was used as initial heads for the top model layer.

Model Refinements and Sensitivity to Changes in Simulated Aquifer Properties

Although some improvements and refinements were made to the model, most changes led to undesired or no significant change. The most positive change was the inclusion of a general-head boundary to represent the hydrologic effects of the Chuska Mountains on underlying aquifers in the regional system; the initial simulation excluded this source of recharge to the regional system. Another change that greatly improved the simulation was reducing the rate of direct recharge to the Lewis Shale and Menefee Formation to one-tenth the rate for the other units, and limiting recharge to only the Ojo Alamo Sandstone subunit of the combined Ojo Alamo Sandstone, Kirtland Shale, and Fruitland Formation hydrostratigraphic unit. This last change represented the high rate of runoff from the near-barren shales and was necessary to prevent the low hydraulic conductivity of these shale units from causing excessive mounding of water in their outcrop areas.

The model was much less sensitive to either of the two previous changes than to changes in hydraulic conductivity and anisotropy. Doubling or halving these properties in the simulations resulted in approximately a 50-foot change in computed hydraulic head in the center of the basin. Changes generally were less elsewhere, especially in the near-outcrop areas.

The model was even less sensitive to changes in simulated vertical conductance (vertical leakance). This probably is due to the relatively low vertical gradients that exist across great thicknesses of units having low hydraulic conductivity. The low vertical gradients support the observation that the primary controls on steady-state potentiometric heads are in the outcrop areas of the aquifers.

The change having the least effect was the simulation of the interaction of the Dakota Sandstone with the San Juan River across the Mancos Shale. A general-head boundary was used to test the effect of simulating leakage from the Dakota Sandstone upward across the Mancos Shale and discharging to the surface-water system of the San Juan River and valley alluvium. No change was noted in computed heads in the Dakota Sandstone. The quantity of water leaking upward across the Mancos Shale is insufficient to affect potentiometric heads in the underlying Dakota Sandstone.

DISCUSSION OF SIMULATION ANALYSES

The most clearly defined conclusion resulting from the simulations was that steady-state hydraulic heads in the San Juan Basin are firmly controlled by boundary conditions and the internal geometry of the hydrostratigraphic units. The primary boundary types that exert the most control are stream-aquifer interaction, recharge from direct precipitation, and recharge to some units of the regional system by leakage through the Chuska Sandstone.

Wide-ranging variations in the values of simulated hydraulic properties resulted in modest changes in computed hydraulic head, especially near the aquifer outcrop areas. The greatest variations in computed head were in the central part of the basin, away from the outcrop boundaries. Finally, the general pattern of head distribution never really changed throughout the analysis of the effects of changes in simulated hydraulic properties. The computed heads for the major water-yielding hydrostratigraphic units are shown in figures 43-53. A hydraulic-head map is not shown for the Lewis Shale because it could not be expected to yield water to a well, nor are heads plotted for the areas of outcrop (except for the San Jose and Menefee Formations), where local topography often dominates ground-water levels.

Although the computed steady-state hydraulic heads compare reasonably well with early measured heads in the major aquifers (Gallup, Dakota, and Morrison) in the central part of the basin, data are insufficient for comparison in the younger units except in the aquifer outcrop areas where water levels are strongly controlled by topographic altitude. Away from the outcrop areas most hydraulic-head measurements in the basin reflect post-development conditions.

Vertical hydraulic-head gradients under steady-state conditions near the center of the basin often were unexpectedly low despite low values of vertical hydraulic conductivity and thick intervening intervals of confining units between the primary aquifers. This is largely attributable to the dominance of outcrop boundary conditions on the potentiometric-head distribution and the similarity of boundary conditions for stratigraphically adjacent units. The vertical flow directions between selected adjacent hydrostratigraphic units are shown in figure 54.

The Dakota Sandstone, Morrison Formation, and Entrada Sandstone exhibit similar hydraulic heads. From the Dakota Sandstone upward the differences in computed hydraulic head between units are greater because of the presence of thick shale sequences. The distinct differences in hydraulic head between the Gallup and Dakota Sandstones and the Point Lookout and Gallup Sandstones are due to the very large isolating thicknesses of the upper and lower Mancos Shale and the thinning and pinch-out of the Gallup Sandstone in the subsurface. Likewise, there are significant head differences across the Ojo Alamo Sandstone, Kirtland Shale and Fruitland Formation, and the Lewis Shale and Menefee Formation.

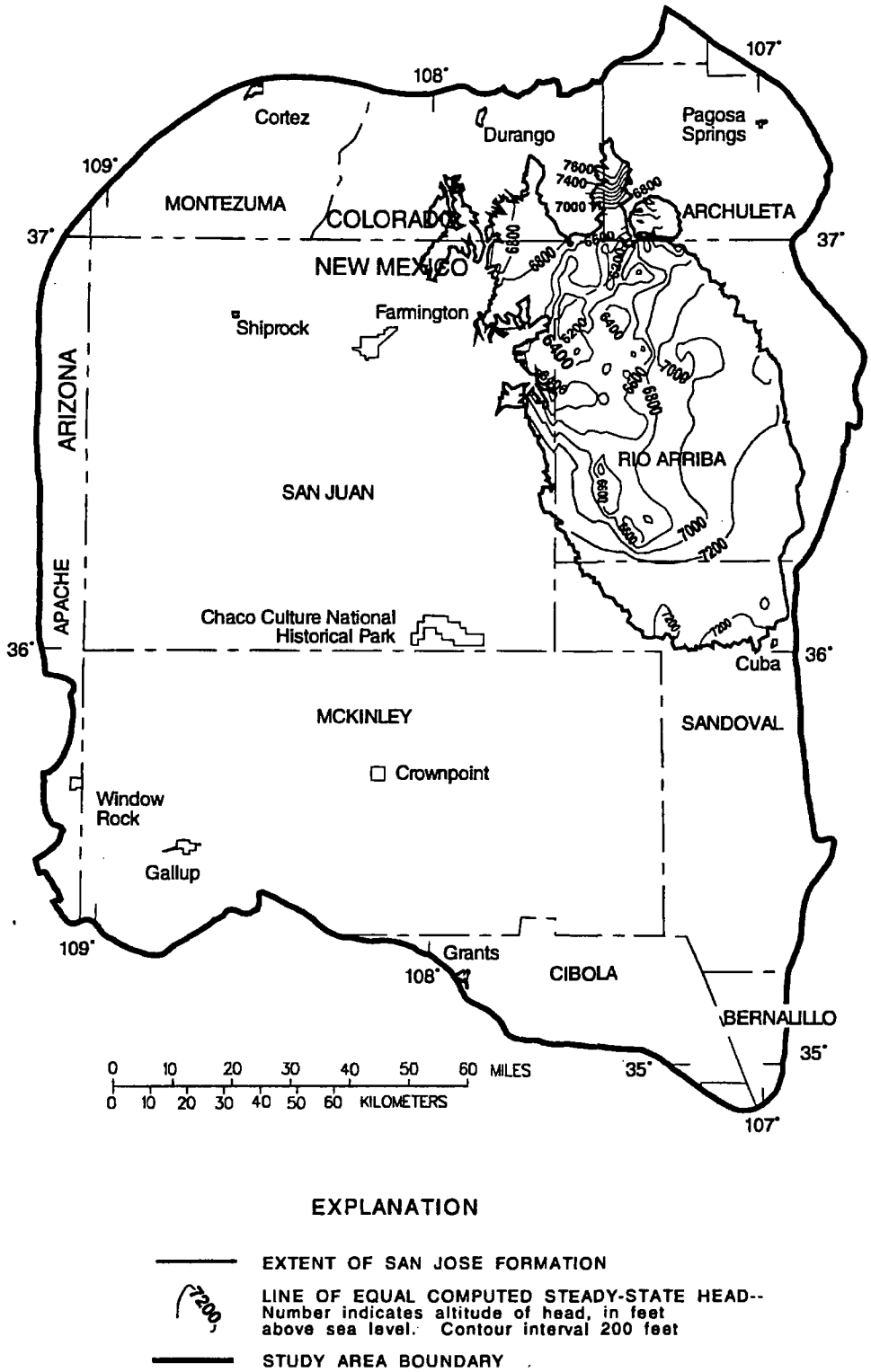

Figure 43.--Computed steady-state head in the San Jose Formation.

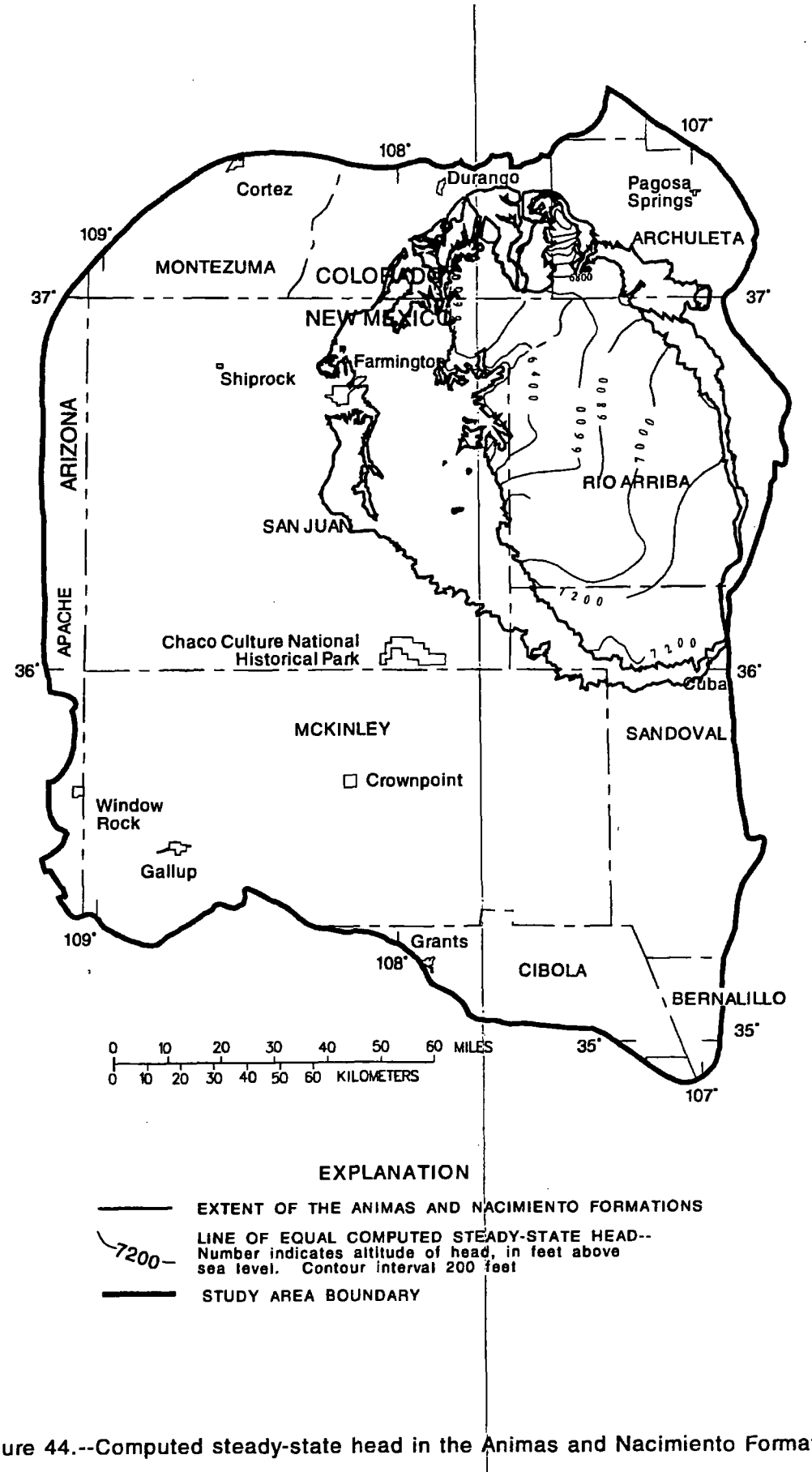

Figure 44.--Computed steady-state head in the Animas and Nacimiento Formations.

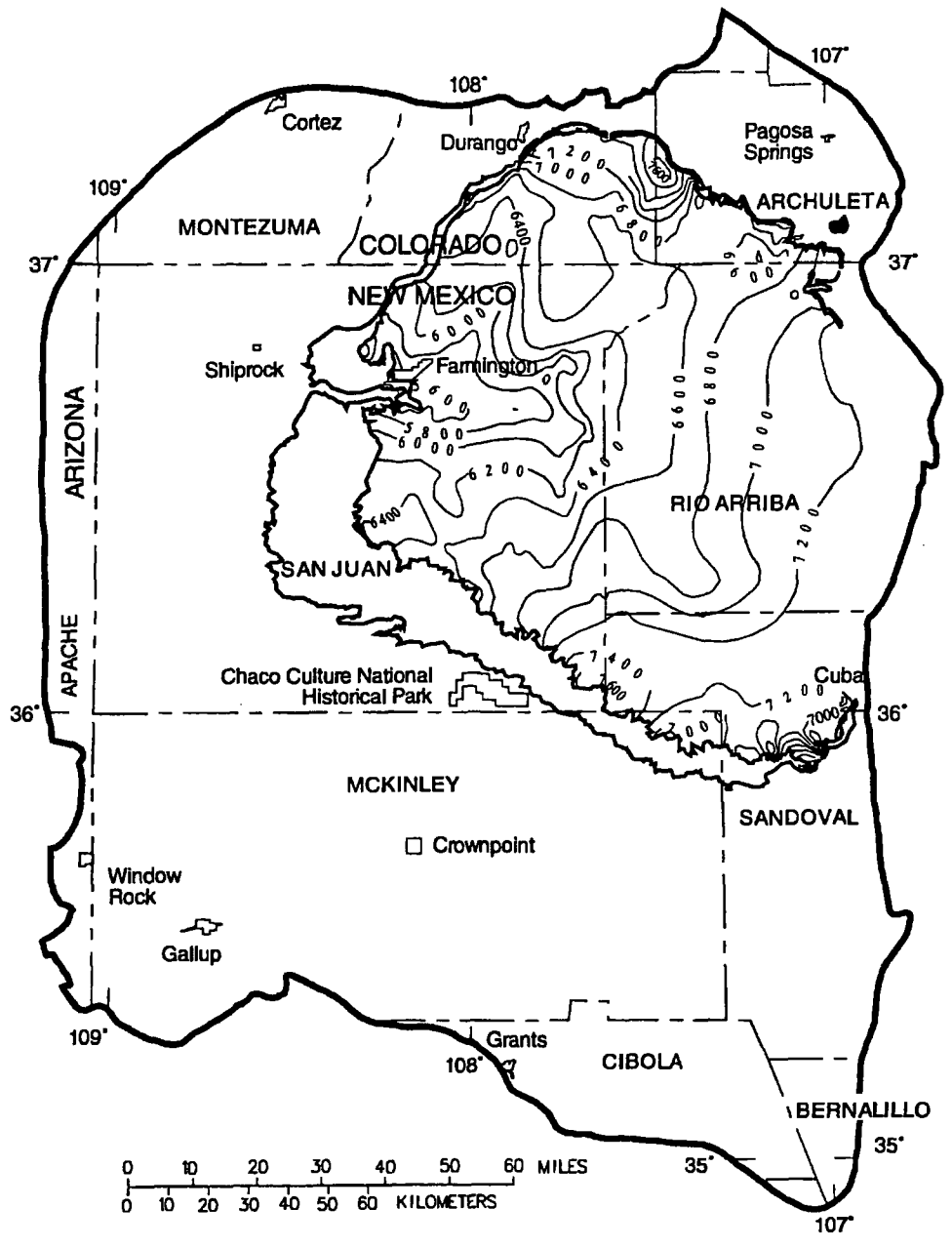

EXPLANATION

EXTENT OF THE COMBINED OJO ALAMO SANDSTONE, KIRTLAND SHALE, AND FRUITLAND FORMATION

7000 LINE OF EQUAL COMPUTED STEADY-STATE HEAD-- Number indicates altitude of head, in feet above sea level. Contour interval 200 feet

STUDY AREA BOUNDARY

Figure 45.--Computed steady-state head in the combined Ojo Alamo Sandstone, Kirtland Shale, and Fruitland Formation.

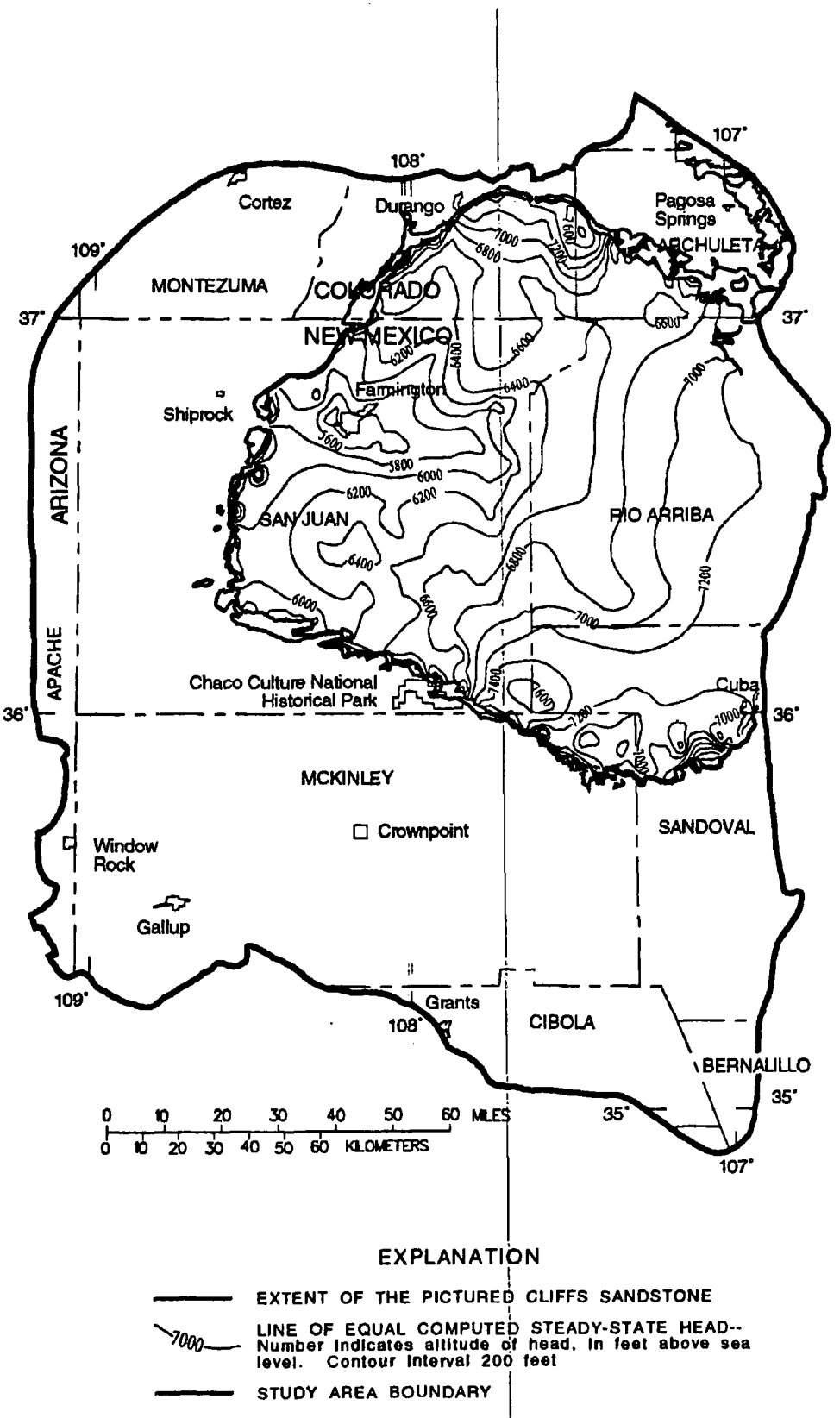

Figure 46.--Computed steady-state head in the Pictured Cliffs Sandstone.

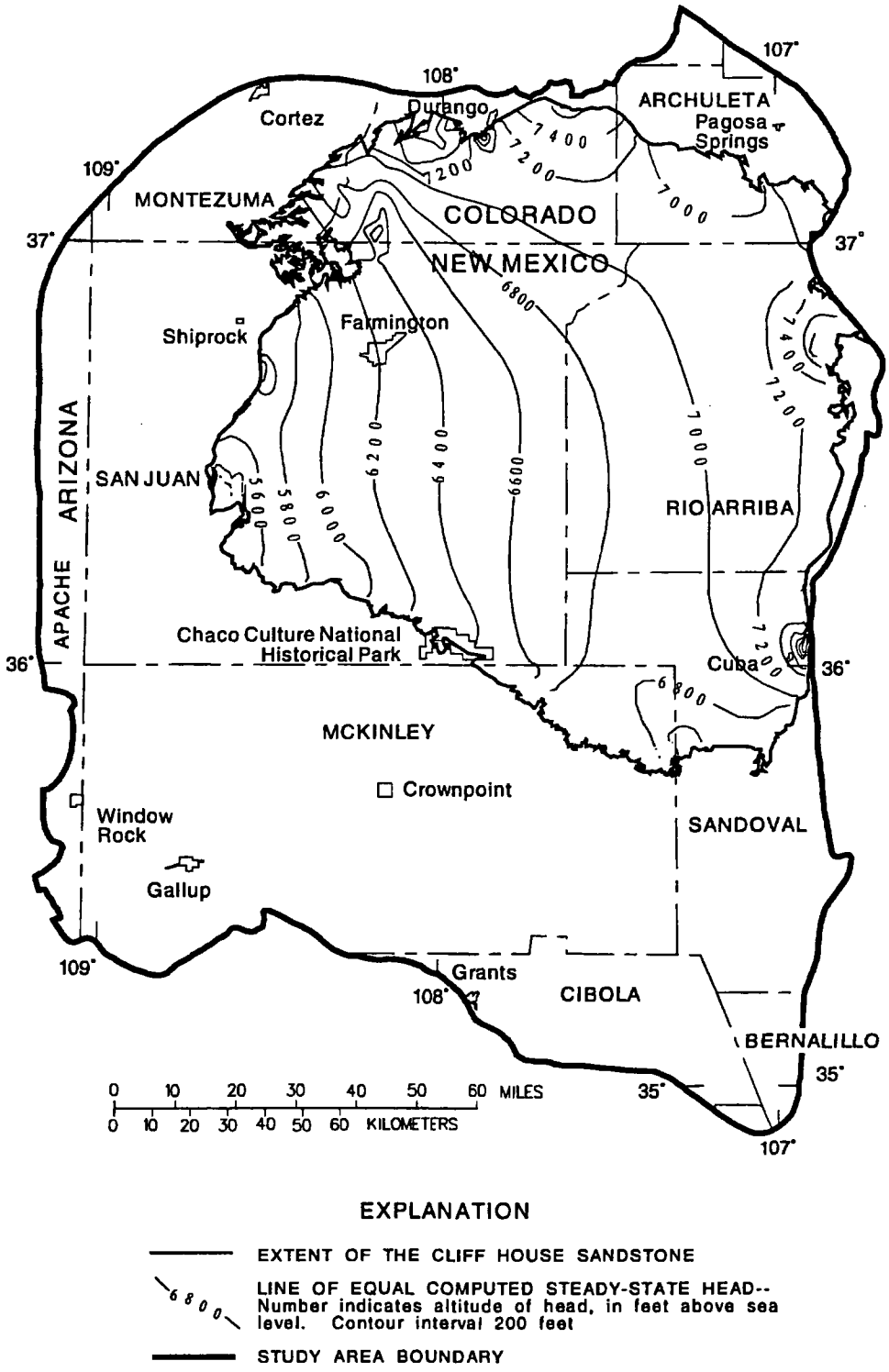

Figure 47.--Computed steady-state head in the Cliff House Sandstone.

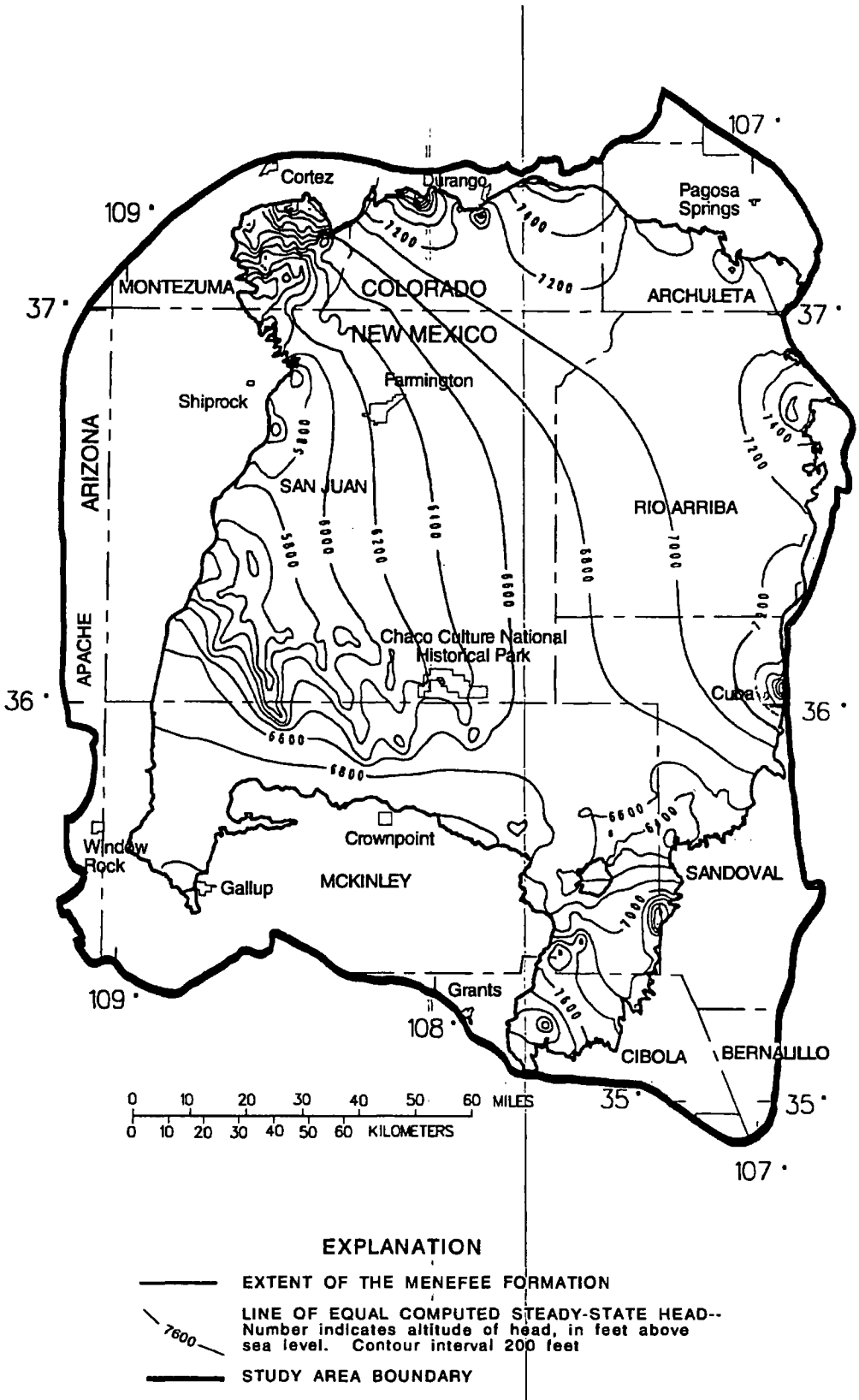

Figure 48.--Computed steady-state head in the Menefee Formation.

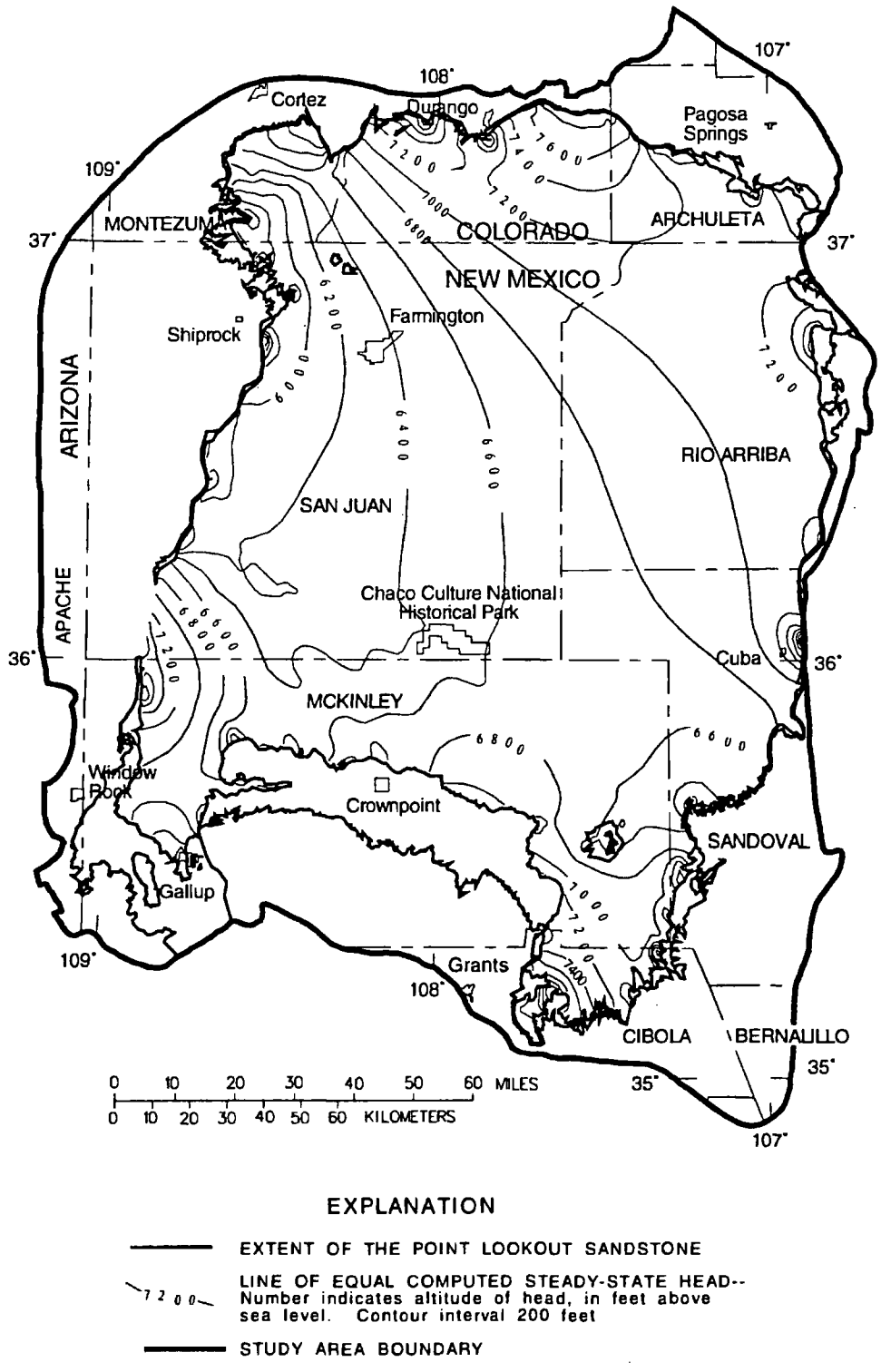

EXPLANATION

EXTENT OF THE POINT LOOKOUT SANDSTONE

7200 LINE OF EQUAL COMPUTED STEADY-STATE HEAD-- Number indicates altitude of head, in feet above sea level. Contour interval 200 feet

STUDY AREA BOUNDARY

Figure 49.--Computed steady-state head in the Point Lookout Sandstone.

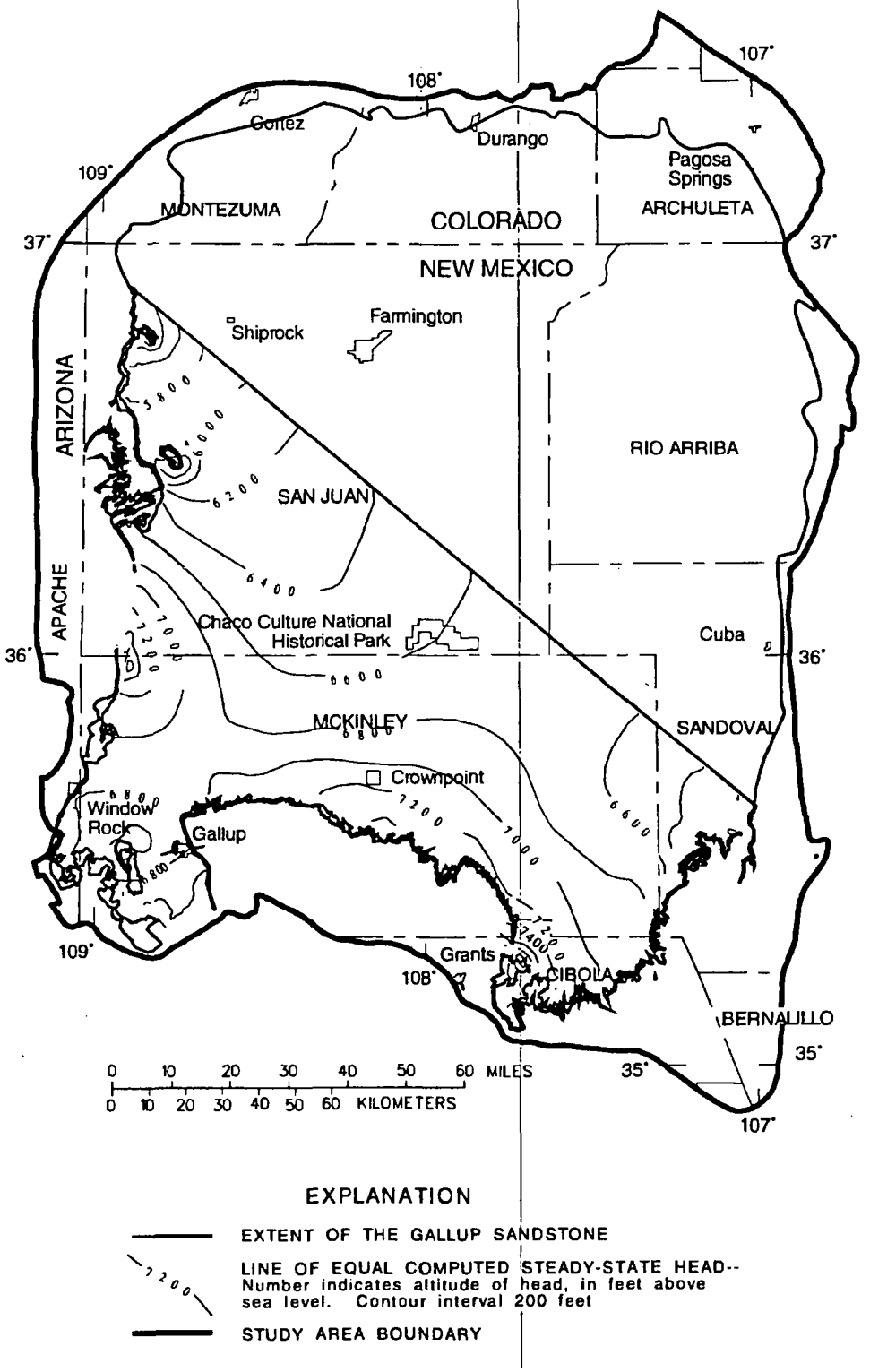

Figure 50.--Computed steady-state head in the Gallup Sandstone.

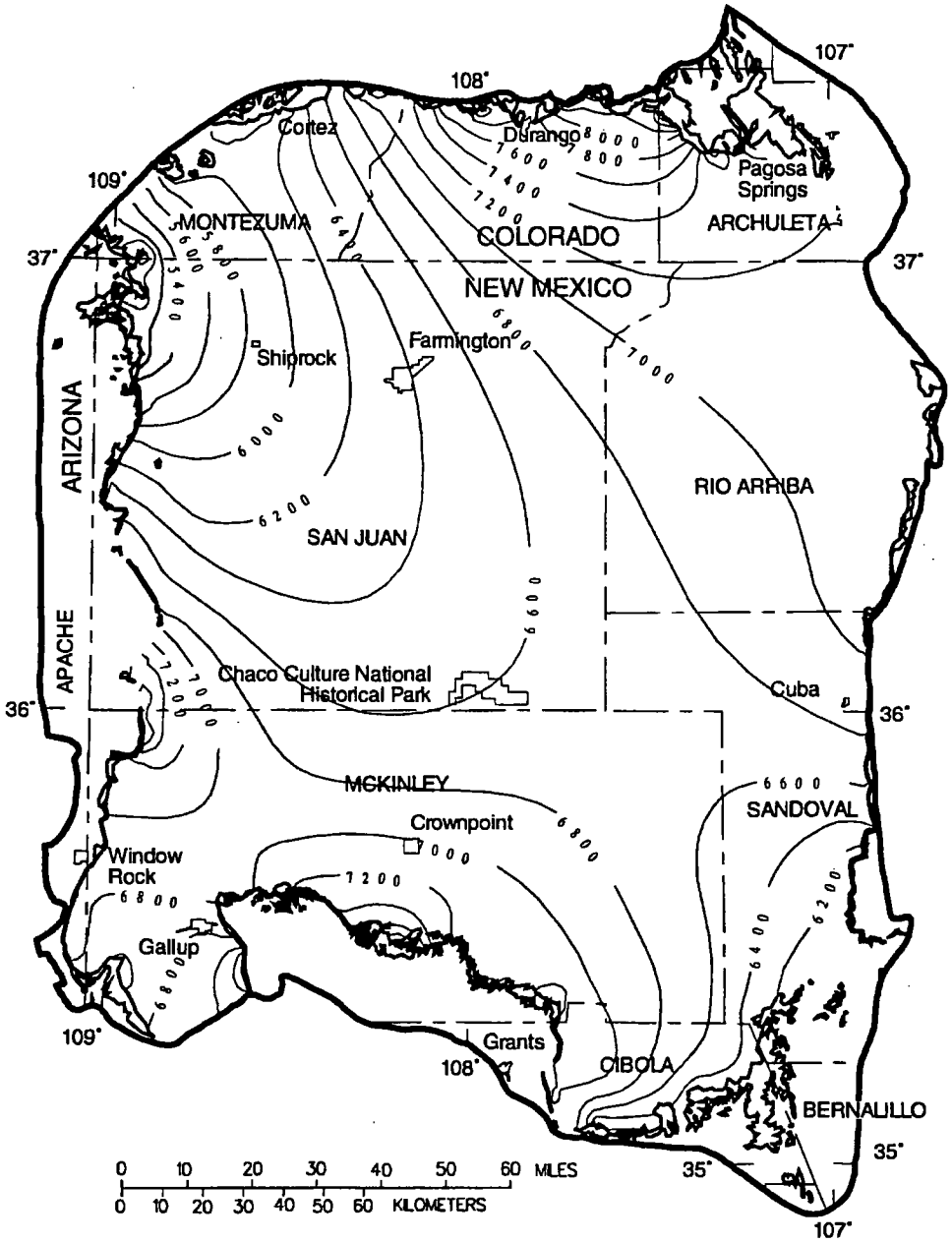

Figure 51.--Computed steady-state head in the Dakota Sandstone.

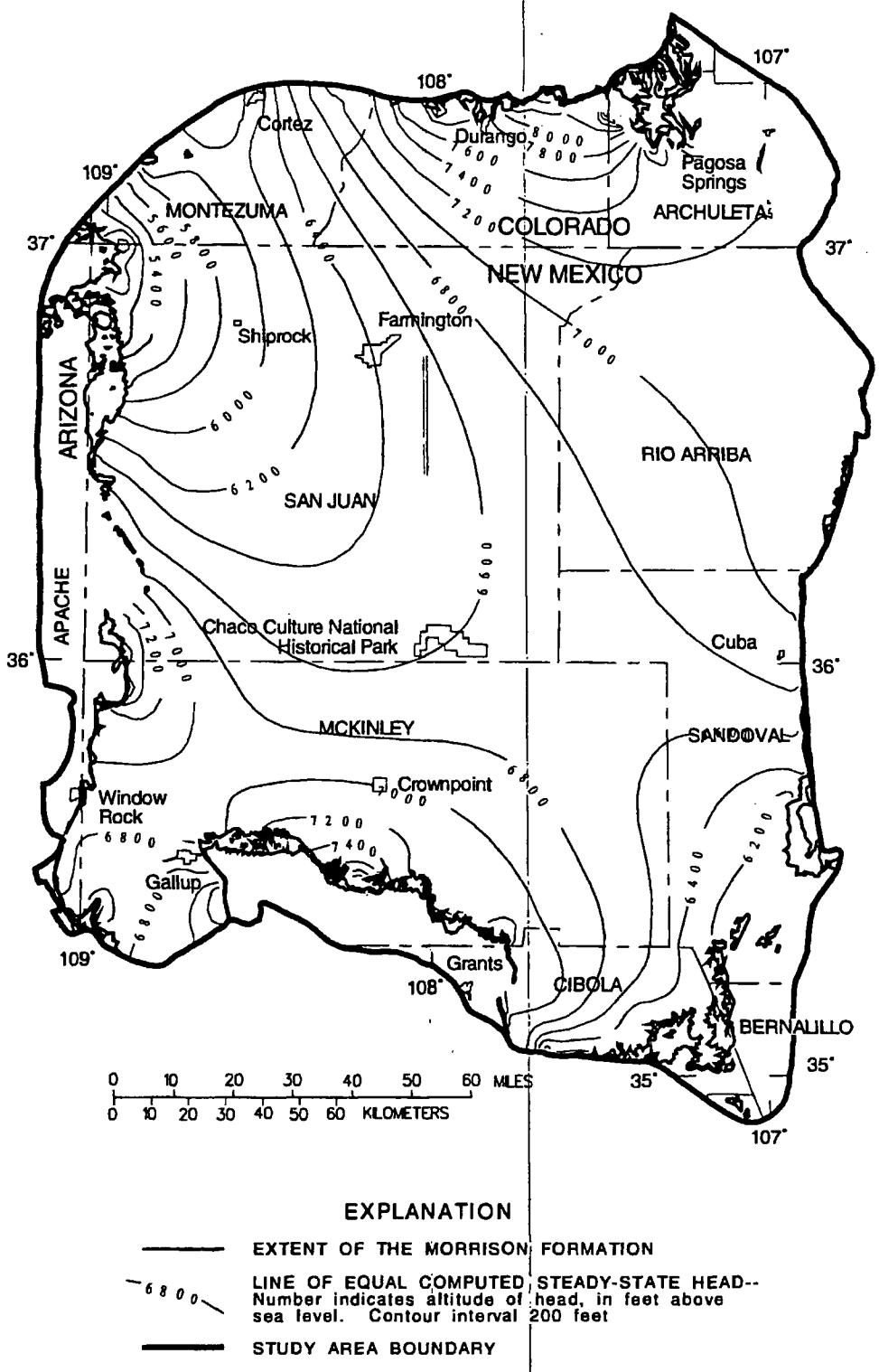

Figure 52.--Computed steady-state head in the Morrison Formation.

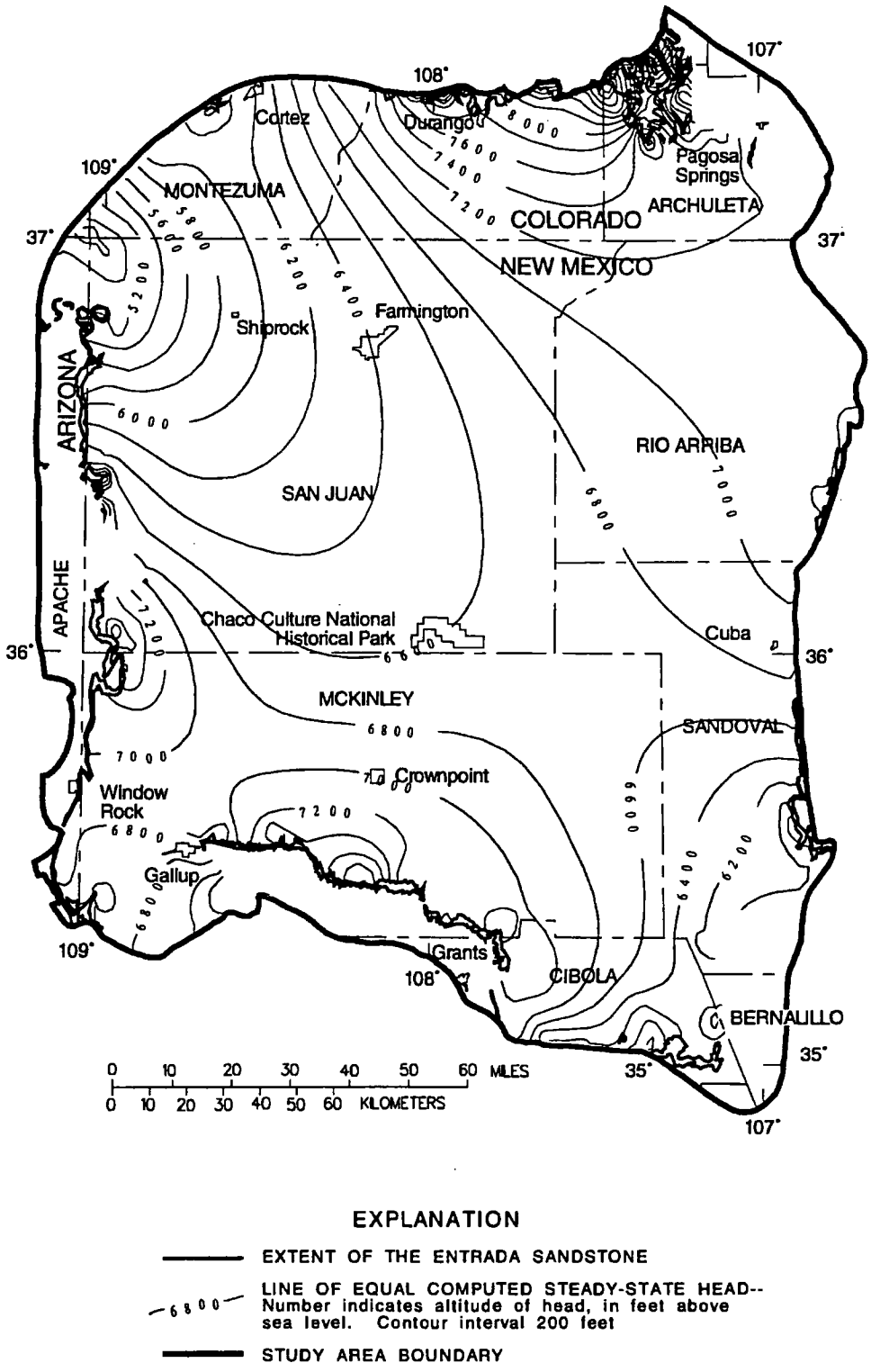

EXPLANATION

EXTENT OF THE ENTRADA SANDSTONE

6800 LINE OF EQUAL COMPUTED STEADY-STATE HEAD--Number indicates altitude of head, in feet above sea level. Contour interval 200 feet

STUDY AREA BOUNDARY

Figure 53.--Computed steady-state head in the Entrada Sandstone.

A. Vertical flow directions between the San Jose and the Animas and Nacimiento Formations.

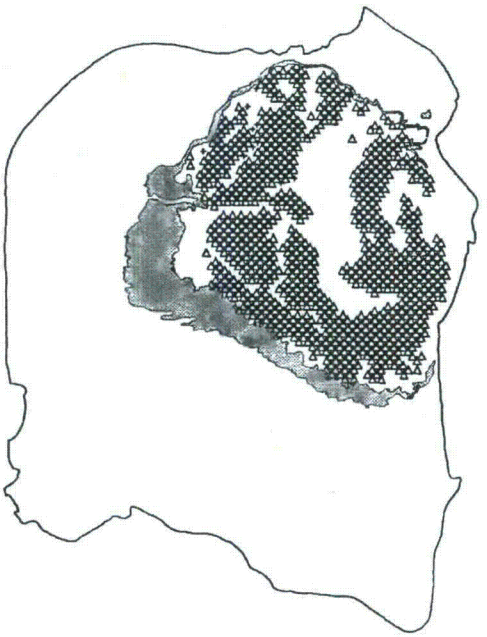

B. Vertical flow directions between the Animas and Nacimiento Formations and the combined Ojo Alamo, Kirtland Shale, and Fruitland Formation.

EXPLANATION

OUTCROP

AREA WITHIN OUTCROP WHERE GRADIENT IS DOWNWARD

AREA WITHIN OUTCROP WHERE GRADIENT IS UPWARD AND HEAD DIFFERENCE IS LESS THAN 100 FEET

AREA WITHIN OUTCROP WHERE GRADIENT IS UPWARD AND HEAD DIFFERENCE IS GREATER THAN 100 FEET

Figure 54.--Vertical flow directions between selected adjacent hydrostratigraphic units in the San Juan Basin.

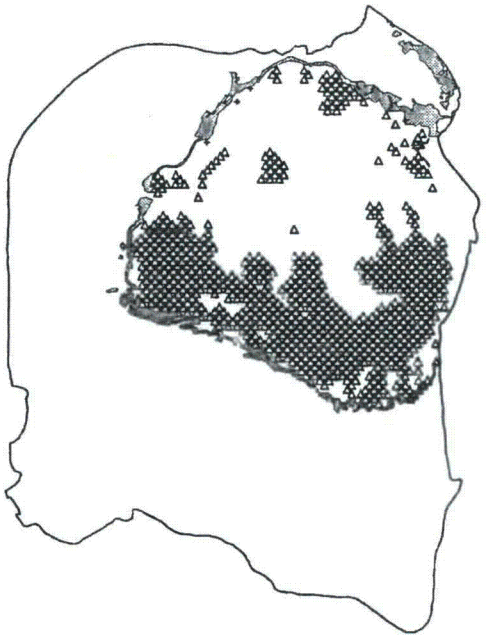

C. Vertical flow directions between the combined Ojo Alamo, Kirtland Shale, and Fruitland Formation and the Pictured Cliffs Sandstone.

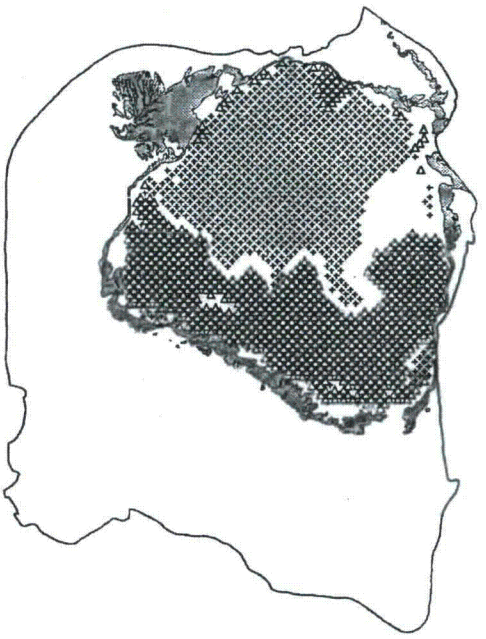

D. Vertical flow directions between the Pictured Cliffs Sandstone and the Cliff House Sandstone.

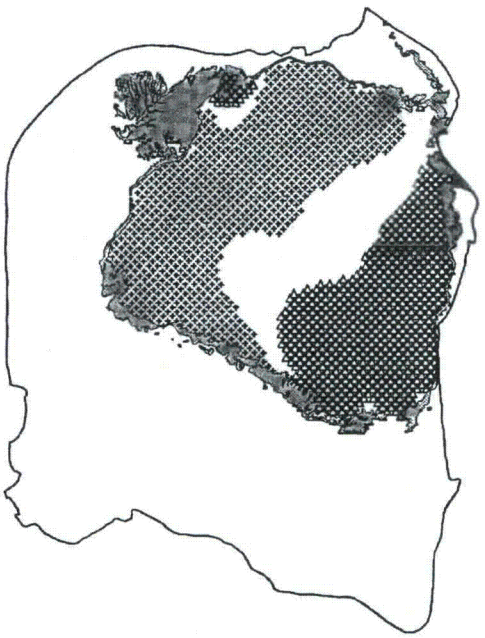

E. Vertical flow directions between the Cliff House Sandstone and the Point Lookout Sandstone.

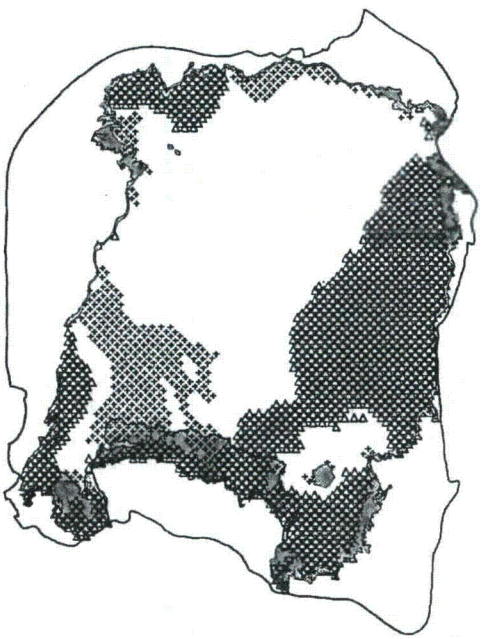

F. Vertical flow directions between the Point Lookout Sandstone and the Gallup Sandstone.

Figure 54.--Vertical flow directions between selected adjacent hydrostratigraphic units in the San Juan Basin--Continued.

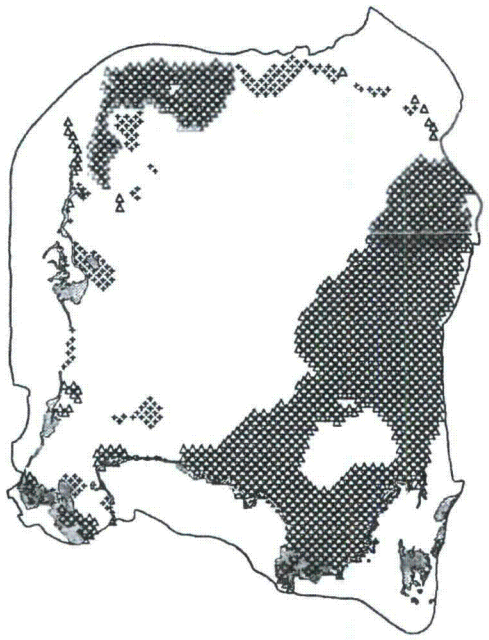

G. Vertical flow directions between the Gallup Sandstone and the Dakota Sandstone.

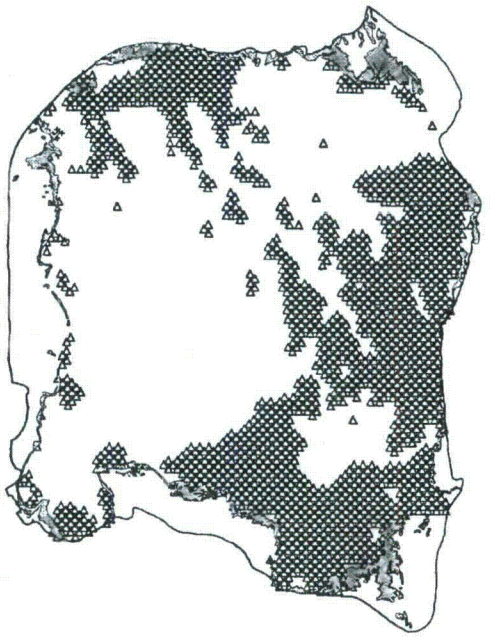

H. Vertical flow directions between the Dakota Sandstone and the Morrison Formation.

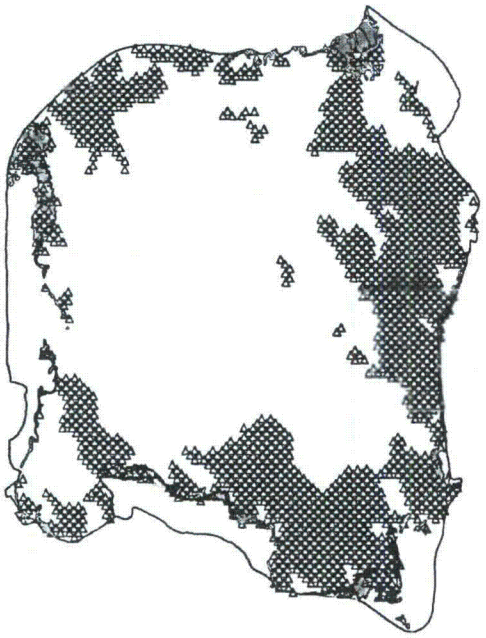

I. Vertical flow directions between the Morrison Formation and the Entrada Sandstone.

Figure 54.-- Vertical flow directions between selected adjacent hydrostratigraphic units in the San Juan Basin--Concluded.

The computed mass balance for water in the ground-water-flow system indicates that the aquifers in the regional system gain 135 cubic feet per second from streambed infiltration, 56 cubic feet per second from direct precipitation, and 4 cubic feet per second from downward leakage from the Chuska Sandstone. The 56 cubic feet per second computed recharge from direct precipitation is roughly one-third of the estimate presented earlier. Because the method used to develop the previous estimate did not differentiate between distributed recharge and local stream losses, however, comparing that estimate with the total computed gain from both streams and direct recharge, about 191 cubic feet per second, is more appropriate.

The total steady-state outflow from the aquifer system is computed to be 195 cubic feet per second, which basinwide is equivalent to 0.14 inch per year or about 1 percent of the average annual precipitation in the basin. All of this is simulated as being discharged to the surface-water system, primarily to the lower reaches of the San Juan and Puerco Rivers and the Rio Puerco. Under steady-state conditions inflow equals outflow. However, when the aquifer system is stressed by withdrawal of water this equilibrium is disrupted: recharge to the system increases and natural discharge from it decreases. Because of the probability of induced recharge to the system in response to ground-water withdrawals, the ground-water system should not be thought of as limited to its computed equilibrium flux of 195 cubic feet per second.

SUMMARY AND CONCLUSIONS

As part of the RASA program a three-dimensional steady-state ground-water-flow model was constructed for the San Juan structural basin in parts of New Mexico, Colorado, Arizona, and Utah. The model encompassed an area of about 19,380 square miles and simulated steady-state ground-water flow in 12 hydrostratigraphic units representing all major sources of ground water from aquifers of Jurassic and younger age.

The geohydrology of 10 of the 12 hydrostratigraphic units previously was described in a series of Hydrologic Investigations Atlases (U.S. Geological Survey HA-720 series). Information presented in the atlases and in this report was processed and stored in digital GIS data bases. The same data bases that were used to prepare the atlases were used to supply geohydrologic data to the ground-water-flow model. The digital data supplied from the GIS included tops and bottoms of units; land-surface altitude; areas of outcrop; locations, widths, altitudes, and vertical hydraulic conductivities of streams and streambeds; and areal distribution and rate of distributed recharge. Additionally, the GIS was used to construct model-input arrays of horizontal hydraulic conductivity and vertical hydraulic conductance.

Stream-aquifer interaction, direct recharge from precipitation, and downward leakage from the Chuska Sandstone were the external boundary conditions that were simulated. Streambed leakage contributed 135 cubic feet per second to the aquifer system, direct recharge contributed 56 cubic feet per second, and downward leakage from the Chuska Sandstone contributed 4 cubic feet per second. A computed discharge of 195 cubic feet per second to the lower reaches of the major streams and rivers in the basin balanced the steady-state water budget of the ground-water-flow system. The total steady-state outflow from the aquifer system is computed to be 195 cubic feet per second, which basinwide is equivalent to 0.14 inch per year or about 1 percent of the average annual precipitation in the basin.

Outcrop boundary conditions were found to most strongly control hydraulic heads and head distributions in the San Juan Basin. Less significant in the simulations were the simulated horizontal hydraulic-conductivity values, and least significant were the simulated horizontal anisotropy and vertical hydraulic-conductivity values.

SELECTED REFERENCES

Allen, J.E., and Balk, Robert, 1954, Mineral resources of the Fort Defiance and Tohatchi quadrangles, Arizona and New Mexico: Socorro, New Mexico Bureau of Mines and Mineral Resources Bulletin 36, 192 p.

Anderholm, S.K., 1979, Hydrogeology and water resources of the Cuba quadrangle, Sandoval and Rio Arriba Counties, New Mexico: Socorro, New Mexico Institute of Mining and Technology, unpublished M.S. thesis, 162 p.

Baltz, E.H., 1967, Stratigraphy and regional tectonic implications of part of Upper Cretaceous rocks, east-central San Juan Basin, New Mexico: U.S. Geological Survey Professional Paper 552, 101 p.

Baltz, E.H., Ash, S.R., and Anderson, R.Y., 1966, History of nomenclature and stratigraphy of rocks adjacent to the Cretaceous-Tertiary boundary, western San Juan Basin, New Mexico: U.S. Geological Survey Professional paper 524-D, 23 p.

Baltz, E.H., and West, S.W., 1967, Ground-water resources of the southern part of Jicarilla Apache Indian Reservation and adjacent areas, New Mexico: U.S. Geological Survey Water-Supply Paper 1576-H, 89 p.

Barnes, Harley, Baltz, E.H., Jr., and Hayes, P.T., 1954, Geology and fuel resources of the Red Mesa area, La Plata and Montezuma Counties, Colorado: U.S. Geological Survey Oil and Gas Investigations Map OM-149, 1 sheet, scale 1:62,500.

Bauer, C.M., 1916, Stratigraphy of a part of the Chaco River valley, *in* Contributions to the geology and paleontology of San Juan County, New Mexico: U.S. Geological Survey Professional Paper 98-P, p. 271-278.

Beaumont, E.C., 1971, Stratigraphic distribution of coal in San Juan Basin, *in* Shomaker, J.W., Beaumont, E.C., and Kottlowski, F.E., eds., Strippable low-sulfur coal resources of the San Juan Basin in New Mexico and Colorado: Socorro, New Mexico Bureau of Mines and Mineral Resources Memoir 25, p. 15-30.

Beaumont, E.C., Dane, C.H., and Sears, J.D., 1956, Revised nomenclature of Mesaverde Group in San Juan Basin, New Mexico: American Association of Petroleum Geologists Bulletin, v. 40, no. 9, p. 2149-2162.

Brimhall, R.M., 1973, Ground-water hydrology of Tertiary rocks of the San Juan Basin, New Mexico, *in* Fassett, J.E., ed., Cretaceous and Tertiary rocks of the southern Colorado Plateau: Four Corners Geological Society Memoir, p. 197-207.

Cadigan, R.A., 1967, Petrology of the Morrison Formation in the Colorado Plateau region: U.S. Geological Survey Professional Paper 556, 113 p.

Chow, V.T., 1964, Handbook of applied hydrology, a compendium of water-resources technology: New York, McGraw-Hill Book Company, 1418 p.

Collier, A.J., 1919, Coal south of Mancos, Montezuma County, Colorado: U.S. Geological Survey Bulletin 691-K, p. 293-310.

SELECTED REFERENCES--Continued

Condon, S.M., 1989, Modifications to Middle and Upper Jurassic nomenclature in the southeastern San Juan Basin, New Mexico, *in* Guidebook of Southeastern Colorado Plateau: New Mexico Geological Society, 40th Field Conference, p. 231-238.

Condon, S.M., and Huffman, A.C., Jr., 1988, Revisions in nomenclature of the Middle Jurassic Wanakah Formation, northwest New Mexico and northeast Arizona: U.S. Geological Survey Bulletin 1633-A, p. 1-12.

Condon, S.M., and Peterson, Fred, 1986, Stratigraphy of Middle and Upper Jurassic rocks of the San Juan Basin--Historical perspective, current ideas, and remaining problems, *in* Turner-Peterson, C.E., Santos, E.S., and Fishman, N.S., eds., 1986, A basin analysis case study--The Morrison Formation, Grants uranium region, New Mexico: American Association of Petroleum Geologists Studies in Geology, no. 22, p. 7-26.

Craig, L.C., Holmes, C.N., Cadigan, R.A., Freeman, V.L., Mullens, T.E., and Weir, G.W., 1955, Stratigraphy of the Morrison and related formations, Colorado Plateau region--A preliminary report: U.S. Geological Survey Bulletin 1009-E, p. 125-168.

Craigg, S.D., 1980, Hydrogeology and water resources of the Chico Arroyo/Torreon Wash area, Sandoval and McKinley Counties, New Mexico: Socorro, New Mexico Institute of Mining and Technology, unpublished M.S. thesis, 272 p.

_____1984, Hydrologic data on the Pueblos of Jemez, Zia, and Santa Ana, Sandoval County, New Mexico: U.S. Geological Survey Open-File Report 84-460, 37 p.

_____in press, Geologic framework of the San Juan structural basin of New Mexico, Colorado, Arizona, and Utah, with emphasis on Triassic through Tertiary rocks: U.S. Geological Survey Professional Paper 1420.

Craigg, S.D., Dam, W.L., Kernodle, J.M., and Levings, G.W., 1989, Hydrogeology of the Dakota Sandstone in the San Juan structural basin, New Mexico, Colorado, Arizona, and Utah: U.S. Geological Survey Hydrologic Investigations Atlas HA-720-I, 2 sheets.

Craigg, S.D., Dam, W.L., Kernodle, J.M., Thorn, C.R., and Levings, G.W., 1990, Hydrogeology of the Point Lookout Sandstone in the San Juan structural basin, New Mexico, Colorado, Arizona, and Utah: U.S. Geological Survey Hydrologic Investigations Atlas HA-720-G, 2 sheets.

Dam, W.L., 1995, Geochemistry of ground water in the Gallup, Dakota, and Morrison aquifers, San Juan Basin, New Mexico: U.S. Geological Survey Water-Resources Investigations Report 94-4253, 76 p.

Dam, W.L., Kernodle, J.M., Levings, G.W., and Craigg, S.D., 1990a, Hydrogeology of the Morrison Formation in the San Juan structural basin, New Mexico, Colorado, Arizona, and Utah: U.S. Geological Survey Hydrologic Investigations Atlas HA-720-J, 2 sheets.

Dam, W.L., Kernodle, J.M., Thorn, C.R., Levings, G.W., and Craigg, S.D., 1990b, Hydrogeology of the Pictured Cliffs Sandstone in the San Juan structural basin, New Mexico, Colorado, Arizona, and Utah: U.S. Geological Survey Hydrologic Investigations Atlas HA-720-D, 2 sheets.

SELECTED REFERENCES--Continued

Dames and Moore, 1977, Geotechnical and hydrologic investigation, production shaft 1, mining unit 1, Nose Rock project: Consultant's report for Phillips Petroleum Company, 56 p.

Dane, C.H., 1936, The La Ventana-Chacra Mesa coal field, *in* The geology of fuels in the southern part of the San Juan Basin, New Mexico: U.S. Geological Survey Bulletin 860-C, p. 81-161.

Dane, C.H., and Bachman, G.O., 1965, Geologic map of New Mexico: U.S. Geological Survey, 2 sheets, scale 1:500,000.

Dane, C.H., Bachman, G.O., and Reeside, J.B., Jr., 1957, The Gallup Sandstone, its age and stratigraphic relationships south and east of the stratotype, *in* Little, C.J., and Gill, J.J., eds., Guidebook to geology of southwestern San Juan Basin: Four Corners Geological Society, Second Field Conference, p. 99-113.

Darcy, H., 1856, *Les fontaines publiques de la ville de Dijon:* Paris, Victor Dalmont, 647 p.

Davies, P.B., 1989, Variable-density ground-water flow and paleohydrology in the Waste Isolation Pilot Plant (WIPP) region, southeastern New Mexico: U.S. Geological Survey Open-File Report 88-490, 139 p.

Dutton, C.E., 1885, Mount Taylor and the Zuni Plateau, *in* Sixth Annual Report: U.S. Geological Survey, p. 105-198.

Emery, P.A., 1970, Electric analog model evaluation of a water-salvage plan, San Luis Valley, south-central Colorado: Colorado Water Conservation Board Water Resources Circular 14, 11 p.

Fassett, J.E., 1974, Cretaceous and Tertiary rocks of the eastern San Juan Basin, New Mexico and Colorado, *in* Guidebook of Ghost Ranch, central-northern New Mexico: New Mexico Geological Society, 25th Field Conference, p. 225-230.

_____1977, Geology of the Point Lookout, Cliff House, and Pictured Cliffs Sandstones of the San Juan Basin, New Mexico and Colorado, *in* Fassett, J.E., ed., Guidebook of San Juan Basin III, northwestern New Mexico: New Mexico Geological Society, 28th Field Conference, p. 193-197.

_____1989, Coal-bed methane--A contumaceous, free-spirited bride, the geologic handmaiden of coal beds, *in* Energy Frontiers in the Rockies: Albuquerque Geological Society, New Mexico, p. 131-146.

Fassett, J.E., and Hinds, J.S., 1971, Geology and fuel resources of the Fruitland Formation and Kirtland Shale of the San Juan Basin, New Mexico and Colorado: U.S. Geological Survey Professional Paper 676, 76 p.

Fassett, J.E., Jentgen, R.W., Black, B.A., Molenaar, C.M., and Woodward, L.A., 1977, Road log second day: Red Mountain Oil Field to El Vado Lake via Pueblo Pintado, Star Lake, Torreon, Cuba, and Llaves, *in* Fassett, J.E., ed., Guidebook to San Juan Basin III: New Mexico Geological Society, 28th Field Conference, p. 19-38.

Freeze, R.A., and Cherry, J.A., 1979, Groundwater: Englewood Cliffs, N.J., Prentice-Hall, Inc., 604 p.

SELECTED REFERENCES--Continued

Frenzel, P.F., 1982, Estimates of vertical hydraulic conductivity and regional ground-water flow rates in rocks of Jurassic and Cretaceous age, San Juan Basin, New Mexico and Colorado: U.S. Geological Survey Water-Resources Investigations Report 82-4015, 59 p.

_____1983, Simulated changes in ground-water levels related to proposed development of Federal coal leases, San Juan Basin, New Mexico: U.S. Geological Survey Open-File Report 83-949, 63 p.

Freyberg, D.L., 1988, An exercise in ground-water model calibration and prediction: Ground Water, v. 26, no. 3, p. 350-360.

Fuchs-Parker, J.W., 1977, Alibi for a Mesaverde misfit--The La Ventana Formation Cretaceous delta, New Mexico, *in* Fassett, J.E., ed., Guidebook of San Juan Basin III, northwestern New Mexico: New Mexico Geological Society, 28th Field Conference, p. 199-206.

Gilluly, James, and Reeside, J.B., Jr., 1928, Sedimentary rocks of the San Rafael swell and some adjacent areas in eastern Utah: U.S. Geological Survey Professional Paper 150-D, p. 61-110.

Green, M.W., and Pierson, C.T., 1977, A summary of the stratigraphy and depositional environments of Jurassic and related rocks in the San Juan Basin, Arizona, Colorado, and New Mexico, *in* Fassett, J.E., ed.,Guidebook of San Juan Basin III: New Mexico Geological Society, 28th Field Conference, p. 147-152.

Gregory, H.E., 1938, The San Juan country--A geographic and geologic reconnaissance of southeastern Utah: U.S. Geological Survey Professional Paper 188, 123 p.

Harshbarger, J.W., and Repenning, C.A., 1954, Water resources of the Chuska Mountains area, Navajo Indian Reservation, Arizona and New Mexico: U.S. Geological Survey Circular 308, 16 p.

Haynes, D.D., Vogel, J.D., and Wyant, D.G., 1972, Geology, structure, and uranium deposits of the Cortez quadrangle, Colorado and Utah: U.S. Geological Survey Miscellaneous Geologic Investigations Map I-629, 2 sheets, scale 1:250,000.

Hearne, G.A., 1977, Evaluation of a potential well field near Church Rock as a water supply for Gallup, New Mexico: U.S. Geological Survey Water-Resources Investigations Report 77-98, 26 p.

_____1985, Mathematical model of the Tesuque aquifer system near Pojoaque, New Mexico: U.S. Geological Survey Water-Supply Paper 2205, 75 p.

Hearne, G.A., and Dewey, J.D., 1988, Hydrologic analysis of the Rio Grande Basin north of Embudo, New Mexico, Colorado and New Mexico: U.S. Geological Survey Water-Resources Investigations Report 86-4113, 244 p.

Hem, J.D., 1985, Study and interpretation of the chemical characteristics of natural water (3d ed., rev.): U.S. Geological Survey Water-Supply Paper 2254, 263 p.

Heywood, C.E., 1990, Use of a geographic information system in the analysis of geophysical and geologic data for ground-water basin studies in New Mexico [abs.], *in* Transactions, American Geophysical Union, v. 71, no. 43, October 23, 1990, p. 1316.

SELECTED REFERENCES--Continued

Heywood, C.E., 1991, Isostatic residual gravity anomalies of New Mexico: U.S. Geological Survey Water-Resources Investigations Report 91-4065, 27 p.

Hintze, L.F., 1981, Geologic map of Utah: Utah Geological and Mineral Survey, 1 sheet, scale 1:500,000.

Holmes, W.H., 1877, Report of the San Juan district, Colorado: U.S. Geological and Geographical Survey Territories, Ninth Annual Report (1875), p. 237-276.

Horn, C.R., 1986, Reach-file manual: U.S. Environmental Protection Agency, Washington, D.C., 40 p.

Kelley, V.C., 1951, Tectonics of the San Juan Basin, *in* Guidebook of the south and west sides of the San Juan Basin, New Mexico and Arizona: New Mexico Geological Society, Second Field Conference, p. 124-131.

Kelly, T.E., 1977, Geohydrology of the Westwater Canyon Member, Morrison Formation, of the southern San Juan Basin, New Mexico, *in* Fassett, J.E., ed., Guidebook of San Juan Basin III, northwestern New Mexico: New Mexico Geological Society, 28th Field Conference, p. 285-290.

Kernodle, J.M., 1992, Summary of U.S. Geological Survey ground-water-flow models of basin-fill aquifers in the Southwest Alluvial Basins region, Colorado, New Mexico, and Texas: U.S. Geological Survey Open-File Report 90-361, 81 p.

Kernodle, J.M., Levings, G.W., Craigg, S.D., and Dam, W.L., 1989, Hydrogeology of the Gallup Sandstone in the San Juan structural basin, New Mexico, Colorado, Arizona, and Utah: U.S. Geological Survey Hydrologic Investigations Atlas HA-720-H, 2 sheets.

Kernodle, J.M., and Philip, R.D., 1988, Using a geographic information system to develop a ground-water flow model, *in* Regional aquifer systems of the United States, aquifers of the western mountain area: American Water Resources Association Monograph 14, p. 191-202.

Kernodle, J.M., Thorn, C.R., Levings, G.W., Craigg, S.D., and Dam, W.L., 1990, Hydrogeology of the Kirtland Shale and Fruitland Formation in the San Juan structural basin, New Mexico, Colorado, Arizona, and Utah: U.S. Geological Survey Hydrologic Investigations Atlas HA-720-C, 2 sheets.

Klausing, R.L., and Welder, G.E., 1983, Data for ground-water studies of the San Juan Basin, New Mexico (1982-83): U.S. Geological Survey Open-File Report 84-135, 46 p.

Knight, R.L., and Cooper, J.C., 1955, Suggested changes in Devonian terminology of the Four Corners area, *in* Guidebook to Four Corners: Four Corners Geological Society, First Field Conference, p. 56-58.

Landis, E.R., Dane, C.H., and Cuban, W.A., 1973, Stratigraphic terminology of the Dakota Sandstone and Mancos Shale, west-central New Mexico: U.S. Geological Survey Bulletin 1372-J, 44 p.

Levings, G.W., Craigg, S.D., Dam, W.L., Kernodle, J.M., and Thorn, C.R., 1990a, Hydrogeology of the Menefee Formation in the San Juan structural basin, New Mexico, Colorado, Arizona, and Utah: U.S. Geological Survey Hydrologic Investigations Atlas HA-720-F, 2 sheets.

SELECTED REFERENCES--Continued

Levings, G.W., Craigg, S.D., Dam, W.L., Kernodle, J.M., and Thorn, C.R., 1990b, Hydrogeology of the San Jose, Nacimiento, and Animas Formations in the San Juan structural basin, New Mexico, Colorado, Arizona, and Utah: U.S. Geological Survey Hydrologic Investigations Atlas HA-720-A, 2 sheets.

Levings, G.W., Kernodle, J.M., and Thorn, C.R., 1996, Summary of the San Juan structural basin Regional Aquifer-System Analysis, New Mexico, Colorado, Arizona, and Utah: U.S. Geological Survey Water-Resources Investigations Report 95-4188, 55 p.

Lohman, S.W., 1972, Ground-water hydraulics: U.S. Geological Survey Professional Paper 708, 70 p.

Mannhard, G.W., 1976, Stratigraphy, sedimentology, and paleoenvironments of the La Ventana Tongue (Cliff House Sandstone) and adjacent formations of the Mesaverde Group (Upper Cretaceous), southwestern San Juan Basin, New Mexico: Albuquerque, University of New Mexico, unpublished Ph.D. dissertation, 182 p.

McDonald, M.G., and Harbaugh, A.W., 1988, A modular three-dimensional finite-difference ground-water flow model: U.S. Geological Survey Techniques of Water-Resources Investigations, book 6, chap. A1, 548 p.

McLean, J.S., 1980, Aquifer tests in the Gallup Sandstone near Yah-Ta-Hey, New Mexico: U.S. Geological Survey Water-Resources Investigations 80-25, 25 p.

Mercer, J.W., 1969, Hydrology of Project Gasbuggy site, Rio Arriba County, New Mexico: U.S. Geological Survey Report PNE-1013, 45 p.

Merrick, M.A., 1980, Geology of the eastern part of the Regina quadrangle, Sandoval and Rio Arriba Counties, New Mexico: Albuquerque, University of New Mexico, unpublished M.S. thesis, 91 p.

Molenaar, C.M., 1973, Sedimentary facies and correlation of the Gallup Sandstone and associated formations, northwestern New Mexico, *in* Cretaceous and Tertiary rocks of southern Colorado Plateau: Four Corners Geological Society Memoir, p. 85-110.

_____1974, Correlation of the Gallup Sandstone and associated formations, Upper Cretaceous, eastern San Juan and Acoma basins, New Mexico, *in* Siemers, C.T., ed., Guidebook of Ghost Ranch, central-northern New Mexico: New Mexico Geological Society, 25th Field Conference, p. 251-258.

_____1977a, San Juan Basin time-stratigraphic nomenclature chart, *in* Fassett, J.E., ed., Guidebook of San Juan Basin III: New Mexico Geological Society, 28th Field Conference, p. xii.

_____1977b, Stratigraphy and depositional history of Upper Cretaceous rocks of the San Juan Basin area, New Mexico and Colorado, *with a note on* Economic resources, *in* Fassett, J.E., ed., Guidebook of San Juan Basin III: New Mexico Geological Society, 28th Field Conference, p. 159-166.

_____1989, San Juan Basin stratigraphic correlation chart, *in* Finch, W.I., Huffman, A.C., Jr., and Fassett, J.E., eds., Coal, uranium, and oil and gas in Mesozoic rocks of the San Juan Basin--Anatomy of a giant energy-rich basin: 28th International Geological Congress, Washington, D.C., Guidebook for Field Trip T120, p. xi.

SELECTED REFERENCES--Continued

Myers, R.G., and Villanueva, E.D., 1986, Geohydrology of the aquifers that may be affected by the surface mining of coal in the Fruitland Formation in the San Juan Basin, northwestern New Mexico: U.S. Geological Survey Water-Resources Investigations Report 85-4251, 41 p.

National Oceanic and Atmospheric Administration, n.d., Annual free water surface evaporation: National Oceanic and Atmospheric Administration Technical Report NWS33, Map 3, scale 1:5,000,000.

Noon, P.L., 1980, Surface to subsurface stratigraphy of the Dakota Sandstone (Cretaceous) and adjacent units along the eastern flank of the San Juan Basin, New Mexico and Colorado: Bowling Green, Ohio, Bowling Green State University, unpublished M.S. thesis, 113 p.

O'Brien, K.M., and Stone, W.J., 1983, A two-dimensional hydrologic model of the Animas Valley, Hidalgo County, New Mexico: Socorro, New Mexico Bureau of Mines and Mineral Resources Open-File Report 133, 60 p.

O'Sullivan, R.B., and Beikman, H.M., 1963, Geology, structure, and uranium deposits of the Shiprock quadrangle, New Mexico and Arizona: U.S. Geological Survey Miscellaneous Geologic Investigations Map I-345, 2 sheets, scale 1:250,000.

O'Sullivan, R.B., Repenning, C.A., Beaumont, E.C., and Page, H.G., 1972, Stratigraphy of the Cretaceous rocks and the Tertiary Ojo Alamo Sandstone, Navajo and Hopi Indian Reservations, Arizona, New Mexico, and Utah: U.S. Geological Survey Professional Paper 521-E, 65 p.

Owen, D.E., 1973, Depositional history of the Dakota Sandstone, San Juan Basin area, New Mexico, *in* Fassett, J.E., ed., Cretaceous and Tertiary rocks of the southern Colorado Plateau: Four Corners Geological Society Memoir, p. 37-51.

_____1984, The Jackpile Sandstone Member of the Morrison Formation in west-central New Mexico--A formal definition: New Mexico Geology, v. 6, no. 3, p. 45-52.

Owen, D.E., and Siemers, C.T., 1977, Lithologic correlation of the Dakota Sandstone and adjacent units along the eastern flank of the San Juan Basin, New Mexico, *in* Fassett, J.E., ed., Guidebook of San Juan Basin III, northwestern New Mexico: New Mexico Geological Society, 28th Field Conference, p. 179-183.

Peeters, L.A., 1983, An isotopic investigation of ground-water resources in the Ojo Alamo Sandstone, San Juan Basin: Socorro, New Mexico Institute of Mining and Technology, unpublished M.S. thesis, 104 p.

Pentilla, W.C., 1964, Evidence for the pre-Niobrara unconformity in the northwestern part of the San Juan Basin: The Mountain Geologist, v. 1, p. 3-14.

Peter, K.D., Williams, R.A., and King, K.W., 1987, Hydrogeologic characteristics of the Lee Acres landfill area, San Juan County, New Mexico: U.S. Geological Survey Water-Resources Investigations Report 87-4246, 69 p.

Phillips, F.M., Peeters, L.A., Tansey, M.K., and Davis, S.N., 1986, Paleoclimatic inferences from an isotopic investigation of groundwater in the central San Juan Basin, New Mexico: Quaternary Research, v. 26, p. 179-193.

SELECTED REFERENCES--Continued

Powell, J.S., 1973, Paleontology and sedimentation models of the Kimbeto Member of the Ojo Alamo Sandstone: Four Corners Geological Society Memoir, p. 111-122.

Reeside, J.B., Jr., 1924, Upper Cretaceous and Tertiary formations of the western part of the San Juan Basin, Colorado and New Mexico, *and* Flora and fauna of the Animas Formation, by F.H. Knowlton: U.S. Geological Survey Professional Paper 134, 117 p.

Reneau, W.E., Jr., and Harris, J.D., 1957, Reservoir characteristics of Cretaceous sands of the San Juan Basin, *in* Little, C.J., and Gill, J.J., eds., Guidebook to geology of southwestern San Juan Basin: Four Corners Geological Society, Second Field Conference, p. 40-43.

Risser, D.W., Davis, P.A., Baldwin, J.A., and McAda, D.P., 1984, Aquifer tests at the Jackpile-Paguate uranium mine, Pueblo of Laguna, west-central New Mexico: U.S. Geological Survey Water-Resources Investigations Report 84-4255, 26 p.

Risser, D.W., and Lyford, P.F., 1983, Water resources on the Pueblo of Laguna, west-central New Mexico: U.S. Geological Survey Water-Resources Investigations Report 83-4038, 108 p.

Robinove, C.J., 1986, Principles of logic and the use of digital geographic information systems: U.S. Geological Survey Circular 977, 19 p.

Sanford, R.F., 1989, Late Jurassic paleohydrology of San Juan Basin--Simulated effects of variable transmissivity and lake levels [abs.]: Proceedings, American Association of Petroleum Geologists 1989 Rocky Mountain Section Meeting, Albuquerque, N. Mex., October 1-4, 1989, p. 90.

Sears, J.D., 1925, Geology and coal resources of the Gallup-Zuni Basin, New Mexico: U.S. Geological Survey Bulletin 767, 53 p.

Sears, J.D., Hunt, C.B., and Dane, C.H., 1936, Geology and fuel resources of the southern part of the San Juan Basin, New Mexico: U.S. Geological Survey Bulletin 860, 166 p.

Sears, J.D., Hunt, C.B., and Hendricks, T.A., 1941, Transgressive and regressive Cretaceous deposits in southern San Juan Basin, New Mexico, *in* Shorter contributions to general geology, 1938-40: U.S. Geological Survey Professional Paper 193-F, p. 101-121.

Shetiwy, M.M., 1978, Sedimentologic and stratigraphic analysis of the Point Lookout Sandstone, southeastern San Juan Basin, New Mexico: Socorro, New Mexico Institute of Mining and Technology, unpublished Ph.D. dissertation, 262 p.

Simpson, G.G., 1948a, The Eocene of the San Juan Basin, New Mexico: American Journal of Science, v. 246, pt. 1, p. 257-282.

_____1948b, The Eocene of the San Juan Basin, New Mexico: American Journal of Science, v. 246, pt. 2, p. 363-385.

Steven, T.A., Lipman, P.W., Hail, W.J., Jr., Barker, Fred, and Luedke, R.G., 1974, Geologic map of the Durango quadrangle, southwestern Colorado: U.S. Geological Survey Miscellaneous Investigations Map I-764, 1 sheet, scale 1:250,000.

Stone, W.J., Lyford, F.P., Frenzel, P.F., Mizell, N.H., and Padgett, E.T., 1983, Hydrogeology and water resources of San Juan Basin, New Mexico: Socorro, New Mexico Bureau of Mines and Mineral Resources Hydrologic Report 6, 70 p.

SELECTED REFERENCES--Continued

Sun, R.J., ed., 1986, Regional Aquifer-System Analysis program of the U.S. Geological Survey, summary of projects, 1978-84: U.S. Geological Survey Circular 1002, 264 p.

Tabet, D.E., and Frost, S.J., 1979, Environmental characteristics of Menefee coals in the Torreon Wash area, New Mexico: Socorro, New Mexico Bureau of Mines and Mineral Resources Open-File Report 102, 134 p.

Thomas, B.E., 1989, Simulation of the ground-water system in Mesozoic rocks in the Four Corners area, Utah, Colorado, Arizona, and New Mexico: U.S. Geological Survey Water-Resources Investigations Report 88-4086, 89 p.

Thorn, C.R., Levings, G.W., Craigg, S.D., Dam, W.L., and Kernodle, J.M., 1990a, Hydrogeology of the Cliff House Sandstone in the San Juan structural basin, New Mexico, Colorado, Arizona, and Utah: U.S. Geological Survey Hydrologic Investigations Atlas HA-720-E, 2 sheets.

_____1990b, Hydrogeology of the Ojo Alamo Sandstone in the San Juan structural basin, New Mexico, Colorado, Arizona, and Utah: U.S. Geological Survey Hydrologic Investigations Atlas HA-720-B, 2 sheets.

Trescott, P.C., 1975, Documentation of finite-difference model for simulation of three-dimensional ground-water flow: U.S. Geological Survey Open-File Report 75-438, 32 p.

Tweto, Ogden, 1979, Geologic map of Colorado: U.S. Geological Survey, 2 sheets, scale 1:500,000.

U.S. Bureau of the Census, 1980, Master area reference file for 1980 Census.

_____1985, Technical documentation, population, and per capita income estimates: Governmental Units, Washington, D.C., 6 p.

U.S. Department of the Interior, 1986, Final environmental impact statement for the Jackpile-Paguate uranium mine reclamation project, Laguna Indian Reservation, Cibola County, New Mexico: U.S. Department of the Interior, 244 p.

U.S. Department of Commerce, n.d., Normal October - April precipitation 1931-60: U.S. Department of Commerce Map, 1 sheet, scale 1:500,000.

U.S. Environmental Protection Agency, 1986a, Maximum contaminant levels (subpart B of part 141, National interim primary drinking-water regulations): U.S. Code of Federal Regulations, Title 40, Parts 100 to 149, revised as of July 1, 1986, p. 524-528.

U.S. Environmental Protection Agency, 1986b, Quality criteria for water, 1986: U.S. Environmental Protection Agency Publication EPA 440/5-86-001.

_____1986c, Secondary maximum contaminant levels (section 143.3 of part 143, National secondary drinking-water regulations): U.S. Code of Federal Regulations, Title 40, Parts 100 to 149, revised as of July 1, 1986, p. 587-590.

_____1987, Municipal facility/waterbody computerized information, an introduction: U.S. Environmental Protection Agency.

U.S. Geological Survey, 1987, Digital elevation models: U.S. Geological Survey Data Users Guide 5, 51 p.

SELECTED REFERENCES--Concluded

Waltemeyer, S.D., 1989, Statistical summaries of streamflow data in New Mexico through 1985: U.S. Geological Survey Water-Resources Investigations Report 88-4228, 204 p.

Waltemeyer, S.D., and Kernodle, J.M., 1992, Computation of snowpack-loss component for a water-budget model for the San Juan aquifer basin in New Mexico and Colorado: Proceedings, Western Snow Conference, Jackson, Wyo., April 14-16, 1992, p. 141-145.

Watson, R.A., and Wright, H.E., Jr., 1963, Landslides on the east flank of the Chuska Mountains, northwestern New Mexico: American Journal of Science, v. 261, June 1963, p. 525-548.

Welder, G.E., 1986, Plan of study for the Regional Aquifer-System Analysis of the San Juan structural basin, New Mexico, Colorado, Arizona, and Utah: U.S. Geological Survey Water-Resources Investigations Report 85-4294, 23 p.

Welder, G.E., and Klausing, R.L., 1990, Geohydrology of the Morrison Formation in the western San Juan Basin, New Mexico: U.S. Geological Survey Water-Resources Investigations Report 89-4069, 1 sheet.

Wells, S.G., Love, D.W., and Gardner, T.W, eds., 1983, Chaco Canyon Country, A field guide to the geomorphology, Quaternary geology, paleoecology, and environmental geology of northwestern New Mexico: American Geomorphological Field Group 1983 Field Trip Guidebook, 253 p.

Wengerd, S.A., and Matheny, M.L., 1958, Pennsylvanian System of Four Corners region: American Association of Petroleum Geologists Bulletin, v. 42, no. 9, p. 2048-2106.

Wilson, E.D., Moore, R.T., and Cooper, J.R., 1969, Geologic map of Arizona: Arizona Bureau of Mines and U.S. Geological Survey, 1 sheet, scale 1:500,000.

Woodward, L.A., and Schumacher, O.L., 1973, Morrison Formation of southeastern San Juan Basin, New Mexico: Socorro, New Mexico Bureau of Mines and Mineral Resources Circular 129, 7 p.

Wright, A.F., 1979, Bibliography of geology and hydrology, San Juan Basin, New Mexico, Colorado, Arizona, and Utah: U.S. Geological Survey Bulletin 1481, 123 p.

Wright, H.E., Jr., 1954, Problem of Tohatchi Formation, Chuska Mountains, Arizona-New Mexico: American Association of Petroleum Geologists Bulletin, v. 38, no. 8, p. 1827-1836.

_____1956, Origin of the Chuska Sandstone, Arizona-New Mexico, a structural and petrographic study of a Tertiary eolian sediment: Geological Society of America Bulletin, v. 67, p. 413-434.

Wright, Robyn, 1984, Paleoenvironmental interpretation of the Upper Cretaceous Point Lookout Sandstone--Implications for shoreline progradation and basin tectonic history, San Juan Basin, New Mexico: Houston, Tex., Rice University, unpublished Ph.D. dissertation, 404 p.

Zehner, H.H., 1985, Hydrology and water-quality monitoring considerations, Jackpile uranium mine, northwestern New Mexico: U.S. Geological Survey Water-Resources Investigations Report 85-4226, 61 p., 1 pl.